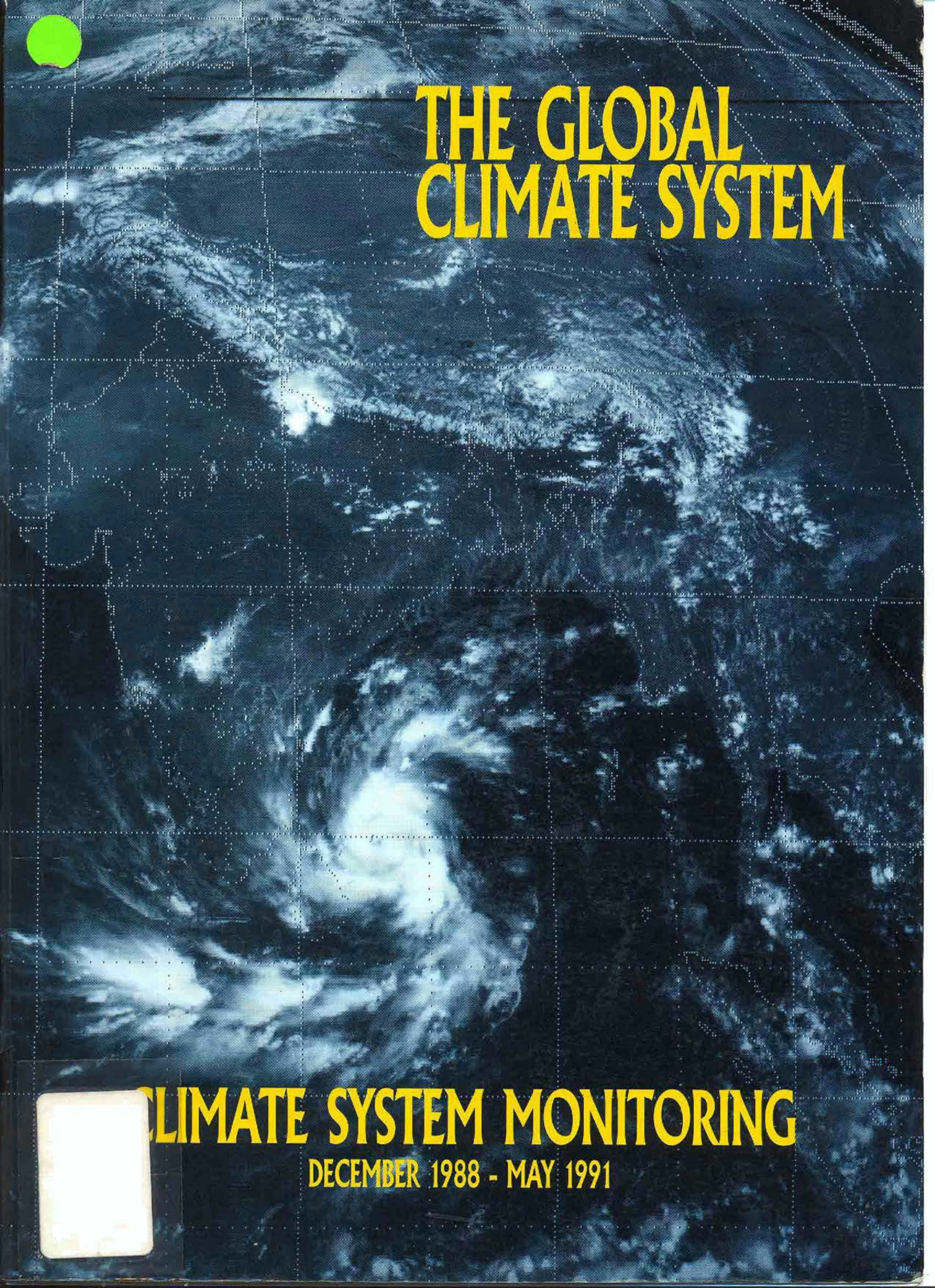

THE GLOBAL CLIMATE SYSTEM

CLIMATE SYSTEM MONITORING

DECEMBER 1988 - MAY 1991

THE GLOBAL CLIMATE SYSTEM

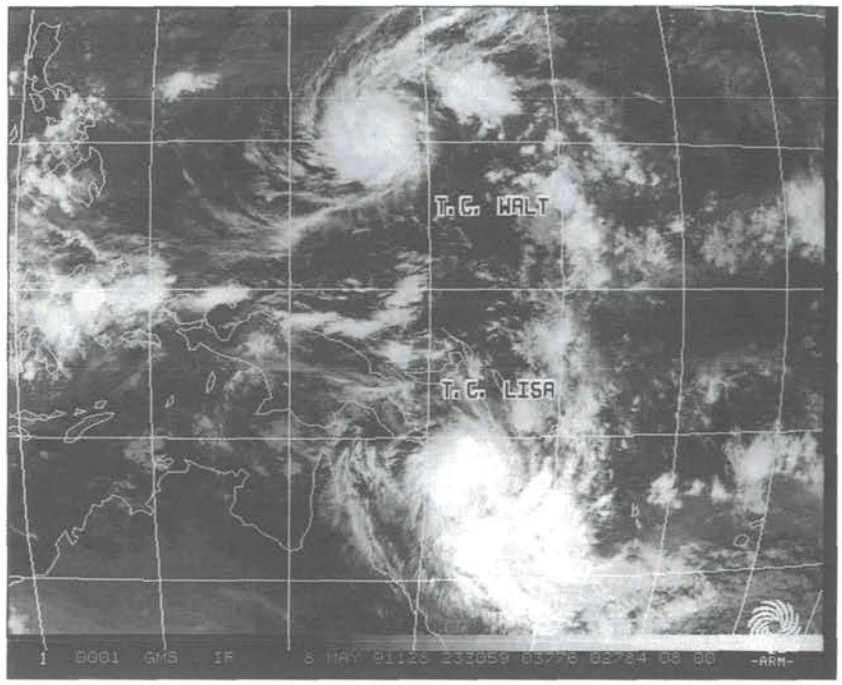

CLIMATE SYSTEM MONITORING

DECEMBER 1988 - MAY 1991

WORLD METEOROLOGICAL
ORGANIZATION
WORLD CLIMATE DATA
AND MONITORING PROGRAMME

UNITED NATIONS
ENVIRONMENT
PROGRAMME

FOREWORD

The Climate System Monitoring (CSM) project of the World Climate Data and Monitoring Programme (WCDMP) was initiated in 1984 following a recommendation of the Ninth Congress of the World Meteorological Organization (WMO) in response to the occurrence of significant climate system anomalies over the last few years associated with adverse impacts on the social and economic activities of many countries. CSM is designed to provide Meteorological Services and other national and international organizations with synthesized information on the state of the climate system and diagnostic insights into significant large-scale anomalies of regional and global consequence. A CSM Monthly Bulletin has been issued since July 1984.

This report, the fourth biennial review of THE GLOBAL CLIMATE SYSTEM, is based on the current scientific understanding of the climate system and provides a basis for the monitoring of global change. This monitoring supports efforts such as the newly formed Climate Change Detection Project of the WCDMP, by facilitating the identification of persistent anomalies on both global and regional scales, which is a necessary first step toward separating the "signal" of climate change from the "noise" of natural variability. Due to deficiencies in the global observing system, the diagnostic analyses of cause-effect relationships are preliminary for some regions and some climatic events or processes.

It is hoped that the review will promote further research and better observing systems that would lead to improved models of the complex interactive processes occurring within the climate system. Much of this report was compiled from the input of a diverse group of experts from various regions around the world, who are acknowledged at the end of the report. Use was also made of readily available scientific literature: an extensive bibliography is provided at the end of the report for further reading. I thank David Phillips of the Canadian Climate Centre for his special contributions in compiling and editing this review.

The co-sponsorship of the CSM project by the Global Environmental Monitoring System (GEMS) of the United Nations Environment Programme and the contribution by the Canadian Climate Centre toward the production of the figures in this review are gratefully acknowledged.

V. Boldirev
Director, World Climate Programme Department

Photo FAO

INTRODUCTION AND HIGHLIGHTS

CHAPTER 1

This report on The Global Climate System, the fourth in a series of biennial reviews, is designed to provide Meteorological Services and other national and international organizations with information about the state of the climate system. In particular, it presents a review of significant climate events and a description of large-scale anomalies of regional and global consequence. Wherever possible, recent events are placed in an historical context through the use of data time series. Also featured is background information on topical climate subjects, such as El Niño, desertification, and greenhouse gases. The Review covers in detail the period from December 1988 to May 1991, inclusive. Brief mention is made of significant meteorological-related events occurring in the remaining months of 1991.

The climate system encompasses the full global domain — atmosphere, oceans, biosphere, and cryosphere. It addresses a multi-disciplinary range of properties and complex, interrelated processes.

The Review contains hemispheric and global anomalies of various atmospheric and oceanic variables, important for interpreting more detailed analyses at subregional, national and local scales. The identification of anomalies requires statistics from long data time series. The significance of climate anomalies is defined by the departures of various components of the climate system from their "normal" values and not necessarily by their impacts.

The Review also includes global analyses of temperature and precipitation anomalies, and atmospheric and oceanic circulation patterns, and details on the persistence of hot/cold, and wet/dry episodes. Events bringing considerable loss of life, much suffering and economic losses — such as floods, drought and major storms — are well documented, as well as information on changes in the concentrations of ozone and various trace gases. To show the full extent of the total climate system, short chapters on vegetation changes, water levels and the cryosphere are presented.

The Review borrows heavily on published analyses of regional and global anomalies carried out by several national meteorological centres. Many of these centres publish the information in monthly bulletins, much of which sees its way into WMO's Climate System Monitoring (CSM) Bulletin published monthly by the World Climate Data and Monitoring Programme.

Highlights

The review period from December 1988 to May 1991 had its share of remarkable extremes and anomalous climate events. Floods and droughts occurred across every continent, sometimes in the same localities during the same year.

Some climate highlights for the period are:

- *The cold ENSO in the Pacific during 1988-89* was one of the coldest episodes of the last 50 years.
- *Global temperatures continued to rise* — 1990 was clearly the warmest year on record.
- *The years 1988 and 1989 were the first consecutive years with normal to higher rainfalls in the Sahel since the mid-1960s*. Dry and hot weather returned to the region in 1990.
- *The "Big Wet" in some areas of eastern Australia during 1989 and 1990* produced the heaviest rains and worst flooding in two centuries.
- *The monsoon over the Indian Subcontinent and eastern Africa was described as excellent* in 1989 and 1990.
- *Cloudiness continued to decrease globally* during 1989 and 1990.
- *Drenching rains struck portions of China in May 1991* and continued well into August of that year, producing the worst floods this century in the Wu River system.
- *The storm that ravaged Bangladesh in April 1991* and inflicted enormous loss of life, much suffering and extensive property damage.
- *Snow cover extent across the Northern Hemisphere in 1990 was below normal in every month*, averaging about 8 to 10% below the annual average.
- *The Antarctic ozone hole continued to increase in both ozone depletion and in spatial extent*. The mean global growth rate of CO_2 for 1989 and 1990 was about 1.4 ppm per year.
- *There was an extraordinary rise in the Caspian Sea level.*

The single most important phenomenon associated with global-scale atmospheric circulation anomalies is the Southern Oscillation (SO). Dominant features in the SO extremes include large-scale warming (cooling) of the equatorial Pacific sea surface temperatures, weakening (strengthening) of the equatorial low-level easterlies, enhanced (suppressed) convection in the equatorial central and eastern Pacific Ocean, and enhanced (weakened) subtropical jet streams in both hemispheres. The two extremes in the SO are often referred to as warm and cold episodes, with the former frequently called El Niño. Historically, the term El Niño has been applied to an abnormal warming of the waters along the west coast of South America. In recent years it has been applied to the larger scale warming that occurs throughout the tropical Pacific during warm episodes.

2.1 EL NIÑO — COLD EPISODE IN 1988-1989 TRENDING TOWARD A WARM EPISODE IN 1990-1991

The 1986-1987 warm episode, described in the last biennial review, was followed by one of the strongest cold episodes in the last 50 years. Cooling was observed throughout the tropical troposphere during 1988-1989; mid-latitude westerlies in both hemispheres shifted poleward of their normal positions. Many anomalous features in the patterns of tropical precipitation (good Southeast Asia and Australia monsoons) and extratropical temperature (above normal temperatures throughout the northern mid-latitudes) seem to be associated with the evolution of the tropical Pacific cold episode.

Anomalous cooling of the sea surface temperatures in the equatorial central and eastern Pacific and of the overlying troposphere occurred during 1988. The peak intensity of the tropical Pacific cold episode, as measured by the Southern Oscillation Index (Figure 2.1) and equatorial central Pacific sea surface temperature anomalies (Figure 2.2), occurred during the Northern Hemisphere autumn of 1988 and winter of 1988-1989. Accompanying the decrease in equatorial Pacific sea surface temperatures, convective activity became anomalously weak. Substantial cooling of the global tropical troposphere was observed and had a significant impact on atmospheric circulation features in the mid-latitudes of both hemispheres (Figure 2.3). This cooling began in the tropical east Pacific and gradually spread throughout the tropics reaching peak intensity in early 1989 (Figure 2.4). By late 1988 and early 1989, zonally averaged tropical

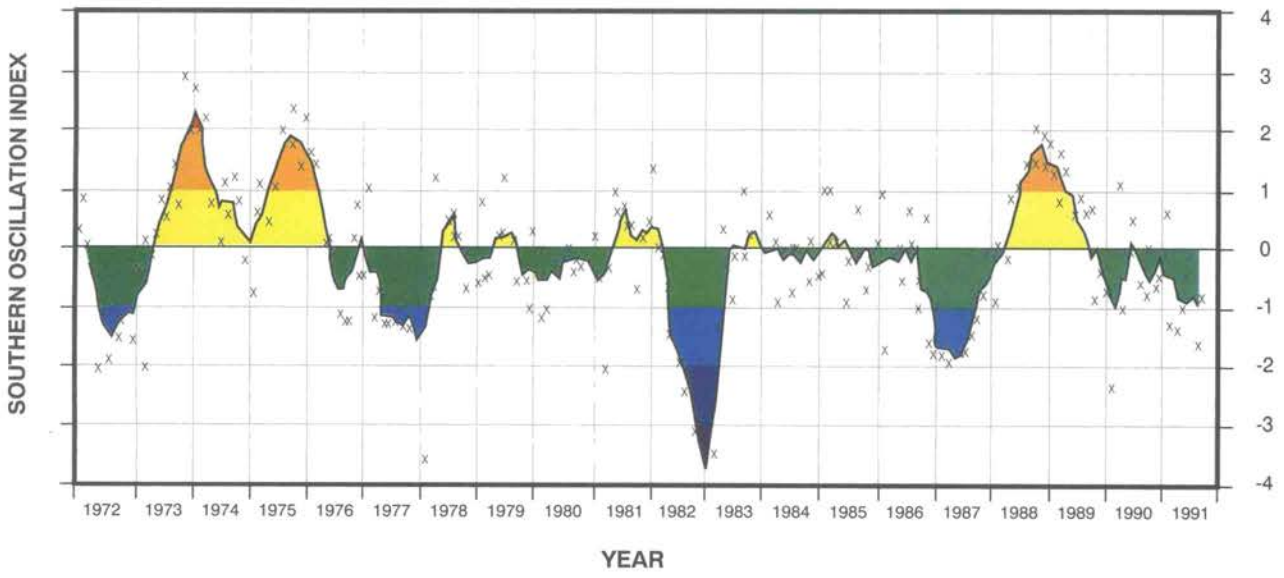

Figure 2.1 - Time series of monthly values of the Southern Oscillation Index (SOI), i.e., the difference between the sea-level pressure anomalies at Tahiti and Darwin (Tahiti-Darwin), standardized with respect to the mean annual standard deviation. The solid line shows the five-month running mean (from NOAA, Climate Analysis Center, Washington, DC).

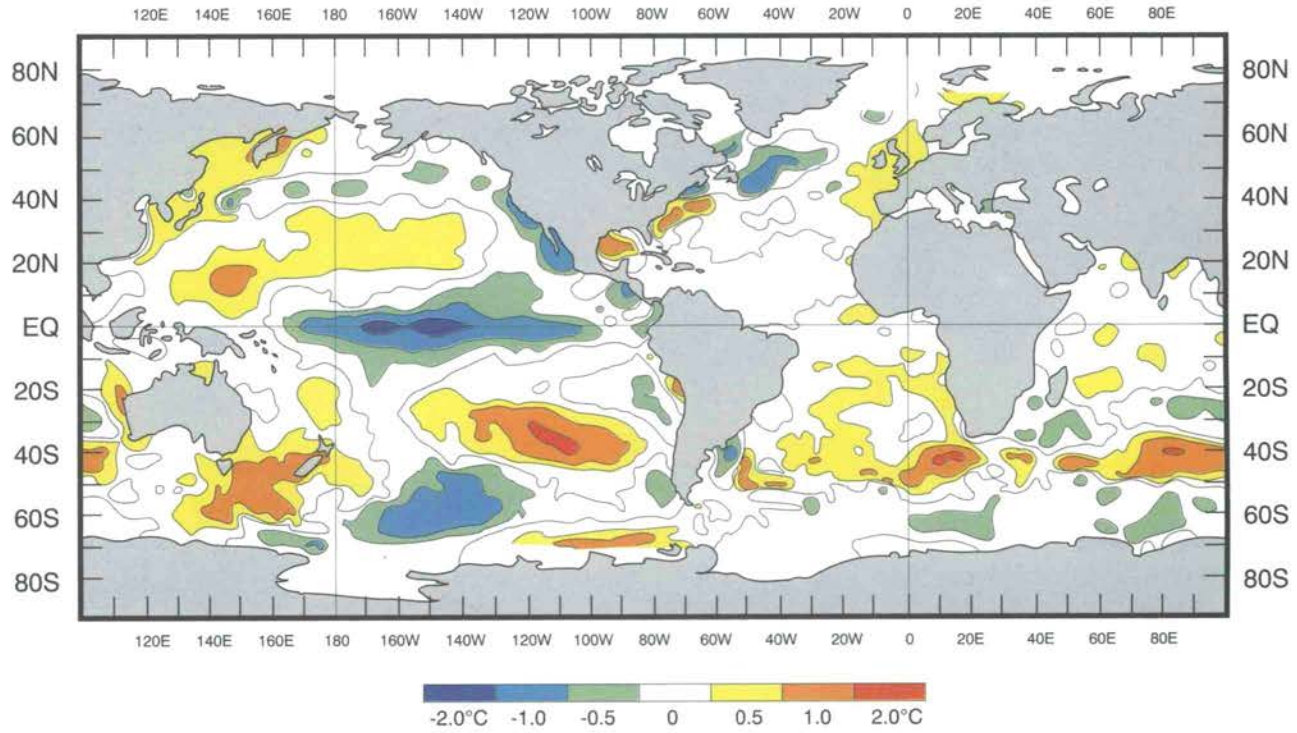

▲ *Figure 2.2* - Anomalous sea surface temperature for December 1988 to February 1989 (from NOAA, Climate Analysis Center, Washington, DC).

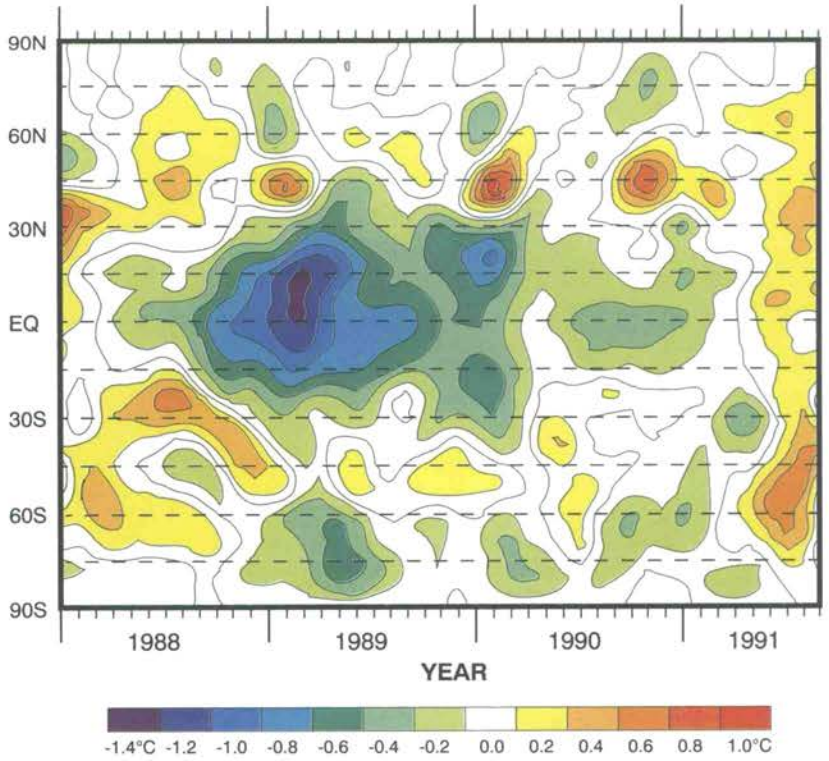

◄ *Figure 2.3* - Time-latitude section of anomalous, zonally averaged 500-hPa virtual temperature (from NOAA, Climate Analysis Center, Washington, DC).

EL NIÑO[1]

El Niño is the invasion from time to time of warm surface water from the western equatorial Pacific Basin to the eastern equatorial region and along the coasts of Peru, Ecuador and northern Chile.

During most of the year, the prevailing southeasterly trade winds produce a surface current flowing toward the equator along the western South American coast. The Earth's rotation adds an offshore component to the current's movement. The waters leaving the coast are replaced by colder water from below, a process referred to as upwelling. This cold current allows nutrient-rich water to upwell off Peru and Ecuador, thus providing one of the world's most productive fisheries.

But when the atmospheric pressure shifts, as it often does before an El Niño, the winds weaken. Sometimes, as in 1991, they can even reverse. That has a huge impact on the ocean. With weak easterly or westerly winds, the layer of warm surface water in the western Pacific slips back towards South America, disrupting the upwelling along the west coast. The warm water over much of the equatorial eastern and central Pacific, sometimes 2 to 3°C or higher above normal, heats the air above it, causing convection, clouds and rain. In the 1982-83 El Niño, one of the strongest on record, spot water temperatures reached 32°C, an unusual 5°C above normal.

In the late 1960s, it became apparent that the year-to-year variations in sea surface temperatures (SST) were closely linked to the Southern Oscillation (SO), an out-of-phase relationship between atmospheric pressures over the southeastern Pacific and the Indian Ocean.

At the height of the ENSO event, a huge area of anomalous westerly winds and warm SSTs lies over much of the equatorial Pacific. The pressure is much higher than average at Darwin and much lower than average at Tahiti, the opposite of anti-El Niño periods, or periods when SSTs are much colder than average.

Figure 2.1 shows the relationship between atmospheric pressures at Tahiti, representing the southeastern Pacific, and at Darwin (Australia), representing the Indian Ocean and Australian region. In years such as 1982-1983 and 1986-1987, when major El Niño occurred, the pressure at Darwin was abnormally high, while at Tahiti it was unusually low. The difference in standardized pressure anomalies, Tahiti minus Darwin, is frequently used as an index of the Southern Oscillation (SOI).

Anomalous SST warmings (El Niño) occur on average about twice every 10 years although the interval between events is irregular. The warm eastern Pacific waters and higher-than-normal Darwin pressures last for about 12 months, commencing around the start of one calendar year and ending just after the start of the next. The years before and after an El Niño episode tend to be cool SST years in the eastern equatorial Pacific.

The relationship between weather patterns in the equatorial Pacific and ENSO is extremely strong and has been well documented for many years. Outside the equatorial Pacific, the strength of the teleconnections varies from area to area and season to season, with the tropics and subtropics generally showing the strongest relationships. In years with an ENSO event, many climate anomalies occur, but, in fact, they occur elsewhere over the earth every year. However, some anomalies tend to recur with particular ENSO events. For North America, the mean westerly air flow accelerates bringing milder Pacific air over most of the continent. El Niño generally means warmer winters for Alaska and western Canada, increased rain over California, Florida and the Gulf Coast. Elsewhere, droughts in Australia, Indonesia, the Philippines and Africa, and tropical storms in Tahiti and Polynesia can be attributed to the effects of the warm current.

1 - Adapted from Nevill Nicholls (1987).

mid-tropospheric temperatures had dropped about 2°C from values observed during the 1986-1987 warm episode and were anomalously cold from 30°N to 30°S. At the same time, the extratropical mid- and upper-tropospheric westerlies weakened in both hemispheres and the main axes of the westerlies shifted poleward. Consistent with the poleward contraction of the jet streams in both hemispheres, warmer than normal conditions were observed at many mid-latitude locations. These features, particularly strong in the Northern Hemisphere, prevailed during the northern winters and springs from late 1988 through 1990. Similar features were also evident in the Southern Hemisphere, although with less seasonal variations.

By late 1989, sea surface temperature anomalies in the central and western equatorial Pacific were once again positive (Figure 2.5), and it appeared that a warm episode was about to develop. Enhanced convection was observed in this

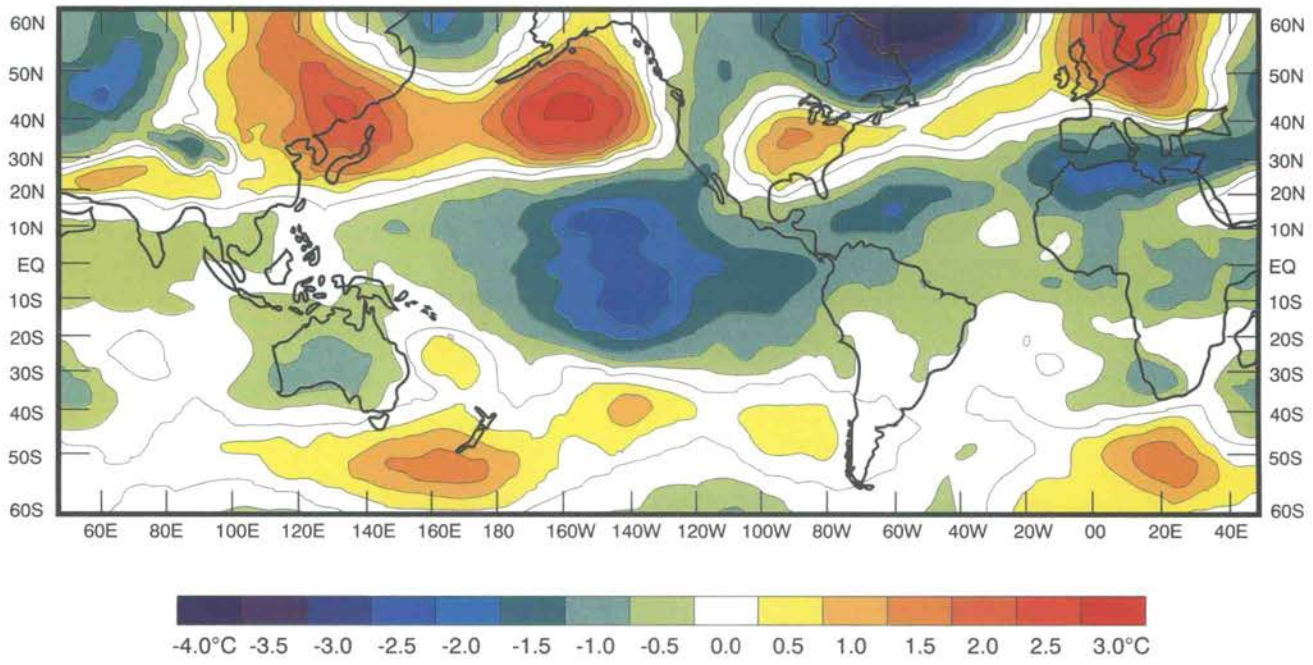

▲
Figure 2.4 - Anomalies of 500-hPa virtual temperature for December 1988 -February 1989, computed with respect to the October 1978-September 1985 base period (from NOAA, Climate Analysis Center, Washington, DC).

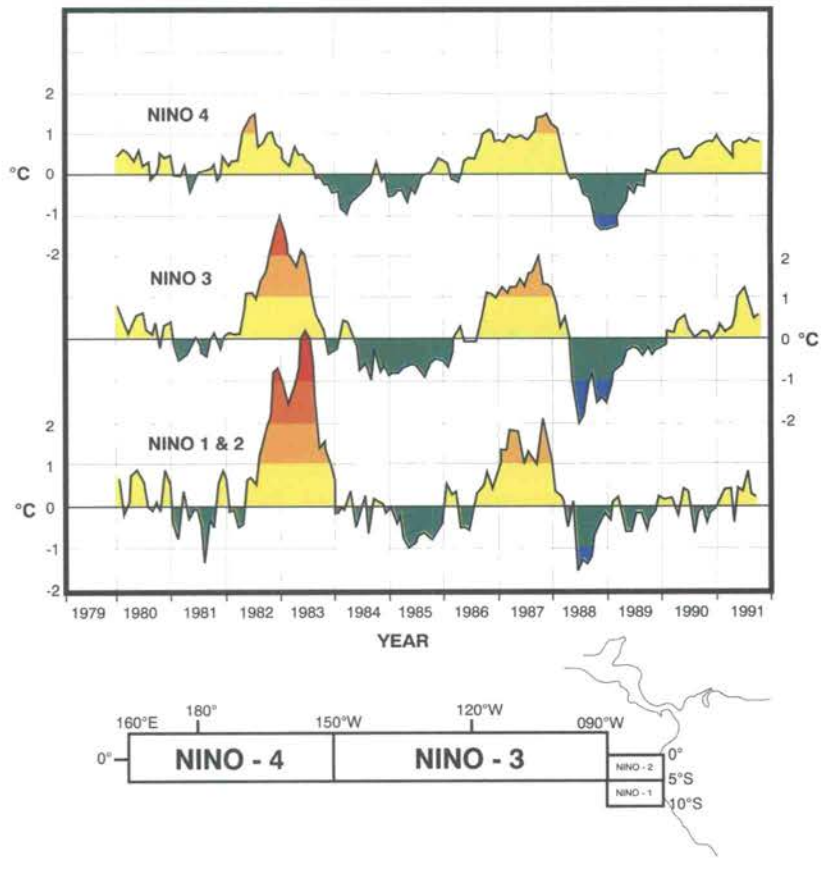

▶
Figure 2.5 - Equatorial Pacific sea surface temperature anomaly indices (°C) for the areas indicated at the bottom of the figure. Niño 1 & 2 is the average over the Niño 1 and Niño 2 areas (from NOAA, Climate Analysis Center, Washington, DC).

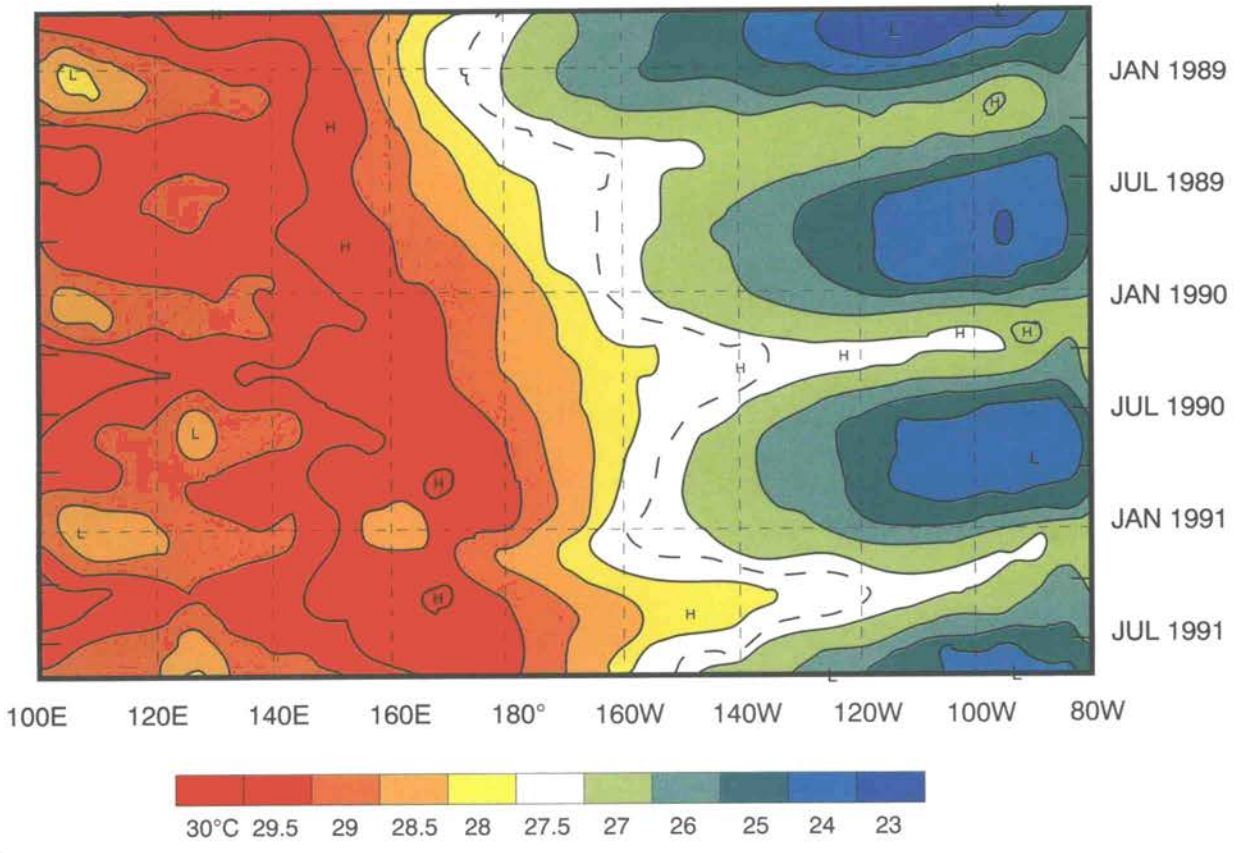

Figure 2.6 - Time-longitude section of the mean monthly sea surface temperature for the latitude band 5°N-5°S (from NOAA, Climate Analysis Center, Washington, DC).

region from December 1989 to February 1990. The Southern Oscillation Index (SOI) featured a large month-to-month variability during late 1989 to early 1990 (Figure 2.1), but by April 1990 the atmospheric circulation returned to near normal and signs of a developing warm episode had disappeared.

From December 1988 to July 1991, the sea surface temperatures in the central equatorial Pacific slowly warmed (Figure 2.6). The 28°C isotherm, considered the threshold for the formation of deep tropical convection, gradually shifted eastward as the area of water with greater values of SST increased. The region of warmest water also shifted eastward. During the 1986-1987 warm episode, the eastward shift of the warmest water to a region along the equator near the date-line appears to have been important in establishing persistent enhanced convection well to the east of the influences of the maritime continent. The lack of development of persistent, enhanced equatorial convection in early 1990 was probably related to both the magnitude of the SST anomalies in the region (only about +0.5°C) and to the lack of a clear separation between the warmest water and the islands of the extreme western equatorial Pacific.

The anomalous depth of the 20°C isotherm in the equatorial Pacific Ocean (Figure 2.7), an indicator of the anomalous depth of the oceanic thermocline, had an interesting pattern during the last five years. Depth anomalies were positive before the 1986-1987 warm episode and negative before and during the early stages of the 1988-1989 cold episode. From early 1989 until mid-1991, except for a brief period in early 1990, depth anomalies have been positive throughout the equatorial Pacific. Positive depth anomalies are consistent with increased heat content in the upper ocean, a characteristic expected before warm episodes. By mid-1991, oceanic and atmospheric indices were consistent in indicating a developing warm episode.

2.2

PERSISTENT ANOMALOUS MID- AND UPPER-TROPOSPHERIC RIDGES DOMINATE THE MID-LATITUDES OF BOTH HEMISPHERES

The strong cooling of the tropical troposphere during the 1988-1989 tropical Pacific cold episode was accompanied by an anomalous warming of the mid-latitude troposphere and a poleward shift of the westerlies in both hemispheres. This pattern is consistent with the zonally averaged 500-hPa temperature anomalies shown in Figure 2.3, which shows mid-latitude (high-latitude) positive (negative) anomalies during the northern winters of 1988-1989 and 1989-1990.

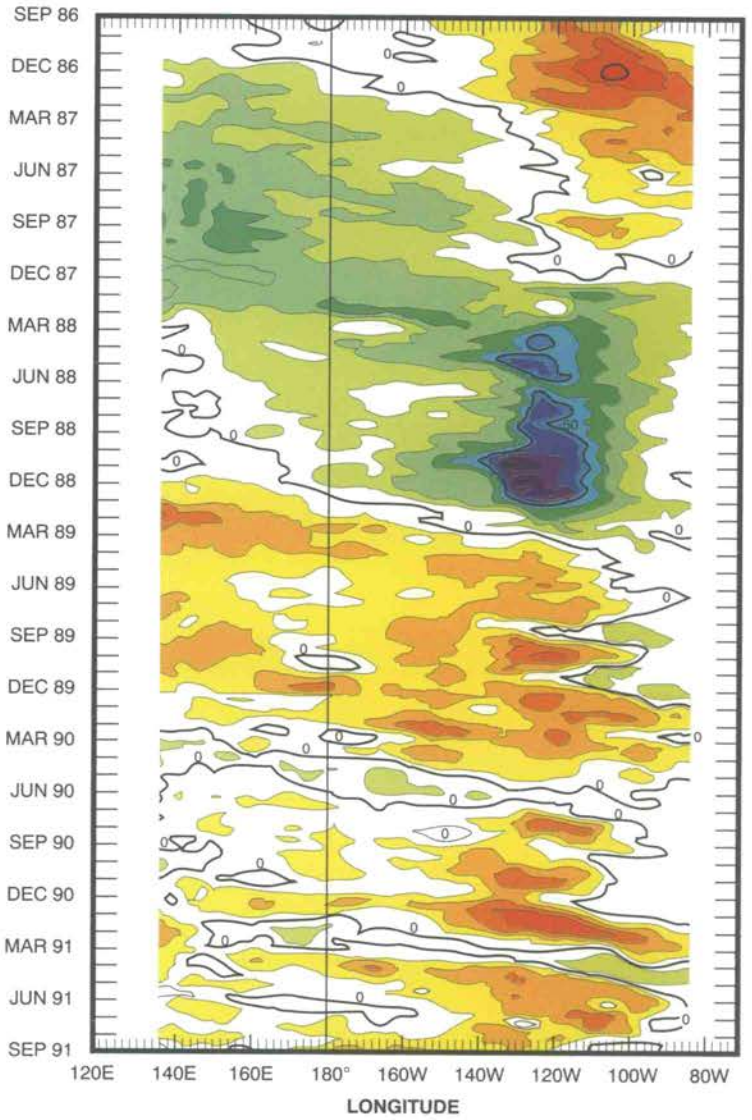

Figure 2.7 - Anomalous depth of the 20°C isotherm along the equator in the Pacific Ocean, September 1986 - September 1991. The contour interval is 10 m with negative anomalies less than -10 m darker and positive anomalies greater than 10 m lighter. Anomalies are computed with respect to the 1985-1990 base period (from NOAA, Climate Analysis Center, Washington, DC).

2.3 NORTHERN HEMISPHERE CIRCULATION — LESS CYCLONICITY BUT SEVERAL VIOLENT STORMS

The pattern of anomalous tropospheric temperature was associated with less than normal cyclonic activity, especially in the western part of the North Pacific and over Canada around Hudson Bay and near Newfoundland (Figure 2.8). Storm tracks shifted north of their normal positions; however, even at higher latitudes the cyclonic activity was less than normal, although in some instances the extratropical cyclones reached record intensities, especially over northern Europe.

Figure 2.8 - Monthly departure from normal of the number of cyclone centres within a 5°x10° grid cell for selected regions with high cyclonic activity in the Northern Hemisphere. Data are for the period December 1988-May 1991; the reference period is 1951-1980 (from Institute for Global Climate and Ecology, Moscow).

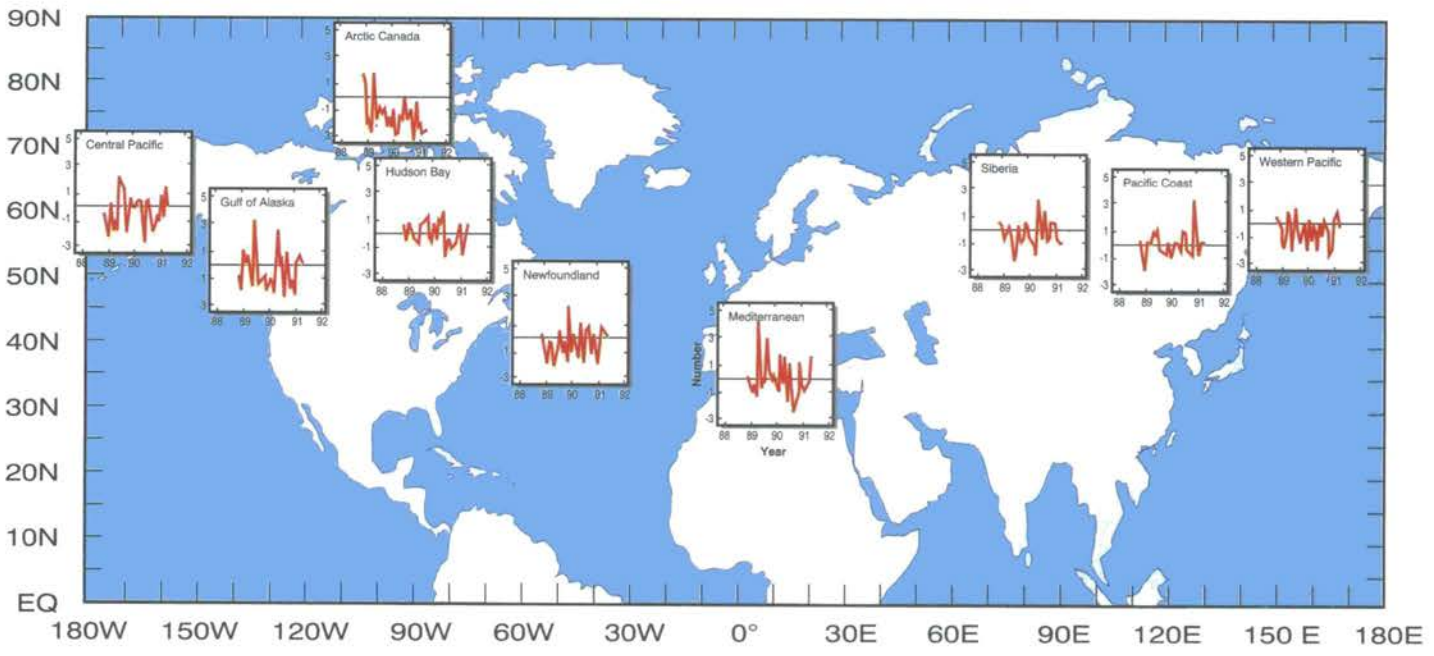

A zonal index, computed as the difference in zonally averaged sea-level pressure between 35 and 65°N, indicates that the northern winters of 1988-1989 and 1989-1990 had the strongest north-south pressure gradient this century for the latitude band centred on 50°N. A series of exceptionally intense extratropical cyclones developed in the North Atlantic during these Northern Hemisphere winter seasons, resulting in a heavy loss of life and property in northern Europe. A European zonal index computed for the longitude band 20°W-40°E for February is shown in Figure 2.9. This figure shows that 1989 and 1990 had the strongest pressure gradients, with departures greater than two standard deviations from normal. The most violent storms affecting northern Europe were experienced during these months. In contrast, February 1991 featured a weaker than normal gradient and a dearth of strong storms.

2.4

NORTHERN HEMISPHERE WINTER BLOCKING — STRONGER AND LONGER

Pronounced atmospheric blocking is one of the main reasons for large weather anomalies that persist from a week to a season. The blocking indices presented in Figure 2.10 characterize duration (TD) and intensity (TI) of blocking ridges for each season. Blocking ridges were stronger and longer lasting during the northern winters 1988-1989 and 1990-1991, and tended to occur at their normal climatological longitudes.

In the northern winter 1988-1989, maximum blocking indices were well above normal over three regions: Western Europe (TD reached 30 days above normal), Eastern Siberia (21 days) and Western Canada (18 days). In the northern spring of 1989, blocking systems lasted longer, were more intense than usual and were displaced east of their climatological positions in the European sector. The Atlantic-European blocking area was displaced into eastern Europe-Siberia, where durations reached 58 days, i.e., 31 days above normal.

Winter 1990-1991 was marked by high blocking activity over most of the Northern Hemisphere, being greatest in two regions: the eastern Atlantic to the Urals (TD anomaly reached 27 days), and the Pacific Ocean to northeast of North America (up to 31 days above normal). In the first region, two periods of uninterrupted blocking were observed: one started in October over the eastern Atlantic and reached the Urals by December, before weakening. The other started in the second half of January and lasted to the end of winter. Over North America the blocking ridge began at the end of December in the west, spreading by the middle of January over the entire northern Pacific Ocean. During the second half of January, this ridge moved

Figure 2.9 - February (1970-1991) zonal index for Europe (20°W - 40°E) computed as the difference in zonally averaged sea-level pressure between 35 and 65°N (from Deutscher Wetterdienst - Seewetteramt).

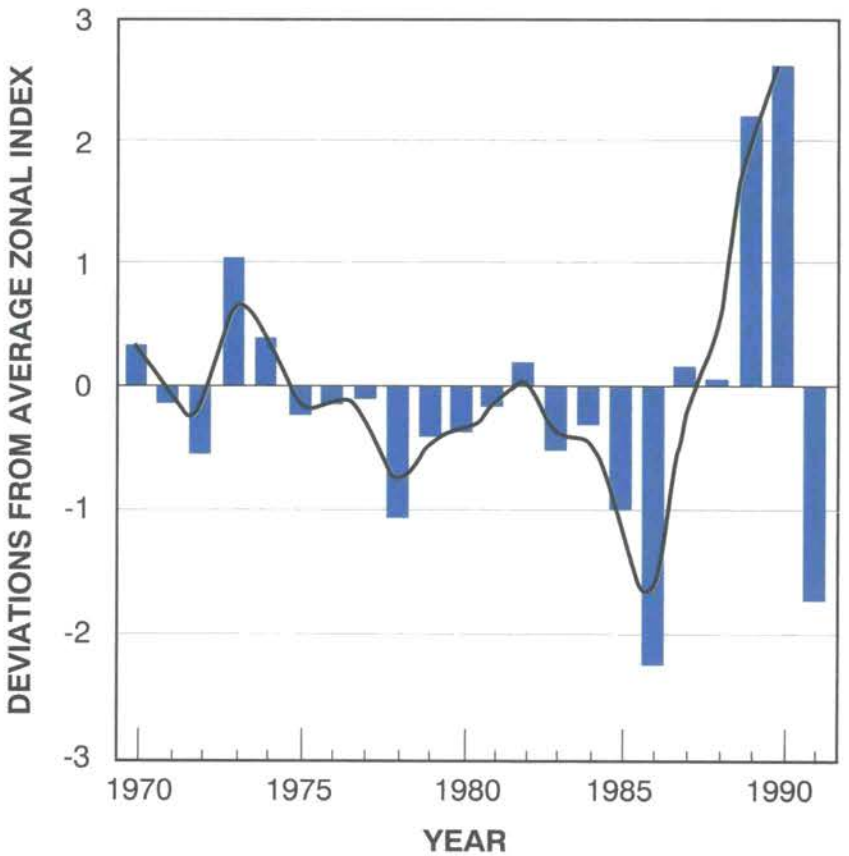

Figure 2.10 - Northern Hemisphere blocking indices: total seasonal duration in days (TD) and total seasonal intensity in decametres (TI) at 60°N latitude as a function of longitude. Blocking is defined as a positive 500-hPa geopotential height deviation from the latitudinal mean value for seven or more days. TD values are shown by a downward dashed line; TI, by an upward solid line across every 10° of longitude. The 30-year mean (1951-80) is shown by a solid curve (from Institute for Global Climate and Ecology, Moscow).

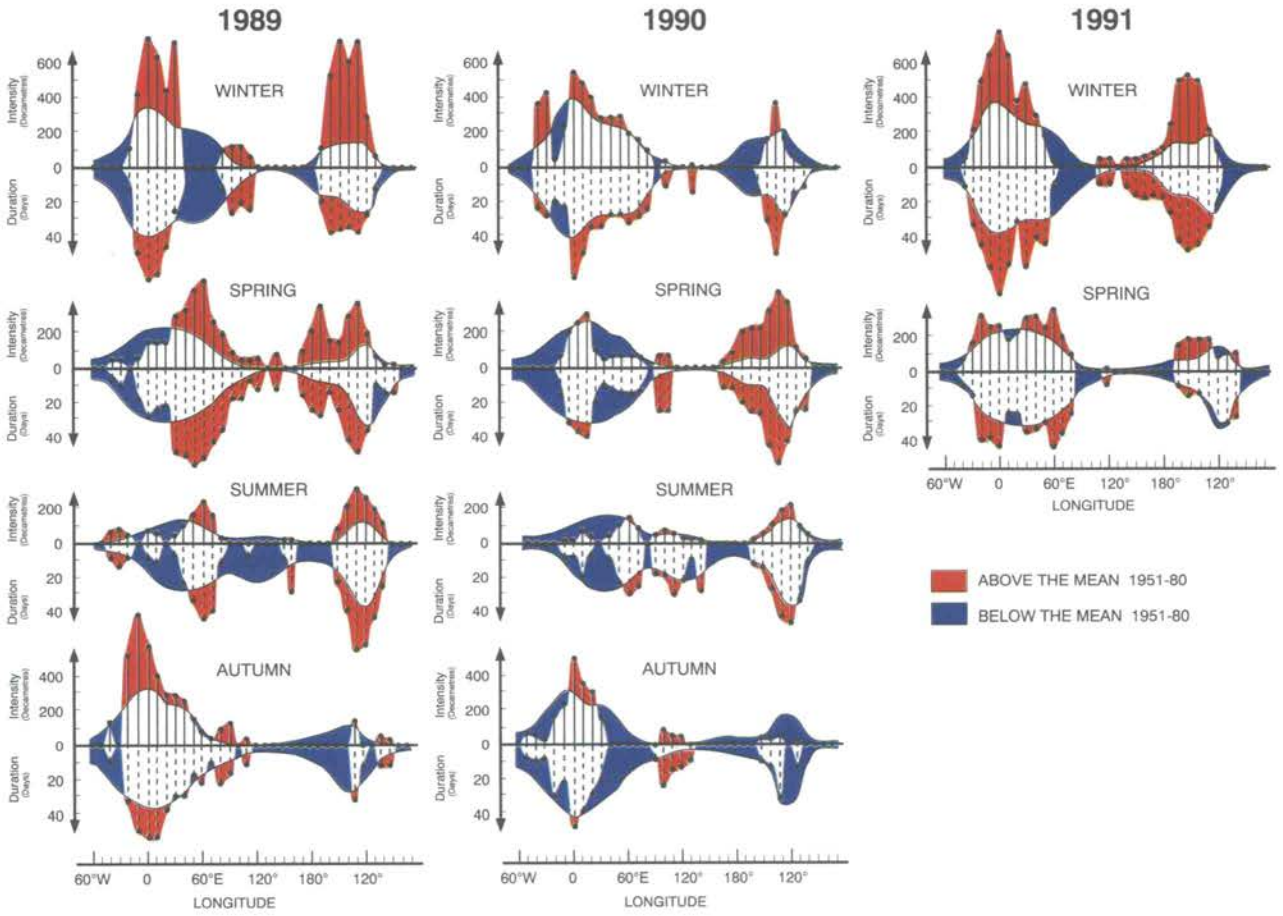

eastward and then moved westward at the end of February.

The northern spring of 1990 had less than normal blocking in the European sector and more than normal blocking in the eastern North Pacific. In spring 1991, three strong blocking areas persisted over Great Britain (up to 15 days above normal), the Urals-Western Siberia (up to 18 days above normal) and northwest of North America (up to 13 days above normal). In February-March a broad blocking ridge was located over Europe, before migrating west. Blocking developed in the last half of April over Great Britain, the Urals and North America. The Pacific Ocean-North America blocking ridge persisted during the spring with different duration breaks (1-3 weeks), while migrating from the central Pacific Ocean to North America.

Although the thermometer was invented a few centuries ago, only since the mid-to-late nineteenth century have measurements been extensive enough to allow estimates of average global and hemispheric temperatures to be made. An excellent review of various temperature datasets was produced by the Intergovernmental Panel on Climate Change (IPCC). The dataset used to construct the time series shown in this issue of *The Global Climate System* is not simply an average of all available data. Considerable care has been taken to ensure that the constituent data, both from the land and marine areas, are homogeneous.

The time series for the Northern Hemisphere, which includes 1991 (Figure 3.1), shows an increase in temperature since the middle of the last century on the order of 0.5°C. The rise is not gradual, however, being principally concentrated in two major periods — first from about 1920 to 1940. After 1940 there was a slight cooling mainly during the 1960s and early 1970s. The warmth of recent years is readily apparent in the long hemispheric time series. The second period, a more rapid, but shorter warming, began in 1976 culminating in the warmest year of the entire record in 1990. The 1980s are the warmest decade although only slightly warmer than the 1940s. The four warmest years in the Northern Hemisphere are, in descending order 1990, 1991, 1988 and 1981.

The Southern Hemisphere time series shows more of a gradual warming since about 1930. The warming was greatest, however, during the 1930s and since the mid-1970s. Unlike the Northern Hemisphere there is no evidence of a cooling between the two warming periods. Thus the 1980s are clearly the warmest decade and every year between 1983 and 1991 has been warmer than 1973, the previous warmest year.

The globally averaged increasing temperature trend, which reached record-high values in 1990 and 1991, was not a result of a worldwide uniform rise in temperature; rather it was an average of regional warm and cold temperature anomalies in which the warm anomalies predominated. The warmth of the recent decade is most striking. The 1980s are the warmest decade, 0.2°C warmer than any other. The annual value for 1990 is clearly the warmest in the global record. The average of 0.39°C for 1990 is 0.06°C warmer than the previous warmest year's (1988). All seven of the warmest years in the global record occurred since 1980 — in descending order: 1990, 1991, 1988, 1987, 1983, 1989 and 1981.

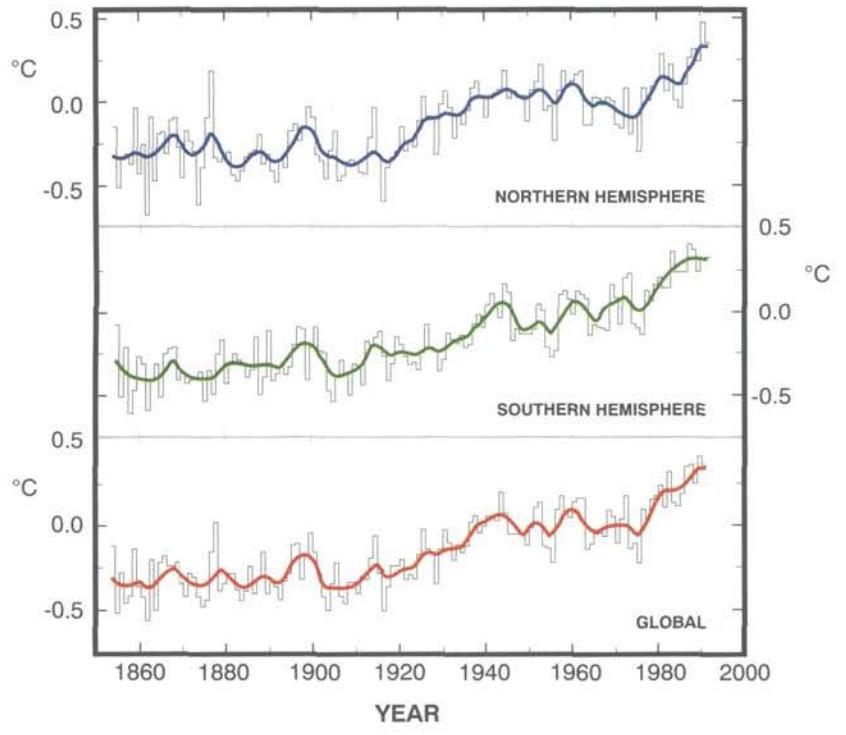

▲ *Figure 3.1* - Annual temperature anomalies for the land and marine regions of both hemispheres and their average, i.e., the global series. Data are expressed as departures from the 1950-1979 values. The smooth line in these and subsequent plots depicts variations on decadal and longer time-scales (from Climatic Research Unit of the University of East Anglia and the U.K. Meteorological Office).

3.1 HEMISPHERIC SEASONAL TEMPERATURE ANOMALIES

The warmth of 1990 is particularly interesting (Figure 3.2). Although this is the warmest year, and many areas of the northern land masses had large positive

Figure 3.2 - Seasonal temperature anomalies for both hemispheres, December 1989-February 1990 (on the left), and March, April and May 1990 (on the right). All data are plotted as departures from the 1950-1979 values. Shaded areas have insufficient data for analysis (from Climatic Research Unit of the University of East Anglia and the U.K. Meteorological Office).

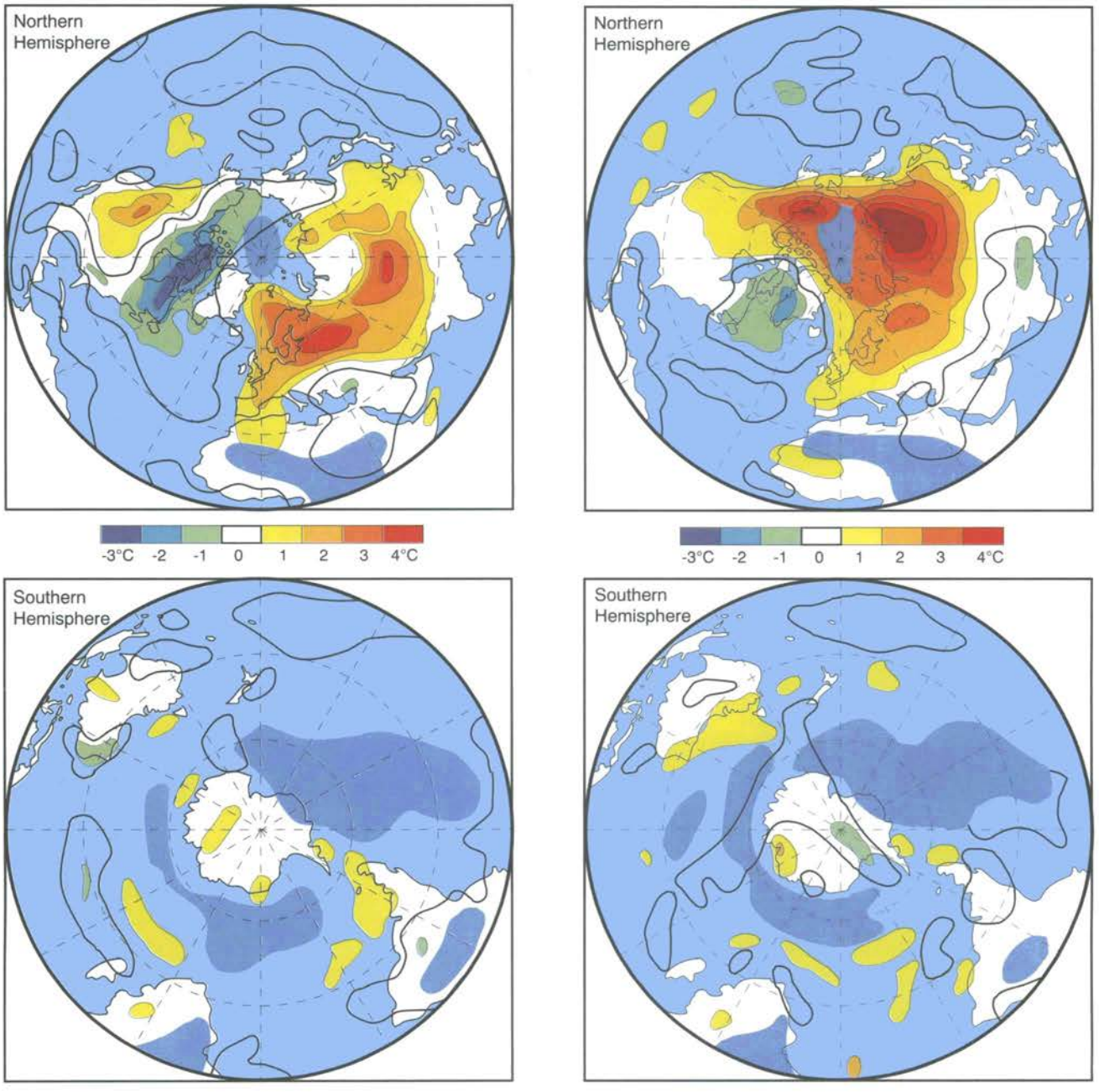

anomalies, some areas of the northern oceans, in particular the North Pacific and the northwestern Atlantic, had cooler than normal temperatures during this period. The latter are clearly apparent in the December-January-February and March-April-May series over northeastern Canada and Greenland. The warmth of 1990 throughout the two northern continents, Eurasia and North America, dominates particularly during the northern winter and spring seasons. The northern summer and fall periods (not illustrated) have smaller and more localized temperature change patterns. In this respect, 1990 continues the 1980s trend of greater anomalous warmth in the first half of the year than in the second.

Anomalies over the Southern Hemisphere generally have smaller magnitudes but are almost always positive, thus the extent of the warmth is more hemispheric.

3.2 REGIONAL ANNUAL TEMPERATURE SERIES

The dramatic rising trend of globally averaged surface temperatures during the 1980s and early 1990s is not always evident or pronounced in the long time series of annually averaged temperatures for selected

UNCERTAINTIES IN DETECTING THE GREENHOUSE EFFECT

The world has warmed by 0.5°C since the late nineteenth century. Can we relate all or part of this warming to the greenhouse effect of increasing trace gas concentrations in the atmosphere? The issue is, however, not as black and white as this question implies, nor as detailed or explained as in the IPCC report. In short, the answer to the question must be that we just don't know. Modelling results indicate the average temperature of the Earth should rise by 1.5-4.5°C if the equivalent concentration of greenhouse gases were doubled. Concentrations have risen by 40%, and as we expect the climate response to lag the greenhouse forcing because of the thermal inertia of the ocean, the warming of 0.5°C agrees with expectations. This agreement does not allow us to claim that we can relate the effect (the temperature rise) to the cause (trace gas buildup). Several factors run counter to conventional model-related wisdom. Much of the 0.5°C warming occurred before 1940 yet greenhouse concentrations have risen dramatically since the 1950s. The warming that has occurred has generally been more pronounced in middle and low latitudes, whereas models suggest an increase in polar latitudes. In short, more research and longer data series will be needed to resolve these issues.

regions or countries. Typically, large anomalies of both signs occur during the last few years; however, regional anomalies can become very strong.

Contiguous United States

Data from about 600 high quality stations in the United States Historical Climate Network (HCN) were averaged to determine a national temperature value for the contiguous United States. Annual temperatures (Fig. 3.3.1) for 1900-1990 show four general long-term regimes (as shown more clearly by the darker smooth curve): a cool regime from about 1900 to 1930; a warm period from about 1930 to 1959; another relatively cool period from about 1960 to the late 1970s; and another warm period beginning in the early 1980s, but becoming very marked during the last half of the decade.

The warmth of the last half of the 1980s is comparable overall to that of the warmest decade: the 1930s. Unusual warmth throughout most of 1990 made it the fourth warmest year out of 91, and 1989 averaged slightly cooler than normal (ranking as 52nd warmest, or 40th coolest).

India

The annual temperature anomalies for India (Figure 3.3.2) are based on data from 73 stations for 1900-1990. From 1900 to 1940 negative anomalies predominated whereas from 1941 to 1970 positive anomalies prevailed. Afterwards mixed trends were noted with a negative anomaly in 1990.

FREE ATMOSPHERE TEMPERATURE VARIATIONS

Changes in the temperature of the troposphere and stratosphere have been estimated since the late 1950s using data from the global radiosonde network. Angell (1988) estimated temperatures in the layers, 850-300 hPa (lower troposphere) and 100-30 hPa (stratosphere), and at various levels. The stratospheric temperatures show a cooling in recent years, much of which may be due to the dramatic cooling over Antarctica as a result of ozone depletion. The lower atmosphere data shows most of the features of the surface-based record. The agreement with the surface is, however, not perfect, nor should it be. The two sets of observations are different measurements of the state of the climate system. The link between the surface and the lower atmosphere breaks down when inversions form at high latitudes, during winters when the anomalous warmth at the surface appears confined to lower levels and over some tropical oceans, such as in 1981, 1983 and especially March 1990.

Recent estimates of lower tropospheric temperatures have been made with the microwave sounding units (MSU) on board NOAA polar-orbiting satellites (Spencer and Christy, 1990). Time series of monthly temperature estimates are available since 1979. Agreement between these satellite-derived data and the radiosonde data is excellent ($r \geq 0.90$ for hemispheric averages over the 12 years 1979-1990). Agreement is poorer with the surface data, and correlations are similar to those between the surface and radiosonde data ($r \geq 0.80$ for 1958-1990). The somewhat poorer agreement means that recent warm year extremes at the surface are not always extremes in the lower troposphere. For example, 1990 was the warmest at the surface, yet only the fourth warmest in the 12 years of MSU data. Many of the discrepancies relate to the decoupling of the surface and the upper atmosphere, so that only broad agreements should be expected.

Figure 3.3 - Annual mean temperature anomaly series. Unless otherwise stated the anomalies are based on the 1950-1979 reference period and the time series is from the Climatic Research Unit of the University of East Anglia and the U.K. Meteorological Office.
Figure 3.3.1 - Annual mean temperature anomaly series for the United States. Based on about 600 high quality climate stations across the contiguous United States for 1900-1990. Departure from the 1951-1980 normal (from NOAA, National Climatic Data Center, Asheville, NC).
Figure 3.3.2 - India (from V. Thapliyal, India Meteorological Department).
Figure 3.3.3 - Greenland and northeastern Canada, including adjacent sea areas.

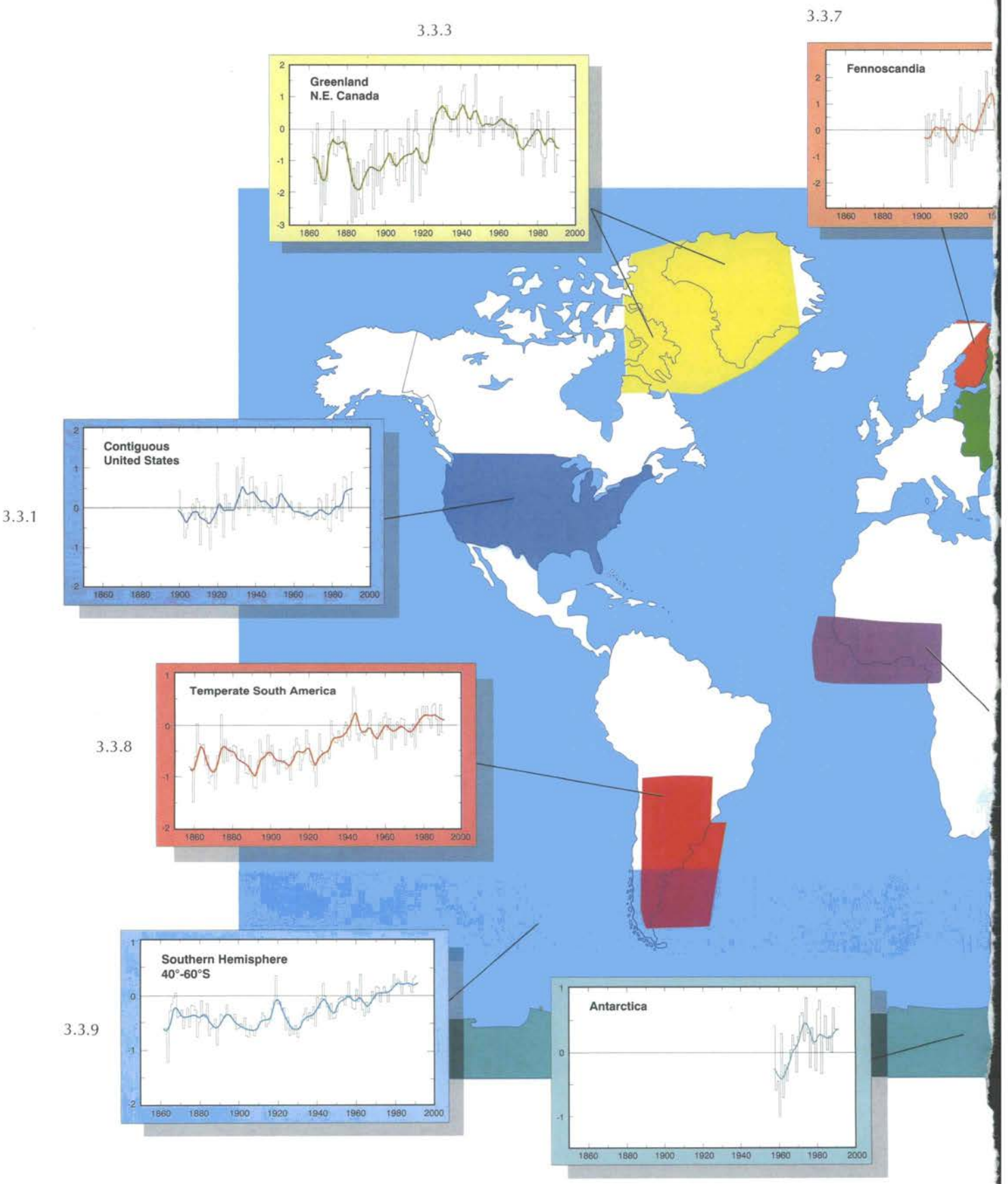

Figure 3.3.4 - Annual mean temperature anomaly series for the former territory of the USSR, 1891-1990, computed using the reference period 1951-1980; 11-year running mean (from Institute for Global Climate and Ecology, Moscow).
Figure 3.3.5 - Japan.
Figure 3.3.6 - Eastern Australia (from Bureau of Meteorology, National Climate Centre, Melbourne, Australia).
Figure 3.3.7 - Fennoscandia.
Figure 3.3.8 - Temperate regions of South America (20-50°S, 50-70°W), including adjacent sea areas.
Figure 3.3.9 - Southern Hemisphere middle latitudes (40-60°S), including land area in southern South America.
Figure 3.3.10 - Antarctica (south of 65°S). Data are expressed as anomalies from the 1951-1975 reference values.
Figure 3.3.11 - West Africa, including adjacent sea areas.

3.3.4

3.3.5

3.3.2

3.3.6

3.3.11

MARCH MILDNESS CONTRIBUTES TO A RECORD WARM YEAR

In March 1990, all of Eurasia was warmer than normal by up to 10°C in Siberia, and most of North America had anomalies exceeding 4°C (Figure 3.4). Greenland temperatures were, however, up to 4°C colder than normal and northern and southern ocean area temperatures were near to or slightly above 1950-1979 reference period values. The whole Northern Hemisphere was nearly 1.2°C above the reference period average, so that March was relatively warmer than any other month by at least 0.4°C.

Possible reasons for the warmth were the dramatic reduction in snow cover over North America, and particularly Eurasia, in January and February; and the enhancement of the zonal flow over Europe from January to March allowing warmer air from the Atlantic to reach Siberia. The excess warmth is very much a surface phenomenon. As in the winters of 1981 and 1983, the warmth did not penetrate through middle levels of the troposphere, and temperatures there were only marginally above normal.

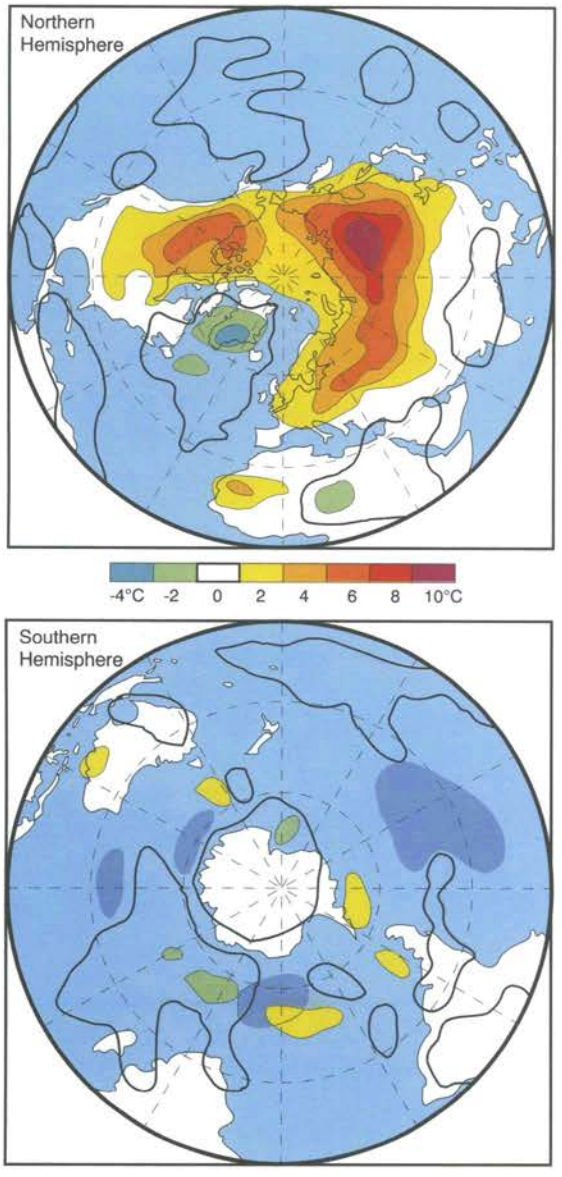

Figure 3.4 - Average temperature anomalies during March, 1990 compared with prevailing temperatures during the 1950-1979 reference period. Shaded areas in the Southern Hemisphere have inadequate coverage (from Climatic Research Unit of the University of East Anglia and the U.K. Meteorological Office).

Greenland and Eastern Canada

Colder than normal temperatures over northeastern Canada and Greenland during the 1980s contrasts with the higher than normal values around the Earth generally (Figure 3.3.3). This region has been cooling since 1940. Anomalies indicate that most of Canada west and south of Hudson Bay was nearly 1°C warmer than the long-term average during the 1980s, whereas the northeast, including most of Baffin Island, the Ungava region of Quebec, Newfoundland and Labrador, was correspondingly cooler.

The 1980s began with relatively mild conditions becoming cooler than normal by 1982. Warm temperatures appeared in 1985, lasting until the end of 1987, when an intense cold regime returned, along with increased ice cover. Generally, cold months are associated with negative 100-50 kPa height anomalies over Baffin Bay, when cold air from the northwest is drawn southward. This in effect dislodges ice from the polar pack south and east into the Labrador Current through Davis Strait and into the Labrador Sea.

Territory of the Former Soviet Union

This territory gradually warmed with considerable year-to-year variability after 1895 (Figure 3.3.4). Although 1987 is the fourth coldest year on record, 1990 and 1991 are the first and second warmest. Much of the record warmth in 1990 resulted from a spectacular February and March warming when positive temperature anomalies ranged from 5°C over Europe to above 10°C over central Siberia.

Japan, Australia, Fennoscandia, South America, Southern Hemisphere Mid-latitudes, Antarctica and West Africa

Regional temperature series are presented for seven regions: Japan, eastern Australia, Fennoscandia, temperate South America, mid-latitudes in the Southern Hemisphere, Antarctica and West Africa. Their definitions are given in Table 3.1. The time series for Fennoscandia, temperate South America and mid-latitudes of the Southern Hemisphere include marine and land-based observations.

All regions show a gradual warming during the twentieth century, but masked by considerable year-to-year variability particularly over Fennoscandia, Japan, eastern Australia and Antarctica. The warming is clearer, and more significant, over temperate South America and mid-latitudes of the Southern Hemisphere where the year-to-year variability is smaller. In most

Table 3.1 - Regional Definitions for Temperature Series		
Figure	**Region**	**Definition**
3.3.1	Contiguous U.S.A.	48 states
3.3.2	India	within national boundaries
3.3.3	Greenland/N.E. Canada	60-80°N, 30-80°W
3.3.4	Territory of the former USSR	within former boundaries
3.3.5	Japan	23 sites
3.3.6	Eastern Australia	Queensland, Victoria and New South Wales
3.3.7	Fennoscandia	60-70°N, 20-30°E
3.3.8	Temperate South America	20-50°S, 50-70°W
3.3.9	Southern Hemisphere middle latitudes	40-60°S, all longitudes
3.3.10	Antarctica	South of 65°S
3.3.11	West Africa	5-15°N, 15°W-15°E

regions the 1980s was the warmest decade. In eastern Australia the warmest year was 1988.

3.3

WINTER WARMING IN NORTH CHINA

Significant warming enveloped most of China during three recent winters (1988-1990), with an average monthly temperature anomaly of greater than +2°C (relative to 35 past winters: 1951-1985). The number of abnormally warm winter months was also high. The warmth was most pronounced in north China (north of 35°N), with a maximum temperature of +5°C over northern Heilongjiang and Inner Mongolia. However, some places in south China (south of 35°N) had a weak negative temperature anomaly (Figure 3.5).

Most winter warming years in north China appeared only within a year after El Niño. This relationship, however, broke down after the 1988 winter, since the significant winter warming years occurred during the negative phase of the Southern Oscillation (even during the cold episode years of 1988-1989).

The winter warming has generally meant a later first frost in autumn and an earlier last frost in spring. The cumulative temperatures above 0°C caused an increase of 100-300 degree-days, and chilly or frosty days were reduced markedly. The depth of frozen soil also tended to diminish.

Such winter warmings have complex effects for all components of the economy and for society, favouring an overall reduction in energy costs, and helping the winter crop growth. The date for cessation of winter wheat growth in north China was postponed by 15 days, and the date for sprouting after winter was advanced by about ten days. Wheat seedling growth during winter was good, with

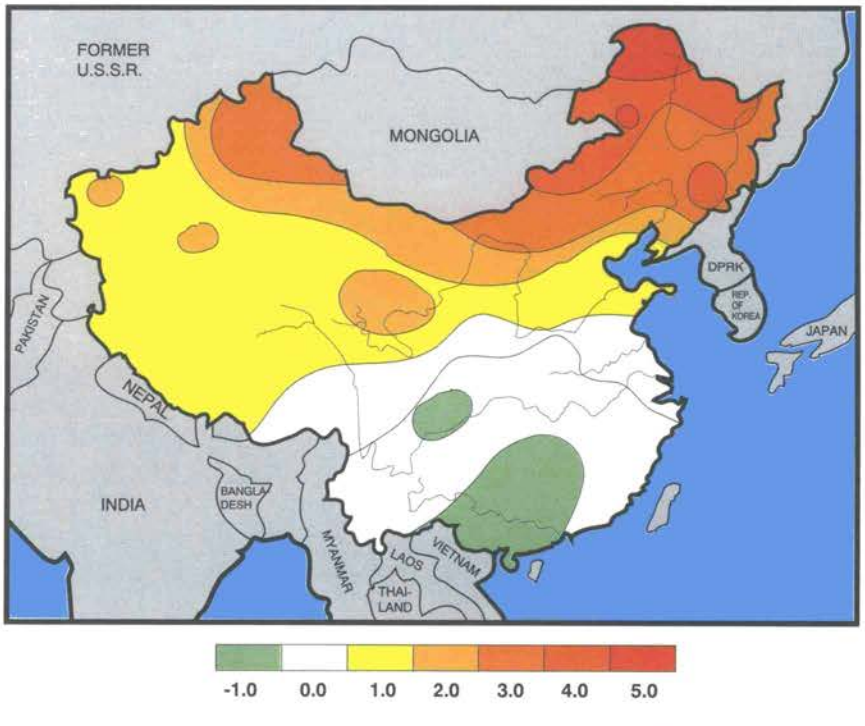

Figure 3.5 - Distribution of average seasonal temperature anomalies (°C) in China for three recent winters (1988-1990); the normal period is based on the average of 35 winters, 1951-1985 (from Jiangsu Meteorological Institute, Nanjing, China).

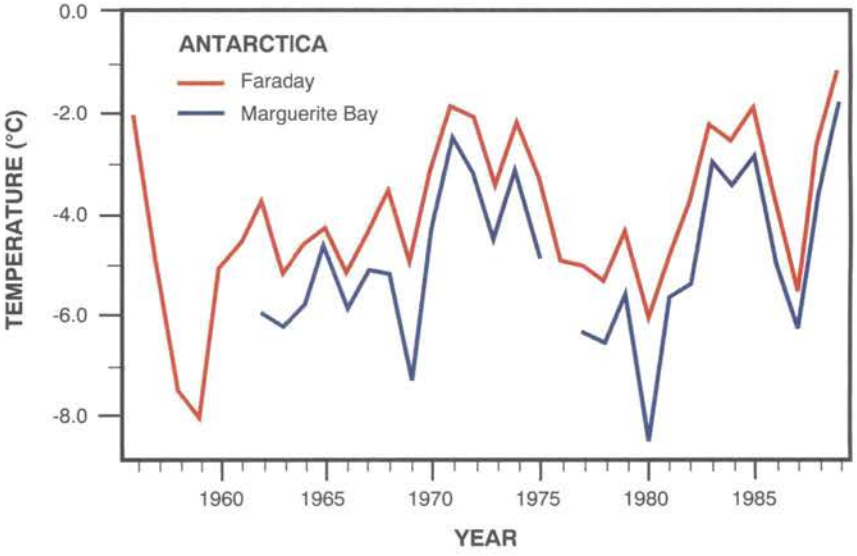

Figure 3.6 - Mean annual temperatures (°C) at Faraday and Marguerite Bay, Antarctica (see Morrison, 1990). ►

reductions in freeze damage and dead seedlings, both favouring greater production. However, warm and dry winters also tend to raise the probability of fire in cities and forests, and encourage the growth of micro-organisms that may lead to disease.

1989 - POSSIBLY THE WARMEST YEAR ON RECORD IN THE ANTARCTIC PENINSULA

Surface meteorological observations have been made at Faraday station in the Argentine Islands (65.25°S, 64.27°W) continuously since 1947 and at Marguerite Bay on Adelaide Island (67.57°S, 68.13°W) since 1962. The annual temperature plots in Figure 3.6, show that 1989 was the warmest year ever recorded at these stations. The mean annual temperature recorded at Faraday was -1.2°C compared with a mean of -4.1°C for the years 1956-1989, and that recorded at Marguerite Bay was -1.8°C compared with a mean of -4.9°C for the years 1962-1989.

The high annual 1989 mean temperature results from the lack of any cold periods, particularly during the winter months.

Despite cold winters in 1980 and 1987, which affected the Weddell Sea to the east and the South Orkney Islands to the north, as well as the Antarctic Peninsula, the warm years of 1988 and 1989 make the late 1980s a warm period comparable to that of the early 1970s or the mid-1980s.

The high spatial variability of precipitation makes it difficult to construct meaningful averages for large areas. A dense observing network is needed to obtain an adequate sample of precipitation measurements in order to minimize the effects of extreme variability. Precipitation averages for global, hemispheric, or even regional or national areas, could be dominated by very high or very low precipitation amounts from a small cluster of stations.

For many years, studies of large-scale changes in precipitation have been hindered by the lack of a database that is geographically and temporally extensive. For example, precipitation was being measured globally at more than 20,000 stations in 1900, and at more than 40,000 meteorological stations and 140,000 precipitation-only stations in 1990. However, only about 5% of the data are in digital form and thus available for climatological research. The oceanic areas are very poorly represented.

Precipitation measurements also suffer from instrumentation inhomogeneities and biases. Seldom are the data corrected to account for such gauge-induced biases as systematic errors caused by wind, wetting on the interior walls of the gauge and evaporation from the gauge.

4.1 PRECIPITATION PATTERNS FOR 1989 AND 1990

Annual precipitation for the review period showed a typically large spatial variability. Notable patterns include the persistently below normal conditions during 1989 and 1990 in north-central Canada, western United States, western Africa, north-central Australia, the Pacific coast of South America, most of northern and southern Africa — including major areas of the Sudan-Sahel belt — and portions of the Mediterranean and Caribbean. Annual precipitation was above normal during both years in north-central South America, eastern North America, eastern Europe, as well as southern, central and eastern monsoon Asia. A notable change from wet to dry (or dry to wet) from 1989 to 1990 occurred in the Nordeste region of Brazil, and the Iberian peninsula/northwestern coastal Africa area.

4.2 GLOBAL AND REGIONAL PRECIPITATION TRENDS

Only in the last few years have sufficiently large datasets been assembled that allow a reasonable description of global precipitation trends. One such land precipitation dataset is shown in Figure 4.1 for 1882 to 1990. Data are taken from as many as 5000 stations for the period up to 1989; and for about 1000 stations for the year 1990. Precipitation departures are based on the reference normal period 1951-1970. Globally, 1989 averaged slightly wetter than normal and 1990 slightly drier than normal. It is noteworthy that precipitation values tend to be above or below the mean for extended periods of time. In general, land-area precipitation averaged below normal from about 1900 to 1950 and above normal from 1950 to 1980.

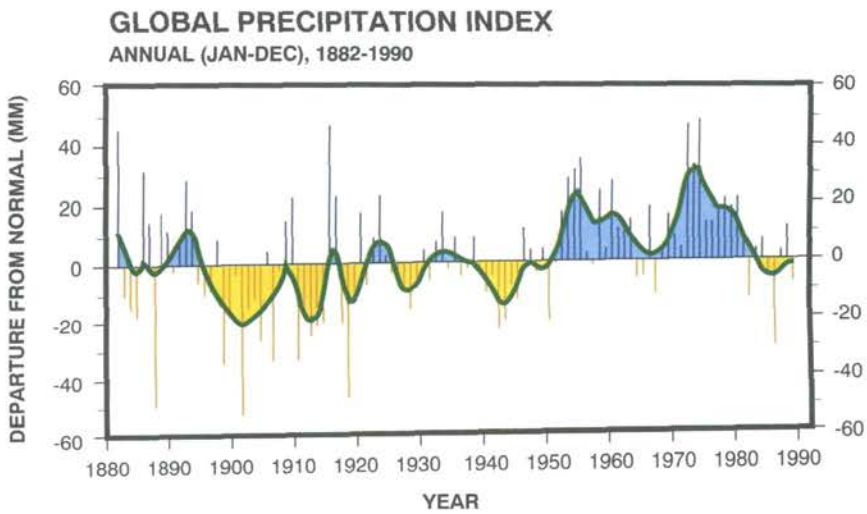

*Figure 4.1** - Annual (January-December) global precipitation index for 1882-1990. Precipitation departures are based on the reference period 1951-1970 (from NOAA, Environmental Research Laboratories, Climate Research Division, Boulder, CO).

*Figure 4.2** - Annual (January-December) national precipitation trend for the contiguous United States for 1895-1990 (from NOAA, National Climatic Data Center, Asheville, NC).
▼

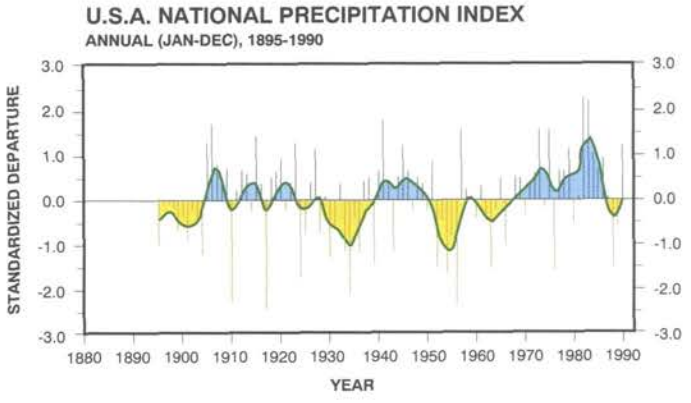

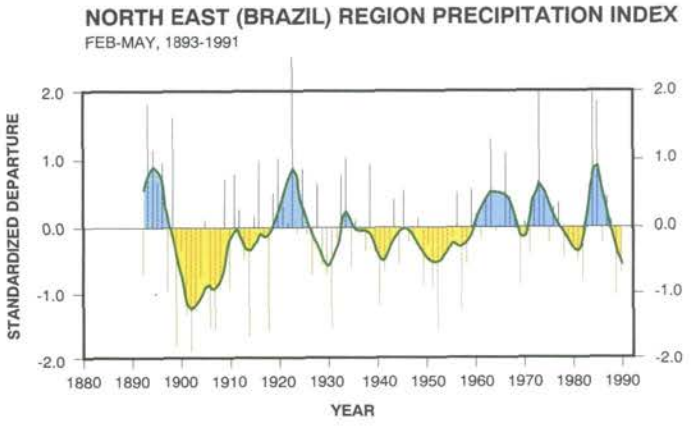

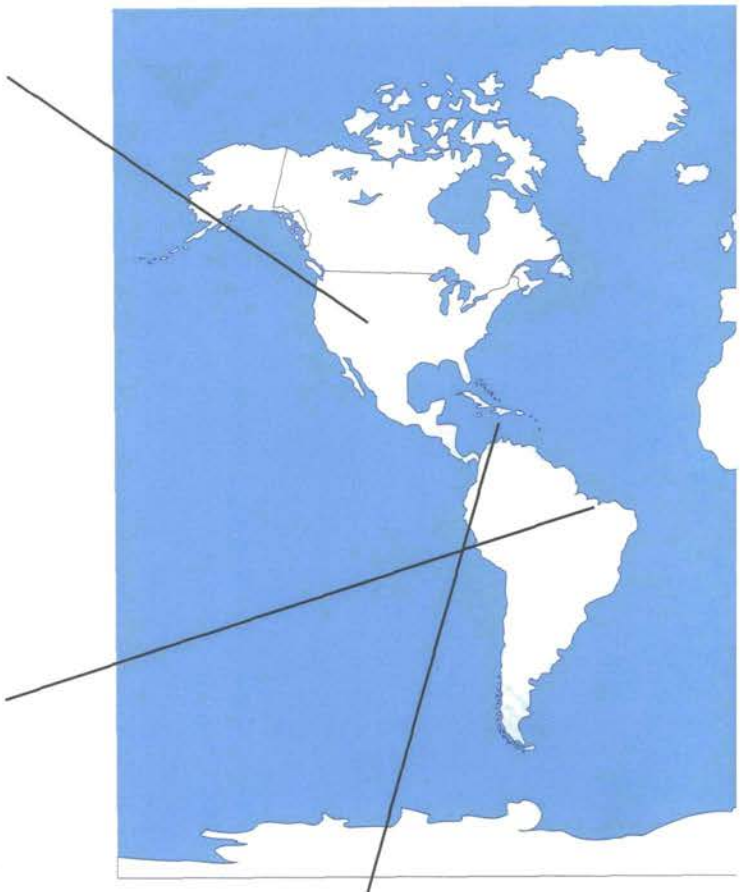

▲
*Figure 4.5** - Standardized regional February-May precipitation values for the Nordeste region of Brazil, 1893-1991. The region is defined as the zone bounded by 0°-12°S latitudes and 30-44°W longitudes (from Climatic Research Unit of the University of East Anglia, Norwich, United Kingdom).

*Figure 4.6** - Caribbean precipitation index for the wet season, May-October (which includes the hurricane season), 1901-1990. Data for eight Caribbean stations (from southern Florida to Trinidad) were used in the analysis (from NOAA, National Climatic Data Center, Asheville, NC). ►

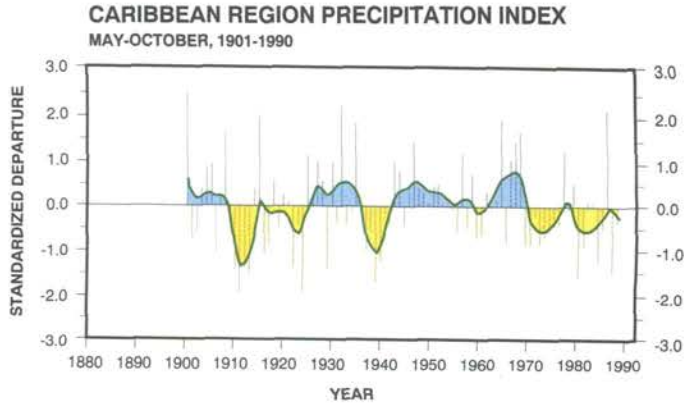

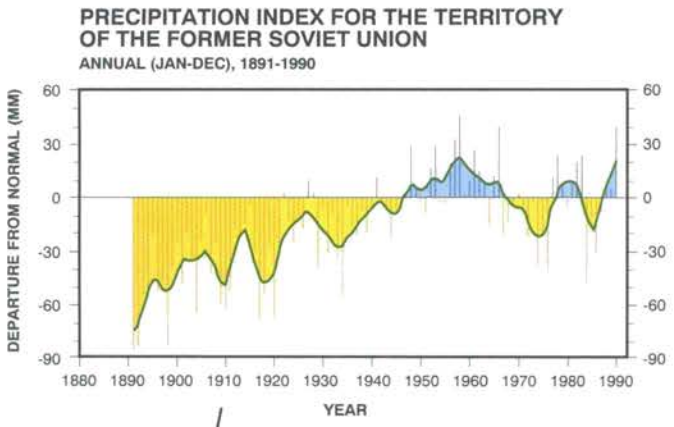

◄

Figure 4.3 - National annual precipitation anomalies for the territory of the former Soviet Union, calculated from the 1921-1960 period average (from the State Hydrological Institute, Leningrad).

Figure 4.7 - National annual rainfall anomalies over India, 1880-1990 (from India Meteorological Department, New Delhi, India).

▼

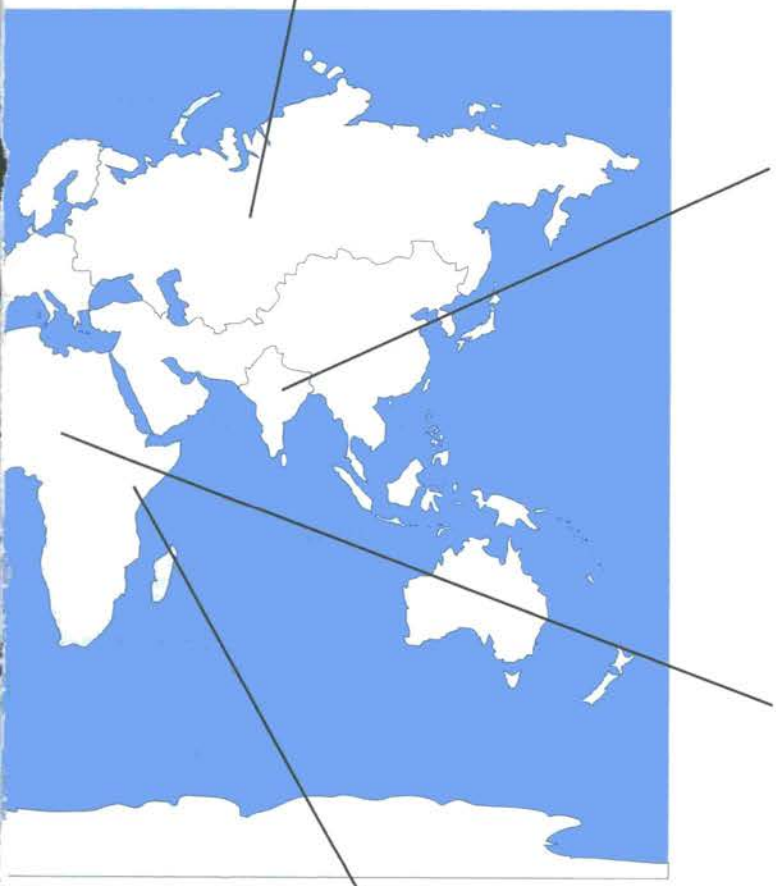

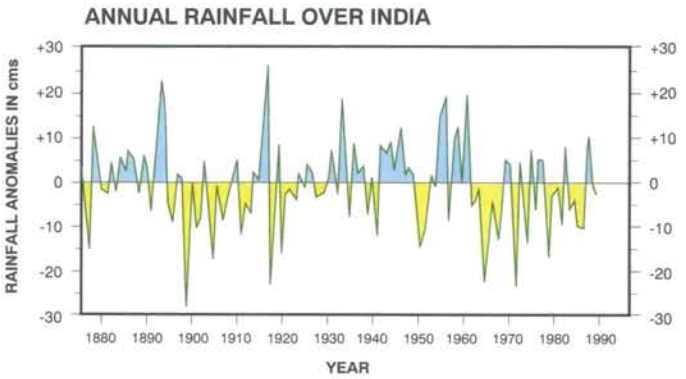

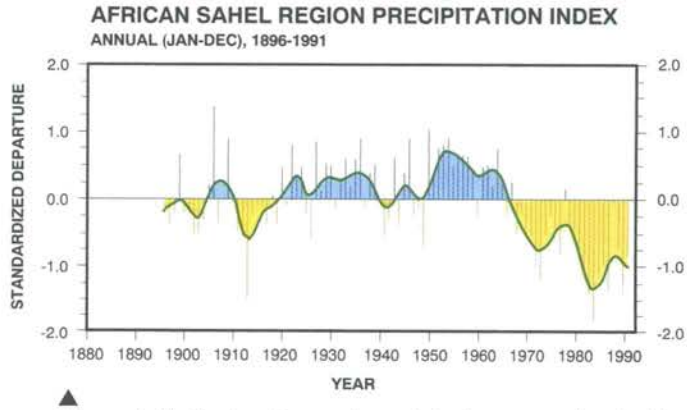

▲

*Figure 4.4** - Regional annual precipitation anomalies for the African Sahel for 1896-1991. Each yearly value is the average of the available station values standardized using the mean (1951–1980) rainfall (from Climatic Research Unit of the University of East Anglia, Norwich, United Kingdom).

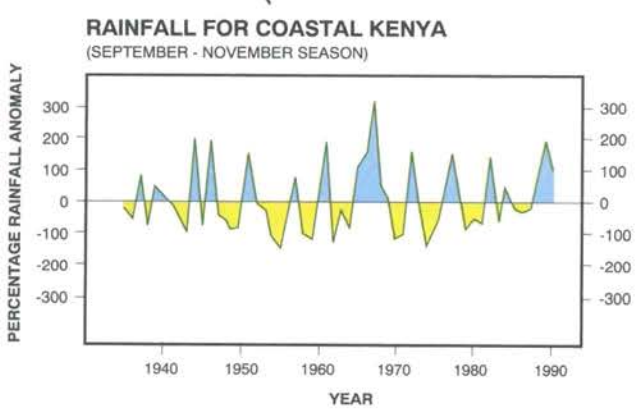

Figure 4.8 - Regional rainfall anomalies for the September-November rainy season for coastal Kenya, 1935-1990 (from University of Nairobi, Department of Meteorology, Nairobi, Kenya).

◄

* The vertical bar depicts the difference between the annual and normal precipitation totals divided by the standard deviation; the smooth curve is a nine-point binomial filter designed to highlight decadal-scale variations.

INCREASE OF WINTER PRECIPITATION IN EASTERN CHINA

With the northwestern cold airstream from Siberia weakening during recent years, winter precipitation in eastern China has tended to increase owing to the strengthening of warm moist air from the southwest. For example, the average January precipitation anomaly (relative to the average for 1951-1985) for 1989-1991 shows a significant increase in eastern China east of 105°E longitude (Figure 4.9). This is especially so in the Yellow River valley where positive anomalies were as much as 100-300%, reaching a record maximum in the last forty years. Soil moisture was ample for winter crops in northern China.

Abundant storm rainfalls added to the winter precipitation, especially in south-central Hubei as early as mid-February 1990, a rare occurrence in the preceding forty years. Also, during the first ten days of March 1991 widespread storm rains fell in the Huaihe-Yangtze Valley; and at the end of November 1990, storm rainfall occurred in the southern Yangtze Valley.

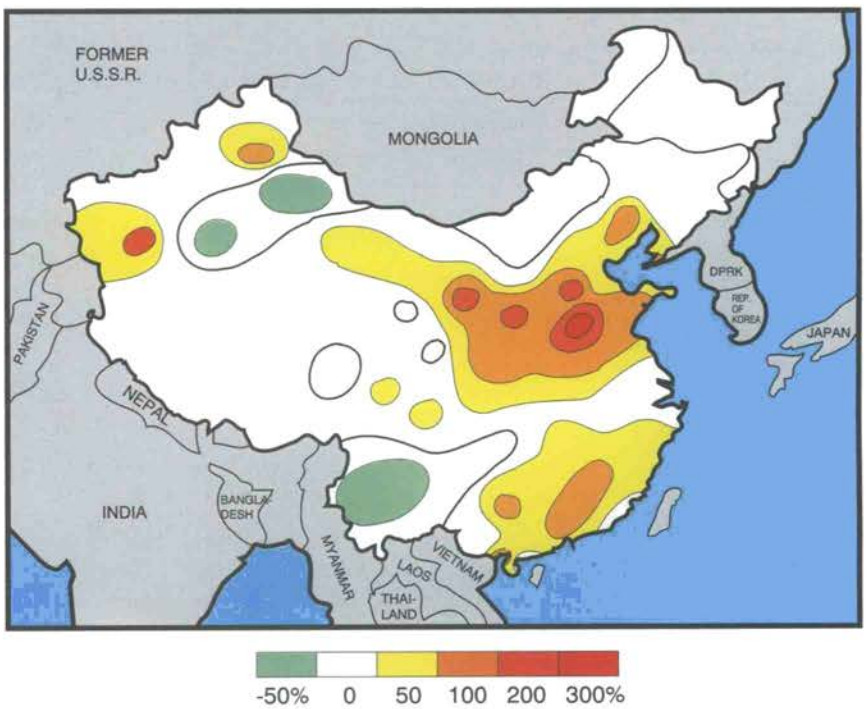

▲ *Figure 4.9* - Percentage departure (relative to the 1951-1985 normal) of the total monthly January precipitation in China for 1989-1991 (from Jiangsu Meteorological Institute, Nanjing, China).

The 1970s, an unusually wet decade, was followed by a return to drier conditions during the mid-1980s. The overall increasing trend in annual precipitation is reflected in the seasonal data (not shown) for the equinoctial seasons (March-May and September-November); and for the northern winter season (December-February) of the last 40 years; however, the June-August period exhibits little overall trend.

Diaz et al. (1989) suggested that most of the observed rainfall trends in global precipitation could be explained by an observed increase in tropical sea surface temperature and the resulting higher evaporation. Precipitation in tropical land areas is strongly controlled by the phases of ENSO, being generally lower during warm events and higher during the cold ones. Years clearly fitting this pattern are the dry years during the 1982-1983 and 1940 warm ENSO events, and the wet years during the 1974-1975 and 1954-1956 cold ENSO events.

Annual precipitation indices for the United States and the territory of the former Soviet Union are shown in Figures 4.2 and 4.3, respectively. Both countries had wetter than normal conditions in 1990. In 1989, the United States was drier than normal whereas the then Soviet Union was near normal. Time series for both countries show several pronounced wet and dry periods. For the United States, the 1930s and 1950s stand out as very dry, whereas the 1940s, 1970s, and 1980s were predominantly wet. The territory of the former Soviet Union experienced a pronounced increase in precipitation from the 1890s to about 1960. The late 1940s to mid-1960s was the wettest period, followed by two periods of pronounced dryness nationwide, the mid-1970s and mid-1980s.

Rainfall variations over the African Sahel in recent years continued the trend of deficit years that began in the late 1960s (Figure 4.4). Since 1969 only two years (1978 and 1988) experi-

enced near or above normal (1951-1980) rains. Deficits during 1989 and 1991 were about the 1971-1990 average. In the eastern Sahel during 1989, substantial convective activity occurred, especially in western Ethiopia and southern Sudan, which received normal to above normal rainfall from mid-August to the end of September. In the western Sahel, heavy flooding occurred in Ghana and Nigeria during the last week of August because of extremely heavy rains. In contrast, 1990 was an exceptionally severe drought year, being exceeded only by 1984 and 1913. During 1990, rainfall deficits occurred throughout the entire region, but were particularly severe in the Sudan.

The Nordeste region of Brazil, in contrast to the African Sahel, shows oscillatory patterns of dry and wet February-to-May periods over the last 30 years (Figure 4.5). Recent droughts have not had the durations nor the intensities of those in the 1900s, the late 1920s-early 1930s, the early 1940s, and the 1950s. The last few years, however, have had a shift to drier conditions. Compared with the exceptionally wet years of 1985 and 1986, the last two years, 1990 and 1991, have been relatively dry.

Hurricane season precipitation in the Caribbean averaged below normal during 1989 and 1990 (Figure 4.6). Prolonged dry periods occurred in the early 1910s, late 1930s to early 1940s, and most of the 1970s. With the exception of 1988 (which was unusually wet), the 1980s was generally near or below normal.

Prolonged wet and dry periods can be seen in the annual precipitation time series for India (Figure 4.7). Rainfall was predominately below normal from the mid-1890s to the mid-1910s and from the 1960s to 1980s, but was generally near to above normal from the 1930s to early 1960s. Both 1989 and 1990 averaged above normal.

Rainfall over coastal Kenya shows no discernible trend in September-November over the past 50 years (Figure 4.8), but as in India, averaged above normal in both 1989 and 1990.

Figure 5.1 - Areas where precipitation anomalies were estimated to be within the driest 10% of climatological occurrences, January to December, 1989 and 1990 (from NOAA, Climatic Analysis Center, Washington DC). ▼

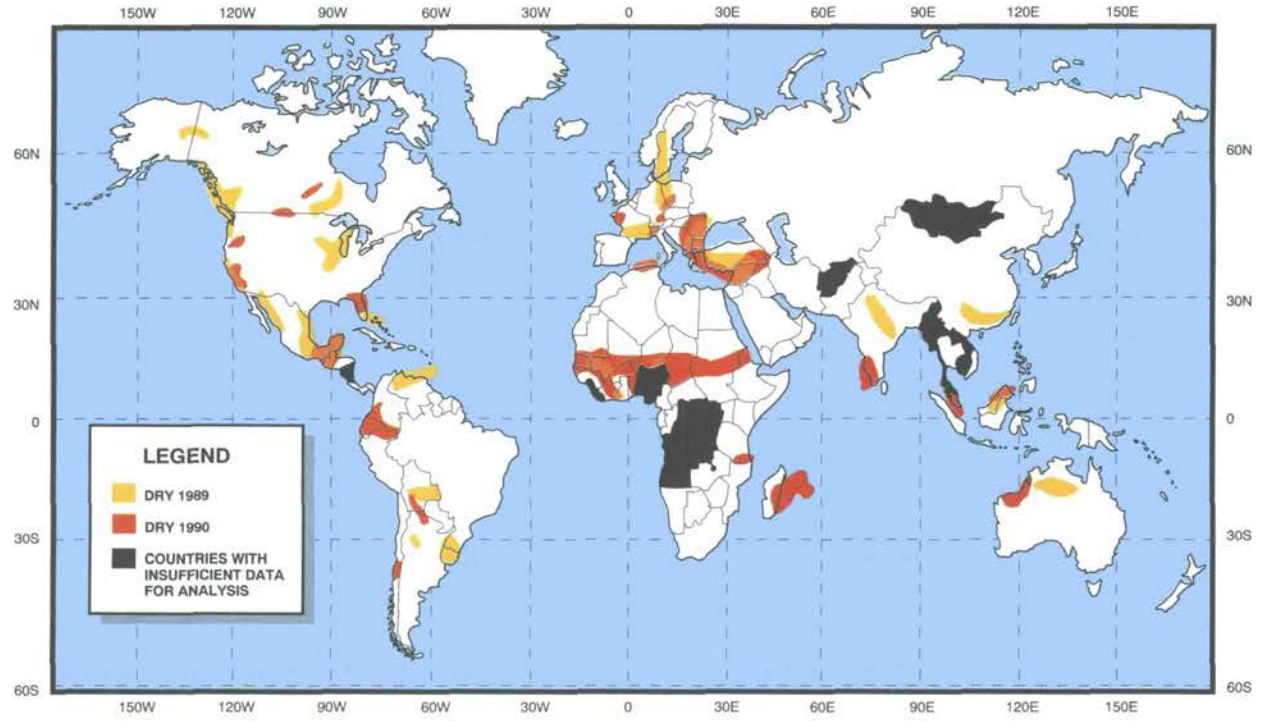

DROUGHT - LESS SEVERE AND LESS EXTENSIVE THAN IN 1988

Drought is a natural disaster of immense consequences, being disruptive of the economy, society and the environment. At any given time drought can occur somewhere in the world. Its start cannot always be readily identified and, in most cases, neither can its termination. Drought may occur over a wide range of time-scales from a season to years to decades.

Droughts are the direct cause of famine, which can kill hundreds of thousands of people and disrupt the society and livelihood of millions of the most vulnerable of the world's inhabitants. For example, the prolonged Sahel drought of the 1970s and early 1980s killed many people, displaced more and disrupted the lives of millions, and the more recent droughts in the Mediterranean and in California (USA) have been calamitous for many.

The causes of droughts are many, complex, and still not fully explained. Some possible physical, causal mechanisms include El Niño/Southern Oscillation (ENSO) events; abnormal sea surface temperature patterns; soil-moisture desiccation; and non-linear behaviour of the climate system. The disasters caused by droughts are also strongly affected by such diverse factors as agricultural practices, changes in population density, and the country's ability to provide alternative supplies of food, water and employment.

During the review period, severe regional droughts occurred in North and South America, the Mediterranean Basin, the Sahel, southern and eastern Africa, eastern Asia, and Australia (Figure 5.1). Apart from drought in the Sudan in 1990, droughts were generally not as severe or extensive, compared with those of the last review period especially during 1988.

5.1 MAJOR DROUGHTS IN THE AMERICAS

Weather in the fall of 1988 across the Canadian Prairies did little to dispel fears of the threat of a second consecutive drought year. The region was generally dry with little soil moisture recharge. However, because of a series of major snowfalls in January 1989, an above normal snowpack covered southern agricultural areas by the end of the 1988-1989 winter. Concern switched from

drought to possible spring flooding, mainly along the Red River and its tributaries. In contrast, signs of drought were evident across the northern farming zone. Blowing dust occurred during the time of the year when blowing snow is expected. Spring 1989 was dry across the Prairies and local flooding was averted. Fears of drought resurfaced but were lessened when heavy rains soaked western areas in May and more eastern areas in June. However, potential bumper crops withered to average yields in a dry midsummer heat wave.

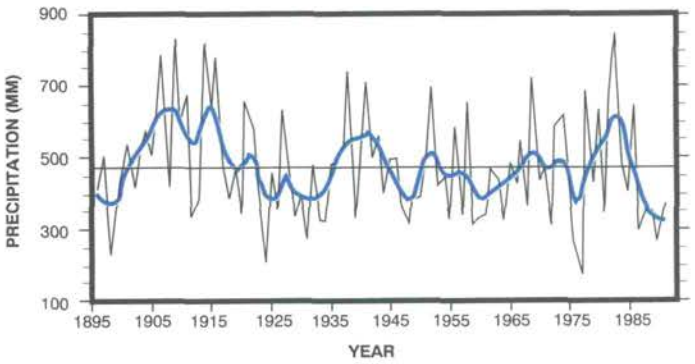

▲ *Figure 5.2* - Statewide average October-March precipitation for California (USA) from 1895-1896 to 1990-1991 (from NOAA, National Climatic Data Center, Asheville, NC).

Fall and winter (1989-1990) were dry with little soil moisture recharge. However, timely, above normal rainfalls in late spring and early summer resulted in near-record prairie grain yields in 1990. The latter part of the summer and the fall turned dry. At many sites the July-to-October precipitation ranked in the lower 10 percentile. As in the previous year, precipitation during the 1990-1991 winter was below normal and provided little soil moisture recharge into the 1991 growing season.

Although a major drought afflicted a considerable portion of the contiguous United States during the review period, no evidence supports the notion that the frequency, areal extent, or severity of droughts in this region is increasing. Karl and Heim (1990) showed that drought conditions increased in frequency and severity from 1895 to the mid-1930s (the decade of the "Dust Bowl") and decreased thereafter.

The precipitation pattern in the United States was highly variable during the review period, both spatially and temporally. Unusually heavy precipitation fell during some months in areas that had experienced precipitation shortfalls in the months before, whereas other areas that had been wet frequently found themselves in the midst of severe short-term dry spells. The United States recovered only partially from the drought of 1988. Unusually dry conditions occurred in many areas during the following winter (December 1988-February 1989), especially in the central plains states. Sections of the central Great Plains experienced record or near-record dryness during the October 1988 to April 1989 winter wheat-growing season, resulting in reduced crop yields. By April 1989, the dry conditions in the northeastern states prompted local water use restrictions. By the end of 1989, southeast Florida was experiencing the most extreme drought on record — part of a basin-wide dry spell occurring across much of the Caribbean.

Subnormal precipitation persisted throughout the review period across a region extending from the west coast to the north central states. Conditions became especially severe in California, where rainy season (October-March) precipitation was much below normal for the last five consecutive years (1986-1987 to 1990-1991). The drought was comparable in severity with the record drought from 1928 to 1934 (Figure 5.2), although the population of California then was 6 million compared with 30 million today. The cumulative effects of the California drought include the following: reservoir reserves were drawn down to extremely low levels; some fisheries populations were brought to the verge of extinction; groundwater reserves were severely depleted in many agricultural regions; hydroelectric power generation was greatly reduced; income from recreation and tourism was reduced; and residential water was widely conserved. March 1991 rains, more than 300% of normal, provided some short-term relief. However, it was not enough to end the drought, especially for those along the hard-hit central coast region from Santa Barbara to San Francisco.

Nationally, severe drought persisted across 18% or more of the contiguous United States from May 1988 to February 1991 — a total of 34 months. Although the area covered was not as large as that of many

Figure 5.3 - Percentage area of the contiguous United States experiencing severe to extreme long-term drought, as defined by the Palmer Drought Severity Index (%), from January 1895 to September 1991. The 1988-1991 drought continued at 18% or above for 34 months, and is surpassed only by the 1953-1957 drought, which persisted at this percentage for 45 months (from NOAA, National Climatic Data Center, Asheville, NC). ▼

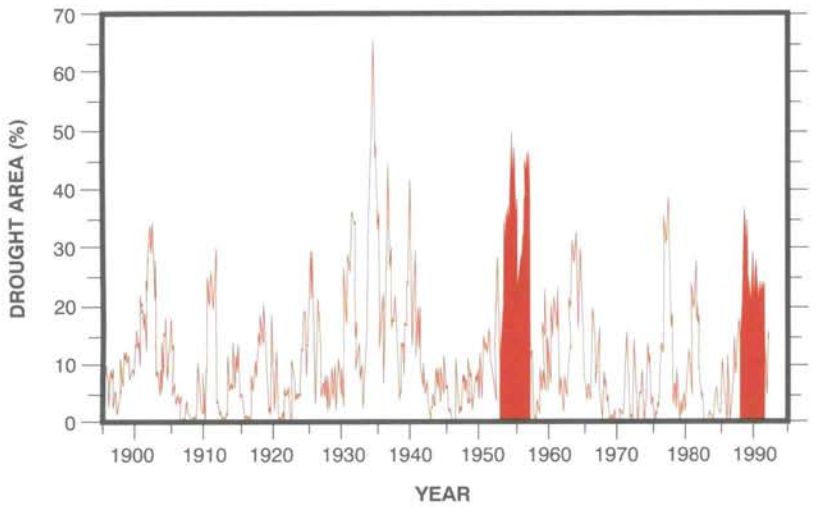

past major droughts, the persistence of a drought of this severity rivalled the major twentieth century droughts (Figure 5.3). Only one other drought (August 1953- April 1957) was as severe for a longer period — 45 consecutive months. Widespread rains over much of the afflicted area brought the areal percentage well below 10% by the end of spring (May 1991).

The Caribbean region experiences little convective activity, especially in the Lesser Antilles, from early June until the middle of September 1989. A precipitation index based on 10 stations in the Caribbean region, from Miami, Florida, to Lamentin, Martinique, reveals that 1989 had the driest summer in the twentieth century, and that the last 16 summers have been generally drier than average (Figure 5.4). Spotty rains, mainly confined to the Windward Islands, fell in the middle of August and again in early September, but did little to alleviate the drought. Heavy rains, however, that accompanied Hurricane Hugo during the middle of September, did dispel the dryness. Drier weather prevailed across the region again from March through June 1990. Scattered heavy thunderstorms provided some relief during July to September, but failed to overcome the long-term precipitation deficits. The drought was aggravated by a week of extreme heat in early September. In mid-October, moisture from the remnants of Tropical Storms Marco and Klaus combined with a stationary front, deluging some areas with over 500 mm of rain, but unfortunately, missing many others.

Unusually dry weather, which began in 1988 and continued through much of 1989, plagued both Uruguay and northern Argentina. In northern, central and eastern parts of Uruguay, the accumulated rainfall for 1988 and 1989 was less than 30% of normal. In northern and central Argentina, the dryness was exacerbated by a series of heat waves during the first three months of 1989 that sent temperatures close to 38°C. Corn production was only half of the previous year's, resulting in the worst harvest in 26 years. The dry weather reportedly killed 800,000 head of cattle.

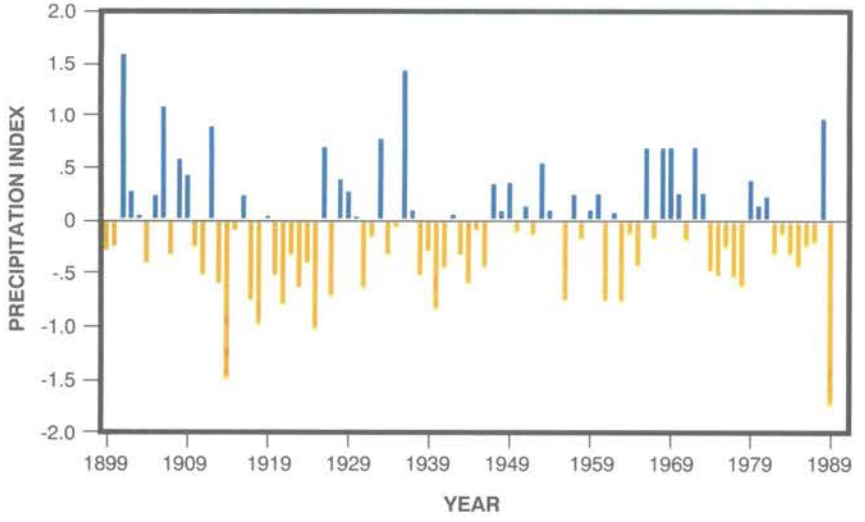

◄ *Figure 5.4* - Summer Caribbean precipitation index June-August 1899 -1989. The index is calculated by averaging precipitation data from at least half of 10 selected stations in the region and standardizing the data using the normal period 1951-1980 (from NOAA, National Climatic Data Center, Asheville, NC).

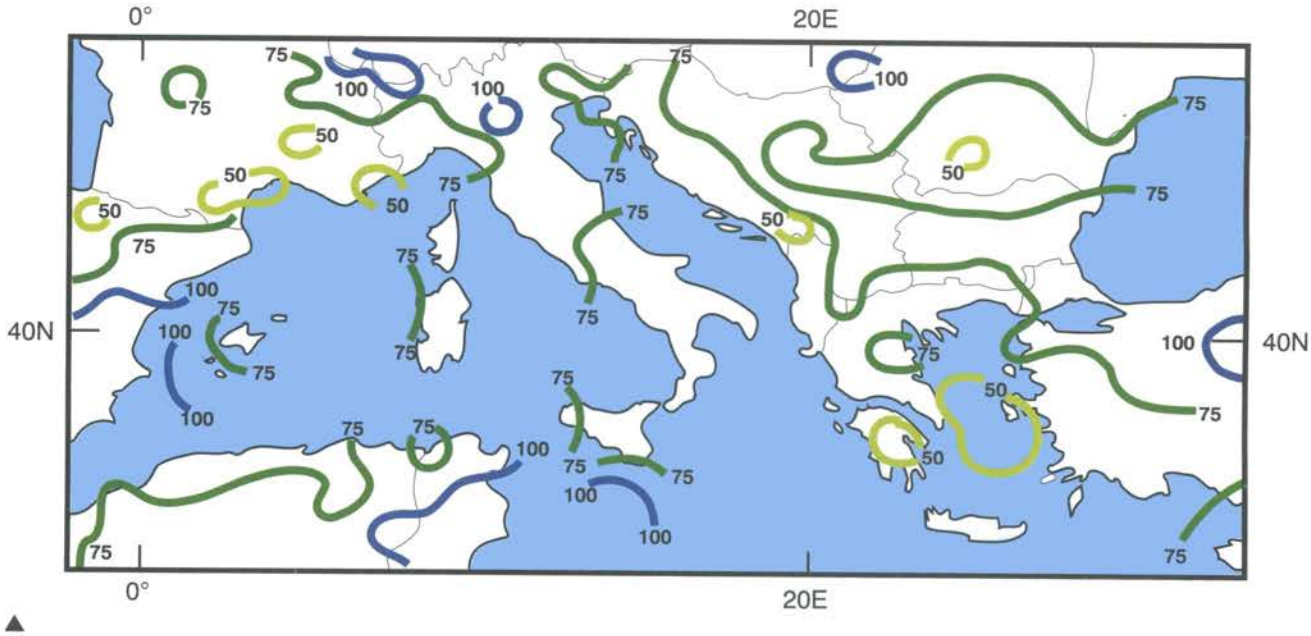

Figure 5.5 - Percentage of normal precipitation from October 1, 1988 to July 28, 1990 (666 days) for the Mediterranean Basin (from NOAA, Climate Analysis Center, Washington, DC).

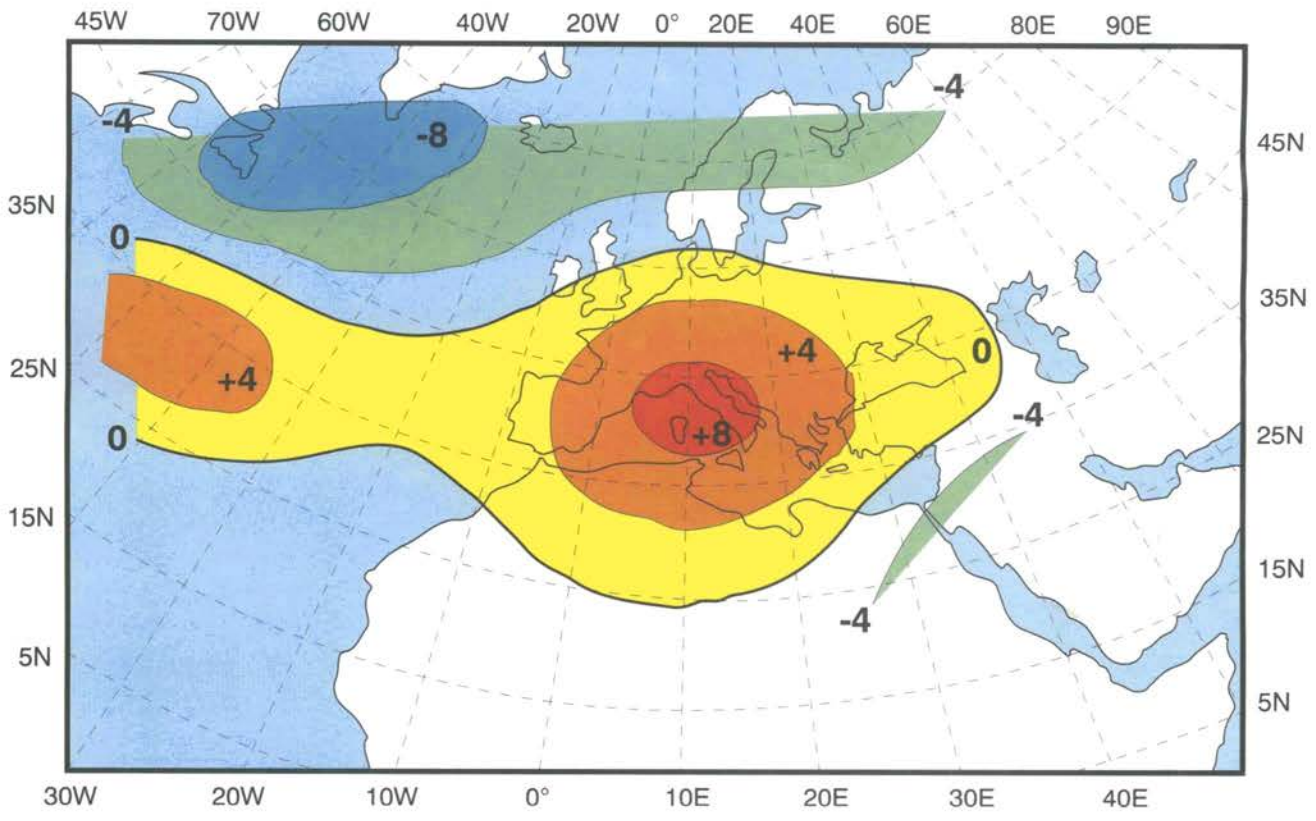

Figure 5.6 - Seasonal-averaged departure of the October 1989 to March 1990 500-hPa geopotential heights from the 1951-1980 mean values (decametres) (from Italian Meteorological Service).

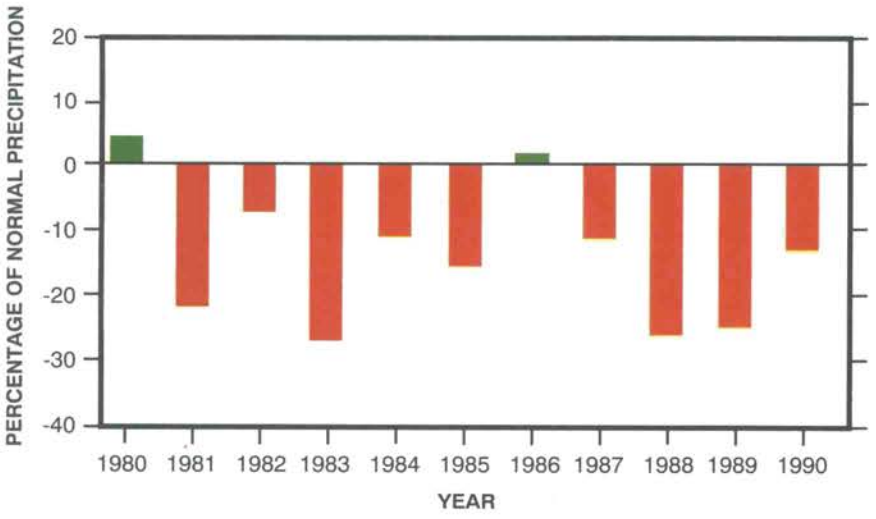

Figure 5.7 - National average annual precipitation departure (%) from the 1951-80 normal for Italy, 1980-1990 (from Italian Meteorological Service).
◄

At the end of 1989 and the beginning of 1990, several weeks of soaking rains brought relief to drought-stricken areas as the region entered another dry, tranquil weather regime from April to September.

5.2 MAJOR DROUGHTS IN EUROPE

Normally most of the Mediterranean basin receives well over half of its yearly precipitation during the cool season (November to April). During the 1988-1989 winter, serious moisture deficiencies began, when much of central and southern Europe experienced exceptionally dry weather. This lack of precipitation continued, only occasionally interrupted by brief periods of wet weather, e.g., April 1990. From October 1988 to July 1990, most of southern Europe and northwestern Africa recorded approximately 75% of normal precipitation (Figure 5.5), generating deficits exceeding 800 mm in parts of eastern Yugoslavia, southern France and Greece and southwestern Turkey, resulting in widespread hydrological drought.

The combination of long-term dryness, sometimes coupled with extreme heat, had adverse impacts on agriculture; lowered or dried up rivers, ponds and lakes; and forced water rationing in many parts of Europe. In Greece, the drought was the worst in 100 years, forcing the government to raise water prices in an effort to lower consumption. Wildfires scorched forest and brush in eastern, southern and northwestern Spain, southern France, and portions of Italy and Greece. Lack of rain left major rivers such as the Loire, Rhone and Garonne at half their normal levels. In Italy, more than half the olive harvest was destroyed. At eight stations in Turkey, 1989 had the driest January-to-April period in 39 years.

Heavy precipitation during the second half of August 1990 alleviated the dryness in Greece and western Turkey, but only the wet 1991 April helped dissipate the dry anomalies. The drought in northeastern Algeria and northern Tunisia was snapped by heavy rains in November 1990. Drought was still afflicting the eastern Mediterranean region. In Cyprus, rainfall from October to December 1990 was only 32% of normal. In Jordan, the drought was unprecedented in 70 years, prompting water rationing in Amman and other Jordanian cities. Precipitation deficiencies in Syria, Israel and Jordan ended in March 1991. Long-term dry anomalies in southern France and northwestern Italy only disappeared at the end of the 1990-1991 winter. One of the few Mediterranean areas that avoided the dryness was Spain, where torrential November and December 1989 downpours produced severe flooding.

The severe drought in the central Mediterranean during the 1988-1989 and 1989-1990 winters was fostered by the persistence of drought-favouring anticyclonic weather systems (Figure 5.6). These steered rain-producing Atlantic storm fronts far to the north into northern Scandinavia, inhibiting the development of Mediterranean storms. Much of the 1980s in Italy was marked by a deficiency of rain (Figure 5.7);

Low water levels at Fontana Lake, North Carolina, USA *Photo Grant W. Goodge*

annual precipitation averaged about 15% below normal, equivalent to a lack of one and a half years of precipitation.

5.3 MAJOR DROUGHTS IN AFRICA

After relatively abundant rainfalls in 1988 and 1989, the 1990 rainy season (June to September) in the Sahel was disappointing, with rainfall averaging only about 70% of the long-term mean (Figure 5.8). The dry conditions were aggravated by temperatures that reached 46°C at some locations in mid-June. Monthly temperatures averaged 2-4°C above normal across much of the western Sahel throughout April, May and most of June. Exceptionally dry weather (less than 60% of normal rainfall) dominated the northern, extreme western and much of the eastern Sahel. The most serious drought occurred in the Sudan. Growing-season rainfall as little as one half of normal and unrelenting August heat devastated crops, raising the spectre of famine. In some northern Sudan farming areas, the drought was as severe as in 1984, when thousands of people died. Dryness also afflicted the marginal growing areas of Sudan's eastern neighbour, Ethiopia. Eritrea's second consecutive summer with below normal rainfall caused much concern. Most areas received 75-90% of normal rainfall, while several areas, including northern Senegal, southern Mauritania, eastern Chad, west-central and east-central Sudan and northern Ethiopia, recorded less than 50%.

Droughts occurred throughout portions of Kenya and Tanzania, and along the Botswana/Namibia border from December 1989 to February 1990. Dry weather returned to northern parts of east Africa during June-August. Djibouti and large sections of Ethiopia and Sudan received below

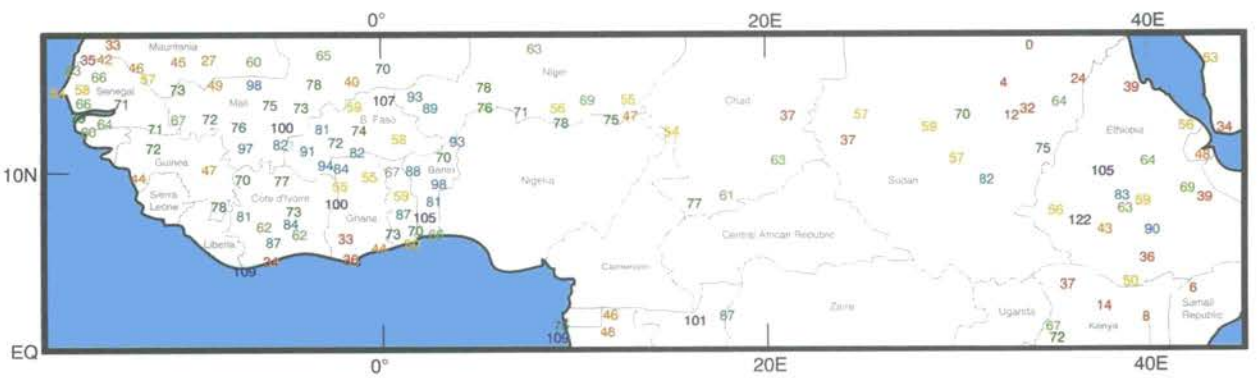

Figure 5.8 - Percentage of normal precipitation from May 1 to September 30, 1990 (153 days) for the African Sahel (from NOAA, Climate Analysis Center, Washington, DC).

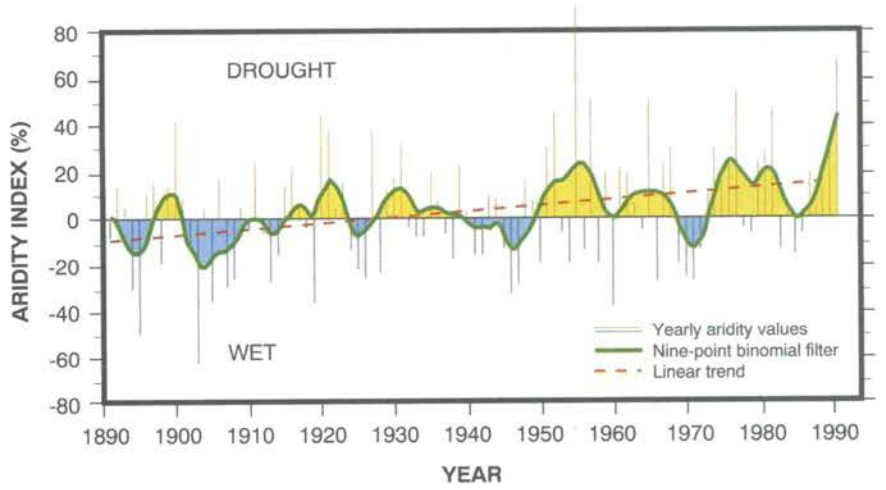

Figure 5.9 - May-June aridity index for the grain-producing areas of the Asiatic territory of the former Soviet Union from 1891 to 1991. The index was calculated by taking the difference between the percentage areas experiencing warm dry and cool wet conditions. "Warm dry" conditions are defined as precipitation less than 80% of the 1891-1975 normal, with temperature anomalies greater than 1°C. "Cool wet" conditions are defined as precipitation greater than 120% of normal, with temperature anomalies less than -1°C (from Institute for Global Climate and Ecology, Moscow).

Figure 5.10 - Percentage of normal precipitation from October 1, 1988 to May 27, 1989 (239 days) for portions of eastern Asia. Isopleths indicate 50, 75 and 100%. Yellow areas depict values less than 50% (from NOAA, Climate Analysis Center, Washington, DC). ▼

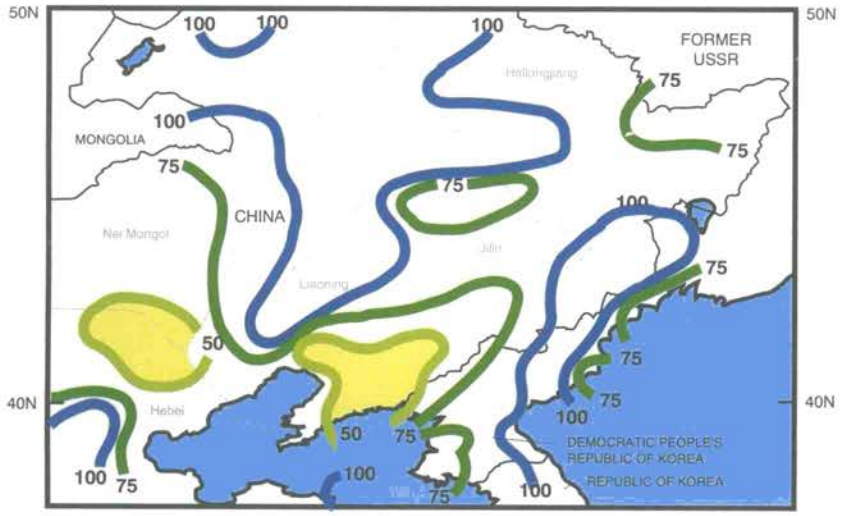

normal rainfall, as did areas around Lake Victoria. The area of below normal precipitation shifted slightly during September-November, into northeastern Kenya and adjacent parts of Ethiopia and Somalia.

The distribution of the seasonal rains during December 1990 -February 1991 was scanty at many locations. Droughts developed in the southwest (along the Angola/Zambia border and again along the Botswana/Namibia border) and east (from the Lake Nyasa area eastward to the coast). These induced severe impacts on the economy and on most of the water-use activities within the region. Although near normal seasonal rainfall amounts were received at many locations during the following season (March-May), the seasonal distribution was poor at most locations. Drought persisted along the Angola/Zambia to Botswana/Namibia border region and in northern parts of Lake Nyasa. Moisture deficits also occurred in northeast Zimbabwe and in and around northwestern Kenya. Some of the droughts were very severe. Some central and northern Tanzania areas, for example, had the driest April this century during 1991. Drought conditions continued to worsen in this region throughout 1991.

▲
Figure 5.11 - Percentage of normal precipitation from October 1, 1990 to May 31, 1991 for southeastern China (from NOAA, Climate Analysis Center, Washington, DC).

5.4 MAJOR DROUGHTS IN ASIA

Summer aridity increased markedly in the basic grain-producing areas of the Asian territory of the former Soviet Union during the last 100 years. The aridity index is the difference between the areas of warm dry and cool wet conditions. The index became steadily more arid during the review period, with 1991 experiencing the second highest index (68%) in the last 100 years (Figure 5.9).

The severe drought over India earlier in the 1980s did not recur during the review period. Of India's 35 rainfall subdivisions during 1989 and 1990 only 6 and 3, respectively, had below normal rainfall, compared with 21 during the 1987 drought.

In Manchuria, across northern China and in parts of the Democratic People's Republic of Korea, precipitation was less than 75% of normal from October 1988 to May

1989 (Figure 5.10). Much above normal temperatures (departures of +2 to +4°C) in the first half of 1989 aggravated the dryness. The Chinese provinces Liaoning and Jilin were the driest in 40 years, where water levels in reservoirs and on rice paddy-fields were 50% below normal.

Widespread drought developed across Taiwan and portions of southeastern China from October 1990 to May 1991 since only 25-75% of normal precipitation fell (Figure 5.11). A spring heat wave combined with low rainfalls to impede the planting and harvesting of rice, grain and vegetables. The drought also hurt industry by limiting water supplies, and electricity to factories.

5.5

MAJOR DROUGHTS IN AUSTRALIA

The summer rainy season for northern Australia is strongly influenced by the circulation systems of the equatorial Pacific. Outgoing long-wave radiation (OLR) anomalies over the central equatorial Pacific became negative (indicating enhanced convection) in November 1989 for the first time since early 1988. Strong equatorial westerlies were observed near and to the west of the International Date-line, and were associated with an eastward migration of warm sea surface temperatures and a minimum in upper-level velocity potential towards the Date-line. As a consequence, the 1989-1990 southern summer was characterized by below average rainfall over most of northern Australia. In fact, large regions in the north recorded their lowest-ever rainfall from December 1989 to February 1990 (Figure 5.12). Less than half the usual rain fell across most of Queensland, severely affecting agriculture. Abnormally hot January temperatures aggravated the abnormal dryness. Heavy rains finally moved into the area in early March 1990, ending the unusually dry weather regime. During the earlier season (August to October 1989), less than half the normal precipitation fell in New South Wales and southern Queensland.

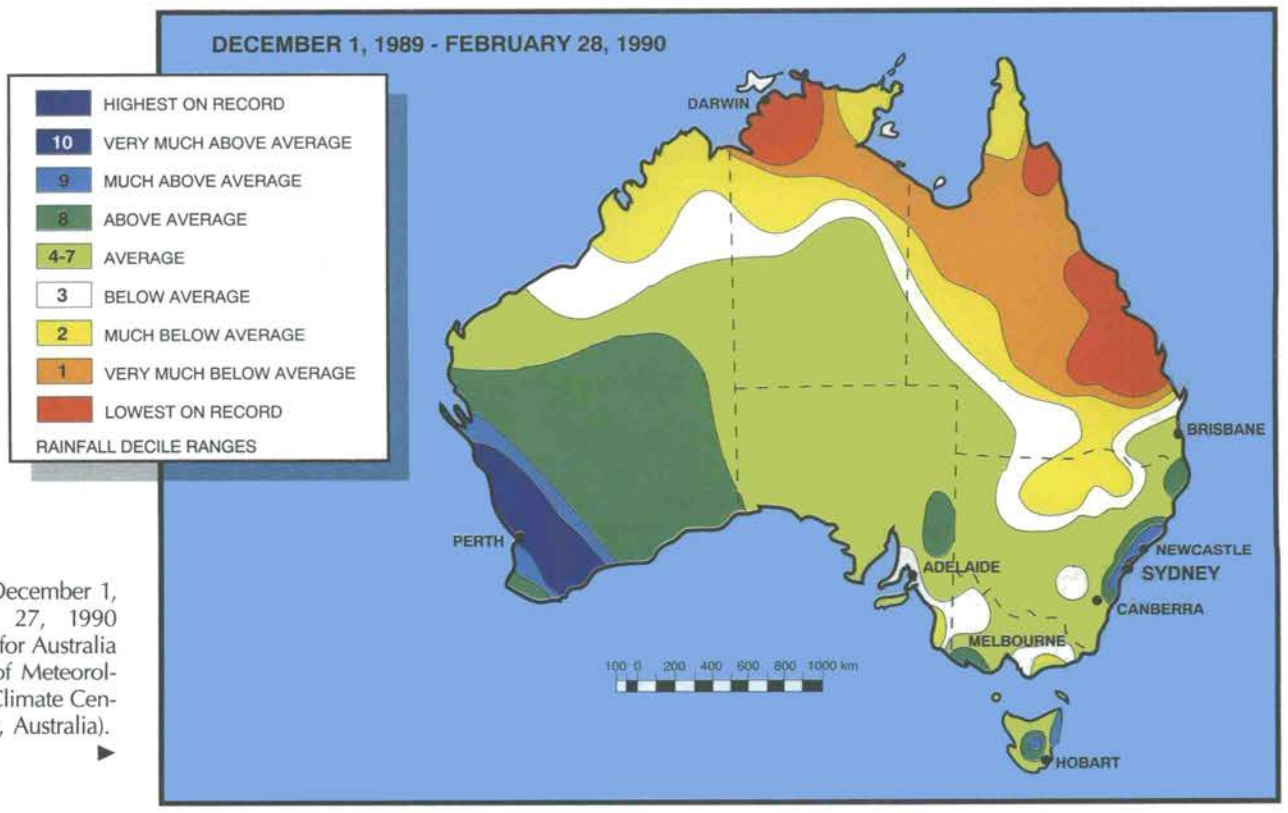

Figure 5.12 - December 1, 1989-February 27, 1990 rainfall deciles for Australia (from Bureau of Meteorology, National Climate Centre, Melbourne, Australia). ►

Photo Grant W. Goodge

Floods are one of the most widespread and destructive of natural disasters. Most floods are caused by too much water arriving in too short a time. Tropical and extra-tropical cyclones and their frontal systems may produce long periods of continuous heavy rain sufficient to cause flooding. Other causes of flooding include rapid snowmelt, ice jams, wind-driven water, high tides, and dam failures.

Storm surges accompanying tropical cyclones, hurricanes and typhoons into low-lying coastal regions have caused some of the highest natural-disaster death tolls on record, exceeded only by some river floods and drought-related famines. During 1980-1985, more than 160 major floods around the world killed and injured more than 120,000 people, and destroyed the dwellings of nearly 20 million with causing $ 22 billion (US) damage.

During the review period several major floods around the world resulted from intense thunderstorms and tropical cyclones (Figure 6.1). Flooding due to tropical cyclones is mentioned in Chapters 7 and 8.

6.1 MAJOR FLOODS IN AUSTRALIA

Torrential downpours, headlined "The Big Wet" by some Australian newspapers, created flash flooding in the normally dry Australian Outback during mid-March 1989.

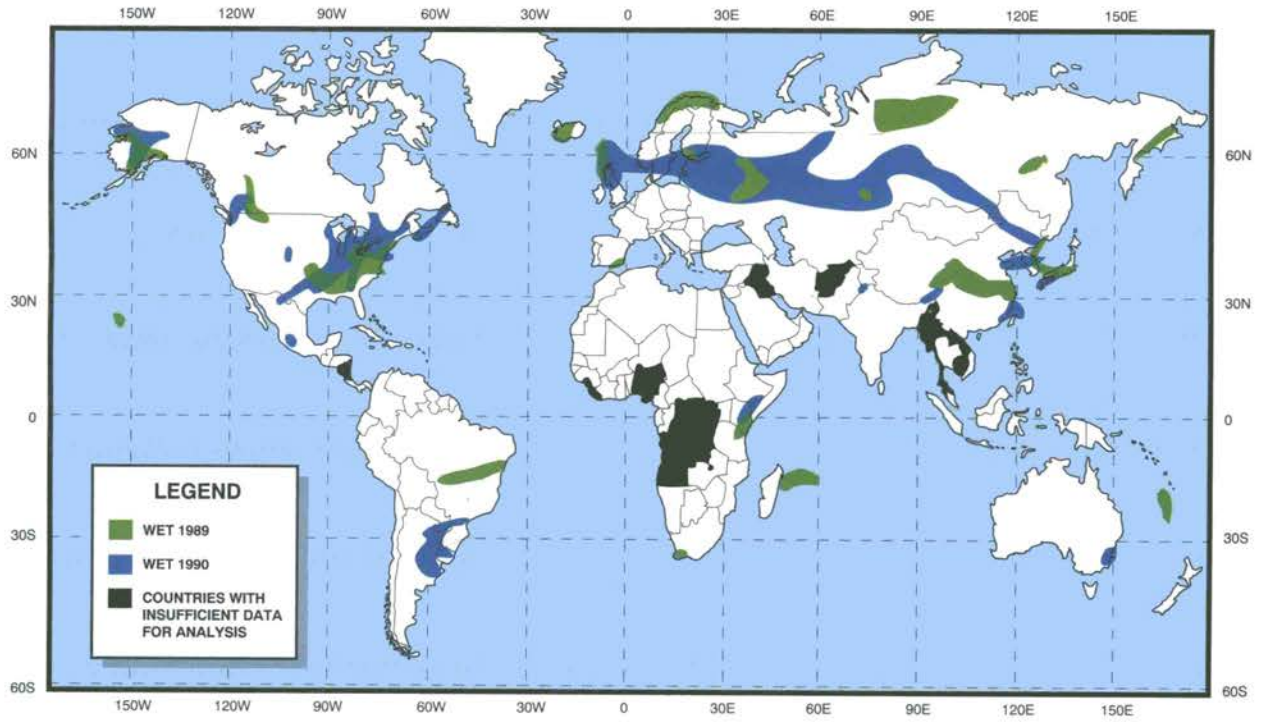

Figure 6.1 - Areas where precipitation anomalies were estimated to be within the wettest 10% of climatological occurrences (from NOAA, Climate Analysis Center, Washington, DC).

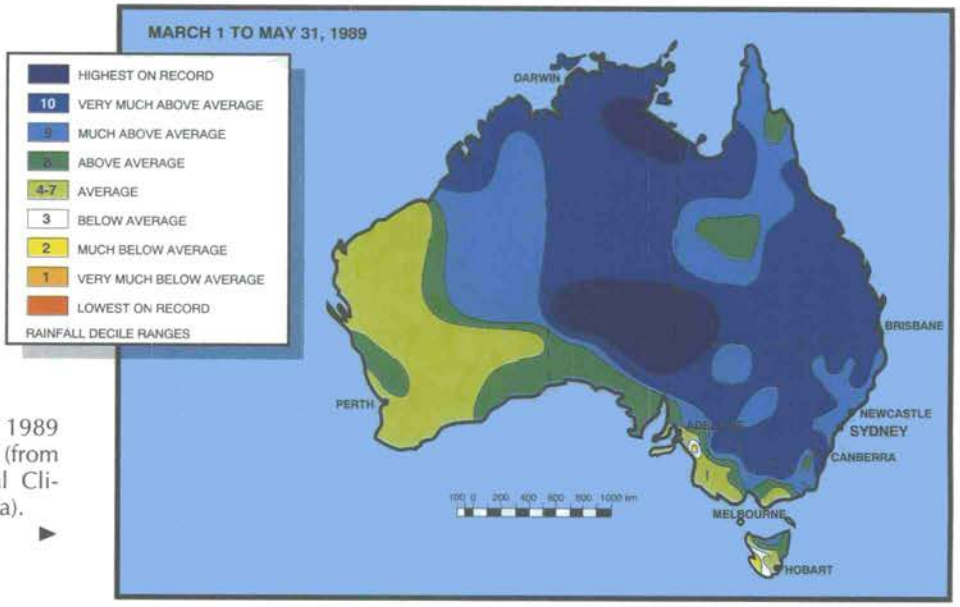

Figure 6.2 - Autumn (March-May) 1989 rainfall deciles for Australia (from Bureau of Meteorology, National Climate Centre, Melbourne, Australia).

►

Floods turned dry creeks into 20-km wide rivers, and marooned remote homesteads. This was the region's worst flooding in half a century, and quite possibly the rains were the heaviest since the country was settled by Europeans in 1788. Some stations received nearly their entire annual rainfall in just two days; e.g., Giles, in western Australia recorded 226 mm of rain, 88% of the annual normal. The excessive rains spread across the central, southern and southeastern areas.

Australia "Big Wet" *Photo NCC, Australia*

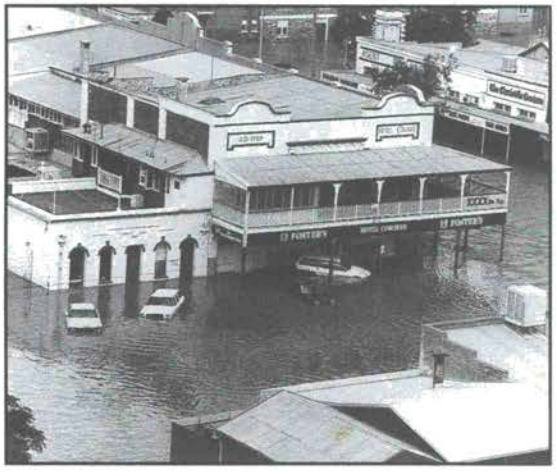

Beginning in April, the wet weather regime, characterized by very heavy showers, was concentrated in the eastern quarter of the continent, then later along the southeastern coast. The "Big Wet" diminished by late June and early July.

The flooding rains during the southern autumns of 1989 and 1990 were associated with the Southern Oscillation. Peaks in the active phase of the 30- to 60-day Southern Oscillation occurred over northern Australia during late November 1988, late January 1989, mid-March 1989 and mid-April 1989. The latter two were associated with cut-off lows over southeastern Australia. The interaction between the extratropical and tropical systems contributed to widespread rains over interior and northern Australia (Figure 6.2).

Other peaks in the oscillation crossed the Australian longitudes in early January, early March and mid-April 1990. The focus of tropical convection during January was to the east of Australia, with little impact on Australian rainfall. The March 1990 peak coincided with the passage of a mid-latitude system along with heavy rains over inland eastern Australia. The peak of mid-April coincided with a trough in the surface easterlies and the formation of a cut-off low. The subsequent widespread rains during April were more than five times normal, and produced some of the worst floods in a century. Queensland was hardest hit: about 570,000 square kilometres, or almost one third of the state, was under water. More than a dozen towns were isolated and 30,000 people marooned. The floodwaters reached 12.5-m depth in some areas, forcing the wholesale evacuation of some towns.

In late December 1990, torrential rains, 200 to 600% of normal, from Tropical Cyclone Joy inundated coastal sugarcane plantations of eastern Queensland. Widespread heavy tropical rains then continued to soak most of Queensland and the remainder of northern Australia during January and February 1991, exacerbating the flooding conditions.

6.2

MAJOR FLOODS IN THE AMERICAS

Record-breaking rains from severe thunderstorms fell on southwestern Ontario, Canada, in July 1989 during a 17-hour period. Torrential downpours flooded homes and farmland, causing property losses of $35 million (US). Official rainfall totals exceeded 250 mm in 24 hours (unofficial totals from an analysis of various non-official rain-gauges and other containers exceeded 400 mm in 24 hours), the highest 24-hour accumulation ever received in Canada east of the Rockies.

Very heavy rains fell in May and June 1989 in the eastern third of the contiguous United States. Flooding occurred in the Ohio River Valley in late May, and again from late August to October.

Heavy thunderstorm rains in late January 1990 also caused considerable flooding in the south-central United States. Severe weather accompanied the heavy rains during much of February, especially in areas extending from Texas and Oklahoma to the Carolinas. More severe weather, heavy precipitation and an ice storm plagued the central states during March. Copious rains during late April and early May in the south-central Great Plains produced the worst flooding in 80 years in eastern Oklahoma, northern Texas and western Arkansas. Recurrent torrential downpours also drenched much of the central and eastern states in May and early June, and many of the storms were accompanied by severe weather. Record and near-record heavy precipitation soaked much of the eastern United States during October and December, generating flooding in sections of the Tennessee and Ohio River valleys, in the Carolinas, and in the central Appalachian Mountains.

During November 1990, a subtropical storm-track dubbed the "Pineapple Express" brought torrential rains northeastward from Hawaii to the central Pacific Coast of North America, generating widespread, severe flooding and landslides throughout western Washington state and British Columbia. Coastal areas recorded more than double their normal

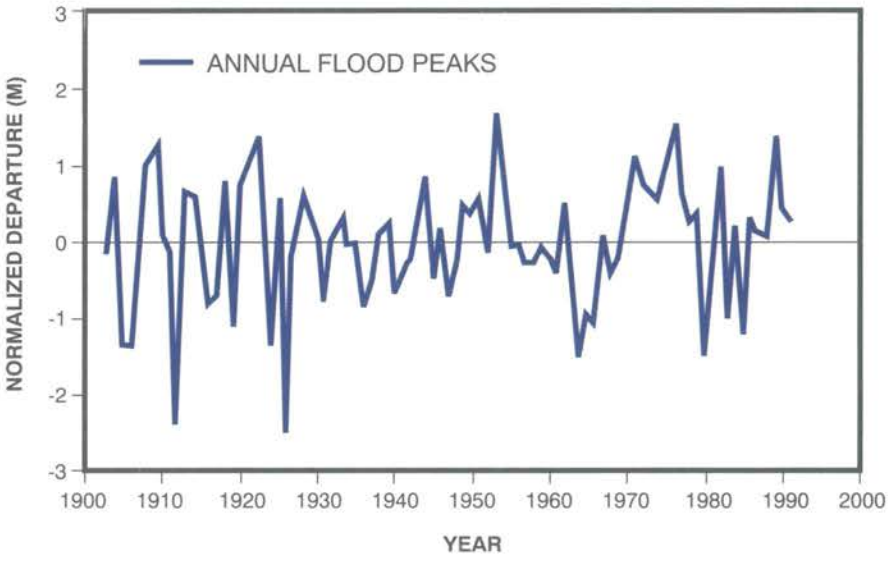

▲ *Figure 6.3* - Annual flood peaks for Rio Negro at Manaus Port, Brazil, from 1903 through 1991 (from Space Research Institute, Manaus, Brazil).

Figure 6.4 - Monthly normalized river discharge for the Trombetas River for January 1971-August 1989 in northern Brazil (vertical bar) and values of the Southern Oscillation Index (SOI) for January 1971-June 1990 (blue line). Negative values of the SOI indicate an El Niño (warm) event, and positive values reflect a cold ENSO event (from Space Research Institute, Manaus, Brazil).

▼

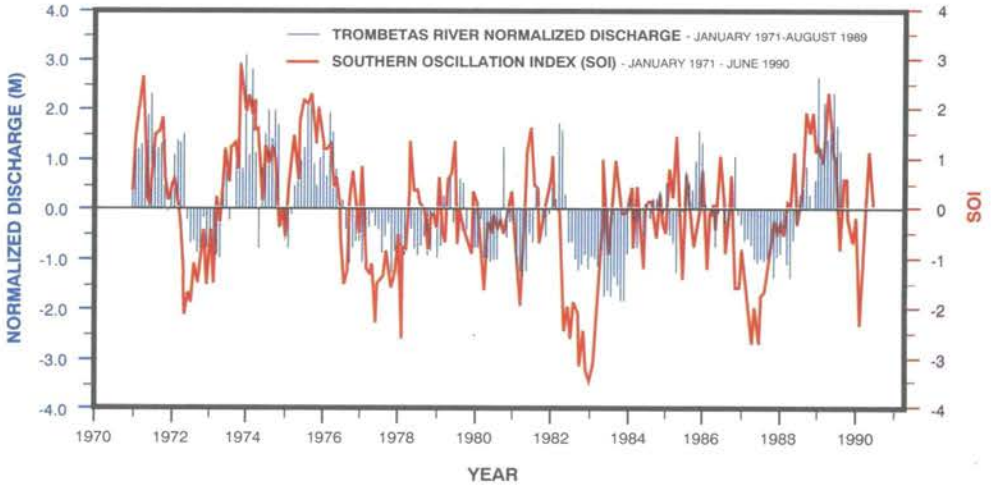

monthly rainfall amounts. At Hope, in the eastern Fraser Valley of British Columbia, precipitation was four times the average, a new all-time record for any month.

The region to the north of the Amazonas River, in northern South America, is strongly influenced by the El Niño/Southern Oscillation (ENSO) phenomenon. Generally cold/anti-El Niño (warm/El Niño) ENSO events produce above (below) normal rainfall, which in turn affects river levels there. Heavy rains fell in association with the cold phase of ENSO in 1989, resulting in near-record high river levels in northern Brazil (Figures 6.3 and 6.4). The 1989 Rio Negro flood peak was the third highest of the century, following 1953 (the highest) and 1976. Abundant rains also fell across much of Brazil during December 1989 and January 1990, causing severe flooding. Very wet conditions caused widespread flooding in Uruguay and southern Brazil in February 1990.

6.3

MAJOR FLOODS IN EASTERN ASIA

More than twice the normal precipitation fell during July 1989 on portions of Korea, the Manchurian provinces of Jilin and Heilongjiang (north of Korea), and southeastern Siberia (Figure 6.5). The rainfall provided welcome relief from long-term dryness, but most of the rain fell during short time spans, causing severe flooding, landslides, extensive property damage, and loss of life.

Surplus rains during mid-February to late April 1990 deluged most of southeastern China, especially Guangdong and Fujian provinces. More than 81,000 ha of rice, vegetable, and other agricultural fields were flooded by the torrential rains in Fujian Province alone; more than 300 roads were blocked by flooding.

Late spring "plum" rains in 1991 flooded large segments of the Huai and Chu river basins and the Tai Lake Basin in southern China. The West Pacific subtropical high was located to the south, and was not only stronger but started moving north some 20 days earlier than usual, in the middle of May — and was situated about 300 km farther north than normal. Rainfall amounted to more than 800-1000 mm from May to mid-July, which is one to three times as much as the average for this period. Rains were heavy, widely distributed and long lasting. The first rains rapidly saturated the soil and filled low-lying areas along the rivers. Some of the country's worst flooding this century occurred in the Wu River watershed.

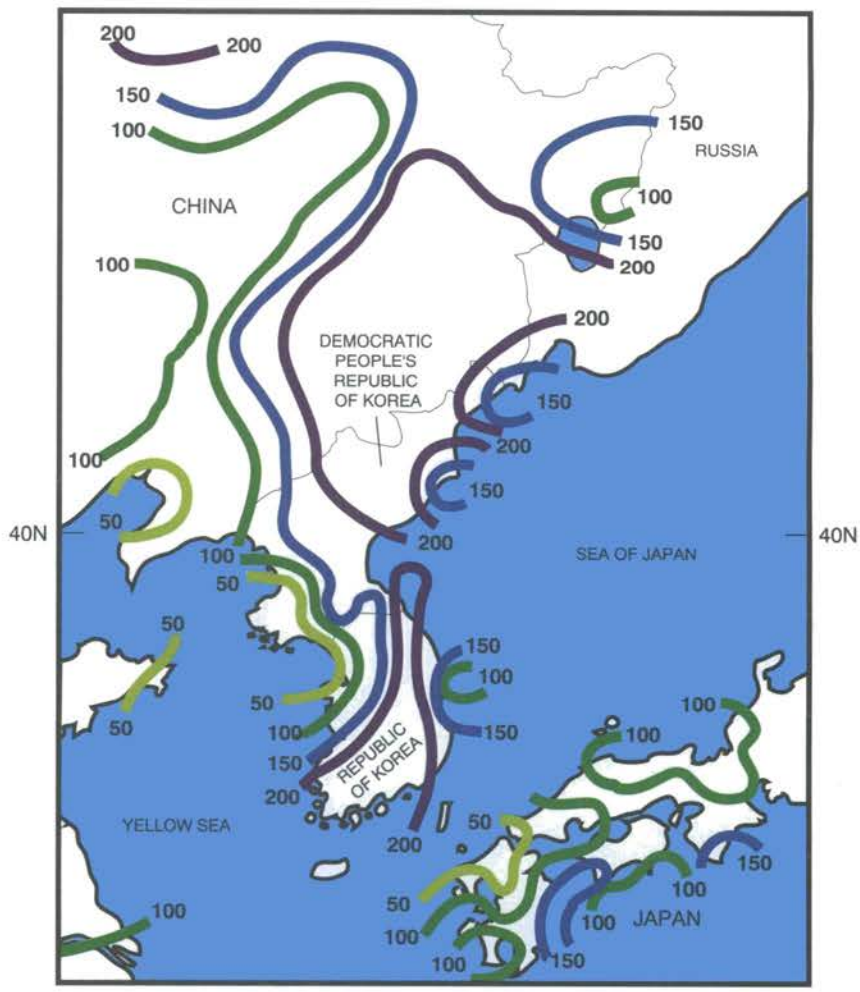

Figure 6.5 - Percentage of normal precipitation during July 9-29, 1989 across eastern Asia (from NOAA, Climate Analysis Center, Washington, DC). ►

A monsoon wind circulation and its associated seasonal rainfall affects a considerable part of the world's land masses. The name "monsoon" has traditionally been used to describe both the rain phenomenon and the southwesterly surface winds that prevail during summer over India and neighbouring regions. Although primarily an Asian phenomenon, it also occurs in eastern Africa, northern Australia and, to a lesser degree, southwestern North America. The year-to-year vagaries of the monsoon, i.e. excessive rainfall leading to floods in certain years or little or no rain in other years causing droughts and famines, cannot be explained without considering interactions with the general circulation.

Although the monsoon seasons over India/China, the equator, and southern parts of eastern Africa are significantly different, high correlations between their monsoonal wind systems have been observed during some years. A good example is the opposite phase relationships between India/China and Eastern African monsoonal wind systems during some El Niño/Southern Oscillation (ENSO) periods.

7.1

ABUNDANT MONSOON RAINS OVER INDIA

India is an agricultural country with large areas that depend on monsoonal rains as the only source of water for cultivation. These rains also provide much needed waters for hydroelectric power generation.

Some of the principal factors controlling the monsoon circulation in India and other Asian subcontinent countries are the "heat-low" over the Baluchistan region of Pakistan, the pressure gradient over the Indian peninsula, the low-level flow pattern, the location of the monsoon trough, the monsoon depression, the strength of cross-equatorial flow, and the sea surface temperature over surrounding areas.

The Indian monsoon season occurs from June to September when about 70% of the annual rainfall is received. Although the monsoon advances into India with a fair degree of regularity, there are significant year-to-year variations in onset date, and temporal behaviour. Any large anomaly with respect to long-term climatic normal monsoon conditions upsets the economy of India and other Asian subcontinent countries. Monsoon rains also bring relief to the people by reducing the extreme high summer temperatures of 40-45°C to more comfortable values near 30°C.

For the review period, the monsoons were generally on schedule and brought ample moisture for India, a welcome change after the severe country-wide drought during 1987. In 1989 and 1990, only 6 and 3 of 19 subdivisions, respectively, received below normal rainfalls (Figures 7.1 and 7.2) compared with 21 subdivisions during the drought of 1987. Excessive or normal rainfalls occurred in 37, 88, 77, and 95% of India for the years 1987 to 1990, respectively.

Ample rains from the southwest monsoon in the summer of 1989 resulted in excellent harvests for Indian farmers but caused considerable flood damage. With the exception of central and north-central India, most areas generally received near normal monsoonal rains. The monsoon began over Kerala on June 3 and over peninsular India and parts of Uttar Pradesh on June 23, and covered the remainder of the country by July 2. The withdrawal of the 1989 monsoon was almost on schedule (Figure 7.3), commencing in mid-September and finishing outside Tamil Nadu and Kerala on October 13.

Between June and September 1989, more than 500 mm fell over most of India and northern Pakistan. As a result, normally arid southern Pakistan and extreme western and much of northern and southern India reported above normal rainfall. The excessive rains in northeastern India flowed into the Ganges and Brahmaputra Rivers, creating disastrous flooding across the delta plains of Bangladesh and extreme eastern India. During July, however, cyclones, copious rains, floods, and tidal waves lashed India's west coast, particularly Maharashtra State, marking an unusually destructive start to the 1989 monsoon season.

The 1990 monsoon started 10 to 14 days earlier than usual over Kerala, Karnataka and western portions of West Rajasthan (Figure 7.4). It was preceded by an intense cyclone during May. The cyclone, considered the most severe in over a decade in India, battered the southeastern Indian coast of Andhra Pradesh State. The monsoon advanced on schedule over Assam and adjacent areas, but was late by 12 to 15

days over the Gujarat region and adjoining areas. Withdrawal of the 1990 southwest monsoon commenced by the end of September, thereby extending the season in northern areas, and finally withdrew from the rest of the country outside Kerala and Tamil Nadu on October 17.

In June 1990, very heavy rains fell over northwestern, southwestern and eastern India and Bangladesh. Rain and flooding continued in July, diminished in early August, and returned later in the month to northeastern India, spreading farther west and causing extensive flooding and landslides. In early September heavy rains fell on north-central Pakistan and northern India, and then the monsoon began its slow southeastward retreat. In late October, the monsoon abated in northeastern India and Bangladesh but only after a violent storm off the coast of Bangladesh had produced strong winds and very heavy rains.

During mid-June, torrential downpours dumped over 560 mm of rain in a 24-hour period on parts of Bombay, with more than 400 mm falling during one 6-hour span. The rains diminished during early August, but returned later in the month to northeastern India. Towards the end of August, downpours in districts south of Katmandu, Nepal, produced flooding and landslides.

Overall, most of central Pakistan, northern, central, and eastern India, and Bangladesh recorded near to above normal monsoonal rains in 1990. Areas with significantly below normal seasonal rains included extreme southern and extreme western India and south-

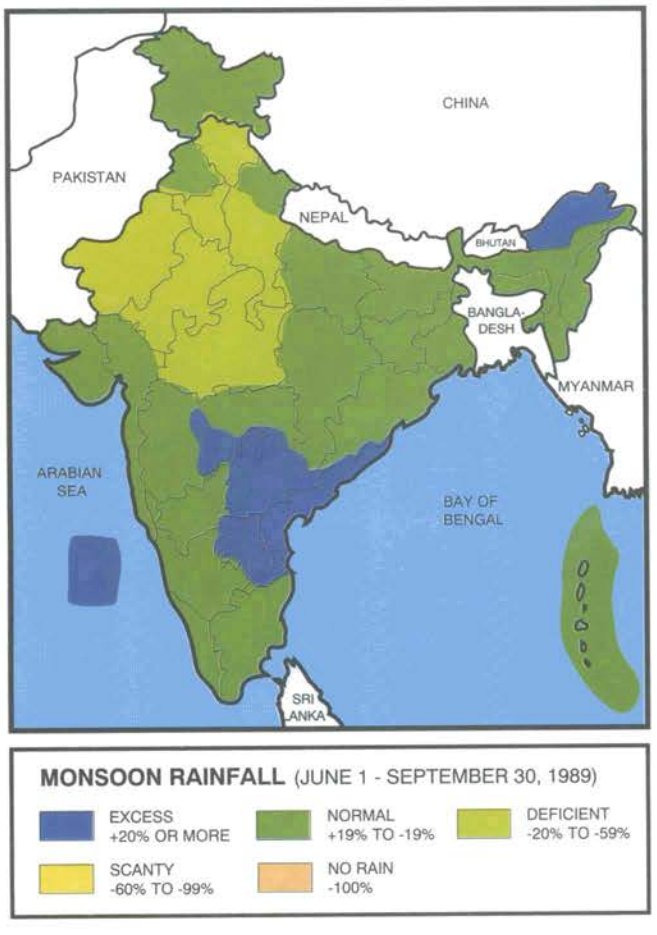

Figure 7.1 - Distribution of anomalous June-to-September rainfall totals over India during the 1989 monsoon (from India Meteorological Department, New Delhi).

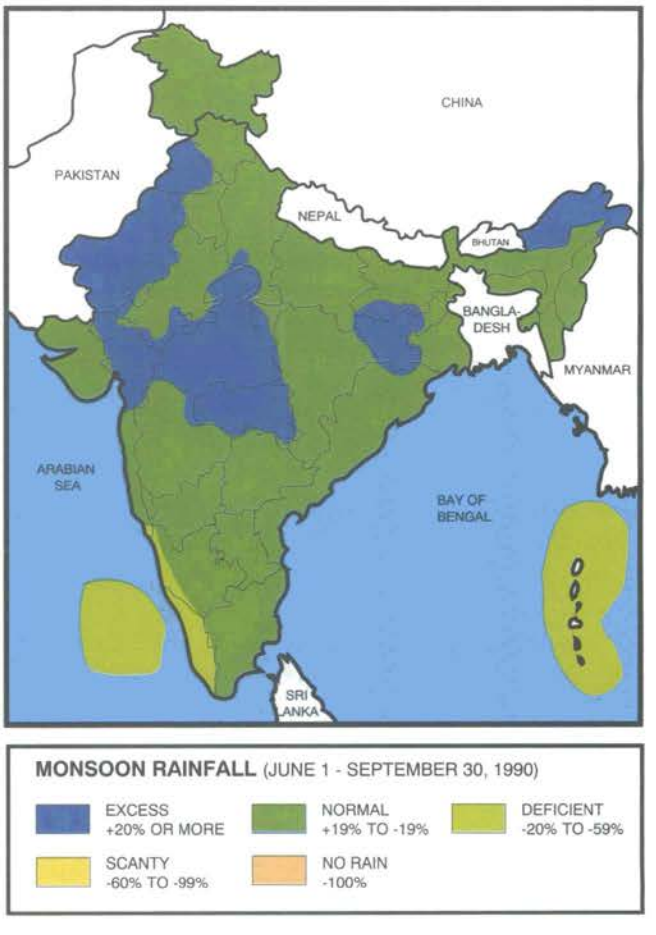

Figure 7.2 - Distribution of anomalous June-to-September rainfall totals over India during the 1990 monsoon (from India Meteorological Department, New Delhi).

eastern Pakistan. The May-September totals of 500-1500 mm in northwestern and central India were well above normal, but the totals of 250-500 mm across much of extreme southern India were below normal.

7.2

VARIABLE MONSOON OVER EASTERN CHINA

The summer "monsoon" of east China (east of 110°E) is generally characterized by a seasonal northward movement of a monsoon-like rainy belt from May to August. Summer monsoon rain in eastern China is directly influenced by the seasonal displacement of the west Pacific High (at the 500-hPa level), which generally moves northward from spring to midsummer. The main monsoon rainy belt is located along the northwestern side of the west Pacific High. During the 1980s, the summer position and interannual variability of the west Pacific High changed significantly compared with the long-term climatology, with resulting changes of the summer monsoon rains of eastern China. Since 1979, the west Pacific High, during high summer, has tended to move to a more southerly position than before. Consequently, northern China has suffered from a deficiency of rain during the high summers of the 1980s, whereas central China (Yangtze and Huaihe basins) was waterlogged several times (Figure 7.5).

Strong statistical evidence correlates the migration of the west Pacific high with direct clear-sky solar radiation during the 1980s. Xu (1990) postulates that owing to an increase in the density of aerosols, either in the troposphere or stratosphere, through the combined result of industrialization and urbanization in China, and the influence of large volcanic eruptions (Mount St. Helens in 1980 and El Chichòn in 1982-1983) direct clear-sky solar radiation has decreased. In turn, the higher density of atmospheric aerosols causes a reduction of surface heating, which leads to a southward retreat of the west Pacific high and the accompanying northern monsoon rainbelt of eastern China during high summer.

The summer monsoon of 1989 in eastern China was active during June to mid-July owing to the more northward shift of the west Pacific high (Figure 7.6.1). The onset of plum rain (Meiyu) by June 3 in the mid-lower Yangtze was abnormally early by about two weeks. The west Pacific High was unsteady and weaker than normal after late July. Its latitude between 110-130°E is situated in the 25 and 27°N belt during the summer, causing more rainfall in central China (especially in the Huaihe Basin), with less rain in southern China (south of 27°N) and northern China (north of 34°N) (see Figure 7.7).

In 1990, the summer monsoon was strongest during June and July. The west Pacific High was more northward than normal (Figure 7.6.2). Its latitude was situated at 26-28°N during the Meiyu (mid-June to early July). This anomaly caused a more northward position of the monsoon rainy belt of east China, locating it along the lower reaches of the Yellow and Huaihe rivers. Meanwhile, the Yangtze

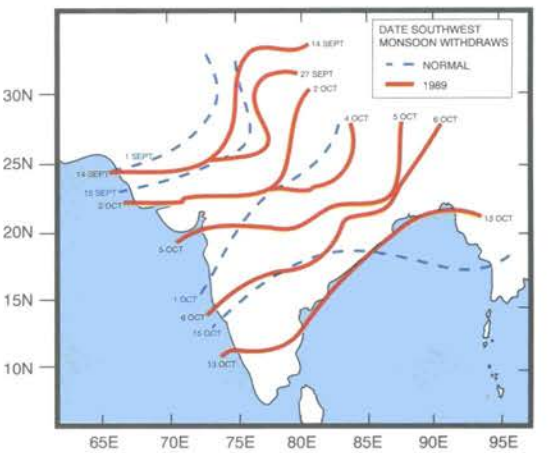

▲

Figure 7.3 - Actual and normal dates of withdrawal of the southwest monsoon over India in 1989 (from India Meteorological Department, New Delhi).

Figure 7.4 - Actual dates of onset of the southwest monsoon over India in 1990 (from India Meteorological Department, New Delhi).

▼

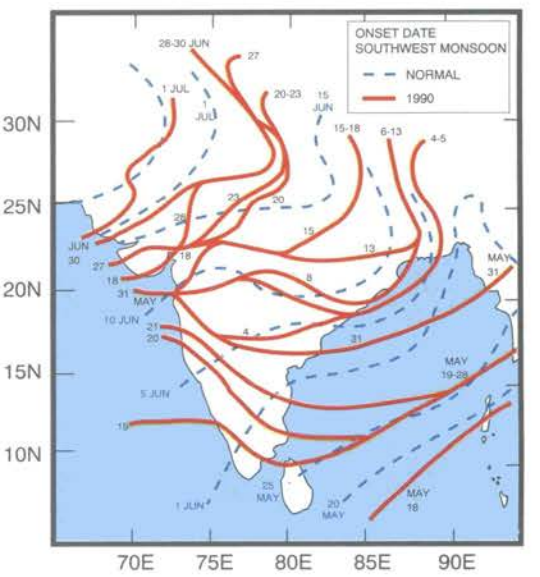

Valley and southern China had no rain. The Meiyu did not appear in summer 1990 — for only the tenth year since 1885. The southern provinces of Jiangxi, Sichuan, Guangxi and Hubei suffered persistent high temperatures during July and August, and the highest daily temperature reached 41°C.

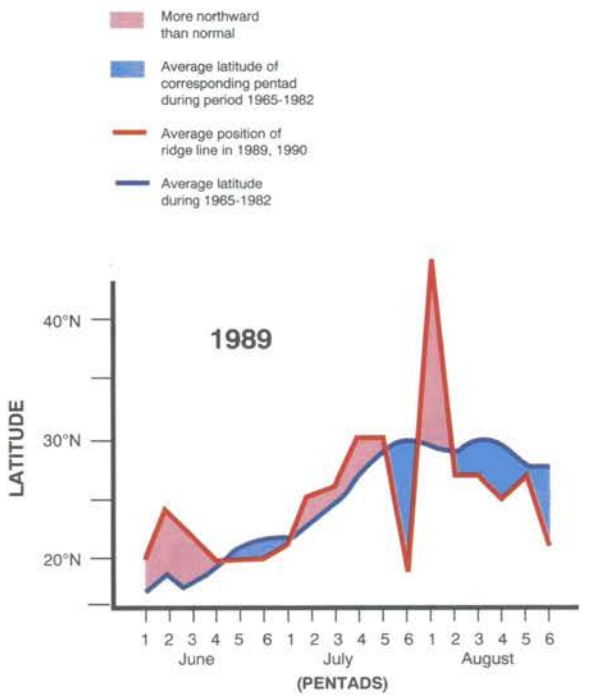

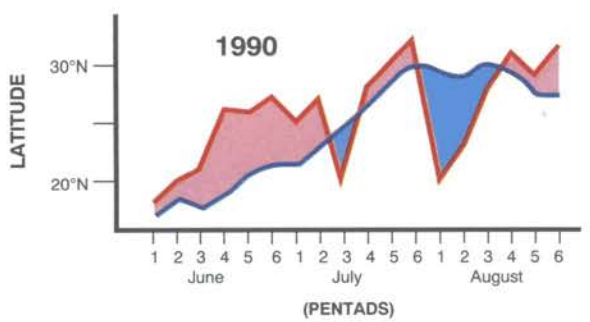

▲

Figure 7.6 - Time variation of the latitude of the west Pacific high-pressure area (500-hPa level) between 110 and 130°E, during the summers of 1989 (7.6.1) and 1990 (7.6.2). The dashed line is the corresponding average during 1965-1982 (from Jiangsu Meteorological Institute, Nanjing, China).

Figure 7.5 - Average summer (July and August) rainfall anomalies during the 1980s for China, expressed as percentage departures from the 1951-1979 normal (from Jiangsu Meteorological Institute, Nanjing, China).

▼

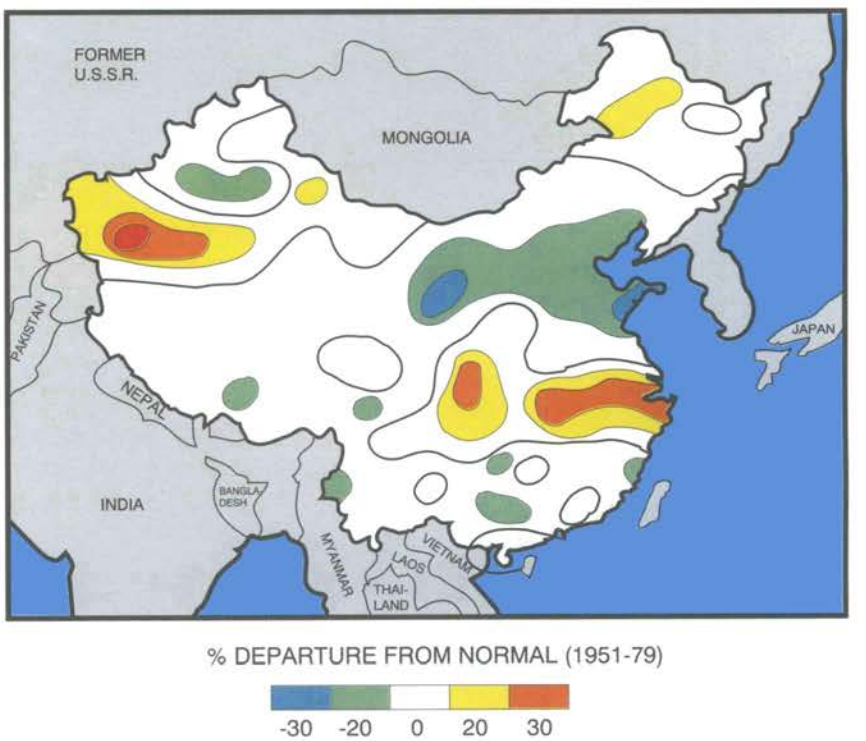

Figure 7.7 - Areal distribution of summer (June to August 1989) rainfall anomaly (percentage departure from the 1951-1979 normal) in China (from Jiangsu Meteorological Institute, Nanjing, China).

▼

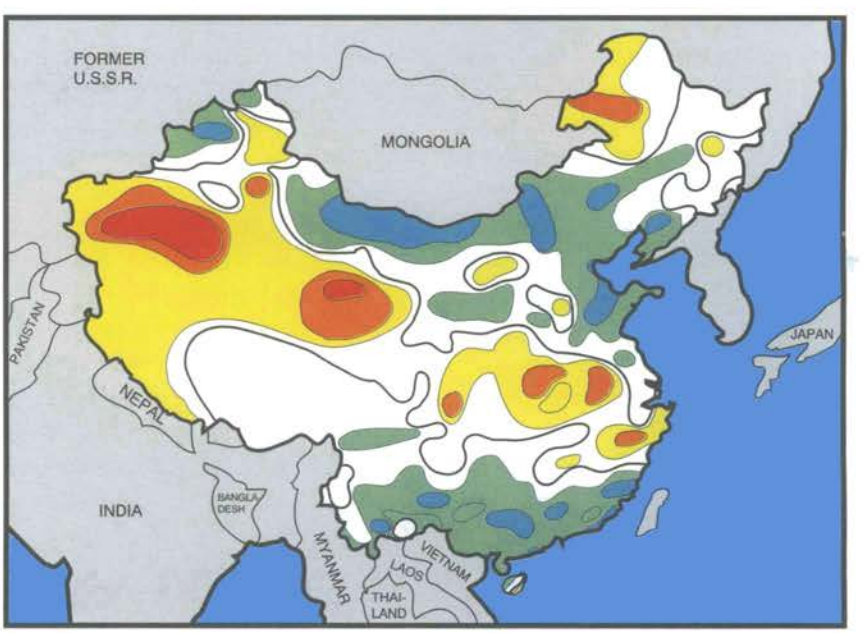

7.3

EASTERN AFRICA MONSOON CONDITIONS IN 1989 AND 1990

The southeasterly (SE) monsoon winds from the Southern Hemisphere and the northeasterly (NE) monsoonal winds from the Northern Hemisphere are the major sources of moisture for rainfall over much of eastern Africa. The patterns of the monsoon wind systems, however, are significantly modified by regional features including complex topography and many large inland lakes. These features often force the convergence zone of the interhemispheric monsoonal wind systems (Intertropical Convergence Zone, or ITCZ) to move both meridionally and zonally during the various seasons. The ITCZ is located over the southern and northern sectors of eastern Africa, which are far from the equator during the corresponding hemispheric summer seasons. Two distinct rainfall seasons associated with the biannual passage of the ITCZ are, however, observed during the spring and autumn seasons over parts of eastern Africa that are closer to the equator and linked to the convergence of the NE and SE monsoon wind systems.

From December 1988 to February 1989, the northeasterly monsoon winds over eastern Africa were anomalously strong. The tropical zonal circulation was dominated by the high circulation index of the El Niño/Southern Oscillation (ENSO). Near to above normal rainfall was recorded over most of southern Africa during the 1988-1989 summer (Figure 7.8). A weakened Indian Ocean monsoon wind system during 1989-1990 resulted in unusually wet and unusually dry areas over southern Africa. A similar pattern occurred during 1990-1991.

June, July and August is the major rainfall season for the northern areas of the region associated with the migration of the ITCZ to the Northern Hemisphere. Western parts of the equatorial sector also receive substantial rainfall associated with incursions of moist unstable low-level westerly winds from the Atlantic Ocean and the moist Congo/Zaire basin. The rainfall patterns for 1989 and 1990 were similar, with drought occurring in the northern areas (see Chapter 5 for details).

A stronger than normal southeast monsoon wind system brought near to above normal rainfall to equatorial Africa from

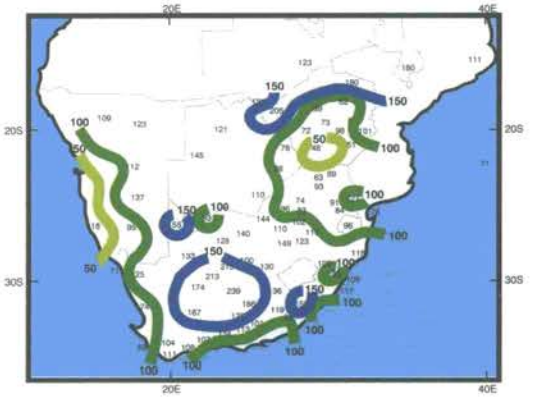

▲ *Figure 7.8* - Percentage of normal precipitation during southern Africa's rainy season (October 1, 1988 to March 25, 1989) (from NOAA, Climate Analysis Center, Washington, DC).

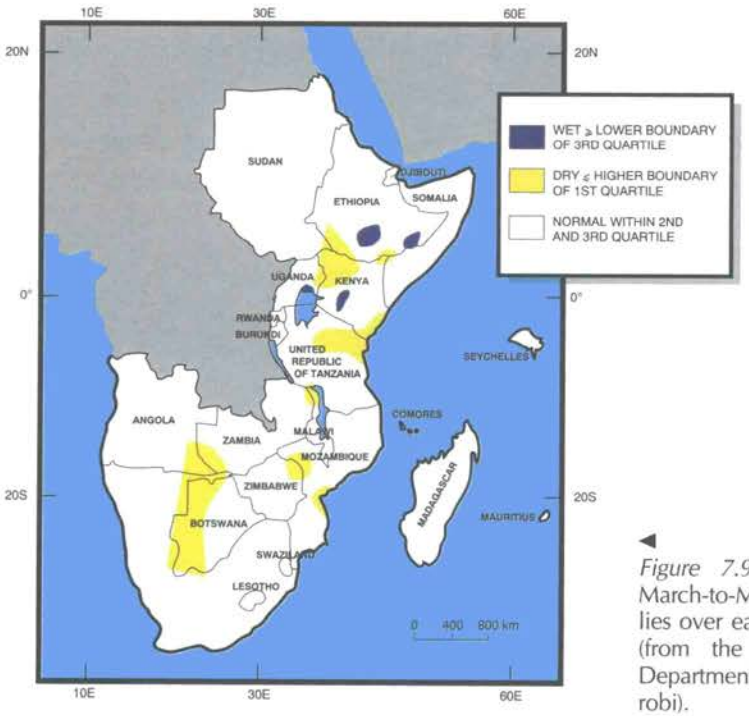

◄ *Figure 7.9* - Distribution of the March-to-May 1991 rainfall anomalies over eastern and southern Africa (from the University of Nairobi, Department of Meteorology, Nairobi).

Figure 7.10 - Sea surface temperature (°C): (a) means, and (b) anomalies for April 1991 (from NOAA, Climate Analysis Center, Washington, DC).

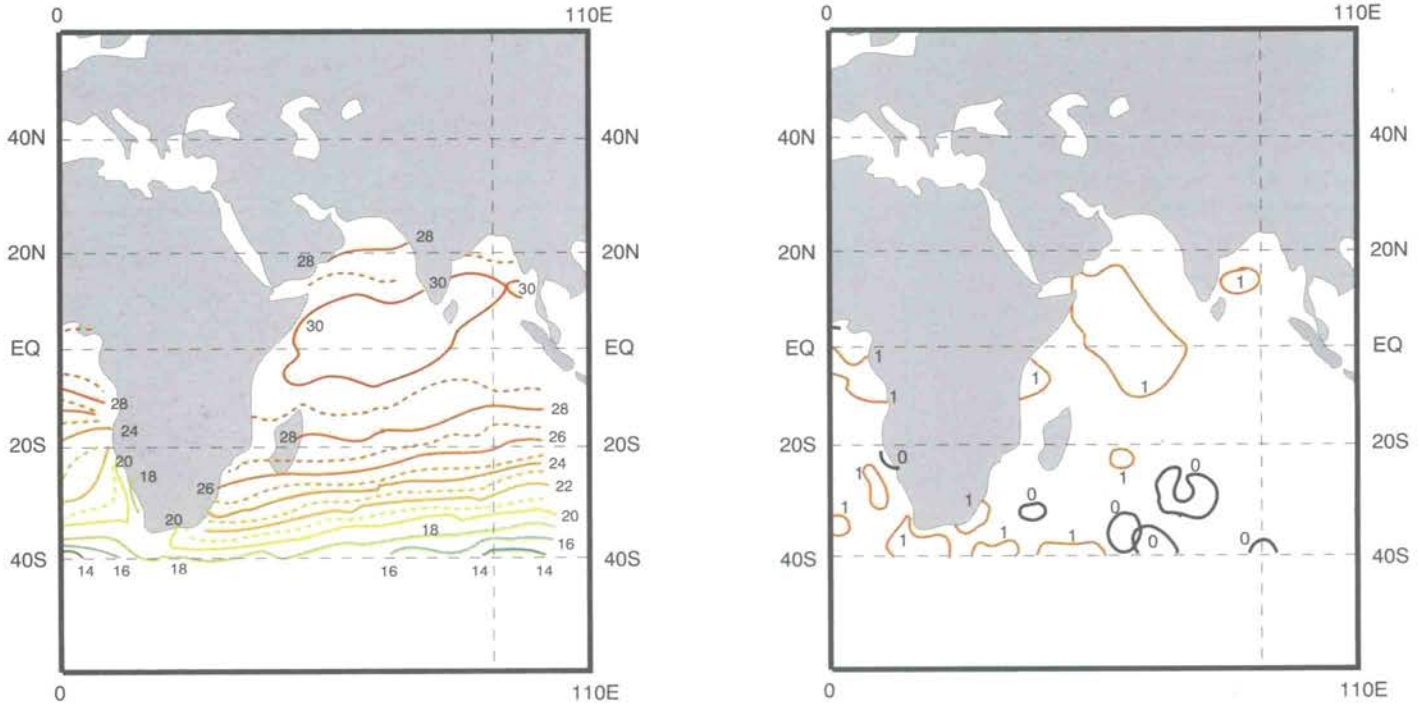

March to May 1989. A similar rainfall pattern occurred during September to November 1989. Anomalies of the southeast monsoon wind system extended over larger portions of the region from March to May 1990 when compared with 1989, resulting in a somewhat greater area of above normal rainfall anomalies. September to November 1990 had near normal rainfall amounts at most locations, but below normal anomalies in portions of the northern equatorial region.

The monsoon circulation was weaker from March to May 1991 than in the two previous years, resulting in a poor seasonal distribution of precipitation over the region and very severe droughts (Figure 7.9). Figure 7.10 shows that warm pools of surface water over equatorial coastal areas of the region and the Arabian Sea were discernible from March to May 1991. Positive sea surface temperature anomalies over this region reduce the intensity of the Arabian subtropical anticyclone and interfere with the normal flow of the east African monsoon wind systems.

SEVERE STORMS: TROPICAL CYCLONES, TYPHOONS HURRICANES, TORNADOES

CHAPTER 8

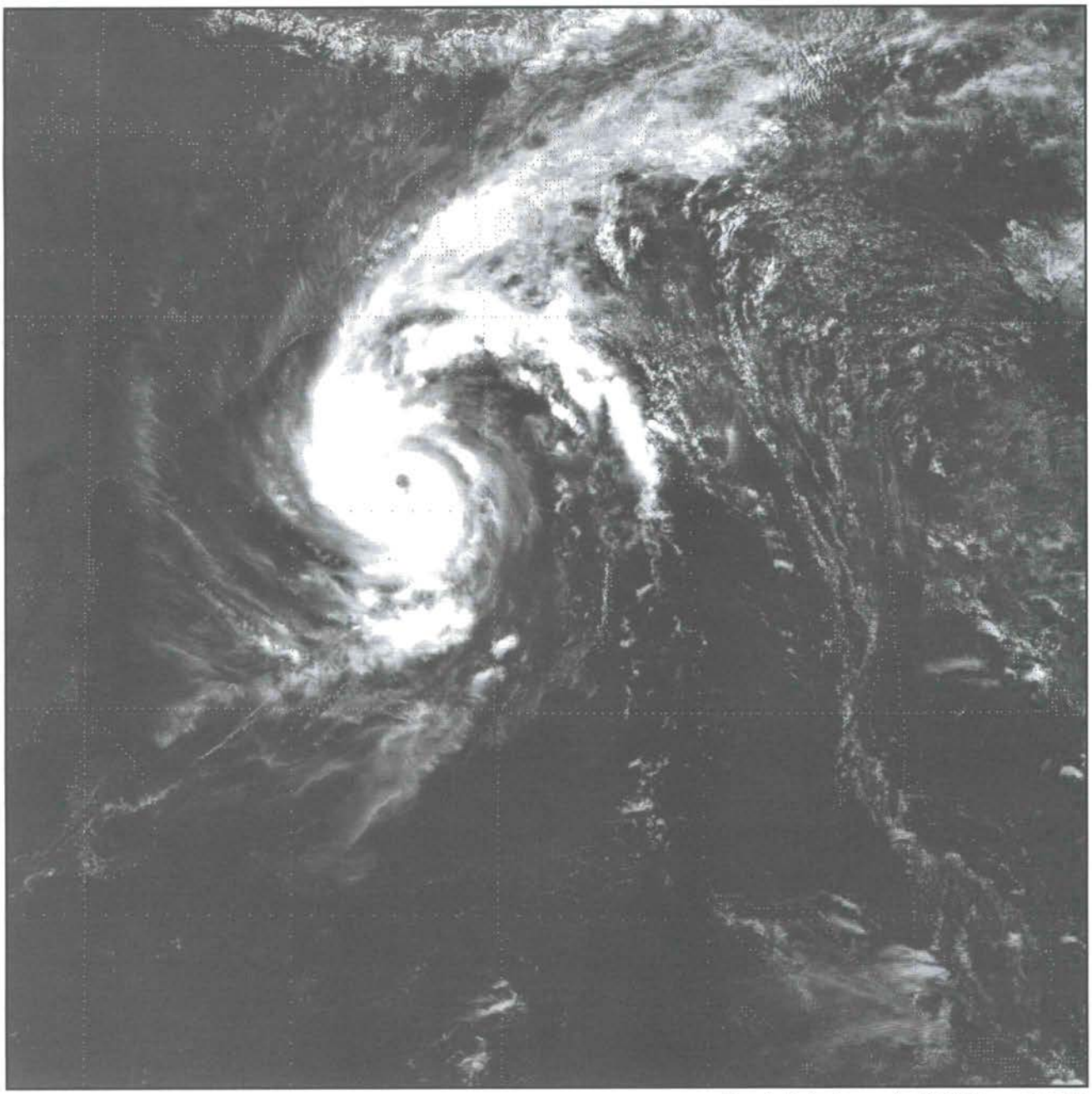

Bangladesh storm, April 1991 INSAT-1D

Tropical cyclones, hurricanes and typhoons are the most devastating of meteorological phenomena. About 80 of these killer storms occur around the world each year. The average annual damage has been estimated at about $1,500 million (US), and the average annual death toll over the past 30 years or so is about 15,000. Drowning contributes heavily to the fatalities, especially through rare events such as the storm surge that caused over 100,000 deaths in Bangladesh in 1991.

Strong winds, storm surges, and associated torrential rains produce heavy damage in coastal areas, especially in developing countries where an adequate infrastructure capable of moving large human and cattle populations in the shortest possible time to safe areas cannot be organized. Attempts are being made by meteorologists in various countries to improve their forecasts in order to give timely warnings to the public about approaching cyclonic storms so as to reduce damage. But there are inherent difficulties because the majority of the hurricanes behave erratically. Available dynamical methods cannot predict them well enough in advance. Climatological records and analogue methods do help to trace and predict tropical cyclones, but they have limited applications. Consequently, the best that can be done is to detect the storms using meteorological satellites, track them by cyclone-detecting radars, and warn the coastal populations to evacuate to pre-determined safe places. A proper all-clear should also be developed to avoid unnecessary movement of the people.

8.1 CYCLONES AND DEPRESSIONS IN THE BAY OF BENGAL AND THE ARABIAN SEA

During 1989, ten tropical cyclonic systems developed over the Bay of

Figure 8.1 - Tracks of tropical cyclones and depressions in the northern Indian Ocean during 1989 and 1990 (from India Meteorological Department, New Delhi). ▼

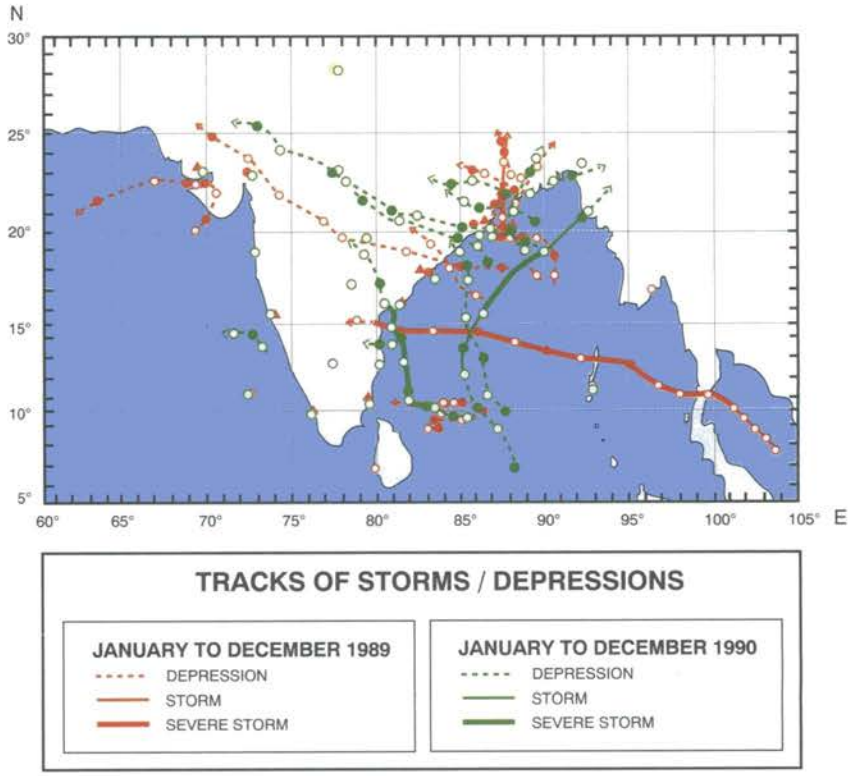

Bengal and the Arabian Sea. Of these in the Bay of Bengal, two hurricanes and one cyclone developed during the monsoon season. One of these hurricanes formed over the north Bay of Bengal, the other over the Gulf of Thailand. The Arabian Sea remained comparatively dormant with only one depression, which formed during the onset phase of the monsoon period. The tracks of these storms and depressions are shown in Figure 8.1. The unusual feature of the cyclonic storm that formed during the monsoon season was its position much farther southward compared to normal. It caused widespread rain over all of India.

A WIND BY ANY OTHER NAME

Tropical systems are classed into several categories depending on maximum strength, usually measured by maximum sustained wind speed. A *tropical disturbance* is simply a moving area of thunderstorms in the tropics that maintains its identity for 24 hours or more. A *tropical depression* is a cyclonic system originating over the tropics that has a highest sustained wind speed of up to 61 km/h. A *tropical storm* has a highest sustained wind speed between 62 and 117 km/h. A *hurricane* has wind speeds of 118 km/h or more.

The word "hurricane", meaning "big wind", has been attributed to Carib Indian origin. Hurricane is used to describe tropical cyclones of hurricane intensity in the North Atlantic and eastern Pacific, whereas "typhoons" are used for similar storms in the China Sea, "baguios" in the Philippines, and "cyclones" in the Indian Ocean region.

KAVALI HURRICANE — AN HISTORIC STORM

Hurricane Kavali developed over the Gulf of Thailand on November 3, 1989. Initially, it moved northwestward for a day, then westward across South Thailand and South Burma, and emerged into the Andaman Sea. Thereafter, it took a west-northwesterly to westerly course, crossed the Andaman group of islands and struck the south Andhra Coast near Kavali around midnight of November 8. Close surveillance of its position and intensity enabled the India Meteorological Department to issue precise cyclone warnings and advisories, well in advance, indicating the intensity, track, time, and place of landfall during its nine-day track. Timely warnings enabled the authorities to take preventive measures to reduce damage. It was one of the most intense cyclones in the seas around India, with a maximum estimated wind speed of 235 km/h. At landfall, its wind speed was 190 km/h with a 5 m storm surge.

About 4 million people in 836 villages in the Nellore district of Andhra Pradesh were afflicted by this hurricane. Its fury was felt within a radius of 17 km from Kavali. According to reports, 69 persons lost their lives and 7,100 cattle perished; on Andaman Island, 709 buildings were damaged and about 1000 trees were uprooted.

Nine tropical cyclonic systems formed in the Bay of Bengal and one in the Arabian Sea during 1990. Of these only two developed into tropical cyclones; the remaining were depressions. Their tracks are shown in Figure 8.1. It is noteworthy that no tropical cyclones have

formed in the Arabian Sea during the last five years.

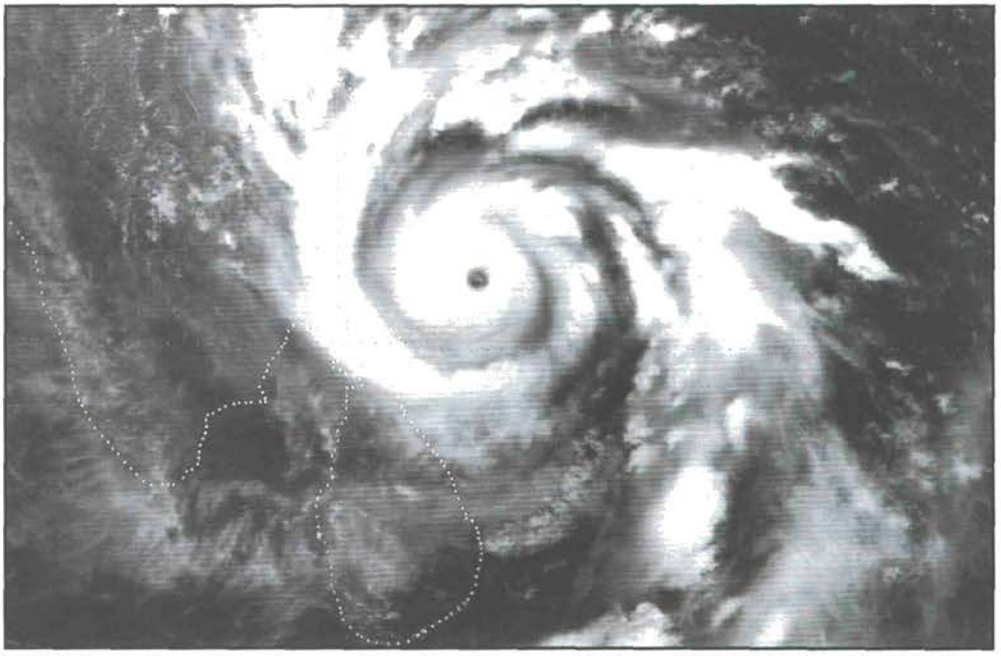

INSAT IB satellite visible picture of the Machilipatnam Cyclone, 0600 UTC May 7, 1990 (from India Meteorological Department, New Delhi).

MACHILIPATNAM CYCLONE

This system originated as a depression over the southwest Bay of Bengal on the morning of May 5, 1990, when it intensified into a cyclonic storm by 1200 UTC and was centred about 500 km southeast of Madras. It moved farther northwestward and became a hurricane on the morning of May 6, then moved north-northwesterly crossing south Andhra Pradesh coast near the mouth of the Krishana River as a severe cyclonic storm at about 1330 UTC, May 9. It weakened on the evening of the 11th. The maximum sustained winds associated with the cyclone were estimated at about 235 km/h. At landfall, its maximum sustained wind was about 167 km/h. Widespread heavy to very heavy rainfall occurred in coastal Andhra Pradesh and adjoining parts of Tamil Nadu during May 8-12, 1990 along with a peak storm surge of 5 m.

The cyclone caused colossal damage to public and private property in

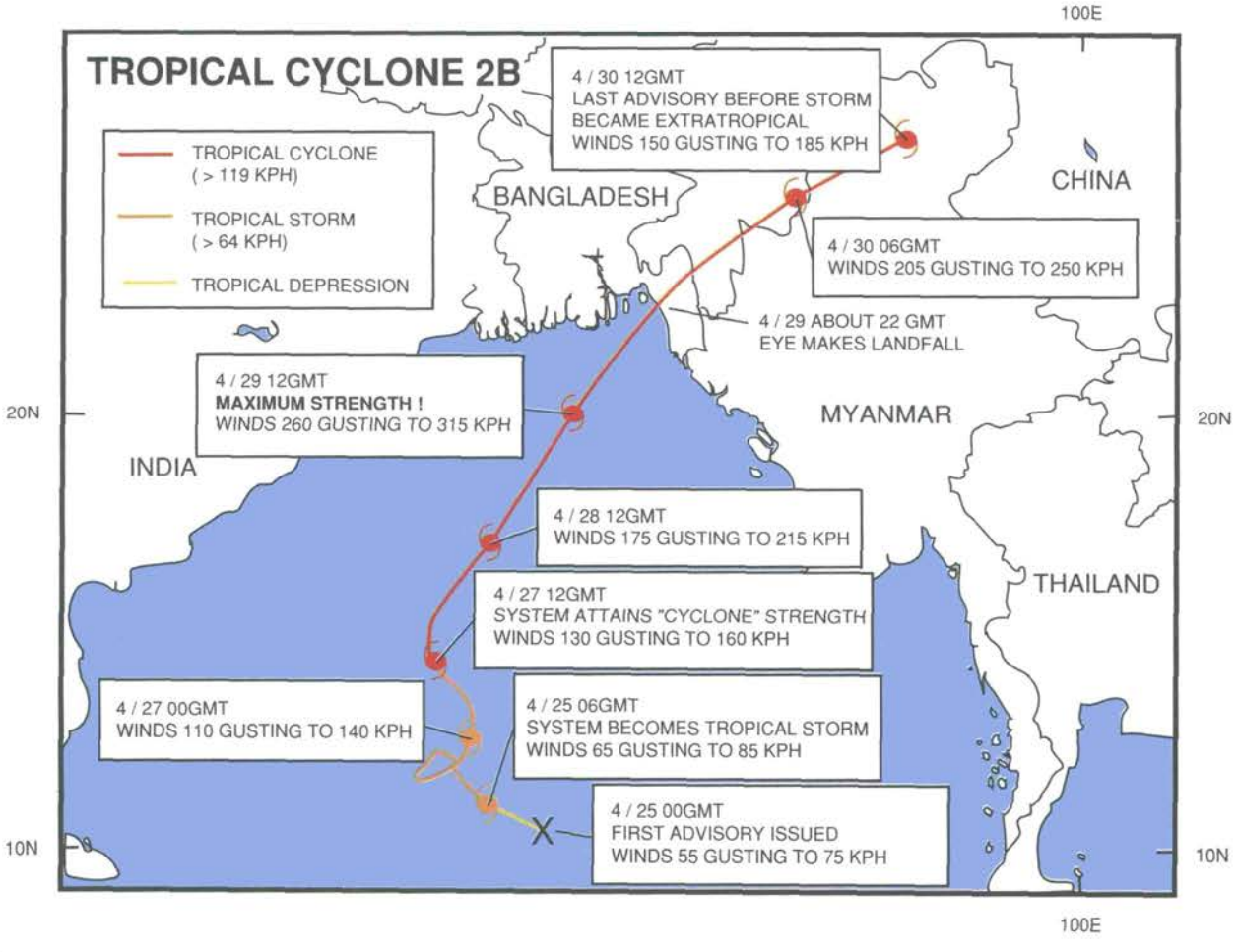

▲ *Figure 8.2* - Track of tropical cyclone 2B that ravaged Bangladesh for more than eight hours on April 30, 1991 (from NOAA, Climate Analysis Center, Washington, DC).

Andhra Pradesh. A total of 5,160 villages was affected; human losses totalled 928; and more than 1.4 million houses were damaged. Timely warnings and preventative measures by the concerned authorities helped in reducing the damage.

8.2

TROPICAL CYCLONES AROUND AUSTRALIA

Figure 8.3 shows the tracks in three hurricane seasons, 1988-89 to 1990-1991. The 1988-1989 tropical cyclone season was very active with 20 cyclones occurring from 70°E to 130°W, and six from 160°E to 170°E longitude. There were only 13 tropical cyclones during the 1989-1990 season with no events east of 170°E. Nine tropical cyclones developed during the 1990-1991 season, three in the Coral Sea and six in the Timor Sea.

The reduction in the number of tropical cyclones each season is consistent with the decline of the cold ENSO episode of 1988-1989. Twelve tropical cyclones originated between 150°E and 150°W during the cold event of 1988-1989 but only three during that of 1990-1991.

Damage and casualties on the Australian mainland resulted from the following four tropical cyclones:

(i) Aivu (April 1989): Hundreds of houses damaged or destroyed;

(ii) Nancy (January 1990): Heavy rain and flooding; 4 deaths.

(iii) Joy (December 1990): Floods resulting in $300 million (Australian $) damage; 5 deaths.

(iv) Fifi (April 1990): Extreme fire-weather conditions due to strong winds; 65 houses damaged.

8.3

WESTERN PACIFIC TYPHOONS

Numerous typhoons and tropical storms battered eastern and southeastern Asia in 1989. The Philippines was hit especially hard during October. Typhoons Angela and Dan struck the north on October 5 and 10-11, respectively, with a combined death toll of 168. On October 19, Typhoon Elsie crossed Luzon about 230 km northeast of Manila with peak winds of 200 km/h. It was judged the most powerful to strike the country since Nina in November 1987.

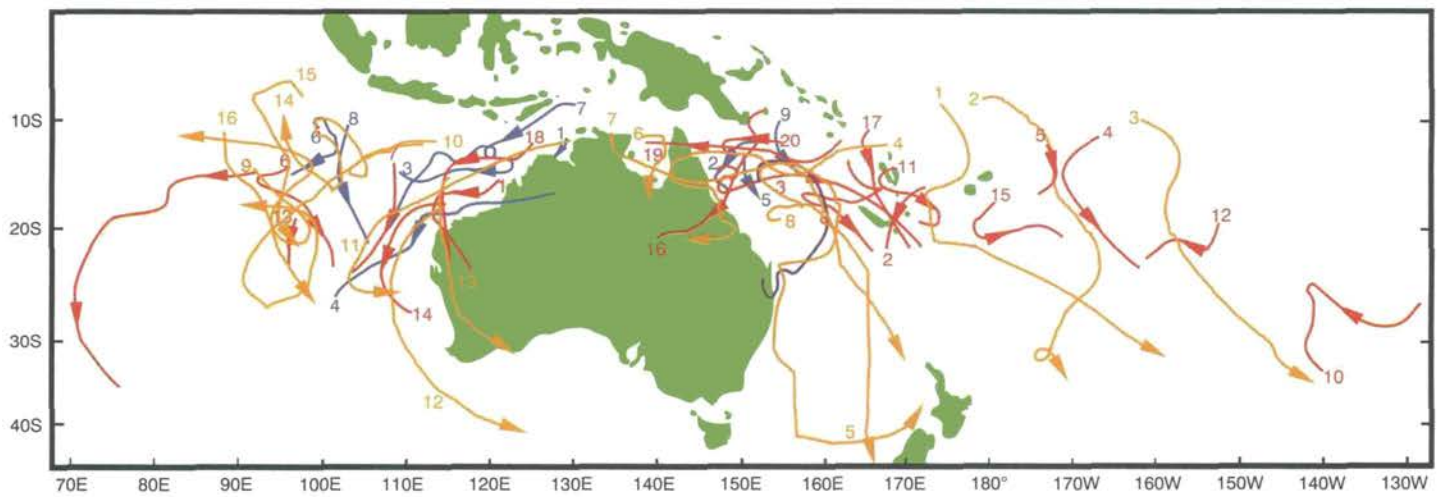

1988 / 1989

1 ILONA	6 JOHN	11 IVY	16 AIVU
2 ESETA	7 KIRRILY	12 JUDY	17 LILI
3 DELILAH	8 HARRY	13 MARCIA	18 ORSON
4 FILI	9 LEON	14 NED	19 MEENA
5 GINA	10 HINANO	15 KERRY	20 ERNIE

1989/1990

1 RAE	7 FELICITY	13 TINA
2 OFA	8 HILDA	14 ROSITA
3 PENI	9 WALTER	15 PEDRO
4 IVOR	10 ALEX	16 BESSI
5 NANCY	11 SAM	
6 GREG	12 VINCENT	

1990 / 1991

1 LAURENCE	4 DAPHINE	7 MARIAN
2 JOY	5 KELVIN	8 FIFI
3 CHRIS	6 ERROL	9 LISA

▲

Figure 8.3 - Tracks of tropical cyclones in the Australian region during the 1988-1989, 1989-1990 and 1990-1991 hurricane season (from Bureau of Meteorology, National Climate Centre, Melbourne, Australia).

BANGLADESH CYCLONE — APRIL 24-30, 1991

A devastating cyclone ravaged Bangladesh for more than eight hours on April 30, 1991, developing in a relatively short period into one of the worst natural disasters on record in the country. Many of the 125,000 deaths occurred on low-lying islands, where 7-m waves swept ashore. Many people survived by moving onto higher ground into concrete buildings that were converted to shelters after the 1970 storm. More bad weather and persistent flooding hampered relief efforts. Little food and unsanitary drinking water aggravated the misery for the estimated 10 million individuals left homeless by the storm.

The storm originated as a depression during the evening of April 24, over the southeastern Bay of Bengal (9.5°N, 89.0°E). The depression initially moved northwesterly and intensified into a cyclone on the morning of April 25, when it was centred near 11.0°N, 88.5°E (Figure 8.2). The system moved slowly westward during the next 24 hours, then recurved northwards and further intensified into a severe cyclonic storm with a core of hurricane winds by the evening of April 27. Moving north-northwest the cyclone lay at about 400 km south-southeast of Calcutta on the morning of April 28, 1991 before crossing the Bangladesh coast around midnight on April 29-30.

This was one of the most intense cyclones on record in the Bay of Bengal for April. Its maximum intensity occurred at 1130 IST on April 29, 1991, with a pressure drop of 80 hPa. The highest estimated wind speed was 235 km/h. At landfall, its pressure dropped 52 hPa and its wind speed approached 200 km/h. The storm surge was 6.0 m.

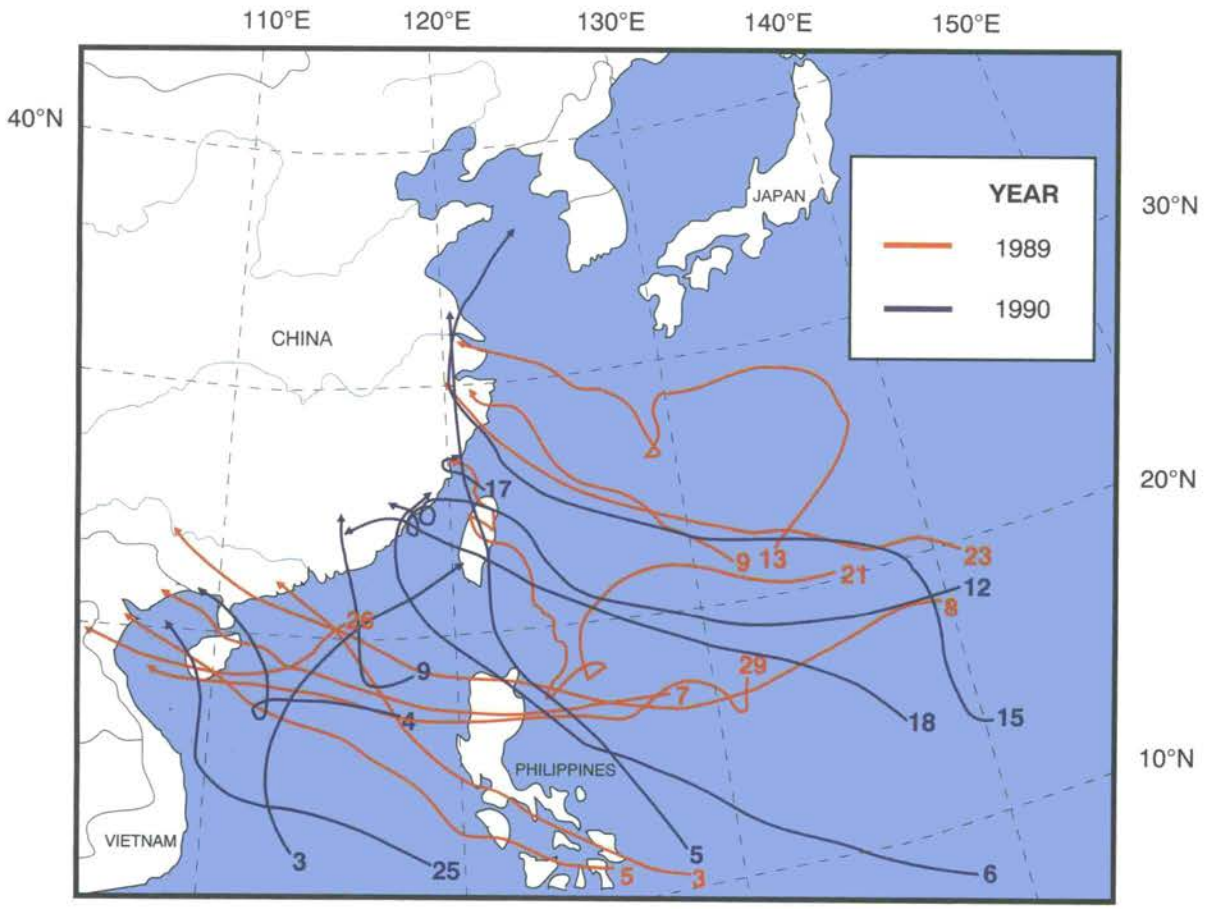

Figure 8.4 - Tracks of typhoons and tropical storms in the western North Pacific striking China during the 1989 and 1990 hurricane seasons (from Jiangsu Meteorological Institute, Nanjing, China).

Severe storms which battered northern Europe during February 1990 caused deaths and destruction to forests Deutscher Wetterdienst

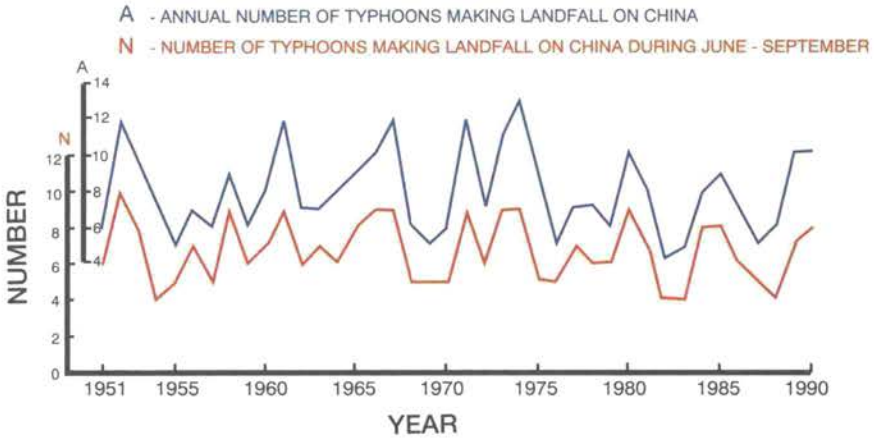

Figure 8.5 - The number of typhoons striking China from 1951 through 1990: (A) annual total, (N) June-September total (from Jiangsu Meteorological Institute, Nanjing, China).

►

From August 1 to September 23, seven typhoons/tropical storms affected Japan. Torrential downpours of more than 200 mm over portions of southern Honshu in less than 24 hours, resulted in landslides and major flooding. Precipitation during the period ranged from 200 to 400 mm over Hokkaido to more than 1000 mm over Shikoku.

On November 4, a rapidly intensifying storm, Typhoon Gay, struck Thailand's southern peninsula with 160 km/h winds. It was reported to be the most powerful storm to hit Thailand in at least 50 years. Nearly 200 ships capsized or sank. More than 1000 people drowned, mostly in Chumpon Province.

Of the 33 typhoons and tropical storms in the western Pacific (as numbered by the Central Meteorological Observatory of China), 10 landed in China. The tracks of landing typhoons in 1989 were more southerly than normal; the most northward only reached the mouth of the Yangtze River (Figure 8.4). Most of the rains were intense and of short duration, causing severe flooding, devastating landslides, and substantial losses of property and lives. Portions of coastal China and Vietnam were battered by Typhoons Gordon, Hope and Irving during the middle of July.

The year 1990 was another active one for tropical storms in the western Pacific with at least 30 depressions. Almost all struck land. The heavy rains were welcomed in drought-stricken parts of the Philippines and Japan, but also caused damaging floods in these countries, and in Taiwan, eastern China and Korea.

Typhoon Flo struck Japan on September 18-19, with sustained winds near 190 km/h at landfall. It was said to be the worst typhoon to hit the country since the early 1960s. Torrential rains greater than 400 mm caused flooding and landslides. In the Philippines, the worst of the 14 typhoons to hit this year, Typhoon Mike, arrived late in the season. Packing winds of 240 km/h, the storm destroyed or damaged over 600,000 houses and left more than 436 people dead.

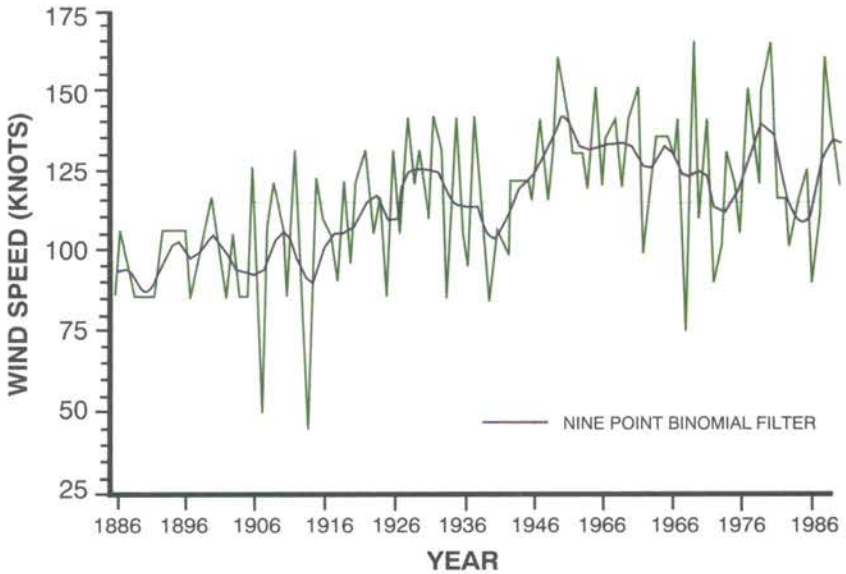

Figure 8.6 - The strongest hurricane-sustained wind speed for each year, 1886 through 1990, for the North Atlantic Ocean (including the Caribbean and Gulf of Mexico) (from NOAA, National Climatic Data Center, Asheville, NC).

►

Although the number of typhoons (29) in 1990 were somewhat less than in 1989 in the tropical western Pacific, the number of typhoons making landfall on China were the same in 1990 and 1989 (10, see Figure 8.5). Landfalls were also more southerly than normal (south of 29°N), but the typhoon damage was significantly larger than in the previous year. From mid-August to mid-September, four tropical cyclones hit southeastern China, including Typhoon Yancy, blamed for over 180 deaths in China and 11 in Taiwan. In 1990, tropical cyclones were responsible for more than 800 deaths, the loss of about 4.67 million ha of cropland and 400,000 houses. However, the abundant rainfall was welcomed in the drought-striken southern provinces.

8.4

EASTERN NORTH PACIFIC TROPICAL CYCLONES

Nine hurricanes and eight tropical storms occurred in the eastern North Pacific during 1989, close to the long-term average number of occurrences. The origins of all but one were associated with westward-moving tropical waves that came from the Atlantic Basin.

Cosme formed as a tropical depression south of Acapulco, Mexico, on June 18. It accelerated northward and moved onshore just east of Acapulco on the night of June 21. Heavy rains accompanied the hurricane over southern Mexico causing flash floods and mudslides over the coastal mountains. Ten deaths due to drowning were reported and many adobe houses were destroyed by floods. Maximum sustained winds were 140 km/h and the lowest sea-level pressure was 979 hPa, both estimated from satellite data just prior to landfall.

Raymond formed on September 25 south of Acapulco . It was the strongest eastern Pacific hurricane in 1989, with 235 km/h winds estimated on October 1 while the storm was a few hundred kilometres southwest of the southern tip of Baja California. Raymond rapidly moved across Baja and into the Mexican state of Sonora, where the mountains weakened the storm. Flash floods were reported over portions of southeast Arizona when it moved into the United States. Its estimated maximum wind of 231 km/h made Raymond the strongest hurricane of the 1989 eastern Pacific season.

A record 20 tropical storms (16 hurricane strength) occurred in

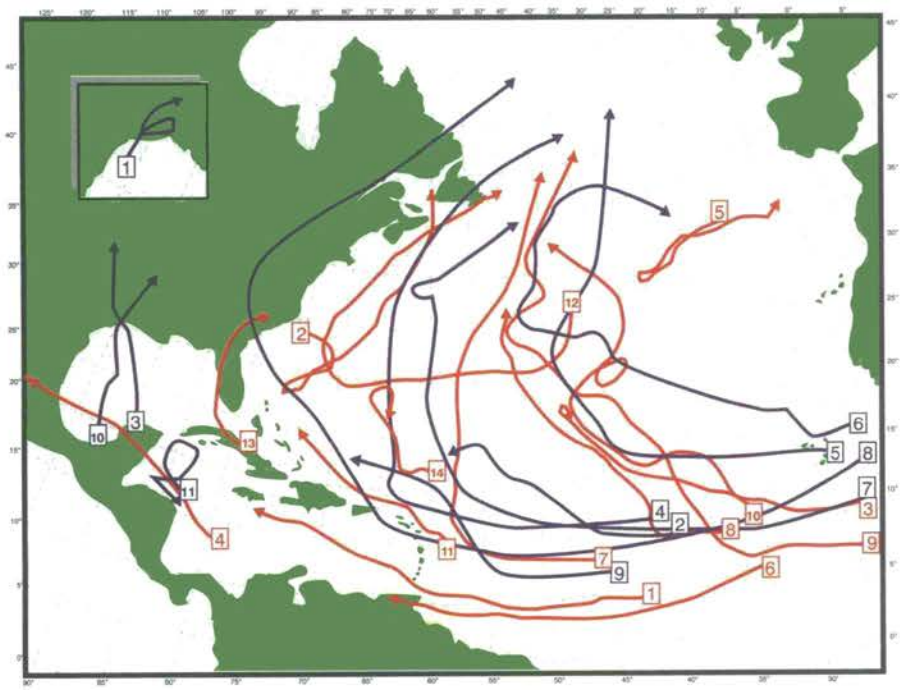

ATLANTIC-CARIBBEAN-GULF OF MEXICO-STORM TRACKS

1989

NUMBER	TYPE	NAME	DATE
1	T	Allison	Jul 24 - 27
2	T	Barry	Jul 09 - 14
3	H	Chantal	Jul 30 - Aug 3
4	H	Dean	Jul 3 - Aug 8
5	H	Erin	Aug 18 - 27
6	H	Felix	Aug 26 - Sep 9
7	H	Gabrielle	Aug 30 - Sep 13
8	H	Hugo	Sep 10 - 22
9	T	Iris	Sep 16 - 21
10	H	Jerry	O ct 12 - 16
11	T	Karen	Nov 28 - Dec 4

1990

NUMBER	TYPE	NAME	DATE
1	T	Arthur	Jul 22 - 27
2	H	Bertha	Jul 24 - Aug 2
3	T	Cesar	Jul 31- Aug 7
4	H	Diana	Aug 4 - 9
5	T	Edouard	Aug 2 -11
6	T	Fran	Aug 11-14
7	H	Gustav	Aug 24 - Sep 3
8	T	Hortense	Aug 25 - 31
9	H	Isidore	Sep 4 - 17
10	H	Josephine	Sept 21- Oct 6
11	H	Klaus	Oct 3 - 9
12	H	Lili	Oct 6 - 14
13	T	Marco	Oct 9 - 12
14	H	Nana	Oct 16 - 21

◄ *Figure 8.7* - Tracks of hurricanes and tropical storms in the North Atlantic during the 1989 and 1990 hurricane seasons (from *Mariners Weather Log*, Spring 1990 and 1990 issues).

the eastern North Pacific during 1990, including several very strong ones. The 16 hurricanes were twice the average number and 4 more than the previous record. (However, reliable records extend only to the mid-1960s for this region.) The origin of all the storms and hurricanes was apparently associated with westward-moving African waves. All but two developed between 5 and 15°N latitude, east of Baja California.

Alma was the earliest eastern Pacific hurricane on record (May 12-18). Locally heavy rains traced to Hurricane Boris affected the southwestern United States, giving San Diego the wettest June on record (since 1850). Satellite-based estimates of the maximum wind

HURRICANE HUGO

The tropical cyclone that spawned Hugo originated from a cluster of thunderstorms that moved off the African coast on September 9, 1989 and evolved into a tropical depression on the 10th just southeast of the Cape Verde Islands. Hugo followed a westerly course across the Atlantic, becoming a tropical storm on the 11th, and a hurricane on the 13th while located about 2040 km east of the Leeward Islands. On the 15th, still several hundred kilometres east of the Islands, Hugo achieved its maximum strength, with an estimated 260 km/h surface wind and a minimum central pressure of 918 hPa.

Hugo's eye passed over the island of Vieques, Puerto Rico, at 1200 UTC on the 18th, then over the eastern tip of the Puerto Rico mainland one hour later. Hugo dumped up to 233 mm of rain in the eastern interior of Puerto Rico and caused water levels estimated at 0.9 to 1.2 m above normal tide during onshore winds at St. Croix and along the eastern end of Puerto Rico.

Hugo continued weakening while moving north, then northwest of Puerto Rico on September 19 and 20. Then, on the 21st, Hugo began to re-intensify and accelerated toward South Carolina in response to a steering flow associated with a major extratropical low that was advancing eastward across the central United States (Fujita and Stiegler, 1989). The hurricane was taking dead aim at Charleston, South Carolina. Just prior to landfall, measurements from reconnaissance aircraft indicated Hugo had a minimum central pressure of 934 hPa and an estimated, maximum one-minute wind speed of 222 km/h.

By the time Hugo made landfall, the system had become quite large, causing the effects of the storm surge to be felt across a sizeable portion of the mid- and south-Atlantic coast. A storm tide of 3.2 m above mean sea level, corresponding to a storm surge of 2.4 m above the predicted normal astronomical tide, was recorded in Charleston, and high-water marks at Bulls Bay indicated a storm tide of nearly 6 m above mean sea level. Even as far north as Hatteras, North Carolina, the surge was 1.2 m above the predicted tide.

The rapid rate of Hugo's forward translation at landfall also carried the hurricane well inland before it could significantly weaken. At 0800 UTC September 22, four hours after landfall, Hugo was still estimated to be of hurricane strength while its centre passed over central South Carolina.

As noted by Fujita and Stiegler (1989), the extent of damage caused by Hugo's winds was enormous. Almost the entire eastern two thirds of South Carolina and much of central North Carolina suffered wind damage, largely caused by falling trees and limbs in heavily forested areas. Extensive long-term power outages occurred and much beachfront property was destroyed. An estimated $7 billion (US) in damage occurred on the U.S. mainland and $3 billion (US) elsewhere, making Hugo the costliest hurricane in history (Mayfield and Case, 1990). An estimated 82 deaths were attributed to Hugo, 41 on the United States mainland. In spite of the excellent warning lead times and rapid government and public response to the warnings, the fury of Hurricane Hugo took many by surprise and will undoubtedly haunt the memories of many people for years to come (Fujita and Stiegler, 1989).

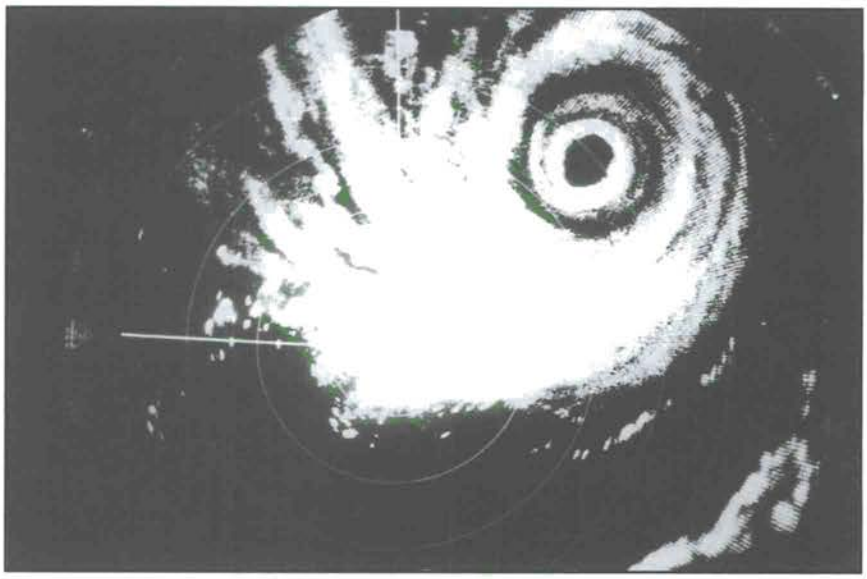

Radar picture of the Machilipatnam Cyclone, 1100 UTC May 8, 1990, taken from the Cyclone Detection Radar site at Madras (from India Meteorological Department, New Delhi).

speeds of 250 km/h, and minimum sea-level pressures of 928 and 925 hPa, respectively, made Hurricanes Hernan and Trudy two of the strongest in recent history in the eastern Pacific, at least as strong as Hurricane Max of 1987 (credited as being the strongest on record for the region). Rachel was the only system to make landfall, which occurred between September 27 and October 3.

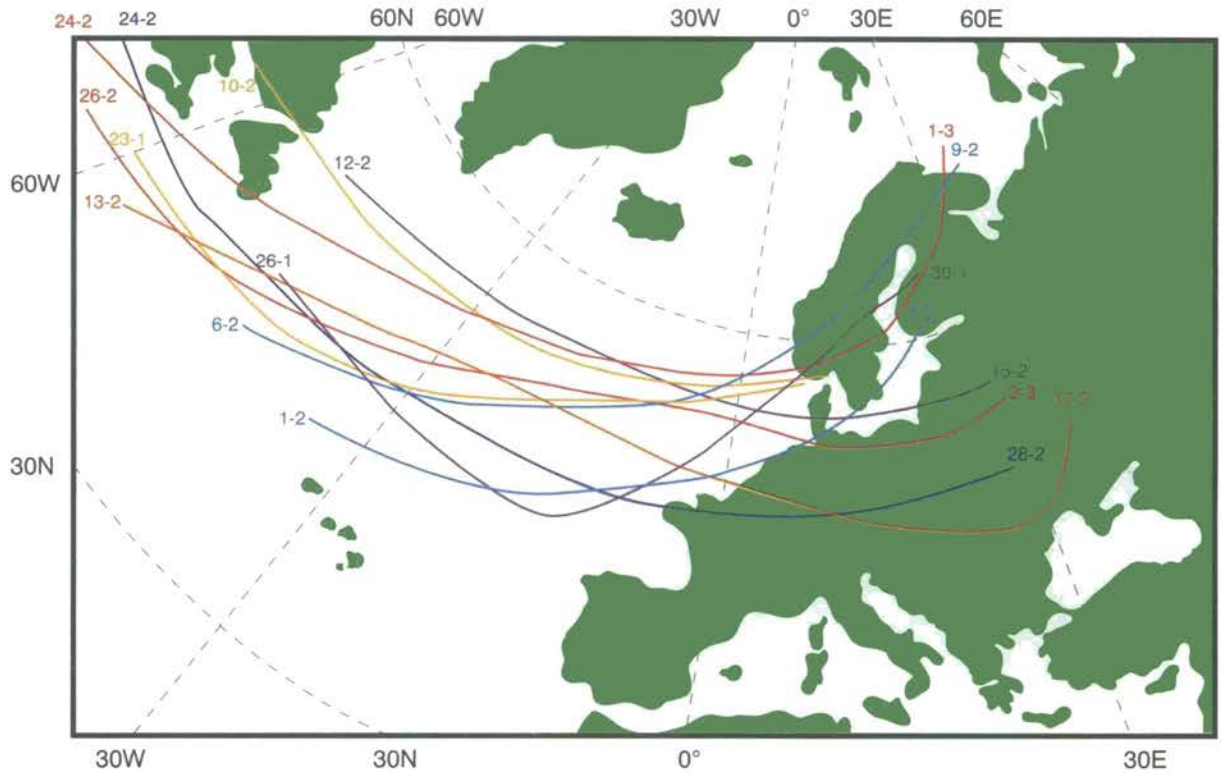

Figure 8.8 - Tracks of nine cyclones with hurricane-strength winds in western and central Europe from January 25 to March 2, 1990 (from Doberitz, 1990).

Kasiviswanathan temple broken and shifted during the Machilipatnam Cyclone (from India Meteorological Department, New Delhi).

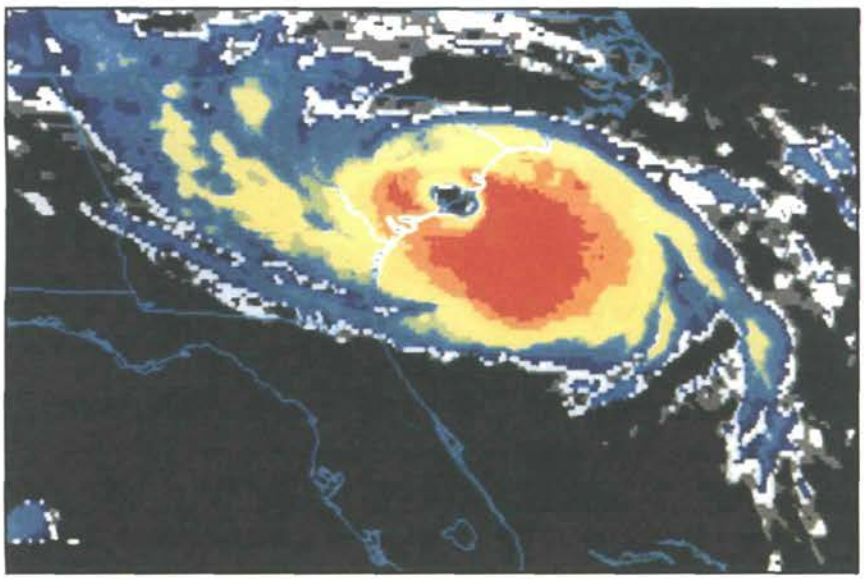

GOES-7 colour-enhanced infrared satellite picture of Hurricane Hugo, 0401 UTC September 22, 1989, making landfall at Charleston, S.C., on the United States mainland (from NOAA, National Climatic Data Center, Satellite Data Services Division, Washington, DC).

8.5

HURRICANES AND TROPICAL STORMS IN THE NORTH ATLANTIC

Though tropical cyclone activity in the Atlantic, Caribbean and Gulf of Mexico during 1989 was just slightly above normal, the trend for large, strong Cape Verde hurricanes continued (see Figure 8.6). Hurricane Hugo reached category five on the Saffir/Simpson scale and caused an estimated $10 billion (US) damage. Gabrielle was another large such hurricane that reached category four, but it remained at sea.

Tropical Storm Allison and Hurricane Chantal caused damage, mainly due to torrential rains and flooding, and deaths, due to drowning, along the upper Texas coast and western two thirds of Louisiana (Figure 8.7). Allison formed from the remnants of eastern Pacific Hurricane Cosme and the northern portion of a westward-moving tropical wave. In all, nearly 750 mm of rain fell at a few locations in north-central Louisiana, and amounts from 250 to 375 mm were common along the upper Texas coast.

The system that provided the embryo for Chantal first appeared on July 24 as an Intertropical Convergence Zone (ITCZ) disturbance near Trinidad. The system moved

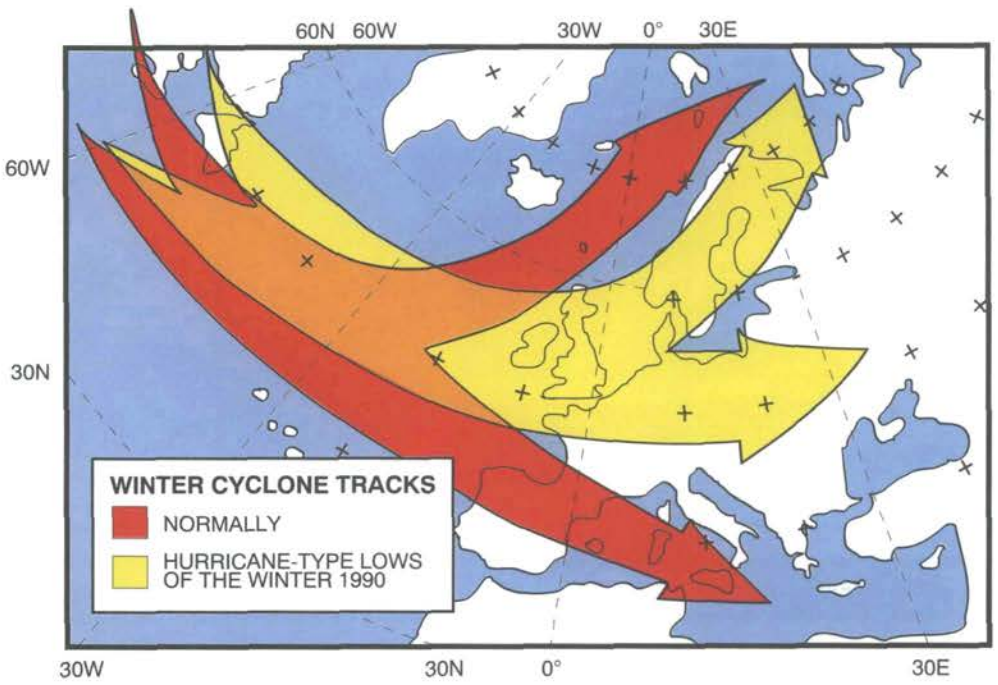

◄ *Figure 8.9* - Winter cyclone tracks. Red arrows depict storm tracks during a normal winter. Yellow arrows depict tracks of major storms during January/ February 1990 (from Doberitz, 1990).

westward across the Caribbean and Central America, forming a depression on the morning of July 30 in the Gulf of Mexico off the northwestern Yucatan peninsula. Hurricane Chantal made landfall near High Island, Texas, during the morning of August 1, with top winds of 130 km/h and a central pressure near 986 hPa. The centre of Chantal continued moving northwestward and dissipated in southwestern Oklahoma after midnight on August 3. The 24-hour rainfall amounts associated with Chantal ranged from 55 to 200 mm.

While never making landfall, the powerful winds of the very large hurricane Gabrielle generated large ocean swells that pounded the shores of the north-

EUROPEAN WINTER STORMS IN 1990 AND THE RESULTING LOSSES

Date	Area	No. of Deaths	Overall Losses Millions of $ (US)	Comments
1990				
Jan. 25, 26	Western and Central Europe	90	6,800	greatest event of storm damage up to now especially in Great Britain, and Benelux countries
Feb. 3, 4	Central Europe	30	1,900	hit Paris, Luxembourg, Germany
Feb. 7, 8	Western and Central Europe	17	300	storm and floods
Feb. 11, 12	Western Europe	1	100	
Feb. 13, 15	Central Europe	25	300	floods, snow storm, avalanches
Feb. 25, 27	Western, Central	64	3,200	storm and tidal wide, huge forest damage in Central Europe
Feb. 28 — March 1	Western and Central Europe	34	2,200	storm and tidal wave, huge forest damage in Central Europe

(from: Munich Reinsurance Co, July 1991)

eastern Caribbean islands, Bermuda, and the North American mainland from central Florida to the Canadian Maritimes during late August and early September. Swells ranged from 3 to 4.5 m along portions of the United States east coast and were as high as 6 to 9 m along the south coast of Nova Scotia. The storm was responsible for eight deaths along the mid-Atlantic and New England coasts.

Hurricane Jerry made landfall on the upper Texas coast on October 16; no hurricane had ever made landfall there so late in the season. Twenty-four hour rainfall totals were in the range, 125 to 175 mm. Tropical Storm Karen was another late-season storm, which has been a trade mark of the 1980s. In the past 100 years, there has been an average of four named November tropical cyclones per decade. During the 1980s, there were eight. Karen formed in the western Caribbean from an African wave on the evening of November 27 and later dropped 250-380 mm of rain over portions of central and western Cuba.

Eight hurricanes and six tropical storms developed during the 1990 hurricane season (Figure 8.7). Although the season was quite active, only one hurricane (Gustav) generated maximum sustained winds greater than 185 km/h, and many of the tropical systems recurved over the central Atlantic in response to a persistent upper-level trough. Gustav reached hurricane strength east-northeast of Barbados on the 26th. Its minimum central pressure of 956 hPa, and maximum sustained winds of 200 km/h occurred about 800 km east-southeast of Bermuda.

Hurricane Diana, which formed from a classical tropical wave off Africa on July 27, reached tropical storm intensity on August 4 and crossed the Yucatan Peninsula of Mexico, then strengthened rapidly while moving into the Bay of Campeche. The minimum central pressure of 980 hPa and maximum sustained winds of 170 km/h occurred just before landfall near Tuxpan, Mexico. The hurricane was estimated to cause 96 deaths while it moved into Mexico, and extensive damage to property, agriculture, and roads in mountainous areas in the states of Hidalgo and northern Veracruz, mostly from torrential rains that triggered mudslides and flooding.

8.6

THE STORMY ATLANTIC — JANUARY/FEBRUARY 1990

During a five-week period in January and February 1990 the North Atlantic bred nine very intense storms that struck northern Europe with hurricane-force winds (Figure 8.8). The winter storms favoured a track across northern and central Europe in contrast to the usual branch pattern over the Mediterranean Sea and the North Sea (Figure 8.9). Storms penetrated well into Europe in the absence of any blocking anticyclone.

The first major storm struck England on January 25. Winds up to 200 km/h knocked out power and phone service to hundreds of thousands of customers. The winds downed trees, blew roofs off buildings, and knocked over trucks. Storm-related deaths in Britain and Europe totalled 93.

Only four days later, on January 29, a second storm battered southwestern England, toppling trees and causing landslides and floods. A third major storm struck during the first week of February, leaving a trail of destruction across northern Europe, It was one of France's worst storms in recent decades. The last of the severe storms hit Europe at the end of February. Winds up to 160 km/h levelled huge stands of trees in central Europe. In Germany, downed timber represented twice the average annual harvest. The last storm killed 63 in addition to at least 25 forest workers who died in accidents during cleanup efforts.

8.7

RECORD TORNADO ACTIVITY ACROSS THE UNITED STATES

Tornadoes are short-lived small-scale severe weather phenomena, each consisting of a destructive whirlwind in the shape of a funnel descending from a cumulonimbus cloud base. The synoptic situation in the United States favouring tornado formation is a southwesterly circu-

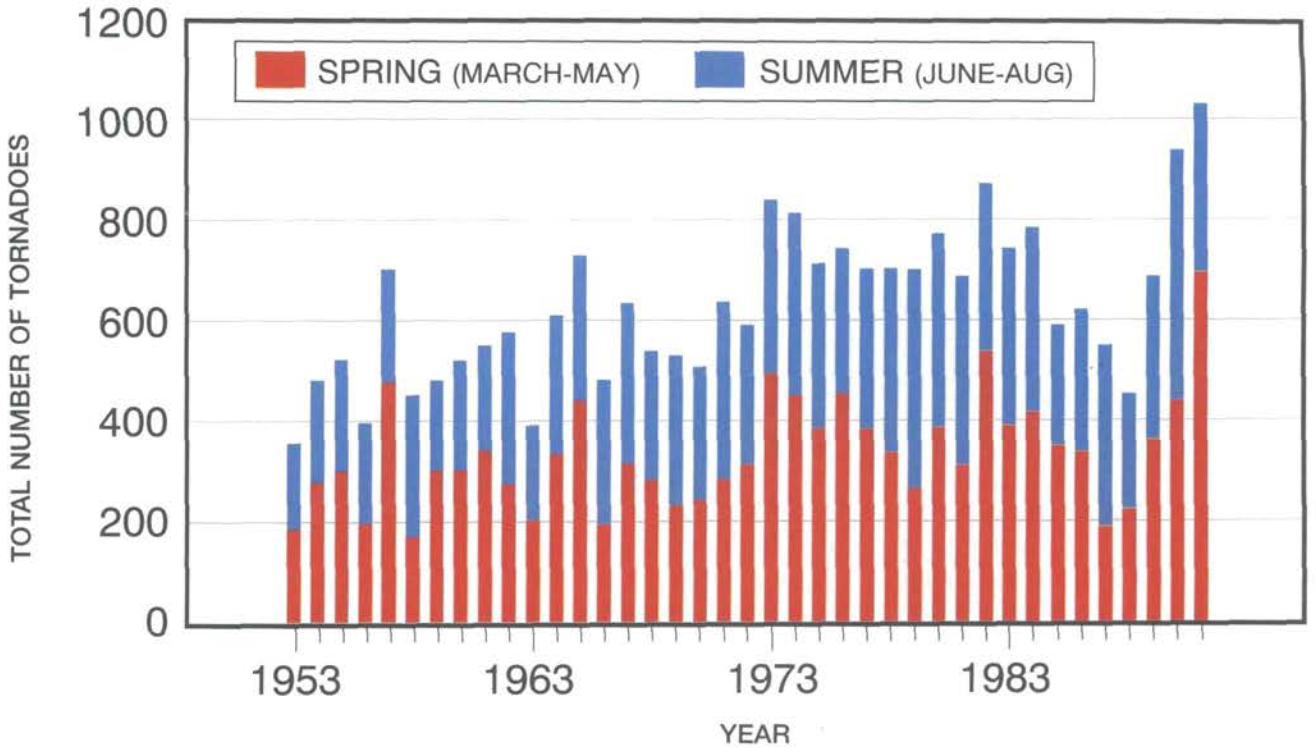

▲
Figure 8.10 - Total number of tornadoes occurring in the United States in spring (March-May) and summer (June-August), 1953-1991. Data prior to the 1950s are considered less complete owing to changes in observing practices and systems (e.g., weather radar, which came into widespread use during this time) (from NOAA, National Climatic Data Center, Asheville, NC).

lation in the upper atmosphere over the western and central states. This pattern directs warm moist air from the Gulf of Mexico into the interior United States. When cold air from the north and west clashes with the warm humid air, the resulting instability enhances tornado development.

After five years of fewer than normal tornadoes, the 1989 and 1990 tornado seasons were well above normal, with 845 and 1126 tornadoes, respectively. The 1990 season set a new yearly record for the most tornadoes. However, the corresponding death tolls, 48 - 53, were each well below the 30-year average of 82. In both years there was an increase in violent tornadoes.

GLOBAL CLOUDINESS CONTINUES TO DECREASE IN 1989 AND 1990

Photo Grant W. Goodge

Information received from the Institute for Global Climate and Ecology in Moscow indicates a continued decrease in average cloudiness over the globe (Figure 9.1) and over both the Northern and Southern hemispheres during 1989 and 1990. The decrease in cloudiness is pronounced after 1986, especially in the Southern ►

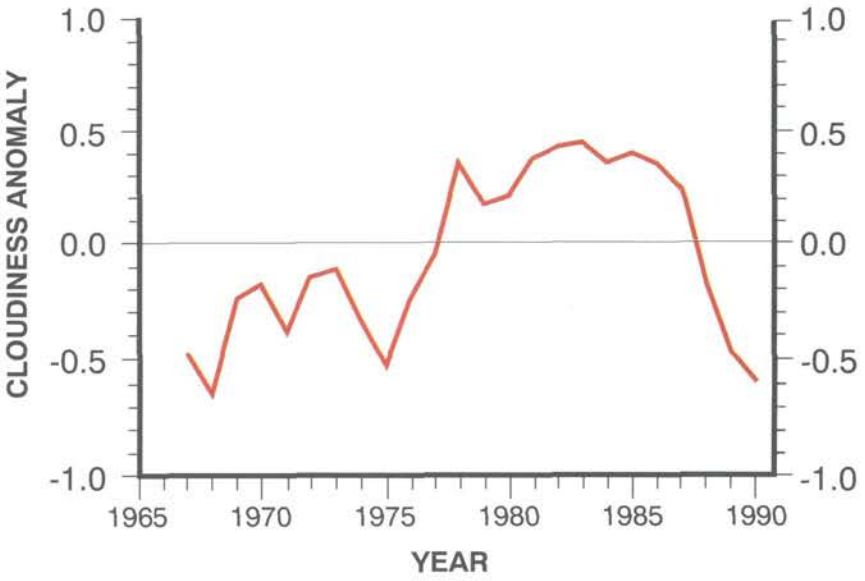

Figure 9.1 - Regionally averaged annual (December-November) total cloudiness anomalies for the world from 1965-1966 to 1989-1990. The anomalies (expressed in tenths) were computed relative to the period 1966-1985 (from Institute for Global Climate and Ecology, Moscow).

Hemisphere. Over the globe and both hemispheres, the cloudiness values dropped below normal in 1988, reaching a minimum by 1990. Average annual cloudiness values for the period 1966 to 1985 over the globe and the Northern and Southern hemispheres are 5.8, 6.2 and 5.3 tenths, respectively. In 1990, average annual cloudiness over the globe was 5.2 tenths — 0.6 less than normal, and 0.5 less than in 1989. In the Northern Hemisphere, average annual cloudiness in 1990 was 0.5 tenths less than in the Southern Hemisphere.

Similar analyses (not shown) for Eurasia and North America show a decreasing trend during the last half of the 1980s; however, cloudiness increased in 1990 to near normal values.

Figure 9.2 shows the variation in cloudiness with latitude for the Northern and Southern hemispheres during the review period. Pronounced regional negative anomalies occurred in the Southern Hemisphere. They developed in tropical latitudes in September 1989 and extended into mid-latitudes by March 1991. Only Antarctica had persistent positive anomalies during most of the review period; however, even these were not large. Positive anomalies occurred over the Northern Hemisphere and mid- and high latitudes (especially over Eurasia) during the northern cold seasons of 1988-1989 and 1989-1990.

The cloudiness data are based on analysis of visible and infrared images from the "Meteor" satellite system (Matveev, 1986). The dataset comprises daily data on a 5° x 10° grid covering the Northern and Southern hemispheres (Aristova and Gruza, 1987). Spatial

Figure 9.2 - Time-latitude section of the monthly mean total cloudiness, averaged for specific latitudinal circles. Cloudiness anomalies (departures from the 1966-1985 normals), expressed in tenths, for December 1988 to May 1991 (solid lines are positive anomalies; dashed are negative anomalies) (from Institute for Global Climate and Ecology, Moscow).
▼

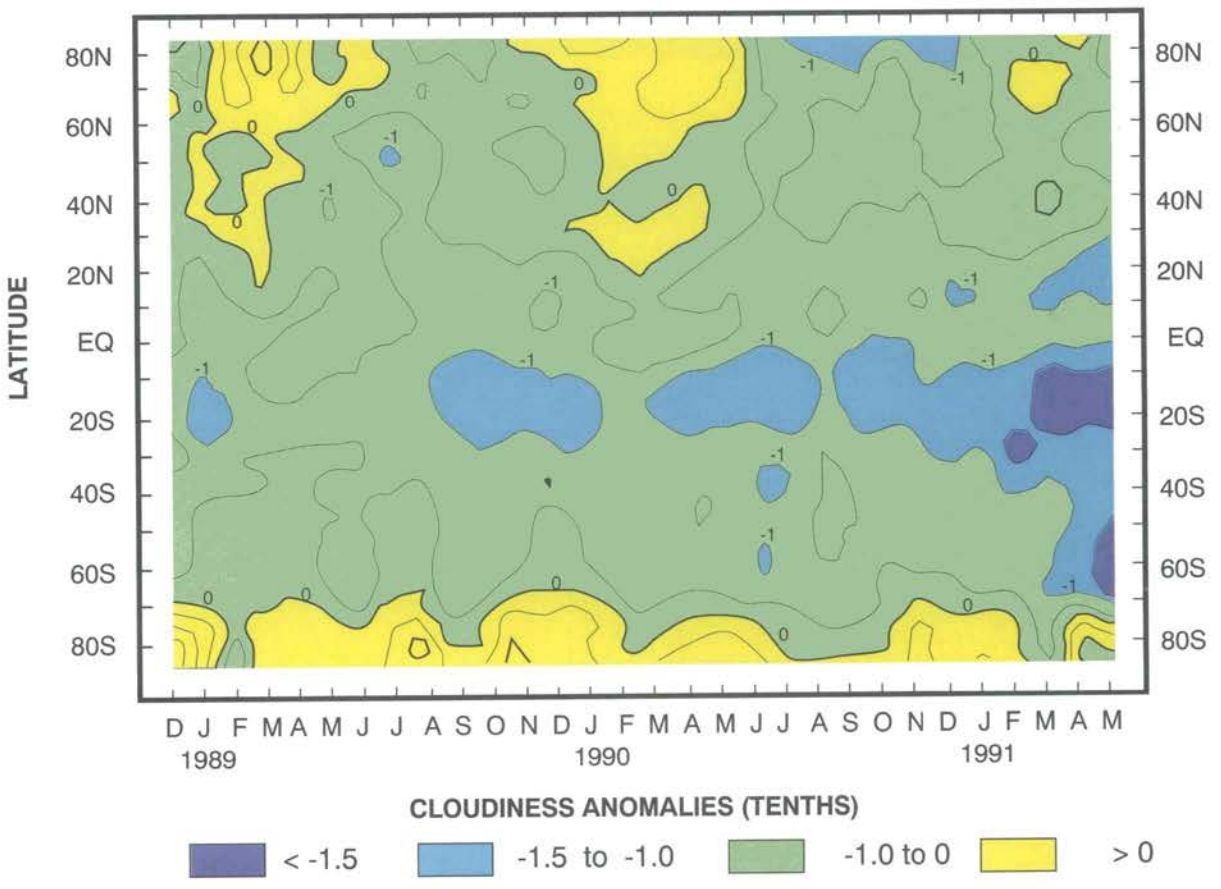

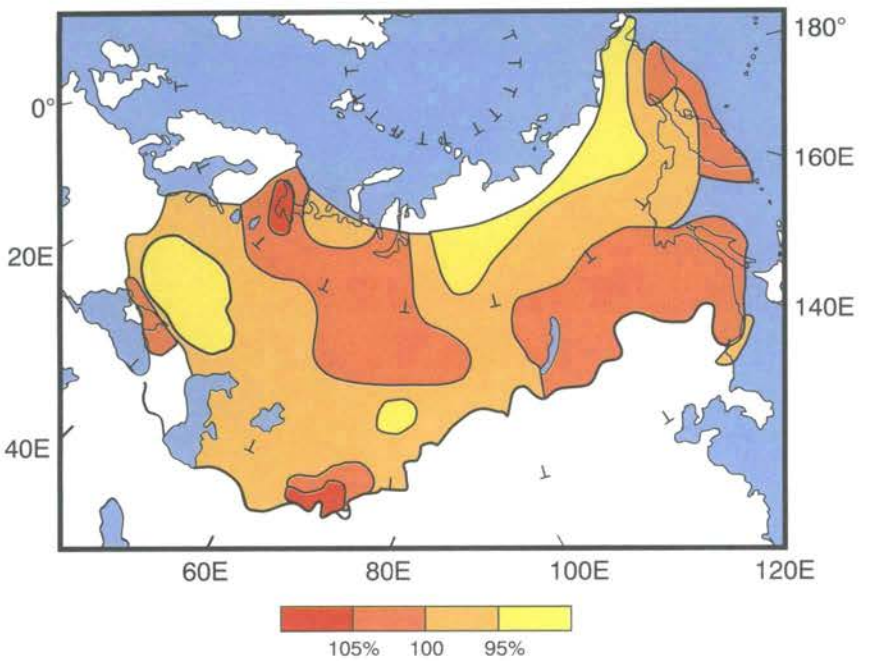

▲
Figure 9.3 - Annual total global radiation anomalies in 1989 (per cent of 1957-1980 normals) for the territory of the former Soviet Union (from Laboratory of Solar Radiation, Main Geophysical Observatory, St. Petersburg).

Figure 9.4 - Annual total global radiation anomalies in 1990 (per cent of 1957-1980 normals) for the territory of the former Soviet Union (from Laboratory of Solar Radiation, Main Geophysical Observatory, St. Petersburg).
▼

averaging is carried out for 62 regions including the globe, the Northern and Southern hemispheres, the continents and oceans, the largest countries, and 10° latitudinal circles and latitudinal zones. Annual values were calculated from mean monthly cloudiness values, which were computed by averaging the daily data.

Figures 9.3 and 9.4 show anomalies (per cent) of annual total global radiation in 1989 and 1990 relative to the averaging period 1957-1980. In 1989 and 1990, the area of most pronounced negative anomalies (less solar radiation reaching the Earth's surface than average) occurred over the European territory and in the near-polar latitudes of eastern Siberia. Extensive areas of positive anomalies during 1989 and 1990 occurred along the Black Sea coast, in western Siberia, in the temperate latitudes of middle Siberia and along the Amur River.

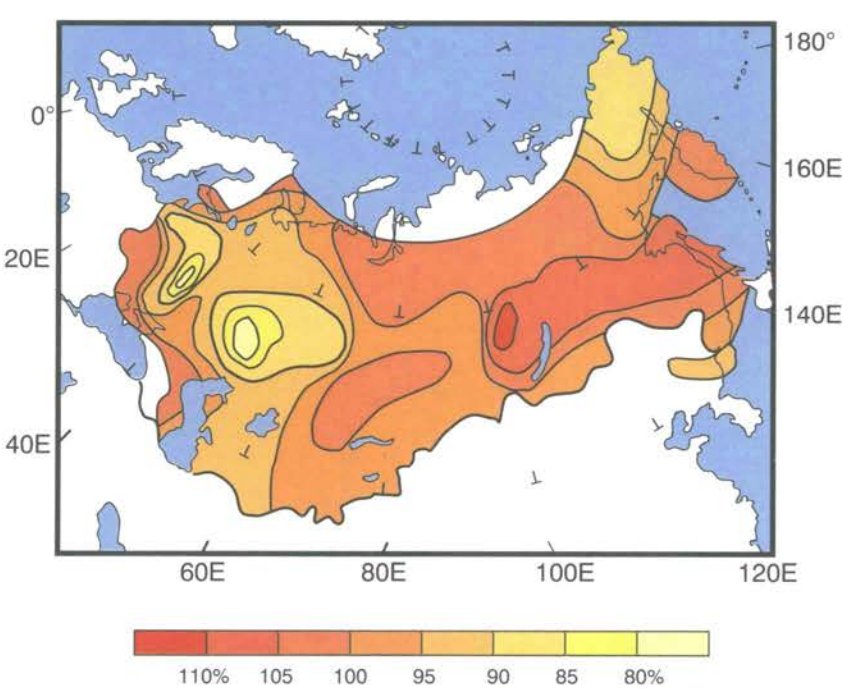

The depletion of stratospheric ozone by anthropogenic trace gases continues to be a topic of great importance and keen international interest. Major assessments of global ozone trends were completed in 1989 (WMO, 1989) and 1991 (WMO, 1991). Readers are referred to the latter report for a comprehensive discussion of stratospheric ozone trends over the last two decades and the related environmental implications. The 1991 report incorporated the newly revised satellite data from the Total Ozone Mapping Spectrometer (TOMS), which used a new, *independent* calibration of its sensor (see Figure 10.1 for a summary of the TOMS ozone trend results). Data from surface-based Dobson and M83/124 stations in the former territory of the Soviet Union were also part of the basis for the assessment and all three instrument types showed, after the known natural variability was accounted for, significant decreases in total column ozone.

The findings from the new 1991 assessment for the period from the late 1960s to 1991 include the following:

- *In the tropics (25°N-25°S):*
  No substantial change in stratospheric ozone has been detected.

- *In the mid-latitudes (35°-64°N and S):*
  A mean decrease of about 2.5% per decade in the total column ozone has been observed. The depletion was greatest during the winter-spring season, and averaged about 1% per decade during the summer, which is still statistically significant.

- *In the Polar Regions (poleward of 64°):*
  The north and south polar regions showed decreases of about 3 and 20% per decade, respectively, with the greatest changes occurring during the winter-spring seasons. The large Southern Hemisphere decreases were strongly influenced by the onset of the Antarctic ozone hole, which first appeared in the late 1970s.

- *In the troposphere:*
  Measurements up to about 10-km altitude above the few balloonsonde stations of the Northern Hemisphere mid-latitudes indicate that ozone amounts have increased by about 10% per decade over the last 20 years. The WMO assessment cautioned, however, that

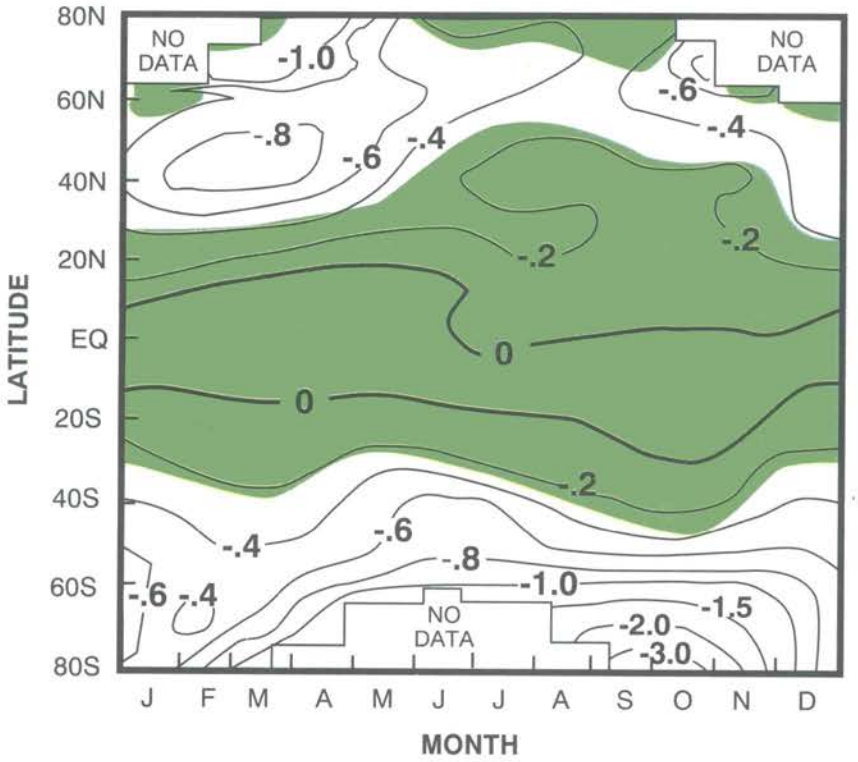

◄ *Figure 10.1* - Total ozone trends (per cent per annum), 1979-1990, as a function of latitude and season, deduced from the TOMS satellite instrument (from Stolarski et al., 1991).

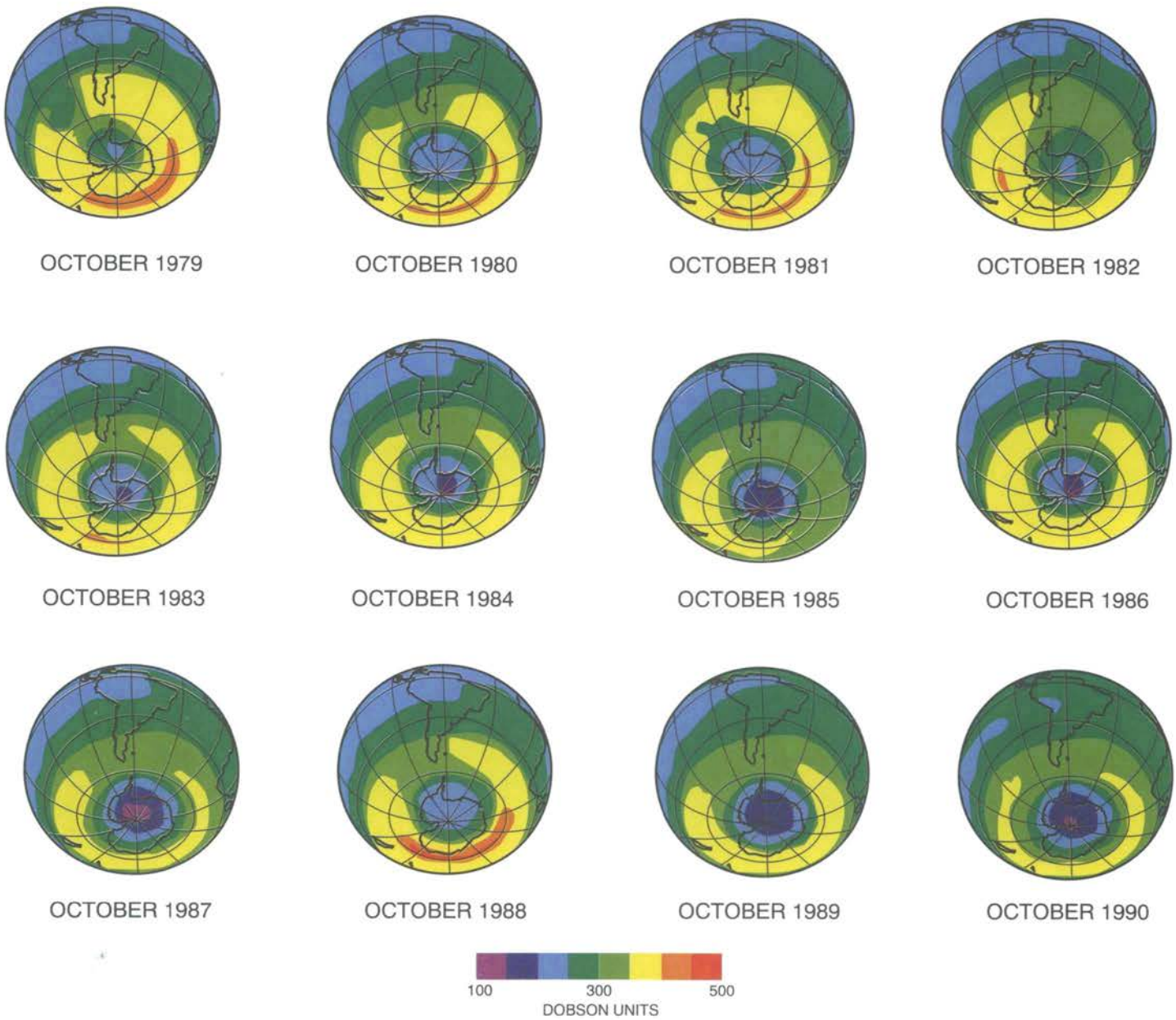

▲ *Figure 10.2* - Monthly mean October total column ozone (colour-coded in Dobson units) over the Southern Hemisphere, 1979-1990, from the NIMBUS 7 TOMS satellite instrument (from NASA/Goddard Space Flight Center).

Table 10.1 - Regional long-term ozone trends (per cent per decade) derived from ground-based Dobson total ozone data from January 1958 to March 1991. Estimates were made using the Allied statistical model with a linear trend fit over the period 1970-1991 (Bishop and Bojkov, 1992).

	Year-Round		Dec-Mar		May-Aug		Sep-Nov	
	Trend	SE	Trend	SE	Trend	SE	Trend	SE
North America	-2.1	0.3	-3.2	0.4	-1.7	0.4	-1.1	0.3
Europe	-1.8	0.3	-2.9	0.4	-1.2	0.3	-1.2	0.3
Far East	-1.2	0.4	-1.8	0.5	-0.9	0.5	-0.4	0.4
36° — 64°N	-1.8	0.2	-2.7	0.3	-1.3	0.2	-1.0	0.2

Causes for the measured global ozone trends could not be fully determined. The most plausible mechanism highlighted is "local heterogeneous chemistry of stratospheric sulphate aerosols" in the presence of mostly anthropogenic chlorine and bromine.

the available data are sparse, especially for the upper troposphere where ozone is an effective greenhouse gas.

The Antarctic ozone hole during the Southern Hemisphere spring of 1991 was again very significantly developed (in both ozone loss and spatial extent) as it was during 1987, 1989 and 1990 (Figure 10.2). In early October 1991, the TOMS satellite instrument measured a minimum value of 108 Dobson units, only 30% of the pre-hole conditions prior to

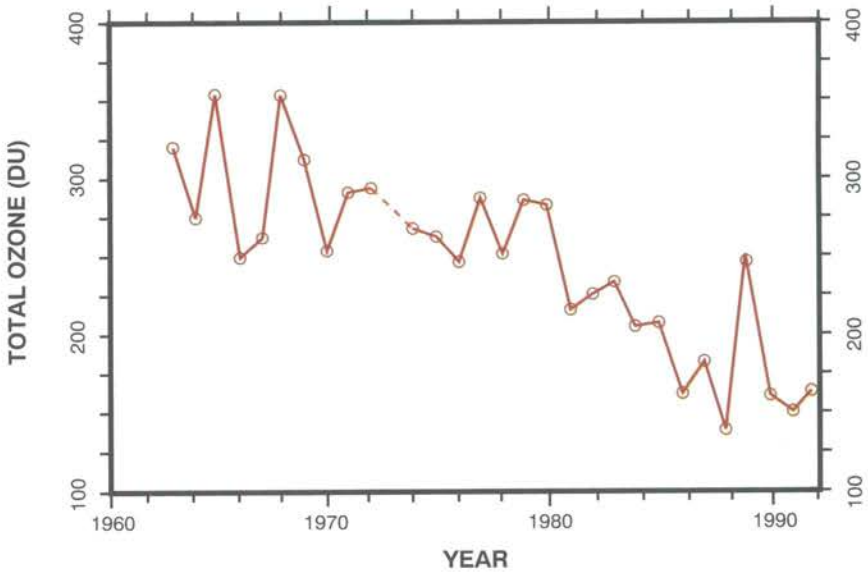

Figure 10.3 - Mean total ozone (in Dobson units) measured at the South Pole, Antarctica, with a Dobson spectrophotometer during October 15-30, 1962-1991 (from W. Komhyr, Environmental Research Laboratories, NOAA, Boulder, CO).

►

the late 1970s. Mean total ozone values for the South Pole for October 15-31 are shown in Figure 10.3, which is an update of Figure 40 from the 1986-1988 edition of *The Global Climate System* review. The weight of experimental (laboratory, ground-based and aircraft-based) and theoretical evidence strongly indicates that anthropogenic chlorine and bromine compounds are primarily responsible for the hole. Polar Stratospheric Clouds (PSC), which form at temperatures below -80°C, facilitate the heterogeneous chemical reactions that initiate the ozone depletion. Over north polar regions, the same potentially ozone-destroying processes have been identified, but the necessary meteorological conditions (i.e., extremely cold stratospheric temperatures) exist only infrequently.

Stratospheric ozone concentrations are modulated by the 11-year cycle of solar variability and the associated ultraviolet radiation output. During the review period, the solar radiation output was near its maximum. The solar sunspot record, which is an approximate indicator of

OZONE*

Ozone is much more reactive than oxygen and is toxic to human beings and living matter. As a pollutant at ground level it is suspected of damaging forests. In the stratosphere it functions both as a greenhouse gas and as a filter for ultraviolet radiation. A fall in the total ozone concentration, and the consequent rise in the penetration of ultraviolet radiation, could cause deleterious effects, such as increased incidence of skin cancers.

The concern that resulted in governments signing the 1987 Montréal Protocol with unusual speed arises from the realization that the ozone layer in the stratosphere is being destroyed by man-made substances called chlorofluorocarbons (CFCs) and halons. These are used as refrigerating fluids and spray-can propellants because they are convenient, cheap and very non-reactive (stable). However, this stability allows them to remain in the troposphere for many decades. As they diffuse eventually into the stratosphere, the chlorine they contain is liberated and catalyses the breakup of ozone. The theory of this process was known since 1974 through the work of Professors Rowland and Molina in California. The most dramatic manifestation of ozone depletion — the famous Antarctic ozone hole — was first detected by Dr. Joe Farman at the British scientific station in Antarctica from routine measurements as part of the WMO Global Ozone Observing System (GO_3OS).

The greenhouse effect depends on ozone in two ways:

- First, it absorbs infrared radiation just as carbon dioxide and the CFCs do, contributing directly to the effect.
- Second, a decrease in total ozone, which allows more ultraviolet radiation to reach the upper layers of the sea, may cause the death of phytoplankton. If this happens the marine biomass will be less able to absorb the carbon dioxide dissolved in the water, reducing the ocean's effectiveness as a carbon sink; the effect would be to leave more carbon dioxide free in the atmosphere.

** Adapted from World Meteorological Organization, 1990: The WMO Achievement — 40 years in the service of international meteorology and hydrology. WMO-No. 729, Geneva, 44 pp.*

Figure 10.4 - Monthly mean Zurich sunspot numbers, 1955-1990 (from National Geophysical Data Center, NOAA, Boulder, CO).
▼

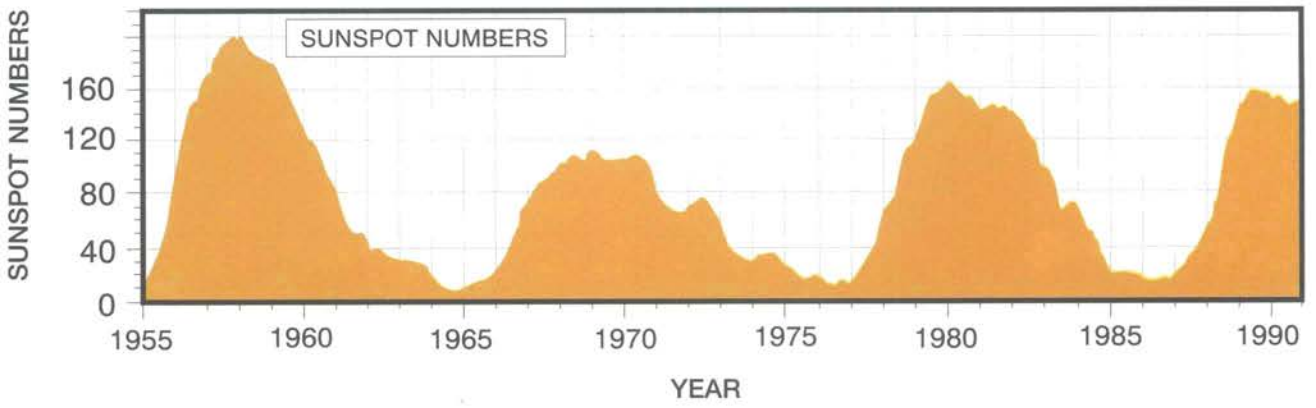

actual output, is shown in Figure 10.4. Stratospheric sulphur gases and particles from volcanic eruptions also facilitate the depletion of ozone through chemical interactions and the reduction of incident ultraviolet radiation. During 1989-1991, stratospheric aerosol amounts were quite low. The record of "apparent" atmospheric transmission from Mauna Loa, Hawaii (Figure 10.5) shows a complete recovery from the El Chichón eruption of 1982. In June 1991, however, the eruption of Mt. Pinatubo in the Philippines injected into the stratosphere amounts of gases and particles similar to, or perhaps slightly greater than, those of El Chichón. A complete assessment of the magnitude of the Mt. Pinatubo eruption is not yet possible. An early satellite analysis (Figure 10.6, NOAA/NESDIS/Robert M. Carey) shows the dust cloud had encircled the earth by July 1991, but was still largely confined to tropical latitudes (10°S to 20°N).

►
Figure 10.5 - Monthly means of "apparent" atmospheric transmission at Mauna Loa Observatory, Hawaii, January 1958 to October 1991 as determined from direct solar radiation measurements (updated from Dutton et al., 1985; courtesy of R. Bojkov).

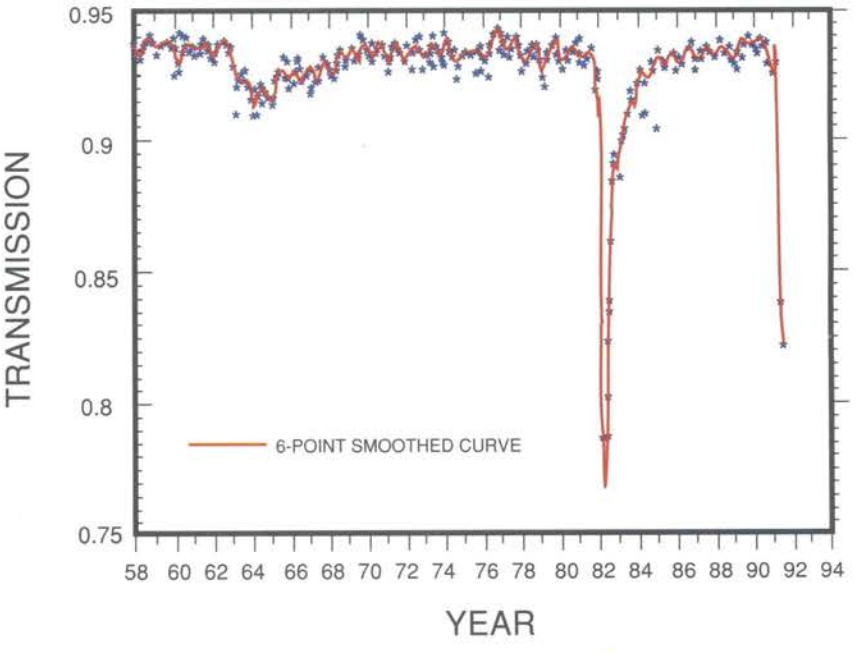

The previous issue of *The Global Climate System* (1986-1988) reported the continuing increase of the concentrations of many atmospheric trace gases. Since 1988, without exception, concentrations of the most significantly important gases for greenhouse climate warming and stratospheric ozone depletion have continued to increase. Four comprehensive, WMO-supported, international reviews of trace gas trends were published during the period (Ehhalt et al., 1988; Megie, 1989; Watson et al., 1990; Fraser et al., 1991). Readers are referred to these for details on concentrations, trends, and impacts of the increases.

11.1 CARBON DIOXIDE

Aside from water vapour, carbon dioxide (CO_2) is the most important gas for greenhouse climate warming. Its atmospheric concentration has been carefully monitored since 1957, when it was about 315 ppm. Today, a global network of 40-plus sites, sponsored by more that 10 nations and coordinated by WMO, documents the rising CO_2 concentration all over the earth. The longest continuing, in situ record is that from Mauna Loa, Hawaii. Monthly mean values from that long term record are shown in Figure 11.1 (which is an extension of Figure 37 from the previous edition of *The Global Climate System* review). The 1990 annual mean concentration at Mauna Loa, which is representative of the global mean value, is about 354 ppm.

For the full review period, the global growth rate averaged about 1.4 ppm per year, slightly less than the mean rate for the 1980s, about 1.5 ppm per year. There was, however, annual significant variability about this mean value. Figure 11.2, which shows the continuous CO_2 growth rate for the 1980s, is derived from the 30-site, globally dispersed NOAA cooperative flask sampling network. The major variability in Figure 11.2 is believed to be linked to the El Niño/Southern Oscillation, although the specific cause/effect mechanism is not completely known. Note the correspondence between Figure 11.2 and the sea surface temperature records in Figure 2.5. For example, after the 1987-1988 ENSO and the subsequent Pacific tropical SST cold event (see Chapter 2), the CO_2 growth rate in 1989 markedly decreased to less than 1 ppm per year.

Figure 11.1 - Monthly mean values of carbon dioxide concentration (ppmv) measured at Mauna Loa Observatory, Hawaii, 1958-1990. Data have been combined from Keeling et al. (1989) of the Scripps Institution of Oceanography and Thoning and Tans (1989) of NOAA.

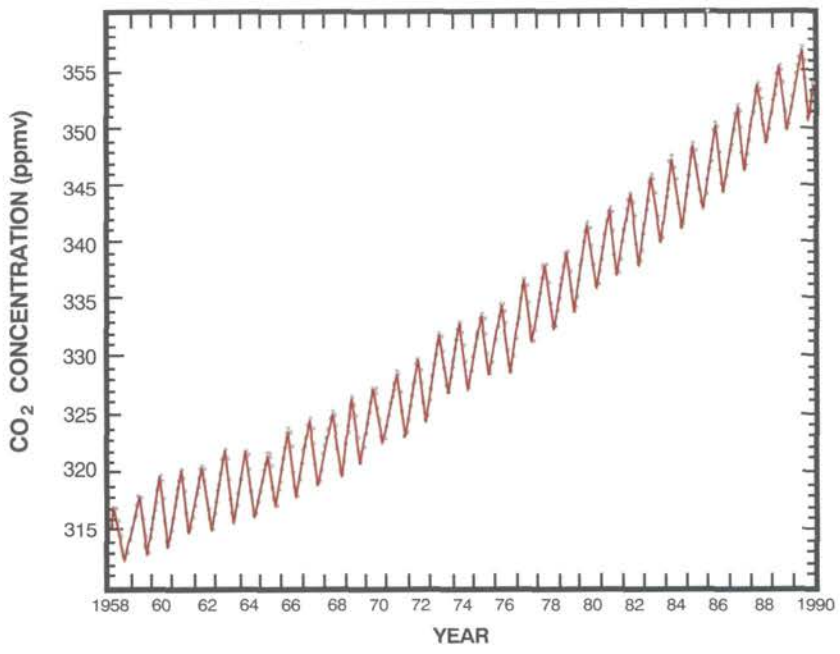

11.2 METHANE

The third most important greenhouse gas is methane. Molecule for molecule it s a far more effective greenhouse gas than CO_2, but with a much reduced atmospheric concentration. The 1990 global mean atmospheric concentration of about 1.7 ppm is more than twice as large as the pre-industrial value of about 0.8 ppm.

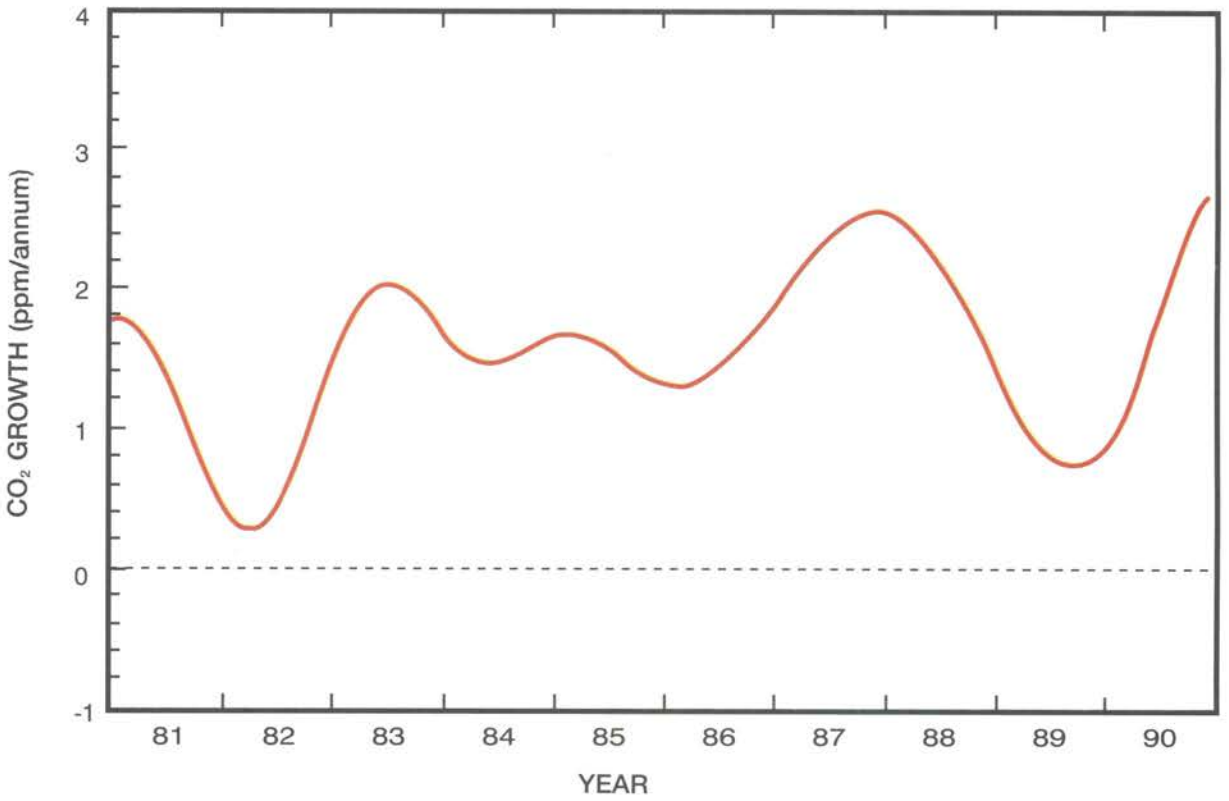

▲ *Figure 11.2* - Global carbon dioxide growth rate, 1981-1990, as derived from the NOAA 30-station flask sampling network (from Conway et al., 1988).

Methane concentrations have been increasing steadily since precise monitoring began in the late 1970s. However, independent measurements from several groups, now show that the rate of growth is slowing (Figure 11.3). Global data from NOAA (Steele et al., 1987), CSIRO (Fraser et al., 1986), Oregon Graduate Institute of Science and Technology (Khalil and Rasmussen, 1990), and University of California at Irvine (Blake and Rowland, 1988) indicate that the growth rates of about 20 ppb per year during 1978-1982 have decreased to about 10 ppb per year during 1988-1990. The cause of this decrease is unknown and might be due to a decrease in sources, an increase in sinks, or both. Moreover, considerable uncertainty still exists about the magnitudes of the various global-scale methane sources and sinks, and remains a continuing high-priority research topic. Comprehensive strategies to restrain atmospheric methane concentrations cannot be reliably developed until the major global sources and sinks of methane are well understood.

11.3 CARBON MONOXIDE

Carbon monoxide itself has neither greenhouse radiative properties nor a direct effect on ozone depletion. It is, however, an important tropospheric trace gas because of its roles in the carbon cycle and in the chemistry of tropospheric ozone production. It is formed in the atmosphere by oxidation of methane and destroyed by further oxidation to carbon dioxide.

More than half of all carbon monoxide sources are anthropogenic, the most significant resulting from biomass burning and fossil fuel combustion. Since these sources are more abundant in the Northern than in Southern Hemisphere, carbon monoxide background concentrations are about twice as large in the Northern Hemisphere.

Despite the importance of carbon monoxide, its short lifetime in the atmosphere has precluded precise determinations of its background mean concentrations and long-term trends. Nonetheless, Fraser et al. (1991) argue that the background marine atmosphere shows no statistically significant trends after 1980. The available data do show, however, a complex Southern Hemisphere interannual variability, which also complicates estimations of a long-term trend.

11.4 PRECURSOR GASES FOR STRATOSPHERIC OZONE DEPLETION

Many gaseous species have significant anthropogenic sources that can either directly or indirectly affect global-scale stratospheric or tropospheric ozone abundances. The most significant species for stratospheric ozone loss are CFC-11, CFC- 12, HCFC-22, CFC-113, the halons, carbon tetrachloride, and methyl chloroform. Nearly all of these are infrared radiative absorbers and, thus, are also potentially important for greenhouse climate warming. In the 1986-1988 issue of *The Global Climate System* review, a comprehensive table (Table 1 on page 44) was presented for the concentrations, growth rates, and lifetimes (as of 1987) of the trace gases that can directly or indi-

Figure 11.3 - Long-term observations of methane mixing ratio (ppbv) from three measurement programs, reported by Fraser et al. (1991).

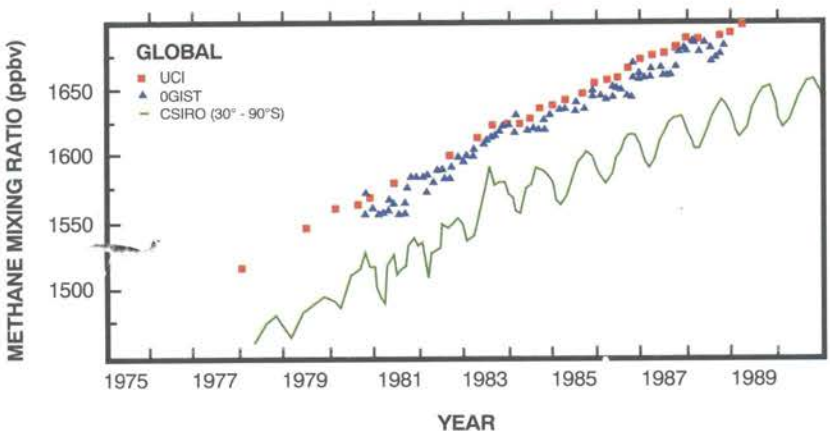

Greenhouse Gases*

Publication in 1894 of the first data on the radiation-absorbing properties of CO_2 led to the recognition that this gas plays a significant role in the heat budget of the atmosphere. In 1896 the Swedish Nobel Prize chemist, Arrhenius, presented a theory of the changes in the world's climate due to fluctuations in the carbon dioxide (CO_2) content of the atmosphere.

A greenhouse gas is one that affects the transmission of long-wave radiation from the Earth's surface through the atmosphere. The major constituents of the atmosphere, oxygen and nitrogen, have no greenhouse qualities, i.e., they have no appreciable effect on the solar radiation re-radiated at long infrared wavelengths. If nitrogen and oxygen were the only atmospheric constituents the Earth's climate would be far harsher than it is, with much greater extremes of temperature.

What makes the difference is a very small volume of water vapour, carbon dioxide, methane, ozone and other "greenhouse gases". These impede the outward flow of radiation from the warm surface of the Earth, acting in some way as the glass in a greenhouse to impede the cooling of the interior, hence the term. Fortunately they create a natural greenhouse effect, and play a critical role in maintaining life on Earth. Overall they are believed to raise the global average temperature by 33-35°C up to the equable average of +15°C.

A major concern is that the CO_2 concentration is rising nearly 1/2% per year because of the activities of humankind. The concentrations of gases, like methane, tropospheric ozone, nitrous oxide and CFCs, grow even faster. Together these other gases are believed to double the rate of temperature rise likely caused by the increasing CO_2 concentration alone.

** Adapted from World Meteorological Organization, 1990: The WMO Achievement — 40 years in the service of international meteorology and hydrology. WMO-No. 729. Geneva, 44 pp.*

rectly affect atmospheric ozone; updated data on global trends and tropospheric concentrations are listed in Table 11.1.

The growth rates for most of these gases, and especially for those with long lifetimes, did not significantly change during the last three years. For example, the rates of CFC-11 (CCl_3F) and CFC-12 (CCl_2F_2), the two most important gases for stratospheric ozone depletion, remained about 4% per year. However, CFC-113 (CCl_2FCClF_2) was a significant exception, showing an increasing rate of about 9% per year (see Figure 11.4). This species, which is primarily used in the microelectronics industry, is now increasing at a rate of about 9% per year. Measurements of CFC-113 made at Hokkaido, Japan, by Makide et al. (1987) of the University of Tokyo (as reported in Fraser et al., 1991) showed a mean annual increase of 7.9 ppt for 1987-1990 compared with only 5.5 ppt for the longer period, 1979-1990.

In September 1987, the Montréal Protocol on Substances that Deplete the Ozone Layer was adopted by the United Nations and subsequently ratified by some 70 nations. It required the nations to reduce their use of CFCs by 50% by the year 2000. In 1990, after more data became available on global ozone depletion, the Protocol was amended to strengthen its terms, including more chemicals to be controlled and a total phase-out of CFCs, halons, and other major ozone-depleting substances. A fund was also established to assist developing nations to identify their use of ozone-depleting species and to implement new technologies. Nonetheless, despite these important and far-reaching agreements, the atmospheric concentrations of CFC-11 and CFC-12, because of their very long atmospheric lifetimes, will still be significant (30-40% of current values) for at least a century (Watson et al., 1990).

Table 11.1 - Global trends and tropospheric concentrations of various source gases for 1989; adapted from Megie (1989) by Fraser et al. (1991).

Source Gas	Concentration 1989 (pptv)	Increase 1989 pptv/year	Increase 1989 %/year
CH_4	1689×10^3	$(12\text{-}14) \times 10^3$	0.7-0.8
H_2	515×10^3	$(2.7\text{-}3.7) \times 10^3$	0.5-0.7
N_2O	$(307\text{-}308) \times 10^3$	$(0.6\text{-}0.9) \times 10^3$	0.2-0.3
CO NH	$(100\text{-}150) \times 10^3$	$(0.4\text{-}1.2) \times 10^3$	0.3-1.0
SH	$(50\text{-}60) \times 10^3$	0	0
CO_2	352.2×10^6	1.6×10^6	0.5
C_2H_6 NH			0.6-1.2
CCl_2F_2	453	16.91-18.2*	3.7-4.0
CCl_3F	255-268	9.3-10.1	3.7-3.8
CCl_2FCClF_2	64	5.4-6.2	9.1
$CClF_2CClF_2$	15-20	~ 1	~ 6
CCl_2FCF_3	~ 5	~ 0.3	~ 6
$CClF_3$	~ 5		
CCl_4	107	1.0-1.5	1.2
CH_3CCl_3	135	4.8-5.1	3.7
$CHClF_2$	110	5-6	6-7
CH_3Cl	600		
$CHCl_3$	~ 10		
CH_2Cl_2	~ 35		
CCl_2CCl_2	~ 30		
CH_2ClCH_2Cl	~ 35		
$CHClCCl_2$	~ 10		
CH_3Br	10-15	?	
CH_2Br_2	2-3		
$CHBr_3$	2-3		
CH_2BrCl	1-2		
$CHBr_2Cl$	1		
$CHBrCl_2$	1		
$C_2H_4Br_2$	1		
C_2H_5Br	2-3		
$CBrF_3$	1.6-2.5	0.2-0.4	15
$CBrClF_2$	1.8-3.5	0.4-0.7	20

** Data subject to revision; significantly lower trends may result.*

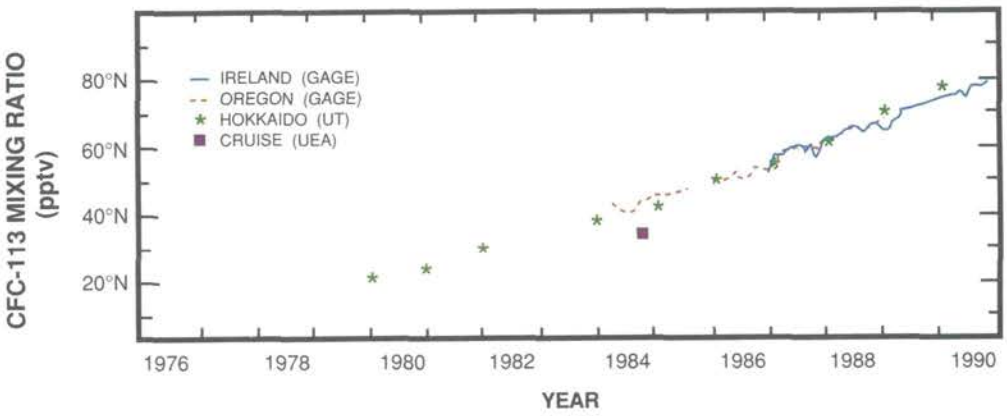

Figure 11.4 - Observations of CFC-113 mixing ratio (pptv) in the Northern Hemisphere (30-90°N), 1980-1990, from three measurement programs, reported by Fraser et al. (1991).

KUWAITI OIL FIRES THREATEN REGIONAL, NOT WORLD, CLIMATE

The Kuwaiti oil fires have been called the "most intense burning source probably in the history of the world". In late February 1991, when more than 600 oil wells were ignited, about 3-5 million barrels of oil a day went up in smoke. The average flux of particles including soot from the fires was determined to be 12,000 tonnes per day, which is about 10% of the emissions from biomass burning worldwide. Approximately 45,000 tonnes of SO_2 were being emitted, 90,000 tonnes of carbon as soot, and more than 700,000 tonnes of carbon dioxide. The CO_2 emission rate was about 2% of the worldwide emissions of CO_2 from fossil fuel and biomass burning. The intense smoke plumes from these fires dramatically affected weather and air quality in the Gulf region. For example, Bahrain experienced its coolest May in 35 years with an average temperature 4°C below normal. Inside the plume at about 900-m altitude and about 30 km downwind of the fires, all sunlight was extinguished.

The dense smoke plume extended for thousands of kilometres to the southeast over the Arabian Sea toward India, and covered large portions of Iran, Iraq, Qatar and the Emirates. Smoke was reported in Pakistan. Black rain fell on Qatar, 645 km away, and black snow fell in Kashmir, 2600 km away. In Kuwait, droplets of unburned oil, soot, sulphuric acid and other toxic substances coated people, livestock, crops, water supplies, and everything else in the landscape.

Only very small amounts of the pollutants reached the stratosphere during rare situations of atmospheric instability, such as thunderstorms. Most of the smoke remained below six kilometres, after residing two days in the air. In the stratosphere, the pollutants could have remained for months; they have affected the regional and global climates by modifying the radiation and energy balances. In the troposphere, the pollutants, which were found to be water-absorbing and not as black as expected, dropped out of the air within days.

The general scientific consensus was that the oil fires' influence on the weather and climate outside the Gulf region was minimal. Episodic events of acid rain and photochemical smog occurred downwind of the plume. Severe environmental phenomena resulted from the Kuwaiti oil field fires, such as damaging sandstorms and long unhealthy temperature inversions that formed over the Gulf States, and perhaps even as far away as Turkey and Afghanistan. Terrestrial and marine environments in the greater Gulf area were severely affected by smoke deposition. For example, the ground in Kuwait was blackened from incompletely burned oil and carbon falling out of the atmosphere.

Consequently, local reflectivities were markedly decreased compared with those of the lighter desert. Significant environmental effects on a worldwide scale such as global cooling, or changes in the Indian summer monsoon rainfall were not expected to occur.

The aerosols injected into the atmosphere by the eruption of Mount Pinatubo contributed to drammatic sunsets

Photo Grant W. Goodge

THE ERUPTION OF MOUNT PINATUBO

The cataclysmic eruption of Mount Pinatubo (15.14°N, 120.35°E) in the Philippines on June 14-15,1991 made the greatest volcanic impact on the stratosphere ever observed by satellite instruments. The eruption yielded an estimated 20 to 30 megatonnes of total H_2SO_4/H_2O aerosol mass, which is about three times that produced by the 1982 El Chichòn eruption. The massive amounts of SO_2, dust, ash and other volcanic effluents created stratospheric clouds to altitudes of greater than 30 km, although most of the clouds were between 20 and 25 km. Stratospheric temperatures increased at altitudes where the cloud resided as a result of the absorption of upwelling infrared radiation. For example, in September increases as much as 3.5°C occurred at 30 hPa at some locations between the equator and 30°N.

The Advanced Very High Resolution Radiometer onboard the NOAA 11 polar-orbiting environmental satellite provided an exceptional opportunity to observe the aerosol optical thickness (AOT) of Mount Pinatubo's stratospheric aerosol layer. AOT is proportional to the intensity of reflected solar radiation. The greater the optical thickness, the greater the amount of reflected solar radiation. Daily and weekly composites of AOT show that the volcanic aerosol layer circled the Earth in 22 days, and most of the early aerosol was confined to the tropics. By August, the entire Southern Hemisphere had experienced a 10-fold increase in optical depth relative to early July due to the layers above 20 km. The layer covered about 42% of the Earth's surface area, over twice the area covered by the El Chichòn aerosol layer two months after its eruption.

Scientists from NASA's Goddard Space Flight Center have suggested that the global shield of stratospheric aerosols caused by Pinatubo will probably have an opacity that exceeds that of any volcanic eruption during the past century. The GISS global climate model forecasts intense aerosol cooling to begin in 1991 and to maximize late in 1992. The model predicts a return to record warm temperatures in the later 1990s.

The varying responses of snow cover, ice extent and other cryospheric variables to fluctuations in climate makes them useful indicators for monitoring changes in the climate system and for revealing long-term climate trends. In linking climate forcing and cryospheric response, however, it is important to consider differences in lag time between those quantities that respond rapidly to change, such as lake ice and snow cover, and those that respond more slowly over decades or centuries, such as continental ice-sheets and permafrost. Regional effects such as latitude, elevation and climatic regime are also important when considering climate forcing and cryospheric response.

12.1 SNOW COVER

Snow cover is the most transient and variable cryospheric form, which can change the surface characteristics of large land areas in just a few days. Monitoring the extent and albedo of snow cover, and more recently its water equivalent on a continental or hemispheric scale has greatly improved with the advent of satellite observing systems. Figure 12.1 is a satellite-derived, 18-year time series of snow cover area anomalies, spanning the years 1973 to 1991, for the Northern Hemisphere, North America and Eurasia, smoothed by a 12-month running mean. The data show considerable variability from year to year, with a range of about ±10 to 15%. Since 1985-1986, there has been a suggestion of a downward trend, especially in the spring after 1987, with 1990 showing a markedly depleted hemispheric snow cover, unlike any other full year since 1973 (Robinson et al., 1991). Every month in 1990 had below normal coverage, and the year was about 8-10% below the annual average. Statistical analyses between snow cover extent and the air temperature records for land areas suggest a causal association, but Barry (1991) cautions that it would be premature to conclude that one actually exists.

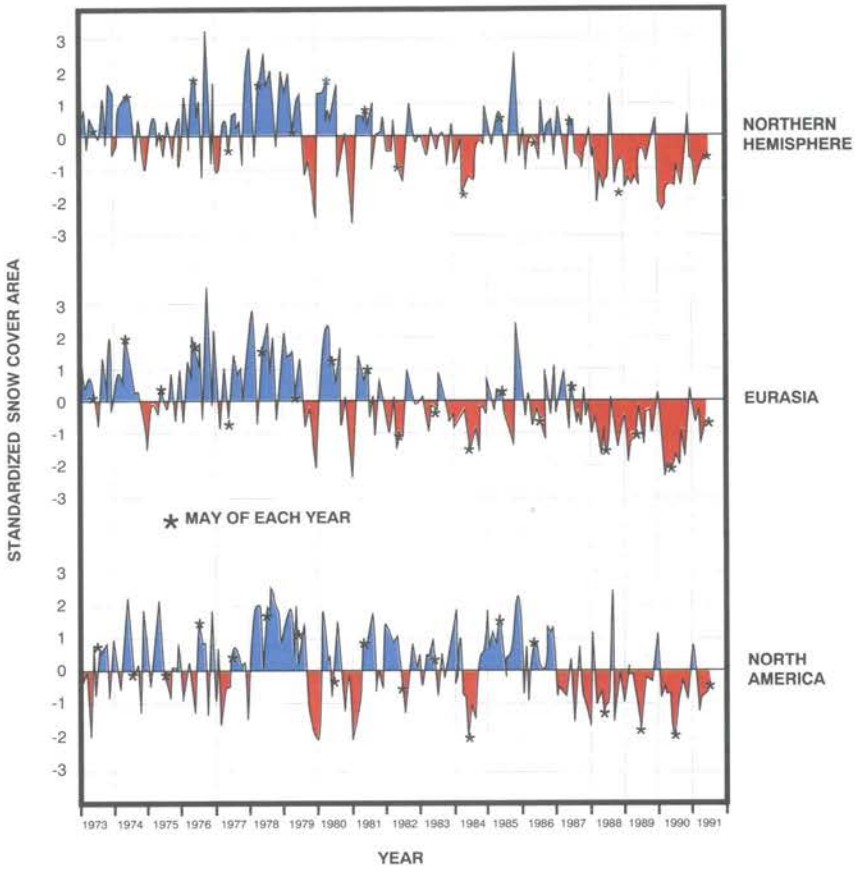

Figure 12.1 - Time series of normalized snow-cover area anomalies for the Northern Hemisphere, Eurasia and North America, 1973-1991, smoothed using a 12-month running mean (from NOAA, Climate Analysis Center, Washington, DC).

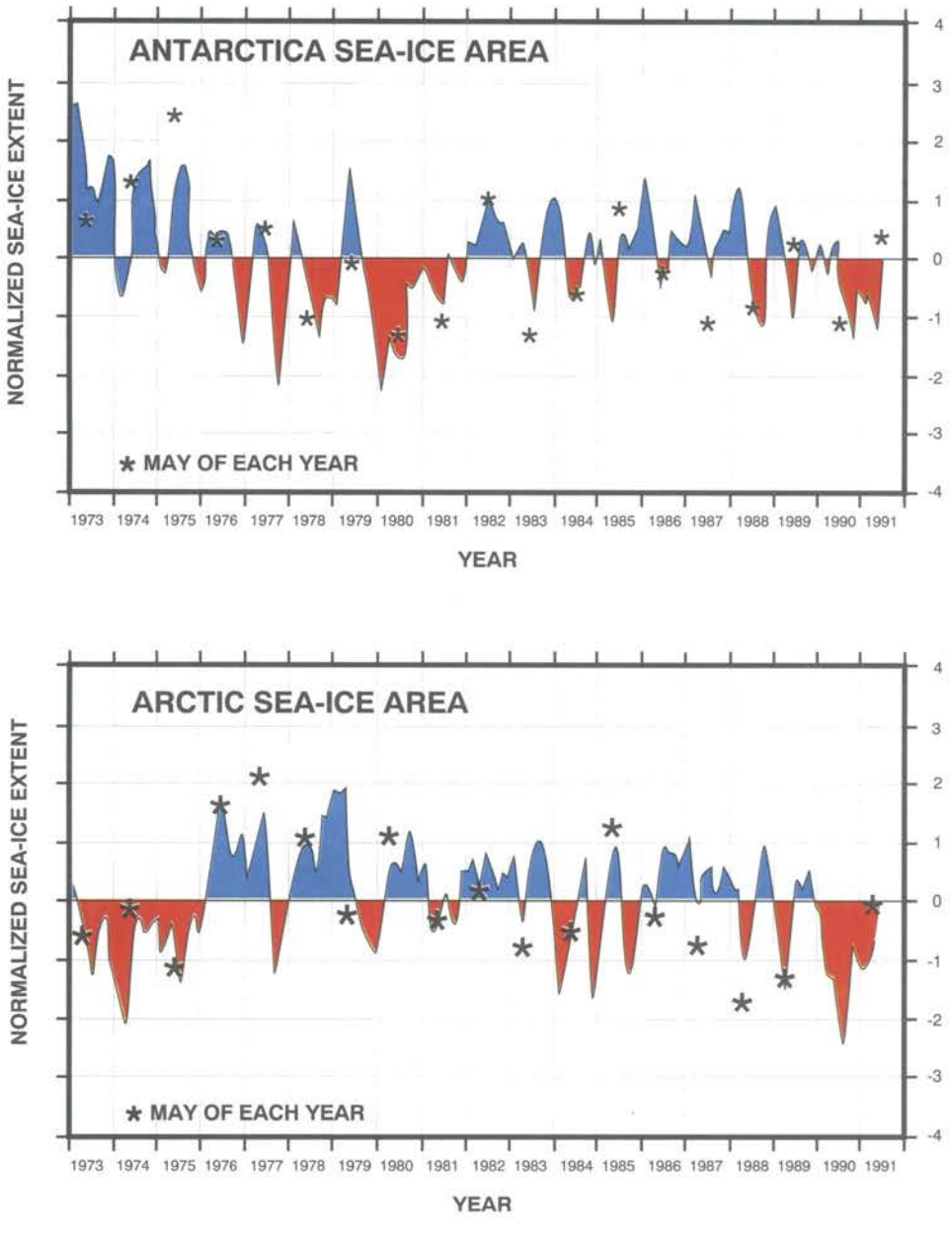

▲
Figure 12.2 - Time series of normalized mean monthly sea-ice extent anomalies for the Arctic and Antarctic, 1973-1991 (from NOAA, Climate Analysis Center, Washington, DC).

12.2

SEA ICE

Records of sea-ice amount and concentration have long been used as climatic indicators. Reasonably consistent sea-ice data for polar regions are available from satellites back to 1973. Figure 12.2 shows the sea-ice extent in the Arctic and the Antarctic, expressed as standardized anomalies with respect to the 1973-1991 mean. For both polar regions over the period, there is no consistent trend in sea-ice extent. Both Arctic and Antarctic sea-ice coverage fluctuated about the mean. It is apparent that Antarctic sea ice has shown less year-to-year variability since 1988 than for any previous review period. In the Arctic, the recent period is characterized by below average sea ice.

Weatherly, et al. (1991) confirm that below normal sea-ice coverage in Antarctica is associated with higher than normal air temperatures. Although the average trends in both sea-ice extent and temperature between 1973 and 1987 were not statistically significant, some regional and seasonal trends were large (winter and summer temperatures became warmer, whereas spring temperatures became colder). The authors found evidence for a complex feedback between sea-ice and air temperature, suggesting that summer temperatures "precondition the near-surface waters, thus predisposing them to above or below normal ice coverage in the following autumn or winter".

Figure 12.3 shows the annual variability in maximum sea-ice extent for the Baltic Sea over 270 winters from 1720 to 1990. The

Figure 12.3 - Maximum ice extent of the Baltic Sea during winter, 1720 to 1990 (from Institute of Marine Research, Finland).

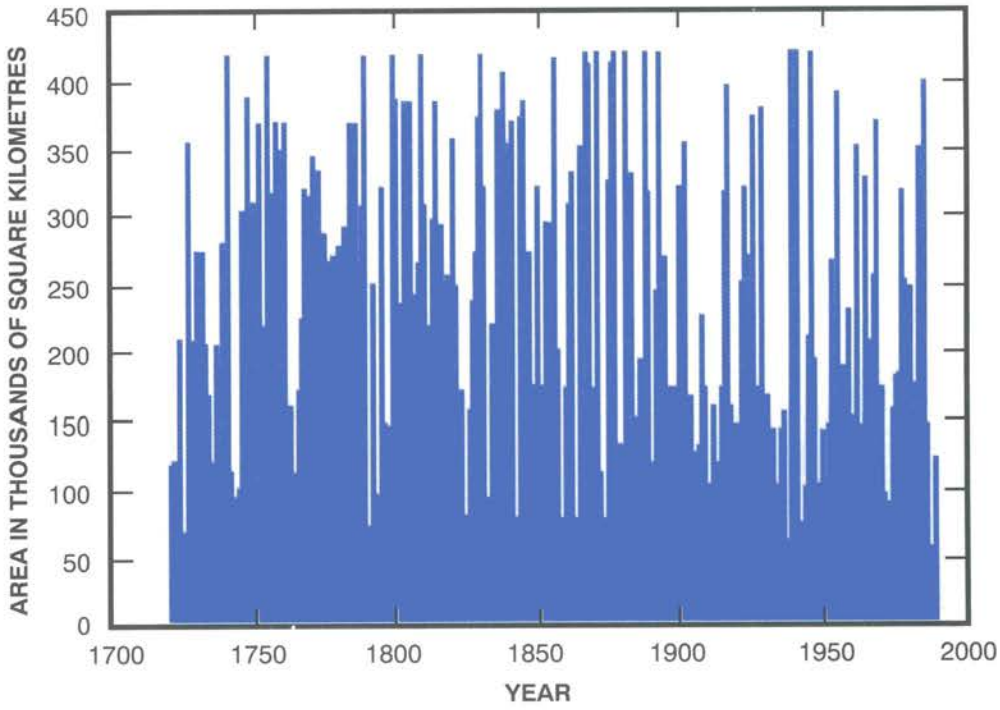

smoothed data (not shown here) showed a slightly increasing trend during the Little Ice Age around 1800, followed by a slightly decreasing trend till about 1900, after which no apparent trend can be detected. During the review period both very mild and very severe winters occurred. In 1988, the second mildest winter with respect to ice coverage occurred, in sharp contrast to 1986, one of the 20 severest on record.

Figure 12.4 is a time-longitude chart of monthly ice conditions along the northern sea route of the former territory of the Soviet Union from January 1988 to August 1991, using a composite analysis of airborne, satellite, ship and observing-station data. The shaded area depicts ice-breaker navigation conditions (concentration greater than 50% and ice thickness greater than 15 cm). The most favourable ice conditions occurred in 1990 east of 110°E when generally open ice conditions lasted 80 to 130 days. Some of the worst, unexpected ice conditions occurred in the warm months of 1989 and 1991 in the vicinity of Severnaya Zemlya (100°E).

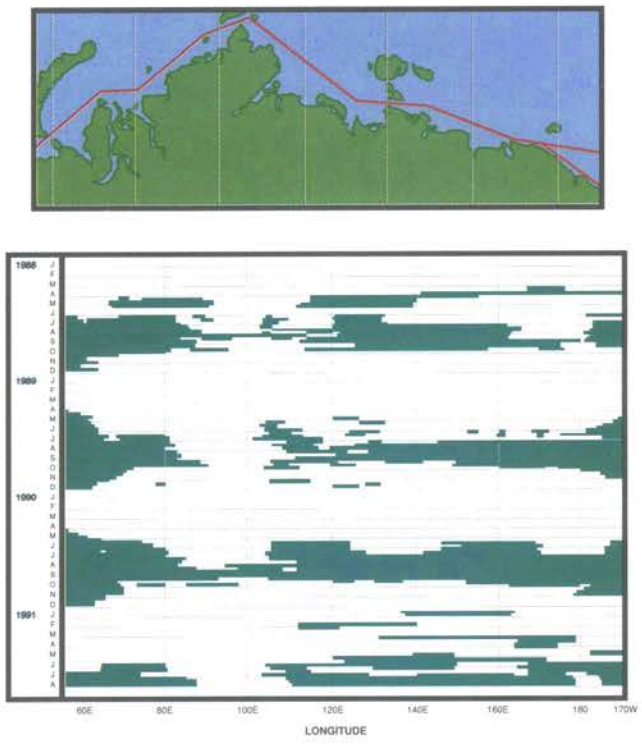

ICE CONDITIONS FOR SHIP NAVIGATION ON THE NORTH SEAWAY ROUTE IN 1988 - 1991:
TOP: NORTH SEAWAY ROUTE
BOTTOM: LONGITUDE-TIME SECTION OF NAVIGATION ICE CONDITIONS
ICE-BREAKER NOT REQUIRED FOR NAVIGATION
ICE-BREAKER REQUIRED FOR NAVIGATION

Figure 12.4 - Ice conditions for the North seaway route in the Russian Federation near Severnaya Zemlya (100°E) for 1988-1991 (from Institute for Global Climate and Ecology, Moscow).

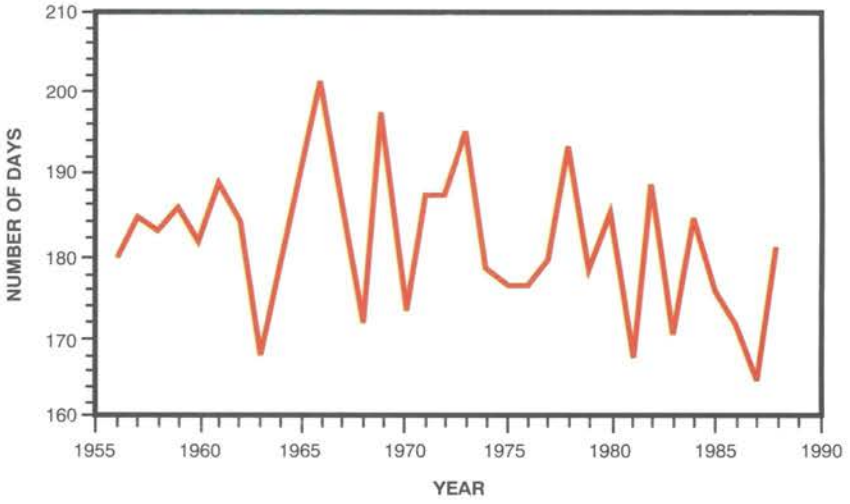

Figure 12.5 - Mean ice-season duration (days) for lakes in the Manitoba-Ontario region of Canada (Skinner, 1991).

12.3 LAKE ICE

Freeze-up and breakup records from lakes in middle to high latitudes provide a useful index of temperature trends in the transition seasons. Lake-ice time series for 20 or more years of data across western and central Canada illustrate a tendency during the 1980s toward earlier breakup of the ice cover (figure 12.5). The duration of the ice-free season has increased by upwards of 20 days over 30 years, mainly because of earlier breakup dates in the spring — a consequence of warmer spring temperatures and reduced snow cover.

Lake-ice duration analysis for southern Finland also reveals a close relationship with air temperatures at Helsinki since the mid-nineteenth century (not shown).

Reliable monitoring of lake-ice coverage for Lake Ladoga dates from the end of the nineteenth century; however, reliable and regular airborne/satellite observations only began in 1960. Figure 12.6 shows the dates of total ice coverage for the most recent three winters, which were generally mild, although 1990-1991 was close to normal.

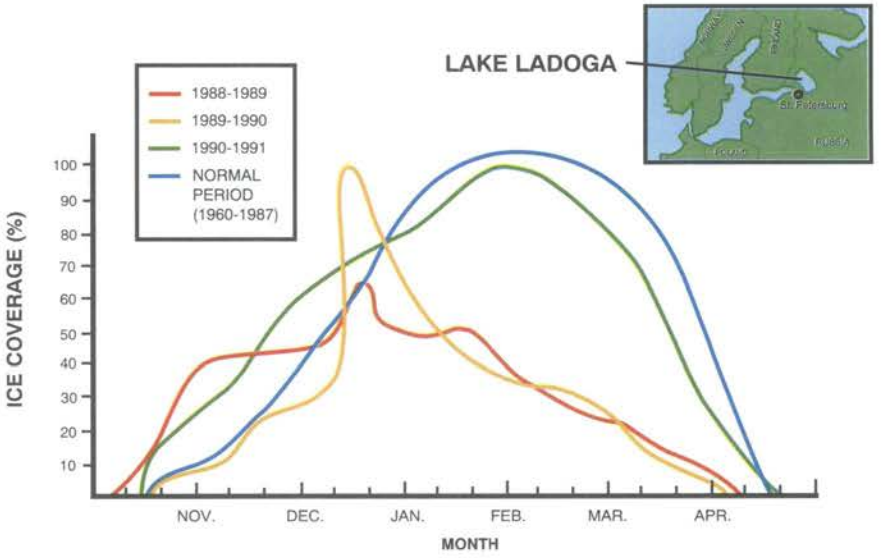

Figure 12.6 - Total ice coverage (including drift ice) on Lake Ladoga for three recent winters and for an average period (1960-1987) (from Hydrometeorological Centre, Moscow).

Figure 12.7 - Estimated number of icebergs south of latitude 48°N (off Newfoundland) 1945-1946 to 1990-1991 (from International Sea Ice Patrol).

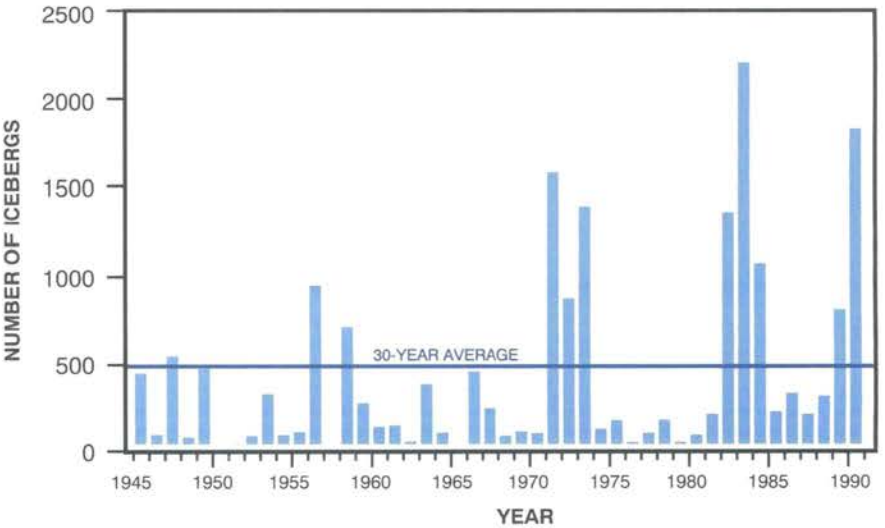

Photo Grant W. Goodge

12.4

LAND ICE

No conclusive evidence is available on whether the massive Greenland and Antarctic ice-sheets are growing or shrinking. Although the Antarctic ice-sheet appears to be growing, the Greenland sheet appears to be in equilibrium. Speculation exists that climate warming has increased the amount of calving from the Greenland and Ellesmere Island glaciers, thus increasing the number of icebergs along the northwest Atlantic Coast.

UNUSUALLY HEAVY ICE DISRUPTS SHIPPING IN ATLANTIC CANADA

Unusually heavy ice conditions prevailed in the Gulf of St. Lawrence and along eastern Newfoundland in 1990 and 1991. Both the ice thickness and the extent reached record values. In 1990, the Gulf became completely covered with ice, which ranged in thickness from 30 to 70 cm. Persistently strong northwesterly winds in February compressed the ice-pack along Newfoundland's west coast, and the heavily rafted and ridged ice attained thicknesses in excess of two metres. At times, ice-breaker-led convoys became stuck in the ice for days waiting for the winds to let up and the ice pressure to ease.

Heavy ice continued to plague the northern Newfoundland and Labrador coasts in the spring and early summer of 1991. The combination of a northwesterly circulation, and the below normal spring mean temperatures in the northwestern Atlantic contributed to one of the worst ice years on Canada's east coast (Figure 12.8). Only towards the end of July did the hard multi-year ice start decaying and break up into patches. Shipping routes leading into the coastal Labrador communities were effectively blocked, preventing supply vessels from entering port.

In some winters the advance of the ice-pack is rapid, whereas in others, it is slow, depending on the persistence of cold northerly winds and the speed and water temperature of the Labrador Current. Good records of sea-ice extent go back to the mid- to-late 1950s. Some of the heaviest east coast ice conditions have occurred during the 1980s, with particularly bad winters in 1982-1983 and 1983-1984; however, a couple of months in the winter of 1985-1986 were quite mild. Changes in atmospheric circulation over the North Atlantic have been observed during both extremely heavy and light ice conditions. During heavy ice-months, intensification of the Icelandic Low between the tip of Greenland and Iceland produces a stronger than normal northwesterly flow of cold air along the eastern Canadian seaboard from Baffin Bay to Labrador.

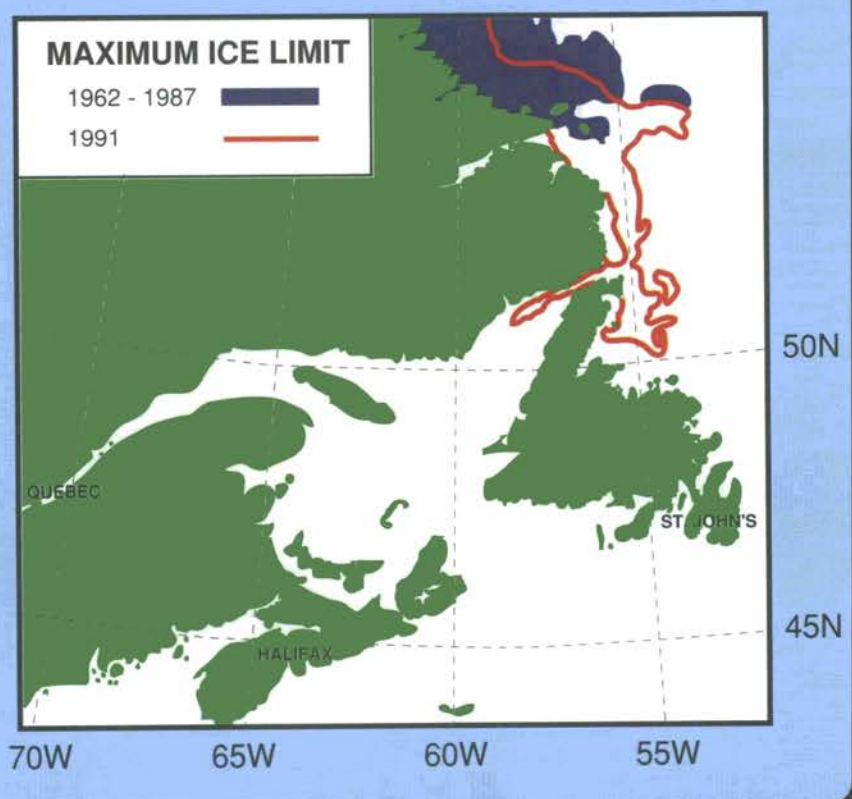

Figure 12.8 - The retreat of the Labrador ice-pack off Newfoundland's north and east coasts was six weeks later than normal in 1991 (from Ice Centre, Environment Canada, Atmospheric Environment Service, Ottawa).

13.1

SELECTED ANALYSES OF OCEAN VARIABLES DURING THE REVIEW PERIOD

With their large heat capacity and mobility, oceans are the world's great heat reservoirs and heat exchangers and the source of much of the moisture that falls as rain and snow. Sea surface temperatures (SST) and their associated heat and moisture fluxes generate atmospheric convection and winds and affect weather events like storms and hurricanes. Oceans are also a source of and a sink for carbon dioxide and other greenhouse gases. The vastness of the oceans alone, covering almost three quarters of the Earth's surface, ensures them a vital role in the dynamics of the atmosphere.

In order to understand and model quantitatively the global circulation of the ocean, and to make the best predictions of weather and climate on time-scales from days to months to decades, we need a full description of the state of the ocean and its variability.

However, in spite of the recognition of the importance of the oceans for climate dynamics, a description of the state of the oceanic circulation is inadequate for several reasons: the measurement problems are formidable, the operational measurements are too few, the processes are not well understood, and the modelling is difficult and complex.

In recent years several operational ocean monitoring global measurement and data management systems have been established by several organizations around the world. Figure 13.1

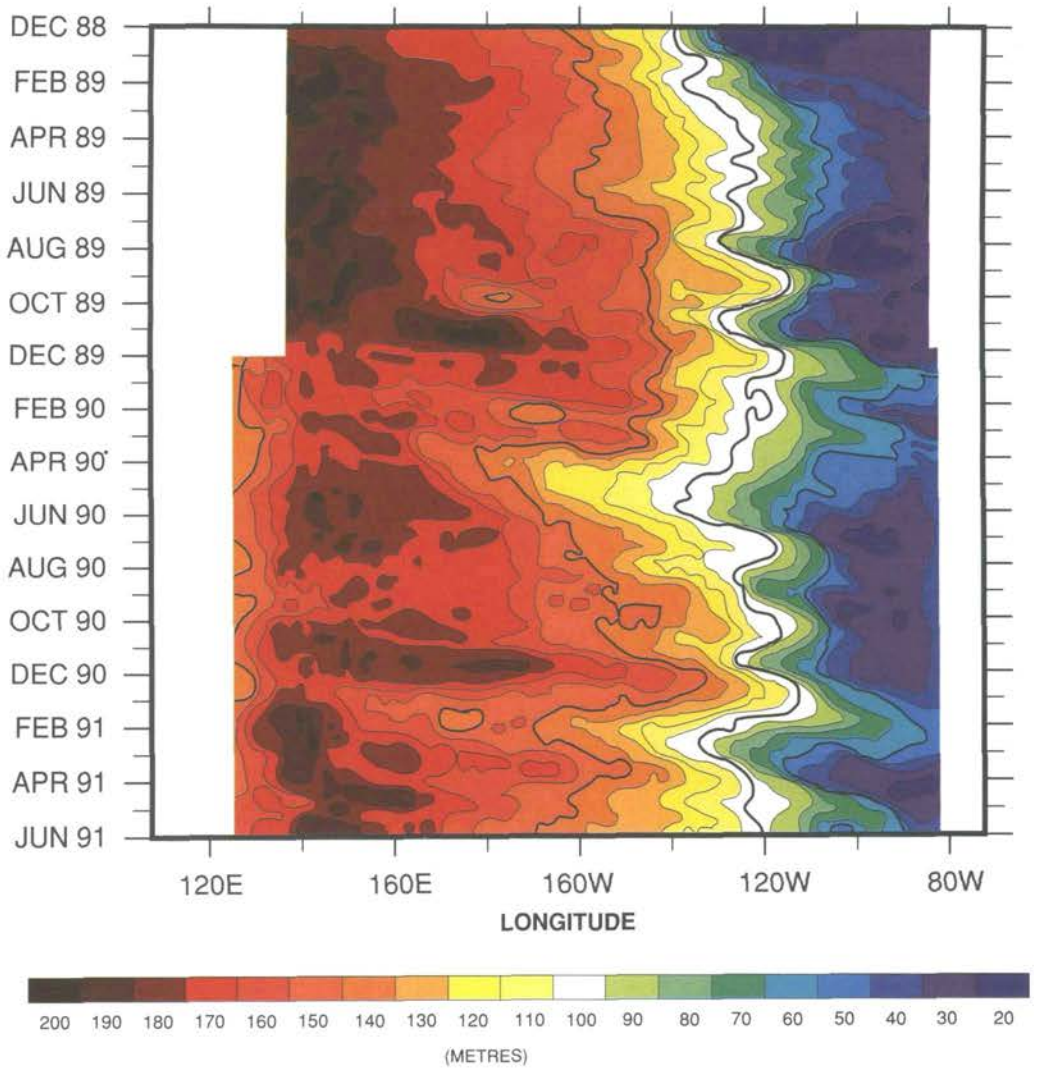

Figure 13.1.1 - Depth of the 20°C isotherm along the equator in the Pacific Ocean. The contour interval is 10 m with shading for values less than 50 m and for values greater than 150 m (NOAA, Climate Analysis Center, Washington, DC). ►

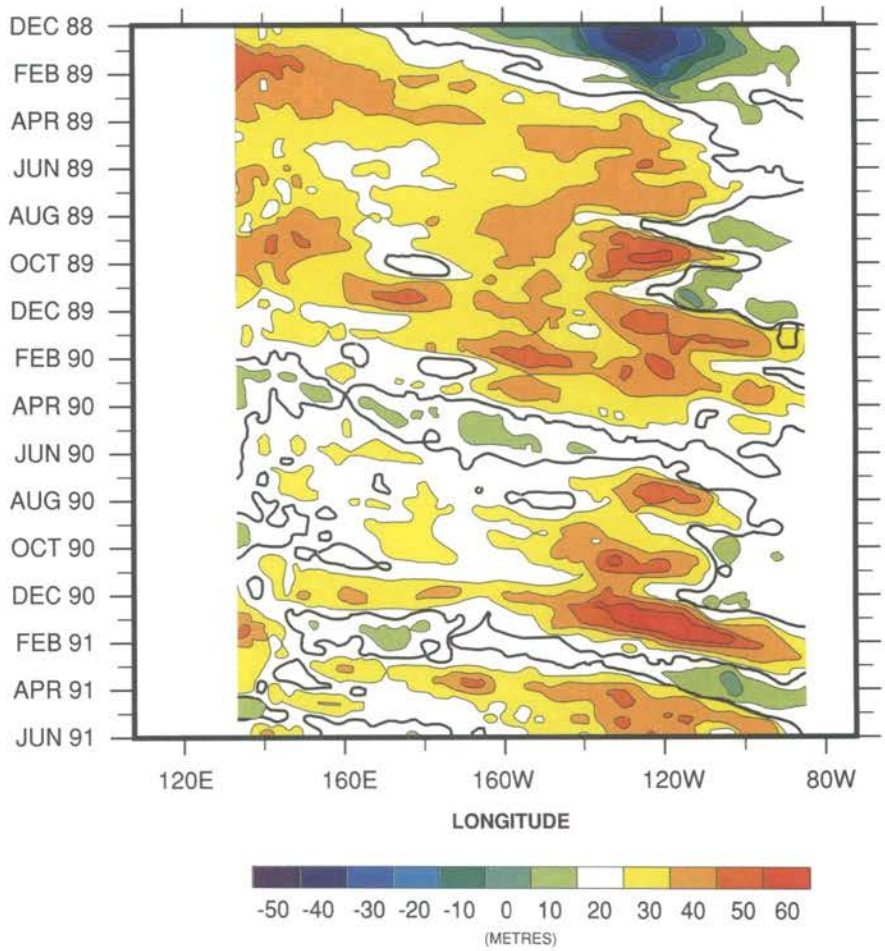

Figure 13.1.2 - Anomalies of heat storage (integrated temperature) along the equator in the upper 408 m of the Pacific Ocean. The contour interval is 10^3 cm °C, with light (dark) shading for anomalies greater than 10^3 cm °C (less than -10^3 cm °C). Anomalies are computed with respect to the 1985-1990 base period (NOAA, Climate Analysis Center, Washington, DC).

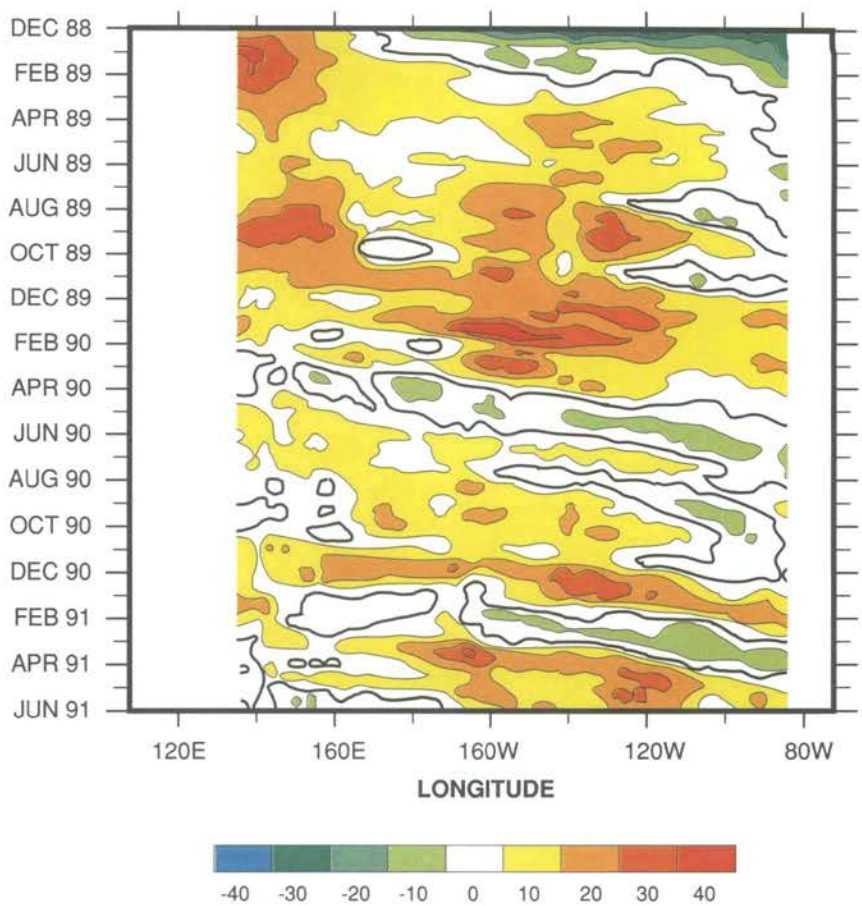

Figure 13.1.3 - Sea surface temperature anomalies along the equator in the Pacific Ocean. The contour interval is 1°C with light (dark) shading for anomalies greater than 1°C (less than -1°C). Anomalies are computed with respect to the 1985-1990 base period (NOAA, Climate Analysis Center, Washington, DC).

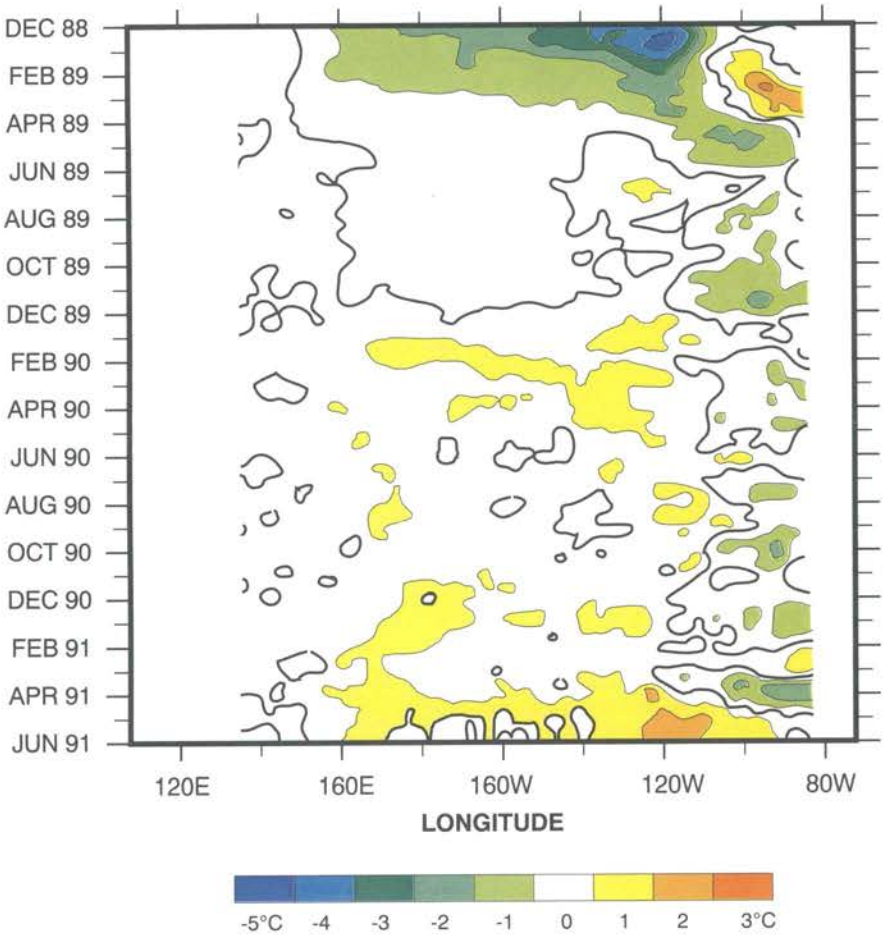

▲ *Figure 13.1.4* - Mean monthly outgoing long wave radiation (OLR) for May 1991 as measure by the NOAA-9 AVHRR IR window channel by NESDIS/SRL (top). Data are accumulated and averaged over 2.5° areas to a 5° Mercator grid for display. Contour intervals are 20 Wm^{-2}, and contours of 280 Wm^{-2} and above are dashed. The mean monthly outgoing long wave radiation anomalies (bottom) are computed as departures from the 1979-1988 base period mean. Contour intervals are 15 Wm^{-2} (NOAA, Climate Analysis Center, Washington, DC).

features a selected analysis of ocean climate fields for the review period.

At the end of the review period, the depth of the 20°C isotherm (Figure 13.1.1) had increased east of 160°W and depth anomalies became positive. This was accompanied by an increase in the upper oceanic heat storage in the eastern equatorial Pacific (Figure 13.1.2) These features are consistent with the observation that the thermocline in the equatorial Pacific shoaled in the west and deepened in the east. Beginning in April 1991, SST anomalies increased dramatically over the eastern half of the equatorial Pacific (Figure 13.1.3 and 13.1.4).

Figure 13.2 is an analysis of SST anomalies for April 1991 as analysed from satellite data by the National Meteorological Centre (Bureau of Meteorology) in Melbourne. The data confirm a significant cooling in the Pacific Niño 1 & 2 area SST and a warming of western Pacific Niño 4 area SST — with anomalies remaining within 2°C of the average. Around the Australian continent, SSTs were near the climate average.

THE WORLD OCEAN CIRCULATION EXPERIMENT

The World Ocean Circulation Experiment (WOCE) is a worldwide oceanographic initiative, led by ICSU's Scientific Committee on Oceanic Research (SCOR) and the Unesco Intergovernmental Oceanographic Commission, and organized as a component of the WMO/ICSU World Climate Research Programme.

The primary goal of WOCE is to develop global ocean models that are useful in predicting climate change on a decadal time-scale and to develop the datasets necessary to test the models. Over the five years (1990-1995) of the programme, there will be an intensive effort to understand the large-scale fluxes of heat and water on a global scale; an upper-ocean measurement programme to determine the annual and interannual oceanic responses to atmospheric forcing on a world domain; and a programme to determine the deep-ocean circulation.

Development of models and data analyses are also key elements of WOCE. For the first time, modellers are expected to simulate the circulation of heat and water in the ocean and its interaction with the atmosphere on a global scale. The modelling effort will include simulation of convection in the upper layers, the flow of deep water, and the eddy exchanges of momentum, heat and salt. WOCE will use measurements from a handful of satellites, dozens of ships, hundreds of moored instruments, and thousands of surface and under-water drifters, tidal gauges, mid-water floats, "pop-up" buoys, and expendable instruments to take a comprehensive "snapshot" of the physical properties of the ocean. Among the variables that will be monitored are salinity, interior- and deep-ocean currents, vertical distribution of eddy energy, oceanic heat fluxes, exchanges of water between ocean basins and their marginal seas, sea surface temperature, and surface wind velocity. Information will be collected on the components of ocean variability on time-scales of months to years and space scales of kilometres to worldwide. WOCE will also make intensive use of historical oceanographic data to assess the longer-term variability of ocean circulation.

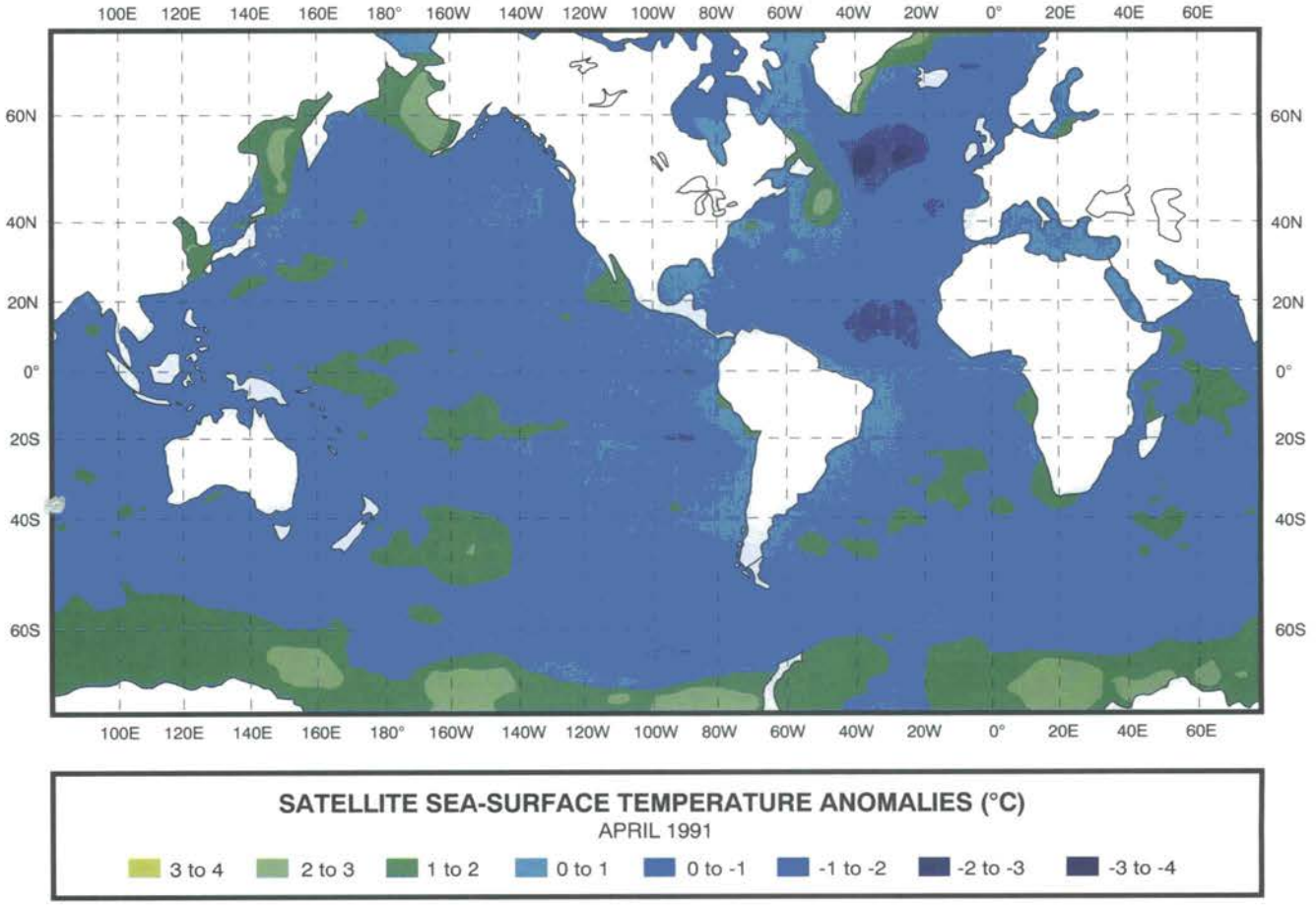

▲

Figure 13.2 - Sea surface temperature anomalies (°C) for April 1991 derived from satellite observations (National Meteorological Centre, Bureau of Meteorology, Melbourne).

▶

Figure 13.3 - Time series of regionally averaged annual (December-November) SST anomalies (°C) for the North Atlantic Ocean (top) and the North Pacific Ocean (bottom) from 1957 to 1990. Anomalies were computed relative to the normal values from 1957 to 1980 (from the Institute for Global Climate and Ecology, Moscow).

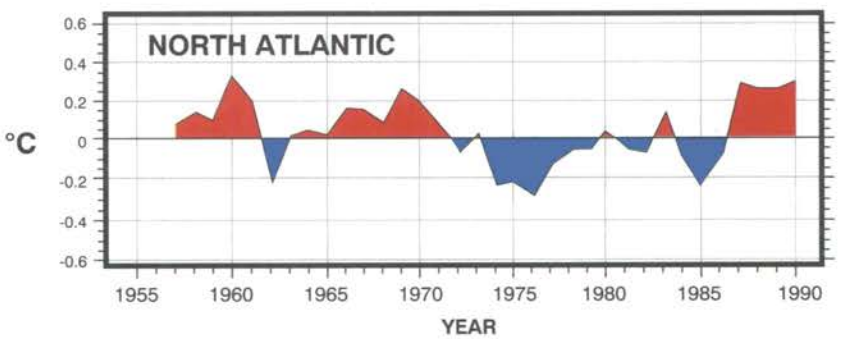

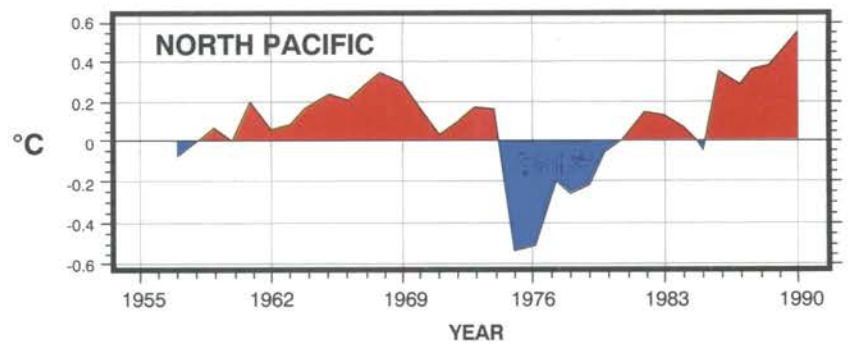

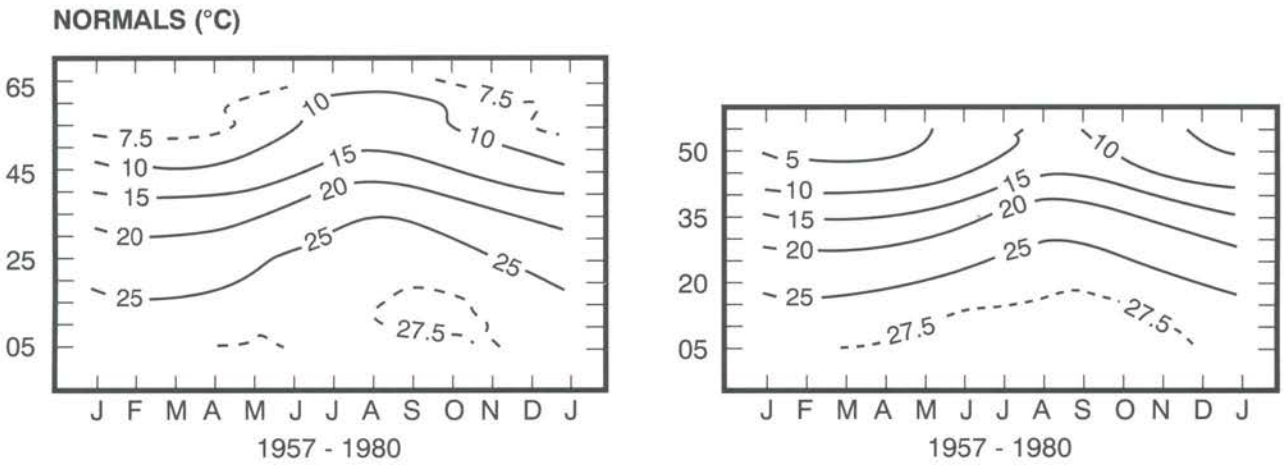

▲

Figure 13.4 - Time-latitude section of monthly, mean SST (°C), averaged for each latitude within the North Atlantic (top) and North Pacific (bottom) oceans. 1957-1980 normal values (°C) (from the Institute for Global Climate and Ecology, Moscow).

Figure 13.5 - Anomalies relative to the 1957-1980 normal values for the period December 1988 to May 1991.

▼

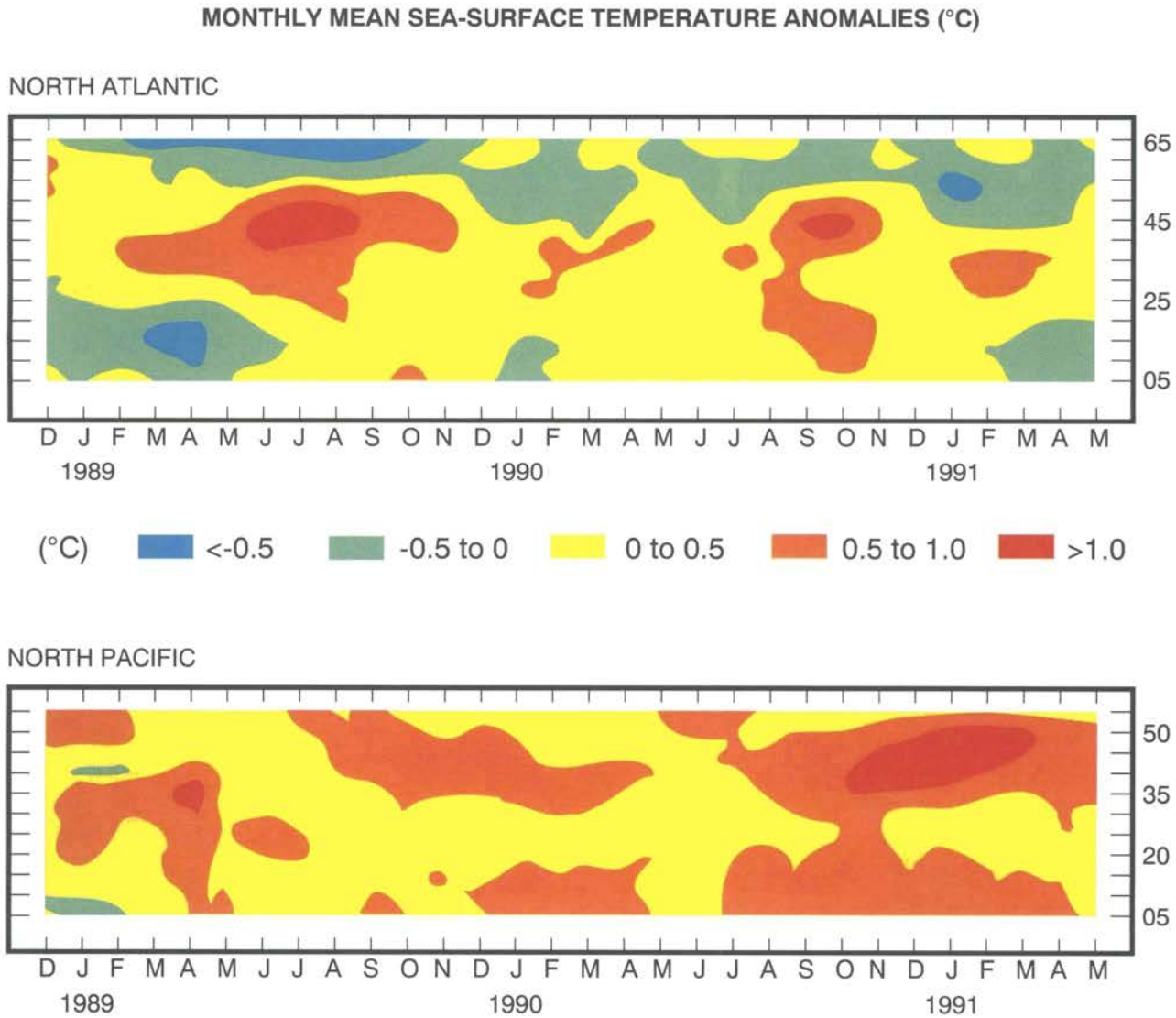

Oregon Coast, USA

Photo Grant W. Goodge

13.2

SEA SURFACE TEMPERATURES IN THE NORTHERN WATERS OF THE ATLANTIC AND PACIFIC OCEANS

Figure 13.3 shows an analysis of monthly mean SST anomalies over the northern regions of the Atlantic and Pacific oceans, using a 5° x 5° grid from 1957-1990. Anomalies are relative to the base period 1957-1980. The Pacific Ocean time series shows positive anomalies for the review period and a maximum in 1989-1990.

The time-latitude section for the North Atlantic Ocean (Figure 13.4) shows positive anomalies during the last 2-1/2 years in mid-latitudes, negative anomalies in high latitudes and two noticeably cold periods in low latitudes i.e., during the first half of 1989 and since March 1991.

For the Pacific Ocean time series, positive anomalies prevailed for the entire period. The warmth was especially pronounced in moderate latitudes from November 1990 to April 1991.

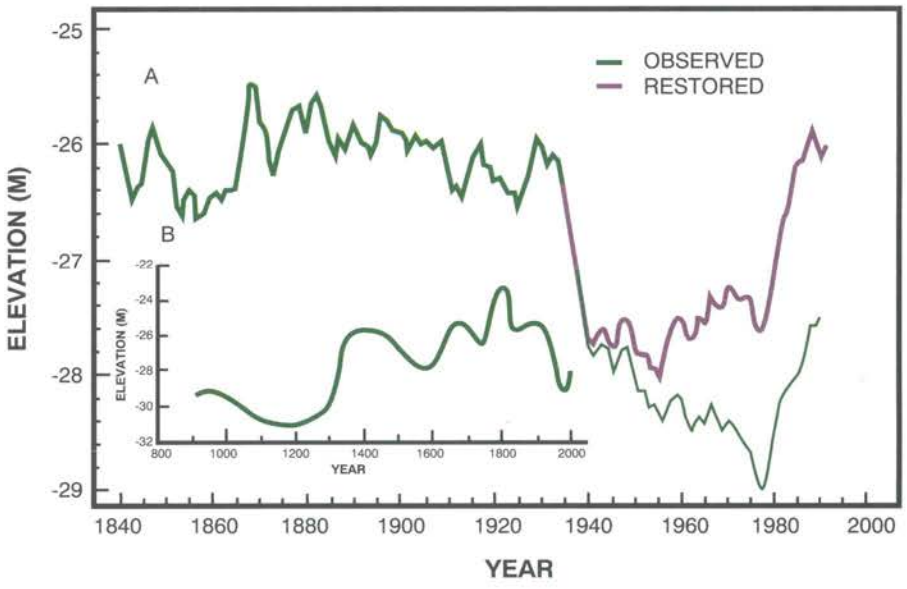

Figure 14.1 - Elevation (m) of the Caspian Sea: (A) annual average for the period 1840 to 1990 from recorded data, and (B) for the last millennium from proxy data. Restored data have been calculated by means of the water balance equation taking into account the water withdrawn for consumptive use from runoff to the sea (from All-Union Research Institute of Marine Fisheries and Oceanography).

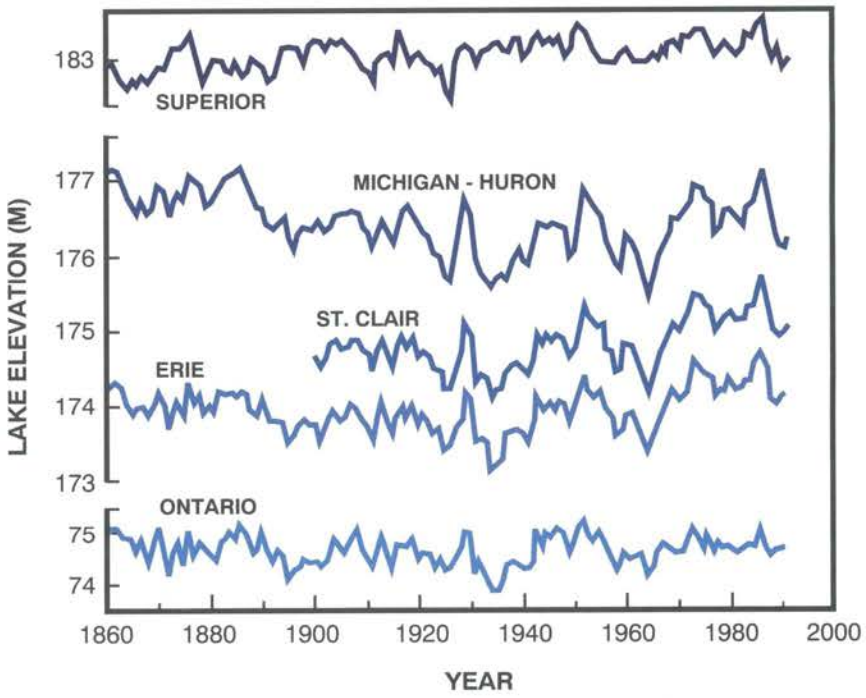

Figure 14.2 - Mean annual elevations (m) of the Great Lakes from 1860 to 1991 (from NOAA, Great Lakes Environmental Research Laboratory, Ann Arbor, Mich.).

14.1

EXTRAORDINARY RISE IN THE CASPIAN SEA LEVEL

The Caspian Sea level is considered to be a good indicator of climate change. Extremely low levels during the medieval warming and extremely high levels during the Little Ice Age, as well as smaller-scale events, are in good agreement with this general rule.

In 1977, the Caspian Sea level reached its lowest recorded value of 29 m below sea level (Figure 14.1). Such a low value has not been observed since at least the fourteenth century. However, later the long downward trend that accelerated in the 1930s reversed, and started to rise. The rise has continued with only a temporary reversal in 1989. Under natural conditions (i.e., if some of the runoff to the sea is not withdrawn for consumptive use, an amount estimated to be about 40 km^3/year) the Caspian Sea level would be as high as before its catastrophic drop in the 1930s.

An analysis of monthly means of Volga runoff for January to May 1991 shows that runoff in each month exceeded that observed in 1990. The total runoff for the first five months in 1991 reached

188 km^3 (compared with 152 km^3 in 1990), which is 80% of the long-term annual mean. This spring flood was one of the most severe for several decades.

14.2

GREAT LAKES REMAIN AT NEAR-NORMAL LEVELS

The North American Great Lakes are one of the world's major water resources, containing about 20% of the world's freshwater supply. The Great Lakes system, comprising lakes Superior, Michigan, Huron, St. Clair, Erie, and Ontario, along with their connecting channels, includes an area of about 766,000 km^2. One third of the system area is lake surface. Two of the lakes, Superior and Ontario, are regulated with control structures at their outlets. The remainder of the system is naturally well regulated owing to the large lake surface areas and constricted outlet channels. Historically this has resulted in small lake-level fluctuations, about 1.8 m. The lake levels have also been modified slightly over the past 100 years by dredging in the connecting channels and by inter- and intra-basin diversions.

The Great Lakes water levels have been gauged since the early 1800s. Continuous water level measurements at the master gauge on each lake, except for Lake St. Clair, are available since 1860. These levels provide one of the longest time series of continuously measured hydrometeorological data in North America. They integrate short-period climate variability and serve as excellent indicators of longer-period water supply variations and climate change.

The annual lake level time series is shown in Figure 14.2. There have been three distinct lake level regimes over the past 130 years: a relatively high regime ending in the 1880s, a low regime lasting from the mid-1880s until about 1940, and a high regime from about 1940 to 1986. From December 1988 to May 1991 the lake levels fluctuated near their long-term means. This was the longest period of near-mean water levels since the 1960s.

GREAT LAKES WATER LEVELS — JULY 1991

LAKE	COMPARED WITH LONG-TERM MONTHLY AVERAGE (1900-1989)	COMPARED WITH JULY 1990
Superior	8 cm below	12 cm above
Michigan-Huron	same	14 cm above
St. Clair	18 cm above	9 cm above
Erie	18 cm above	5 cm above
Ontario	5 cm above	3 cm above

Photo FAO

INCREASING TROPICAL FOREST DEPLETION AND DESERTIFICATION

CHAPTER 15

Tropical forests are disappearing more than 50% faster than a decade ago, with the Earth annually losing forests equal in size to Austria, Denmark and the Netherlands combined. According to the Forest Resources Assessment Project* of the Food and Agricultural Organization of the UN (FAO), 17 million ha of tropical forests are lost to development each year. During the 1980s, about 70% of all deforestation occurred in dense rain forests of Latin America, Asia and the Pacific Ocean. Loss of tropical forests results in extinction of plants and animal species, waste of forest resources, and encroachment of deserts into once-fertile regions, and could contribute to long-term global climate changes.

Forest resource appraisals are made by FAO on a worldwide basis to provide reliable and globally consistent information about the current state of the tropical forest cover and about recent trends of deforestation and forest degradation. FAO's Forest Resources Assessment Project is carrying out the assessment in two complementary phases: (I) the compilation of existing survey data to the reference year 1990; and (II) the monitoring of tropical forest cover and its changes using remote sensing.

Table 15.1, based on Phase I studies, lists revised estimates of forest cover area and rates of deforestation at a subregional level. The figures are based on existing survey data and must be considered provisional since more information is expected for some of the countries, particularly, within Africa.

Forests are defined as vegetal formations with a minimum of 10% crown cover of trees (minimum

*) *For further information contact: Forest Resources Assessment 1990 Project, FAO, Via delle Terme di Caracalla, 00100 Rome, Italy.*

Table 15.1 - Preliminary estimates of forest area and rate of deforestation for 87 countries in the tropical regions (revised 15 October 1991) (FAO Forest Resources Assessment 1990 Project).

SUB-REGION	NUMBER OF CONTRIES STUDIED	TOTAL LAND AREA*	FOREST AREA 1980*	FOREST AREA 1990*	AREA DEFORESTED ANNUALLY 1981-1990*	RATE OF CHANGE 1981-1990
		THOUSANDS OF HA				% ANNUM
LATIN AMERICA	32	1 675 700	923 000	839 900	8 300	– 0.9
1 Central America and Mexico	7	245 300	77 000	63 500	1 400	– 1.8
2 Caribbean Sub-Region	18	69 500	48 800	47 100	200	– 0.4
3 Tropical South America	7	1 360 800	797 100	729 300	6 800	– 0.8
ASIA	15	896 600	310 800	274 900	3 600	– 1.2
4 South Asia	6	445 600	70 600	66 200	400	– 0.6
5 Continental South-East Asia	5	192 900	83 200	69 700	1 300	– 1.6
6 Insular South-East Asia	4	258 100	157 000	138 900	1 800	– 1.2
AFRICA	40	2 243 400	650 300	600 100	5 000	– 0.8
7 West Sahelian Africa	8	528 000	41 900	38 000	400	– 0.9
8 East Sahelian Africa	6	489 600	92 300	85 300	700	– 0.8
9 West Africa	8	203 200	55 200	43 400	1 200	– 2.1
10 Central Africa	7	406 400	230 100	215 400	1 500	– 0.6
11 Tropical Southern Africa	10	557 900	217 700	206 300	1 100	– 0.5
12 Insular Africa	1	58 200	13 200	11 700	200	– 1.2
TOTAL	87	4 815 700	1 884 100	1 714 800	16 900	– 0.9

** Figures may not tally due to rounding.*

height 5 m) and/or bamboos, generally associated with wild flora, fauna and natural soil conditions, and not subject to agricultural practices. Deforestation refers to the change of land use or the depletion of crown cover to less than 10%.

In Asia, forest cover area and rate of deforestation are both lower than in Latin America and Africa owing to the use of new data obtained for India and Myanmar in 1991. In Latin America, the estimates are higher since the whole of Brazil was included (previous estimates were limited to tropical moist zones, viz. Northern Brazil). For Africa, the assessment was completely reviewed using new data for several countries. The present estimates for rate of deforestation are lower for the moist zone. Major efforts are being made to secure an up-to-date and adequate database.

The differences between the present (1990) and FAO/UNEP (1980) assessments are indicated by the following summary statistics for 76 countries common to the two assessments (Table 15.2):

Table 15.2 - Estimated values for reference year (1980)

	FOREST AREA (MILLION HA)	AVERAGE ANNUAL RATE OF DEFORESTATION (MILLION HA)	% DEPLETED
FAO/UNEP(1980)	1935	11.3	0.6 (1976-80)
FAO - Forest Resources Assessment (1990)	1882	16.9	0.9 (1981-90)

LANDSAT image of southeast Amazonia, containing the Tucurui Hydroelectric Power Plant. Huge tracks of tropical vegetation were denuded during the construction of dam, lake and new settlements. More than 230,000 ha of forest cover was removed through other development activities. No measures were taken to prevent soil erosion and lake silting.

TROPICAL DEFORESTATION AND CLIMATE

Transformation of the tropical forest into pastures or other types of short vegetation will cause changes in the microclimate of the disturbed areas. Changes will occur in albedo and in energy and water balances.

A joint Anglo-Brazilian microclimate experiment was set up 80 km north of Manaus in order to compare the climate of a tropical forest with that of a pasture field that had replaced the forest. The data for 1990 showed that deforestation had a significant impact on the local climate. The reflected solar radiation (albedo) was 13% over the forest and 17% over the pasture. This translates into less energy over the pasture for use in evaporation and for heating the air. After a rainstorm the pasture evaporation was 5 mm a day, consuming about 75% of the available energy, a rate quite similar to the forest's.

However, after a 20-day dry spell, the pasture evaporation decreased to 2.5 mm a day or 55% of the available energy, whereas the forest's remained nearly constant. The average daily maximum air temperature was nearly 3°C higher for the pasture, compared to the forest.

If the size of the perturbed area is sufficiently large, the climate of nearby and even distant regions may be altered, depending on the scale of the alterations. It is not yet possible to predict accurately the regional climate changes associated with the observed patterns of deforestation by means of climate model simulations.

Simulation of Amazonia's large-scale deforestation using general circulation models suggests an increase in surface and soil temperatures and in the diurnal fluctuations of temperature and specific humidity deficit, and a reduction in evapotranspiration. In addition, the yearly averaged precipitation and runoff decreased more for the pasture vegetation than for the forest.

The impacts of large-scale deforestation on the global climate are still unknown. To understand and predict any possible large-scale climate change due to tropical deforestation, it is crucial to know to what extent the rainfall patterns will change when rainforests are converted into grasslands. It is well known that the tropical regions function as atmospheric heat sources through the release of latent heat of condensation in convective clouds, which drives the large-scale tropical circulations. Deforestation may also influence the chemistry of the atmosphere, by altering the exchange rates of greenhouse gases.

For an excellent discussion of tropical deforestation and its impacts on local, regional and global climates see the special issue of *Climate Change*, Vol. 19, Nos. 1-2, September 1991, edited by Norman Myers.

In addition to studies on deforestation, work progresses on assessing forest degradation. Indications are that biomass loss in the tropical forest is occurring at a significantly higher rate than the rate of area loss due to deforestation. A recent assessment of the Brazilian Amazon forest by scientists with the Space Research Institute at Manaus, Amazonas, Brazil, using LANDSAT imagery, showed an average annual deforestation rate of 2.2 million ha during the period 1978 to 1989. These rates decreased to 1.9 and 1.4 million ha during the periods 1988-1989 and 1989-1990, respectively. The total area deforested to date is 41.5 million ha, which represents 10.9% of the area originally occupied by the Brazilian forest.

DESERTIFICATION: A SONORAN DESERT STUDY

After the mid-1970s, climatologists debated vigorously about the climatic effects resulting from widespread overgrazing and human-induced desertification. Following a landmark article by Charney (1975), many climate scientists concluded that overgrazing in semi-arid lands would act to increase the surface reflectivity thereby cooling the surface and local air temperatures. However, many others argued that the drying effect of overgrazing and desertification could reduce soil moisture levels and lead to substantial warming in the affected areas. Recognizing the importance of the debate, scientists from Arizona State University, the University of Arizona, and the Jet Propulsion Laboratory initiated a study of climate response to overgrazing along the United States-Mexico border.

The U.S.-Mexico border has a substantial discontinuity in vegetation caused by severe overgrazing of the Mexican landscape. As a result, the Mexican side has a higher reflectivity, more exposed soil and far less vegetation cover. During the summer of 1987, detailed on-site and satellite measurements showed the Mexican side had afternoon air temperatures that were 2 to 4°C higher and surface temperatures that were about 7°C higher. Hydrological measurements revealed that the exposed Mexican landscape dries more rapidly than the U.S. side following summer storms; a few days after the storms, the depletion of soil moisture produces higher surface and air temperatures in Mexico (Balling, 1988, 1989; Bryant et al., 1990).

Recognizing that the spatial discontinuity in vegetation along the border evolved slowly over the past century, Balling (1991) hypothesized differential warming in Mexico with respect to adjacent American territory. Analysis of the Jones et al. (1986a, b, c) gridded temperature database revealed a 100-year warming bias of 0.32°C for the overgrazed area of northern Mexico. Balling (1991) expanded the analysis and found a desertification warming bias of about 0.50°C per century for many areas around the globe. The fundamental conclusion from this study is that widespread desertification is creating a warming signal in the land-based temperature record that could be easily mistaken for greenhouse warming.

16.1

DECEMBER 1988 TO FEBRUARY 1989

This period began with a peak in the high index phase of the Southern Oscillation, which proved to be the strongest since 1975. In southern Africa, where nearly all of the annual rainfall occurs from October to March, the 1988-1989 seasonal precipitation was mostly above normal and evenly distributed temporally across much of the area. The abnormally mild winter regime of late 1988 persisted across Siberia into 1989 and also occurred in northern Europe, where temperature departures as high as 21°C were recorded in February. Unusually dry and warm weather persisted into the beginning of 1989 in both Argentina and Uruguay, with some relief in late January. Similarly, very dry conditions prevailed throughout the eastern United States and southwestern Canada.

16.2

MARCH, APRIL AND MAY 1989

The Southern Oscillation Index continued to decrease during this period. The above normal temperatures lasted into May in much of Asia and until April in Northern Europe. Over much of South America, the very hot, dry weather continued into March, and although scattered showers fell in April, the long-term precipitation deficits remained while the dry season began in May. Very high temperatures were also recorded in northern Mexico and the southern United States. Central and southern Europe experienced the warmest March on record, but the warm conditions ended in April. Above normal precipitation dominated portions of Australia for the entire period.

16.3

JUNE, JULY AND AUGUST 1989

In the tropical Pacific, SST anomalies increased, setting the stage for a warm episode, while low-level easterlies decreased. The above normal temperatures returned to Europe in mid-July while a persistent southerly flow kept feeding warm tropical air over the continent.

Finally rains diminished in Australia and returned to parts of Canada and the United States. A marked lack of convective activity dominated the Caribbean in 1989. In India, the monsoon season was excellent compared with that of 1988, but July cyclones lashed the west coast with rains, floods and high waves. In the African Sahel, 1989 marked the second consecutive year of normal rainfall. Ghana and Nigeria were beset by heavy flooding during the last week in August.

16.4

SEPTEMBER, OCTOBER AND NOVEMBER 1989

The Southern Oscillation Index continued to fall. The 1989-1990 rainy season in southern Africa began with ample amounts of precipitation and, as in the Sahel region, this marked two consecutive years of sufficient rainfall. Heavy precipitation fell on Japan and the Republic of Korea at the beginning of September, accompanying two tropical storms, with several areas reporting the wettest September on record. Hurricane

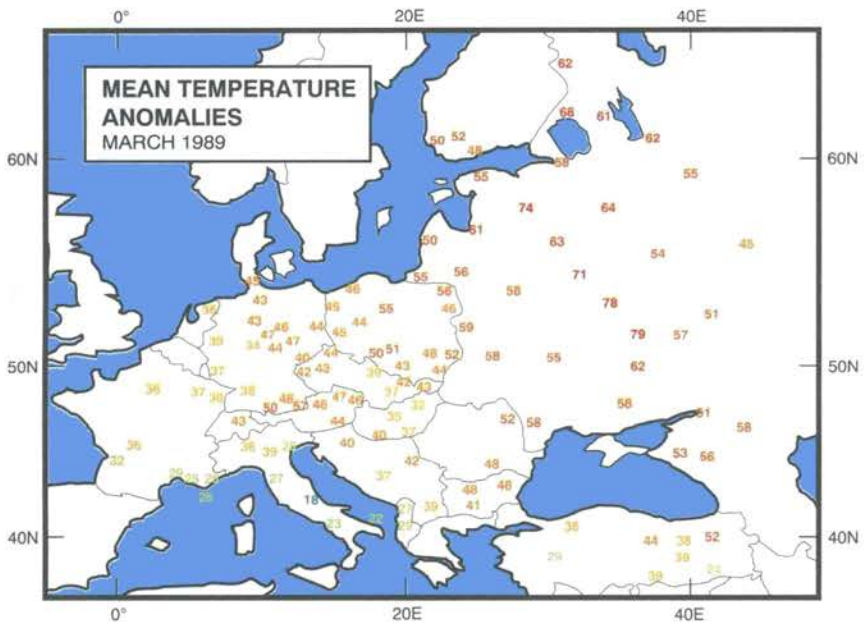

Figure 16.1 - European record high-temperature departures from normal in tenths of °C during March 1989 (NOAA, Climate Analysis Center, Washington, DC).

Hugo brought heavy rains and devastation to the Caribbean and portions of the southeastern United States. In November, unusually wet weather developed across northeastern Australia.

The persistent warm weather started again in portions of Europe after a cooler September. In contrast, record-breaking cold and heavy snows signalled an early winter for much of North America. In the middle of November, Alaska and northwestern Canada became extremely cold.

16.5

DECEMBER 1989 TO FEBRUARY 1990

Very dry conditions spread gradually across south-central and southeastern Europe in January and February when severe storms afflicted northern Europe. Much of southern Europe received less than 75% of normal precipitation from October 1989 throughout this time period. In December, several European areas experienced record-breaking warmth, while record-breaking cold continued in North America.

Conditions in the Pacific continued to evolve toward a warm ENSO episode that never became entrenched. In February, the SOI, during its downward trend, reached its lowest value since 1982-1983. However, no persistent intense convection developed in the equatorial central Pacific.

Torrential rains, as much as 350 mm during one week, fell across southeastern Africa and Madagascar in January and February. Brazil was very wet at the beginning of the year, while in Australia a year that would be characterized by alternating wet and dry spells began quite dry in the northern regions.

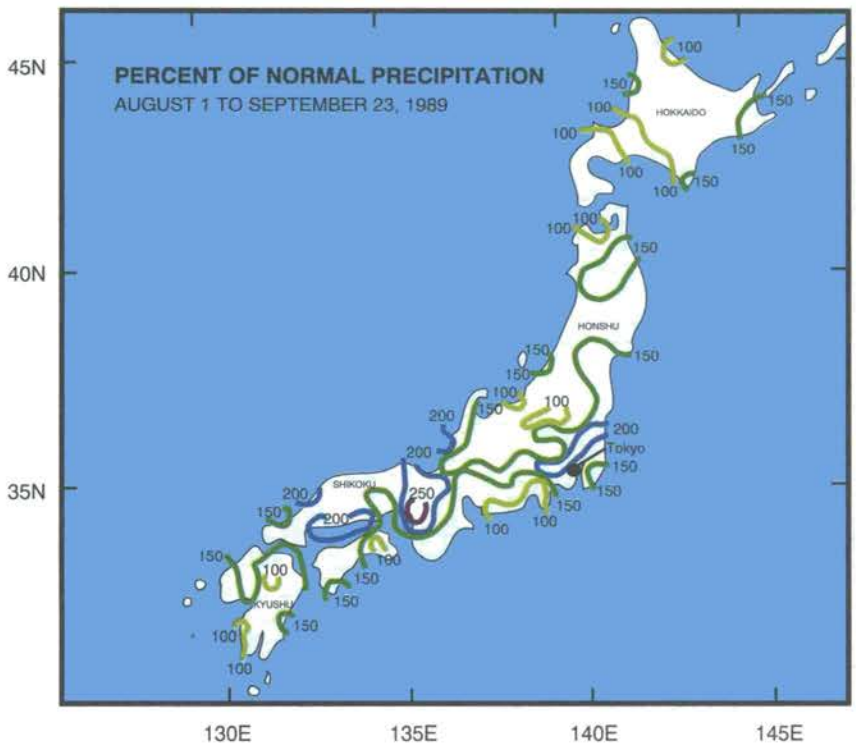

◄ *Figure 16.2* - Percentage of normal precipitation in Japan from August 1 to September 23, 1989 (NOAA, Climate Analysis Center, Washington, DC).

16.6

MARCH, APRIL AND MAY 1990

In March, the SOI was still strongly negative but it reversed its downward trend for the first time in more than a year. Stronger convective activity started in the central Pacific, and SSTs and their warm anomalies began an increase that would last most of the year. These conditions continued to signal the possible beginning of a warm ENSO episode.

Abundant rainfall covered the southwest Pacific by early March, ending the prolonged dry regime. Later in the month tropical storm Ivor produced heavy rains, which generally continued in northeastern Australia in the form of tropical thunderstorms, producing some of the worst flooding of the century.

Heavy rains fell in April and early May across equatorial Africa. Over much of northern Africa and the Sahel, unusually dry conditions prevailed.

Very warm weather spread across northern Asia in March and April as part of an overall pattern that dominated the Northern Hemisphere. The 1990 Indian monsoon started slightly ahead of schedule, preceded by one of the most intense cyclones of the decade along the southeast coast of India in May.

In Brazil a drier regime began for most of March, but rain from severe thunderstorms fell in early April. Later drier weather occurred

across most of Uruguay and portions of Argentina and Paraguay, lasting during May. Long-term dryness persisted across Hispaniola, Puerto Rico and much of the Caribbean.

16.7

JUNE, JULY AND AUGUST 1990

Positive SST anomalies persisted along with a weakening of the equatorial easterly winds. The SOI with its slight upward trend was the only indicator against a developing warm episode.

In Africa, the Sahel rainy season (1 May to 30 September) was hot and dry, except for a short wet spell at the beginning of July, and bore little resemblance to the more favourably moist seasons of 1988 and 1989. Exceptionally dry weather dominated much of the eastern, northern and extreme western Sahel.

August rainfall in southeastern areas of South America was not enough to overcome the persistent excessive dryness. Dryness also affected northern North America, and combined with high temperatures led to the third worst wildlife season ever recorded in Alaska. In Europe, also, a heat wave persisted during most of July and August, accompanied by abnormally dry conditions.

In Asia, typhoons that began in late July affected many areas in much of the Indian subcontinent. The monsoon produced very heavy rains and flooding that continued in July, diminished in early August and returned later in the month to northeastern India, spreading farther west and causing widespread floods and landslides.

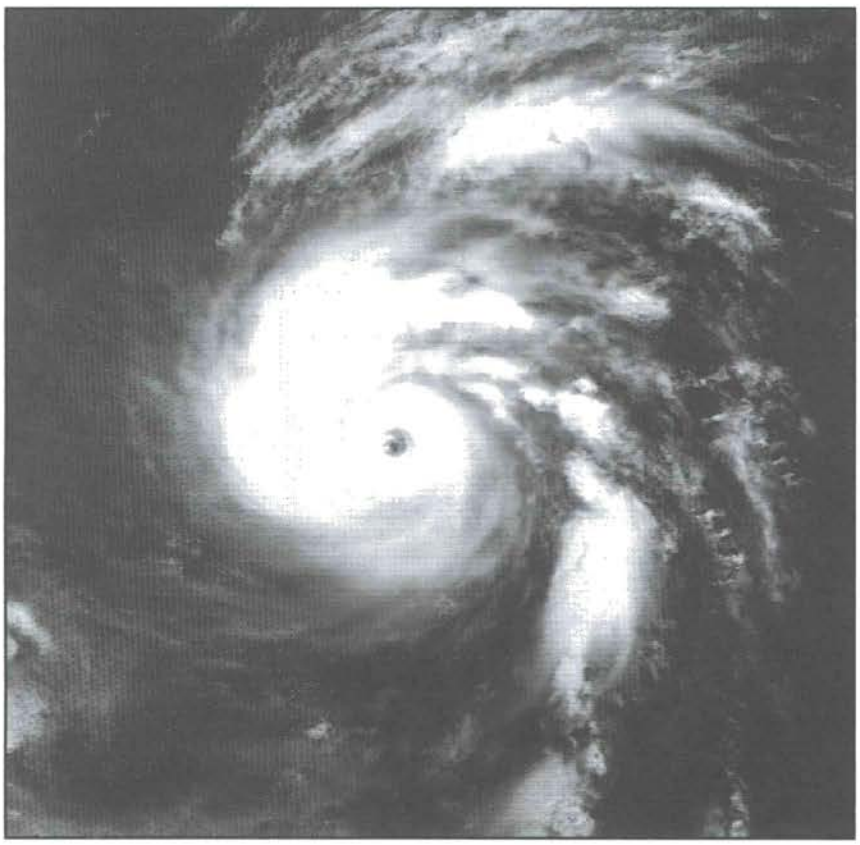

16.8

SEPTEMBER, OCTOBER AND NOVEMBER 1990

Despite increasing positive SST anomalies throughout the equatorial South Pacific Ocean, a significant warm ENSO episode did not materialize toward the end of 1990. Convective activity was only slightly greater than normal, and the SOI averaged near zero.

Southeastern Africa was plagued by abnormally dry weather as seasonal rains were absent. In constrast, the rainy season in southeastern South America began in earnest with heavy rainfalls across eastern Argentina, Uruguay and southern parts of Brazil and Paraguay. Across Japan, torrential rains and strong winds accompanying typhoon Flo in September caused severe flooding and landslides. Dry weather followed, until terminated by typhoon Page in late November.

Unseasonably warm weather returned to much of Europe during late September and early October, but the dry weather in southern Europe was relieved somewhat by moderate to heavy rains along the Mediterranean shores in October, when a significant six-week wet spell was ending in northeastern Europe.

16.9

DECEMBER 1990 TO FEBRUARY 1991

The weak central Pacific warm episode persisted while the depth of the thermocline and the upper ocean heat content remained greater than normal, although SST anomalies decreased.

December brought cold weather and unusually heavy snowfalls throughout a significant portion of continental Europe, although some of Scandinavia remained free of snow cover.

In southern Africa, excessive rains in late January followed a slow beginning to the rainy season. In central South America, the middle of the rainy season was dry and January light rains did little to reduce moisture deficits. In southeastern South America, however, primarily favourable rains provided sufficient moisture for most crops. The west coast of North America endured its fifth consecutive abnormally dry rainy season when January and February had exceptionally low precipitation. Eastern sections of Asia and much of the southwest Pacific also began 1991 with dry weather, although the only Southern Hemisphere growing region to experience widespread, season-long dryness was southeastern Australia.

16.10

MARCH, APRIL AND MAY 1991

The tragic event in this time period was the late April cyclone that swept across Bangladesh with six-metre waves and 270 km/h winds, claiming nearly 125,000 lives.

Positive SST anomalies increased in many sections of the tropical and eastern Pacific, as well as in the eastern equatorial Atlantic and central tropical Indian Ocean. Atmospheric circulation features, such as the blocking pattern that developed during April and May in the central and eastern Pacific, were consistent with these anomalies as indicators of a developing warm episode, which did occur toward the end of 1991. However, at the end of May persistent strongly enhanced convection was still lacking in the central equatorial Pacific region.

Across west-central Africa some areas received very little rainfall, whereas others were deluged. March was exceptionally warm across the western and central Sahel.

In Europe, a very warm spell during March persisted until late April when a cold outbreak invaded much of the continent causing damage to France's grape and fruit crops.

In South America during March, late season warm and drier weather developed, but was ended abruptly by heavy rains in mid-April, which continued in the east-central portion of the continent throughout May.

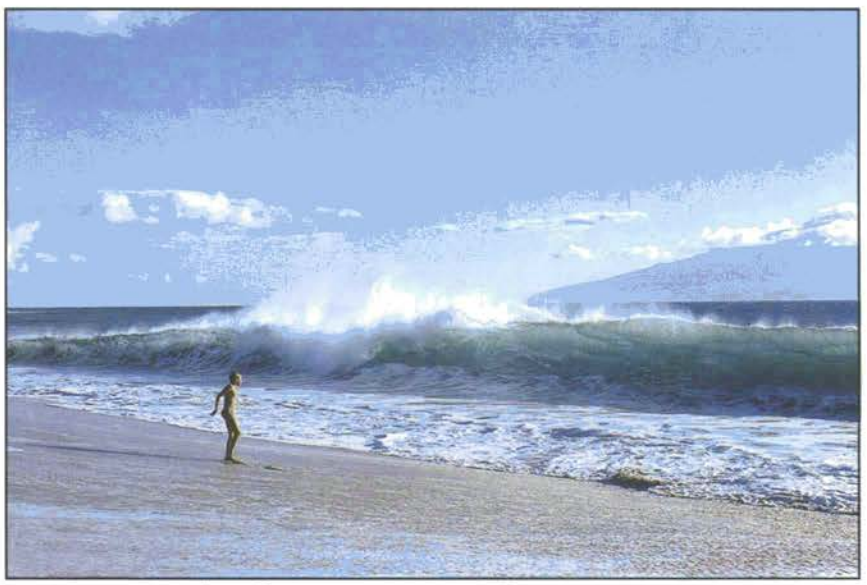

Hurricane generated swell waves - West Coast of Maui, Hawaii

Photo Grant W. Goodge

THE 1980s - A REMARKABLE DECADE FOR CLIMATOLOGY

CHAPTER 17

The 1980s were one of the most remarkable climate decades in recent history. At least three new entries went into the world weather record book. In Antarctica, a new all-time low temperature of -89.6°C was recorded at Vostok on July 21, 1983. Hurricane Gilbert, the most powerful Atlantic hurricane of the century, passed through the Caribbean and the Gulf of Mexico in September 1988, setting a new low-pressure record of 88.8 kPa for the Western Hemisphere. A few months later, in January 1989, a new high-pressure record for North America, 107.5 kPa, was set at Northway, Alaska.

Not surprisingly, there were several brief, localized and exceptionally violent storms that produced extensive wind damage, and in some cases enormous floods. The decade experienced some of the worst summer droughts since the 1930s. Northern Hemispheric tropospheric circulation patterns suggest there have been small, but significant, systematic shifts in the hemispheric circulation patterns. Over the years, tropical monsoon rainfall amounts generally decreased, whereas mid-latitude precipitation may have increased. The 1980s also saw some of the largest year-to-year variability of the twentieth century. In particular, the Southern Oscillation was associated with the strongest warm episode of the century (1982-1983) and the strongest cold episode in 50 years (1988-1989).

But the biggest story of the 1980s was the growing public concern about climate and atmospheric change. The Antarctic ozone hole was first reported in 1985, and similar Arctic depletions were reported in 1986 and confirmed in subsequent years. The extent of these depletions and the suddenness with which they appeared focused attention on the fragility of the atmosphere in a way that few other events could and brought new urgency to international attempts to cut back the use of chlorofluorocarbons.

For the first time, a large segment of the public realized that global warming could be a significant and even imminent threat, when heat and drought affected many parts of the world. In the United States, a heat wave in the summer of 1980 was responsible for more than 1200 deaths, and wheat yields were reduced for much of the decade by drought on the northern plains. In Africa, famine was widespread, especially in the mid-1980s, when the long-standing drought in the western Sahel region intensified, and new droughts developed in other areas, notable Ethiopia. After an unbroken string of more than 20 dry years, the rains finally returned to the Sahel in 1988, but as the 1980s ended the spectre of drought and famine loomed once again over Ethiopia.

The eighties turned out to be the warmest decade globally since the first estimates of average world temperatures were compiled in 1881. Indeed, seven of the ten warmest years on record were all in the 1981-1990 decade, with 1990 being the warmest ever.

17.1 MAJOR EXTREMES IN THE SOUTHERN OSCILLATION (WARM AND COLD EPISODES) DOMINATED THE INTERANNUAL VARIABILITY

Perhaps the strongest warm (El Niño/Southern Oscillation — ENSO) episode of the last century occurred during 1982-1983. That episode featured extreme flooding in western Ecuador, coastal northern

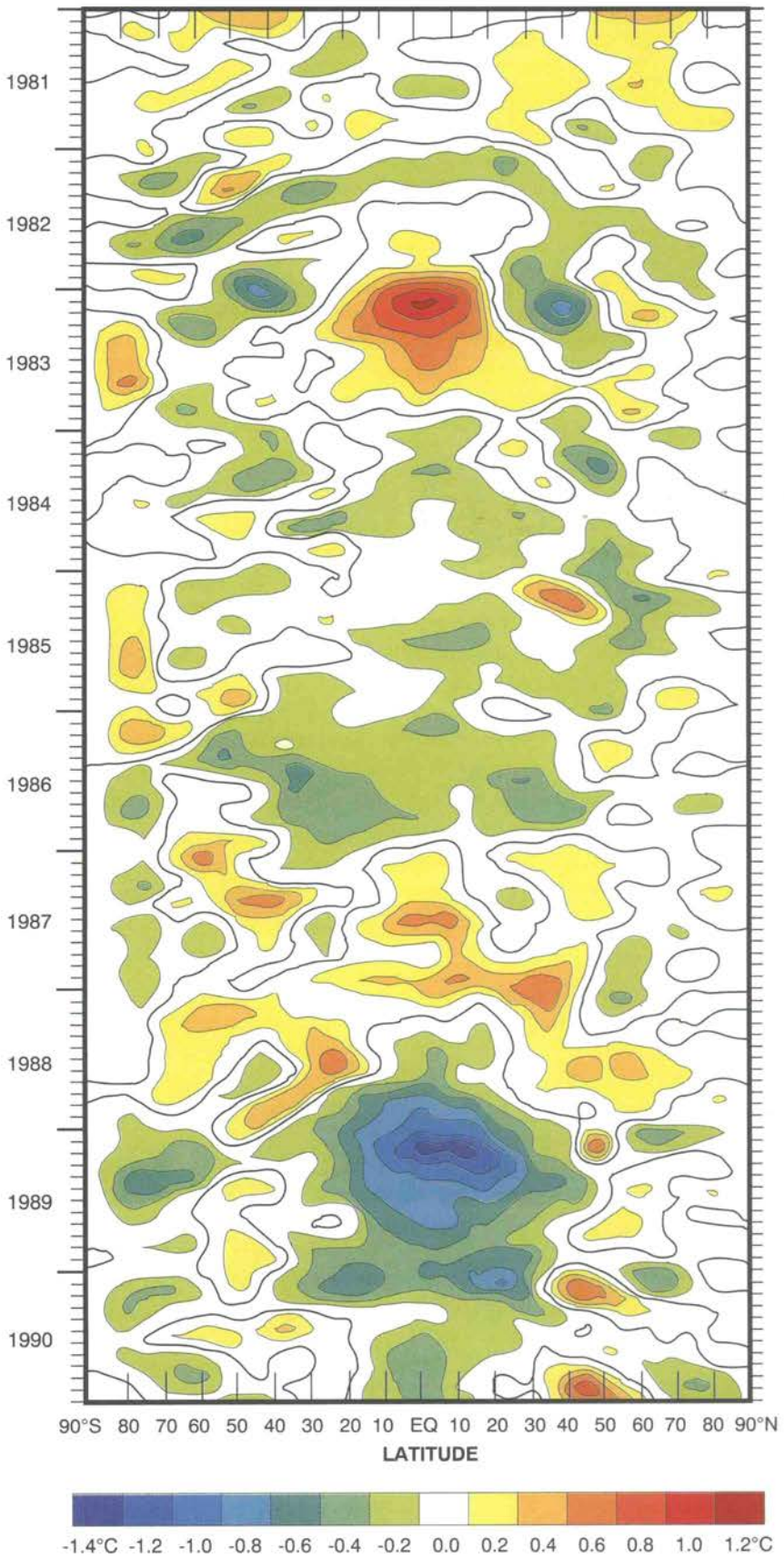

Figure 17.1 - Time-latitude section of zonally averaged 500-hPa temperature anomalies, computed with respect to the 1979-1988 monthly means. Contour interval is 0.2°C (from NOAA, Climate Analysis Center, Washington, DC).
◄

Peru, and southern California. Australia suffered its worst drought since the l860s, and drought also plagued northeast Brazil, Indonesia and India. Another warm episode occurred during 1986-1987. Although much weaker than the 1982-1983 episode, it was a moderately strong event, which affected precipitation, temperature and atmospheric circulation in many regions. Following this episode, a strong Pacific cold episode developed during 1988-1989, which was one of the strongest cold episodes of the last 50 years. This episode featured enhanced precipitation in the monsoons of India and Australia, above normal rainfall in northeast Brazil, and drought in southern Brazil, Uruguay and central Argentina. In contrast to the enhanced strength of the subtropical upper-tropospheric westerlies during warm episodes, the strength of the subtropical westerlies was anomalously weak during 1988-1989 since the main belt of westerlies shifted poleward of its normal position. The northern winters of 1988-1989 and 1989-1990 were characterized by less than normal extratropical cyclone frequencies and above normal temperatures at many mid-latitude locations.

Figure 17.1 is a time-latitude section of the zonally averaged 500- hPa temperature anomalies for the 1980s. The analysis is used as an index of the tropospheric heating and cooling associated

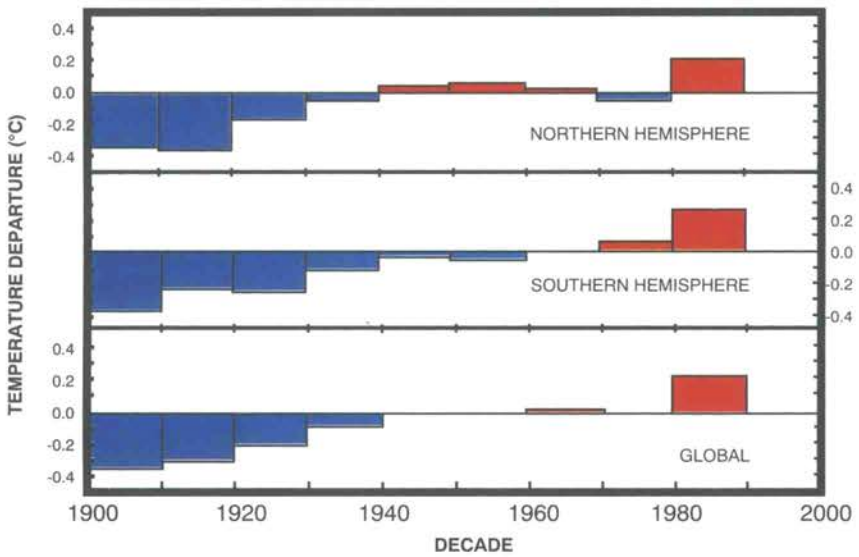

Figure 17.2 - Average temperatures for each hemisphere and the world for each decade of the twentieth century. Data are plotted as departures from 1950-1979 values (from Climatic Research Unit, University of East Anglia). ◄

with variations in the intensity of tropical convective activity. Zonally averaged positive anomalies were observed in the tropics during the two ENSO episodes of 1982-1983 and 1986-1987. However, it is apparent from Figure 17.1 that the cold episode of 1988-1989 also had a remarkable impact on mid-tropospheric, temperatures, with zonally averaged anomalies of less than -1.4°C in the tropical belt.

During periods of anomalously warm or cold conditions in the tropical mid-troposphere, the mid-latitudes tend to experience opposite temperature anomalies. Thus, during warm (cold) episodes when the tropical mid-troposphere is anomalously warm (cold), the mid-latitude mid-troposphere is anomalously cold (warm). It is evident that the cold episode of 1988-1989 affected the tropical and extratropical mid-tropospheric temperature anomalies from early 1988 until early 1990 (a period of about two years). During that period, the mid-latitudes in both hemispheres were dominated by anomalously warm conditions.

17.2 RECORD WARMTH

The 1980s (1981-1990) were the warmest decade since comparable records began in the mid-nineteenth century, and in both hemispheres were at least 0.2°C warmer than all decades during the twentieth century and at least 0.4°C warmer than its first two decades (Figure 17.2). The warmth was not evident everywhere but tended to be concentrated over land masses in the Northern Hemisphere (Figure 17.3). Temperatures cooler than the reference period's were experienced over Greenland, Iceland, eastern Canada and portions of the North Pacific Ocean. In the Southern Hemisphere the warmth was more evenly spread, with the only major area of colder than normal temperatures being situated over eastern Antarctica.

17.3 ANTARCTIC OZONE HOLE AND TRACE GASES

There were several major changes in the chemistry of the atmosphere during the decade. The volcanic eruption of El Chichón in Mexico in April 1982 injected large quantities of dust and gas into the stratosphere as evidenced by the low atmospheric transmission (see Figure 10.5), where it remained for several years. During this time, these particles and gases caused decreases in stratospheric ozone, increases in stratospheric temperature, and decreases in mean surface air temperature (some of which may have been offset by the 1982-1983 ENSO event).

The Antarctic ozone hole was first reported in the scientific literature in 1985, and concentrations of stratospheric ozone over Antarctica during the austral springtime decreased markedly from the beginning to the end of the decade (see Figures 10.2 and 10.3). This phenomenon is expected to continue well into the next century until the impact of the Montréal Protocol controls become effective. Many trace gases, both the greenhouse warming species (e.g. carbon dioxide and methane) and

Figure 17.3 - Annual temperature anomalies for the 1981-1990 decade. Data are plotted as departures from the 1950-1979 values. Shaded areas have insufficient data for analysis (from Climatic Research Unit, University of East Anglia).

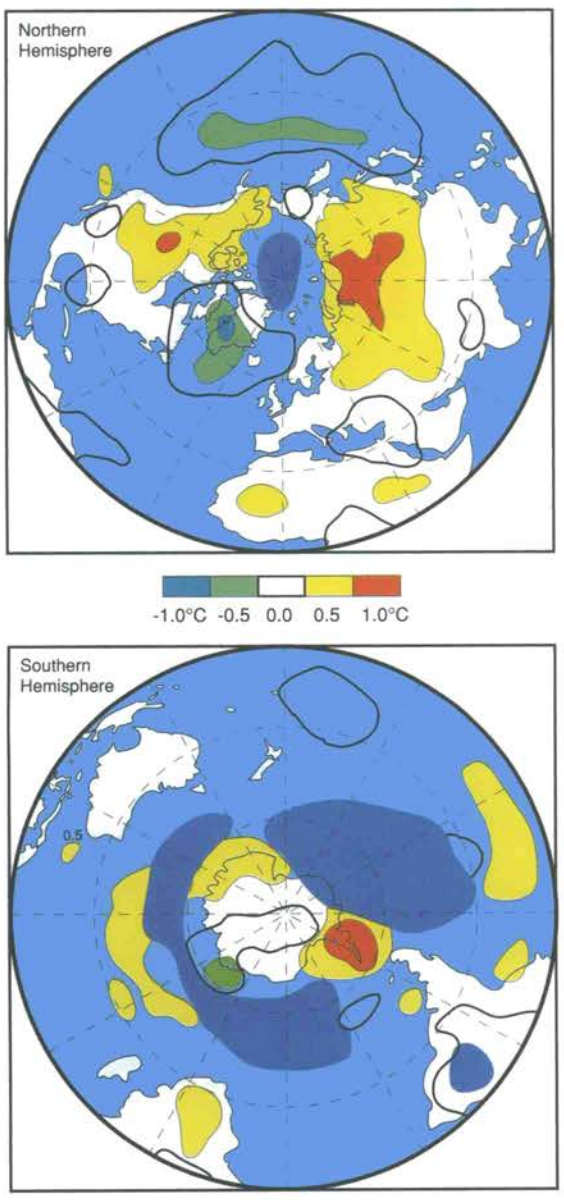

stratospheric ozone-depleting species (e.g., CFC-11, CFC-12, and nitrous oxide), showed continuing increases in their global background concentrations.

17.4 INTERNATIONAL MILESTONES IN RESPONSE TO GLOBAL WARMING

But the 1980s may best be remembered as a remarkable climate decade because of the growing conviction within the international scientific community that the climate system is changing at such a rate that global ecosystems and human society are being threatened. Further, for the first time it was recognized that atmospheric issues are not independent, but are inextricably linked, and that action to deal with both causes and effects must be based on a more holistic approach to atmospheric change and to the human and economic dimensions of such change. That conviction has moved the climate change issue to the forefront of the international political agenda and has led to the convening of several international conferences. Responses to the consequences of atmospheric change include the following:

- First World Climate Conference, Geneva (February 1979)
- Vienna Convention for the Protection of the Ozone Layer (1985)
- International Conference on the Assessment of the Role of CO_2 and Other Greenhouse Gases in Climate Variations and Associated Impacts, Villach (1985)
- Montréal Protocol to control CFCs (September 1987)
- Workshops on Developing Policies for Responding to Climate Change, Villach and Bellagio (1987)
- World Commission on Environment and Development (WCED) report to the United Nations General Assembly (September 1987)
- World Conference on The Changing Atmosphere, Toronto (June 1988)
- Establishment of the Intergovernmental Panel on Climate Change (November 1988)
- Conference on Legal and Policy Aspects of the Protection of the Atmosphere, Ottawa (February 1989)
- Ministerial Conference on Atmospheric Pollution and Climate Change, Noordwijk (November 1989)
- Intergovernmental Panel on Climate Change (IPCC) reports (August 1990)
- Second World Climate Conference, Geneva (October/November 1990)
- United Nations General Assembly resolution to establish the negotiating process for the climate change convention (Fall 1990)
- Start of Negotiations on a Framework Convention Climate Change, Washington (February 1991)
- United Nations Conference on Environment and Development, Brazil (June, 1992)
- Signature by 153 countries of Framework Convention Climate Change, Washington (February 1992)

MAJOR CLIMATE SYSTEM EVENTS AND ANOMALIES DURING 1981-1990

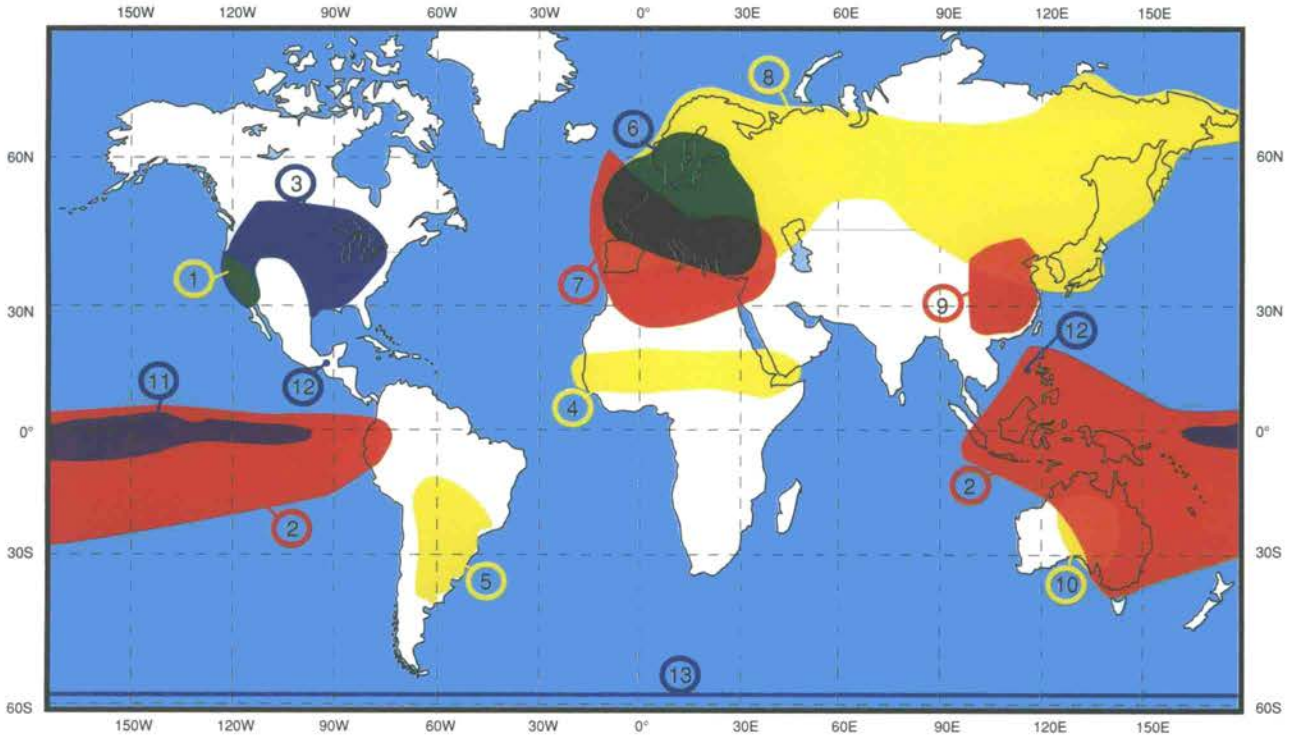

Figure 17.4 - Major climate system events and anomalies throughout the world: 1981-1990 (adapted from Halpert and Ropelewski, 1991):

1. California drought — five consecutive dry winters (1986-1990). Less than 60% of normal precipitation was recorded in San Francisco and Los Angeles.
2. Intense El Niño/Southern Oscillation affects global climate (1982-1983) — Abnormally warm equatorial Pacific waters brought massive floods to portions of Ecuador and Peru, numerous tropical cyclones to French Polynesia, and record drought to Australia and Indonesia.
3. The 1988 drought in the Midwest was the most severe since 1936.
4. The second consecutive dry decade in the Sahel caused widespread crop failures and large-scale human suffering.
5. Prolonged heat and dryness across east-central South America (1988-l989) produced the worst harvests in 26 years.
6. A cold winter and spring occurred across Europe in 1987. Severe winter weather halted shipping in northern Europe, spread snow south to the Riviera and froze citrus crops in Italy and Greece.
7. Heat waves aggravated prolonged dryness in southern Europe, the Middle East and Northern Africa in 1990.
8. Record winter (1988-1989) and spring (1989) mildness spreads across Eurasia. The warmth resulted in weekly temperatures averaging up to 21°C above normal.
9. The spring (1981) drought in China was overtaken by late summer floods. Most of Hebei province recorded only 10-30% of normal precipitation in spring. Torrential rains abruptly ended the drought; the Yangtze River reached its highest level this century.
10. Record rains in l984 caused severe flooding in Eastern Australia.
11. The cold ENSO in the Pacific during 1988-1989 was one of the most severe cold episodes of the last 50 years.
12. Major volcanic eruptions — El Chichón in March 1982 and Pinatubo in June 1991 — injected tens of millions of tonnes of aerosols into the stratosphere, perhaps more than any volcano in this century. Effects of the eruption include more acidic rain, further depletion of the ozone layer and surface cooling of up to 0.5°C.
13. The concentration of stratospheric ozone over Antarctica during September to November decreased markedly during the decade.
14. The mean CO_2 growth rate for the 1980s was about 1.5 ppm per year.

1. INTRODUCTION AND HIGHLIGHTS

AUSTRALIAN BUREAU OF METEOROLOGY, *1988 to 1991: Climate Monitoring Bulletin — Southern Hemisphere*. National Climate Centre, Melbourne. Monthly issue.

AUSTRALIAN BUREAU OF METEOROLOGY, *1988 to 1991: Seasonal Climate Outlook*. National Climate Centre, Melbourne. Seasonal issue.

HALPERT, M.S. and C.F. ROPELEWSKI, *1991: Climate assessment. A decadal review 1981-1990*. NOAA, National Weather Service — National Meteorological Center, Climate Analysis Center. Washington, DC

U.S. DEPARTMENT OF COMMERCE, *1988 to 1991: Climate Diagnostics Bulletin*. NOAA, National Weather Service — National Meteorological Center, Climate Analysis Center, Washington, DC. Issued monthly.

U.S. DEPARTMENT OF COMMERCE, *1988 to 1991: Weekly Climate Bulletin*. NOAA, National Weather Service — National Meteorological Center, Climate Analysis Center, Washington, DC.

WORLD METEOROLOGICAL ORGANIZATION and UNITED NATIONS ENVIRONMENT PROGRAMME, *1985: The Global Climate System. A critical review of the climate system during 1982-1984*. World Climate Data Programme. 52 pp.

WORLD METEOROLOGICAL ORGANIZATION and UNITED NATIONS ENVIRONMENT PROGRAMME, *1987: The Global Climate System. Autumn 1984 — Spring 1986*. World Climate Data Programme. CSM R84/86. 87 pp.

WORLD METEOROLOGICAL ORGANIZATION and UNITED NATIONS ENVIRONMENT PROGRAMME, *1990: The Global Climate System — Climate System Monitoring June 1986 — November 1988*. World Climate Data Programme. CSM R84/86. 70 pp.

WORLD METEOROLOGICAL ORGANIZATION and UNITED NATIONS ENVIRONMENT PROGRAMME, *1988 to 1991: Climate System Monitoring (CSM) Monthly Bulletin*. World Climate Data and Monitoring Programme. Monthly issue.

2. GLOBAL ATMOSPHERIC AND OCEANIC CIRCULATION

ANGELL, J.K., *1990: Variation in global tropospheric temperature after adjustment for the El Niño influence, 1958-89*. Geophysical Res. Lett., 17 (8): 1093-1096.

BARDIN, M.Y., *l990: Statistical properties of cyclonicity at 500 mb in the Northern Hemisphere*. Proceedings of USSR Hydrometcenter, V.304, (in Russian).

DROSDOWSKY, W. and M. WILLIAMS, *1991: The Southern Oscillation in the Australian region. Part I: Anomalies at the extremes of the oscillation. J. of Climate*, 4 (6): 619-638.

ENFIELD, D.B., *1989: El Niño, past and present*. Reviews of Geophysics, 27(1):159-187.

GRUZA, G.V. and L.V. KOROVKINA, *1991: Climatic monitoring of blocking processes of the middle of the westerlies in the Northern Hemisphere*. Meteorology and Hydrology, Number 8 (in Russian).

GRUZA, G.V. and L.V. KOROVKINA, *1991: Seasonal features of space distribution of blocking indices in the Northern Hemisphere*. Meteorology and Hydrology, Number 3 (in Russian).

HASTENRATH, S., *1990: Decadal-scale changes of the circulation in the Tropical Atlantic Sector associated with Sahel drought*. International J. of Climatology, 10: 459-472.

HASTINGS, P.A., *1990: Southern Oscillation influences on tropical cyclone activity in the Australian/South-West Pacific region*. International J. of Climatology, 10: 291-298.

JOSEPH, P.V. and B. LIEBMANN, *1991: Interannual variability of the Australian summer monsoon onset: Possible influence of Indian summer monsoon and El Niño*. J. of Climate, 4 (5): 529-538.

JUILLET-LECLERC, A., L.D. LABEYRIE and J.L. REYSS, *1991: Temperature variability in the Gulf of California during the last Century: A record of the recent strong El Niño*. Geophysical Res. Lett., 18 (10): 1889-1892.

KAROLY, D.J., *1989: Southern Hemisphere circulation features associated with El Niño-Southern Oscillation*. J. of Climate, 2 (11): 1239-1252.

KILADIS, G.N. and H.F. DIAZ, *1989: Global climatic anomalies associated with extremes in the Southern Oscillation*. J. of Climate, 2 (9): 1069-1090.

KOROVKINA, L.V., *1989: Synoptic-climatological characteristics of the blocking processes in the atmosphere*. Reviews. Obninsk (in Russian).

KOUSKY, V.E., *1991: The evolution of recent oceanic and atmospheric anomaly fields in the Tropical Pacific*. Proceedings 15th Climate Diagnostics Workshop, Asheville, NC. October 29 to November 2, 1990. pp. 1-10.

KOUSKY, V.E. and M.S. HALPERT, *1991: The global climate of March-May 1990: An abnormally warm season in both hemispheres*. J. of Climate, 4 (1): 80-105.

LABITZKE, K. and H. VAN LOON, *1989: The Southern Oscillation. Part IX: The influence of volcanic eruptions on the Southern Oscillation in the stratosphere*. J. of Climate, 2 (10): 1223-1226.

LINDESAY, J.A. and C.H. VOGEL, *1990: Historical evidence for Southern Oscillation-Southern African rainfall relationships*. International J. of Climatology, 10: 679-689.

NICHOLLS, N., *1987: The El Niño/Southern Oscillation phenomenon*. In: The Societal Impacts Associated with the 1982-83 Worldwide Climate Anomalies (Michael Glantz, Richard Katz and Maria Krenz, editors). National Center for Atmospheric Research, Boulder, CO. Report of Workshop on the Economic and Societal Impacts Associated with the 1982-83 Worldwide Climate Anomalies, 11-13 November 1985. Lugano, Switzerland. pp.2-10.

NESTEROVA, G.A., *1982: Climatic variability of polar vortex characteristics*. Proceedings of Institute of Hydrometeorological Information World Data Center, Obninsk, Volume 84 (in Russian).

QUING LIU and C.J.E. SCHUURMANS, *1990: The correlation of tropospheric and stratospheric temperatures and its effect on the detection of climate changes*. Geophysical Res. Lett. 17 (8): 1085-1088.

REYNOLDS, R.W., *1988: A real-time global sea surface temperature analysis*. J. of Climate, 1 (1): 75-86.

RICHMAN, M.B., P.J. LAMB and J.R. ANGEL, *1991: Relationships between monthly precipitation over central and eastern North America and the Southern Oscillation*. Proceedings 15th Climate Diagnostics Workshop. Asheville, NC. October 29 to November 2, 1990. pp. 373-383.

SCHONHER, T. and S.E. NICHOLSON, *1989: The relationship between California rainfall and ENSO events*. J. of Climate, 2 (11): 1258-1269.

SOLOW, A. and N. NICHOLLS, *1990: The relationship between the Southern Oscillation and tropical cyclone frequency in the Australian region*. J. of Climate, 3 (10): 1097-1101.

WAGNER, J., *1991: Northern Hemisphere circulation*. Weatherwise, 44 (1): 17-21.

WAGNER, J., *1989: Persistent circulation patterns*. Weatherwise, 42 (1): 18-21.

WAGNER, J., *1990: Northern Hemisphere circulation: High latitude persistence*. Weatherwise, 43 (1): 19-22.

WANG, W-C. and K. LI, *1990: Precipitation fluctuation over semi-arid region in northern China and the relationship with El Niño/Southern Oscillation*. J. of Climate, 3: 769-783.

WANG, W-C. and K. LL, *1990: Precipitation fluctuation ofer semiarid region in Northern China and the relationship with El Niño/Southern Oscillation*. J. of Climate, 3 (7): 769-783.

WOLTER, K. and S. HASTENRATH, *1989: Annual cycle and long-term trends of circulation and climate variability over the tropical oceans*. J. of Climate, 2 (11): 1329-1351.

WOOD, F.B., *1990: Monitoring global climate change: The case of greenhouse warming*. Bulletin of the American Meteorological Society, 71: 42-52.

WYRTKI, K., *1975: El Niño — The dynamic response of the equatorial Pacific Ocean to atmospheric forcing*. J. Phys. Oceanogr., 5: 572-584.

ZEBIAK, S.E., *1989: On the 30-60 day oscillation and the prediction of El Niño*. J. of Climate, 2 (11): 1381-1387.

3. TEMPERATURE

ANGELL, J.K., *1988: Variations and trends in tropospheric and stratospheric global temperatures, 1958-1987*. J. of Climate, l: 1296-1313.

BALLING, R.C., JR., *1988: The climatic impact of a Sonoran vegetation discontinuity*. Climatic Change, 13: 99-109.

BALLING, R.C., JR., *1989: The impact of summer rainfall on the temperature gradient along the United States — Mexico border*. J. of Applied Meteorology, 28: 304-308.

BALLING, R.C., JR., *1991: Impact of desertification on regional and global warming*. Bulletin of the American Meteorological Society, 72: 232-234.

BRYANT, N.A., L.F. JOHNSON, A.J. BRAZEL, R.C. BALLING JR., C.F. HUTCHINSON and L.R. BECK, *1990: Measuring the effect of overgrazing in the Sonoran Desert*. Climate Change, 17: 243-264.

CHARNEY, J.G., *1975: Dynamics of deserts and drought in the Sahel*. Quarterly Journal of the Royal Meteorological Society, 101: 193-202.

DIAZ, H.F., *1990: A comparison of "global" temperature estimates from satellite and instrumental data, 1979-88*. Geophysical Res. Lett., 17 (12): 2373-2376.

ELSNER, J.B. and A.A. TSONIS, *1991: Comparisons of observed Northern Hemisphere surface air temperature records*. Geophysical Res. Lett., 18: 1229-1232.

FINDLAY, B.F. and A. DEPUTUCH-STAPF, *1991: Colder than normal temperatures over Northeastern Canada during the 1980s*. Canada Department of the Environment, Climatic Perspectives, 13 (4): 9-12.

FOLLAND, C.K. and D.E. PARKER, *1990: Observed variations of sea surface temperature*. In Climate-Ocean Interaction. (M.E. Schlesinger, editors), Kluwer, pp. 31-52.

FOLLAND, C.K., T.R. KARL and K. YA. VINNIKOV, *1990: Observed climate variations and change*. In Climate Change: The IPCC Scientific Assessment. (J.T. Houghton, G.J.Jenkins and J.J. Ephraums, editors), Cambridge University Press, pp. 195-238.

GRUZA, G.V., E. YA. RANKOVA and E.V. ROCHEVA, *1989: Analysis of global data on variations in surface air temperature over the period of instrumental observations*. Meteorology and Hydrology, 1: 22-31 (in Russian).

HANSON, K., G.A. MAUL, and T.R. KARL, *1989: Are atmospheric "greenhouse" effects apparent in the climatic record of the contiguous*

U.S. (1895-1987)?. Geophysical Res. Lett., 16: 49-52.

HEIM, R., K. DEWEY, M. ANDERSON and D. LEATHERS, *1990: A December to remember.* Weatherwise, 43:329-332.

HOUGHTON, J.T., G.J. JENKINS and J.J. EPHRAUMS, *1990: Climate Change: The IPCC Scientific Assessment,* Cambridge University Press, 364 pp.

JONES, P.D. and T.M.L. WIGLEY, *1990: Global warming trends.* Scientific American, 263: 84-91.

JONES, P.D., S.C.B. RAPER, R.S. BRADLEY, H.F. DIAZ, P.M. KELLY and T.M.L. WIGLEY, *1986a: Northern hemispheric surface air temperature variations: 1851-1984.* J. of Climate and Applied Meteorology, 25: 161-179.

JONES, P.D., S.C.B. RAPER and T.M.L. WIGLEY, *1986b: Southern hemispheric surface air temperature variations: 1851-1984.* J. of Climate and Applied Meteorology, 25: 1213-1230.

JONES, P.D., T.M.L. WIGLEY and G. FARMER, *1991: Marine and land temperature datasets: A comparison and a look at recent trends.* In Greenhouse-gas-induced climate change: A critical appraisal of simulations and observations. (M.E. Schlesinger, editor), Elsevier, pp. 153-172.

JONES, P.D., P.M. KELLY, C.M. GOODESS and T. KARL, *1989: The effect of urban warming on the Northern Hemisphere temperature average.* J. of Climate, 2 (3): 285-290.

KARL, T.R. and P.D. JONES, *1989: Urban bias in area-averaged surface air temperature trends.* Bulletin of the American Meteorological Society, 70: 265-270.

KARL, T.R., R.R. HEIM JR., and R.G. QUAYLE, *1991: The greenhouse effect in central North America: If not now, when?.* Science, 251: 1058-1061.

KARL, T.R., J.D. TARPLEY, R.G.QUAYLE, H.F. DIAZ, D.A. ROBINSON and R.S. BRADLEY, *1989: The recent climate record: What it can and cannot tell us.* Reviews of Geophysics, 27 (3): 405-430.

MORRISON, S.J., *1990: Warmest year on record on the Antarctic Peninsula?* Weather, 45 (6): 231-232.

PARKER, D.E. and P.D. JONES, *1991: Global warmth in 1990.* Weather, 46 (10): 302-310.

SANSOM, J., *1989: Antarctic surface temperature time series.* J. of Climate, 2 (10): 1164-1172.

SPENCER, R.W. and J.R. CHRISTY, *1990: Precise monitoring of global temperature trends from satellites.* Science, 247: 1558-1562.

STATE METEOROLOGICAL ADMINISTRATION (Beijing), 1991. *Meteorological Working Report No. 4.*

TRENBERTH, K.E., *1990: Recent observed interdecadal climate changes in the Northern Hemisphere.* Bulletin of the American Meteorological Society, 71 (7): 988-993.

TRENBERTH, K.E. and J.G. OLSON, *1989: Temperature trends at the South Pole and McMurdo Sound.* J. of Climate, 2 (10): 1196-1206.

VINNIKOV, K.YA., P.YA. GROISMAN and K.M. LUGINA, *1990: Empirical data on contemporary global climate changes (temperature and precipitation).* J. of Climate, 3 (6): 662-677.

4. PRECIPITATION

ADEJUWON, J.O., E.E. BALOGUN, and S.A. ADEJUWON, *1990: On the annual and seasonal patterns of rainfall fluctuations in Sub-Saharan West Africa.* International J. of Climatology, 10: 839-848.

AUSTRALIAN BUREAU OF METEOROLOGY 1989-90, *Climate Monitoring Bulletin*, Nos. 42-52.

APASOVA, E.G. and G.V. GRUZA, *1982: Climate structure and variability data. Precipitation. Northern Hemisphere.* Obninsk, p. 212 (in Russian).

BRADLEY, R.S., H.F. DIAZ, J.K. EISCHEID, P.D. JONES, P.M. KELLY, and C.M. GOODESS, *1987: Precipitation fluctuations over Northern Hemisphere land areas since the mid-19th Century.* Science, 237:171-175.

CLIMATIC DATA OFFICE, *1989-91, Meteorological Monthly Bulletin. January 1989 — May 1991,* National Meteorological Centre, Beijing, China.

DIAZ, H.F., R.S. BRADLEY, and J.K. EISCHEID, *1989: Precipitation fluctuations over global land areas since the late 1800's.* J. of Geophysical Res., 94 (D1): 1195-1210.

DRUYAN, L.M. and R.D. KOSTER, *1989: Sources of Sahel precipitation for simulated drought and rainy seasons.* J. of Climate, 2: 1438-1446.

GROISMAN, P.YA., V.V. KOKNAEVA, T.A. BELOKRYLOVA, and T.R. KARL, *1991: Overcoming biases of precipitation measurement: A history of the USSR experience.* Bulletin of the American Meteorological Society, 72: 1725-1733.

GROISMAN, P. YA., E.H. MASON, and S. DELGRECO, *1991: Metadata for construction of homogeneous long-term precipitation time series.* Preprints, Seventh Conference on Applied Climatology, 10-13 September 1991, Salt Lake City, pp. 119-122.

GRUZA, G.V. and E.G. APASOVA, *1981: Climatic variability of monthly total precipitation in the Northern Hemisphere.* Meteorology and Hydrology, N.5, pp. 5-16 (in Russian).

HASTENRATH, S., *1990: Prediction of northeast Brazil rainfall anomalies.* J. of Climate, 3 (8): 893-904.

HULME, M., *1991: An intercomparison of model and observed global precipitation climatologies.* Geophysical Res. Lett., 18 (9): 1715-1718.

INTERNATIONAL DROUGHT INFORMATION CENTER, *1989-91, Drought Network News.* January 1989-June 1991, University of Nebraska, Lincoln, NE.

KARL, T.R., J.D. TARPLEY, R.G. QUAYLE, H.F. DIAZ, D.A. ROBINSON, and R.S. BRADLEY, *1989: The recent climate record: What it can and cannot tell us.* Rev. Geophys., 27: 405-430.

LECOMTE, D., *1989: The rains return to the tropics.* Weatherwise, 42 (1): 8-12.

LEGATES, D.R. and C. J. WILLMOTT, *1990: Mean seasonal and spatial variability in gauge-corrected, global precipitation.* International Journal of Climatology, 10: 111-127.

MECHOSO, C.R., S.W. LYONS and J.A. SPAHR, *1989: The impact of sea surface temperature anomalies on the rainfall over northeast Brazil.* J. of Climate, 3 (8): 812-826.

NICHOLLS, N., *1989: Sea surface temperatures and Australian winter rainfall.* J. of Climate, 2 (9): 965-973.

NICHOLSON, S.E., M.L. DAVENPOST and A.R. MALO, *1990: A comparison of the vegetation response to rainfall in the Sahel and East Africa, using normalized difference vegetation index from NOAA AVHRR.* Climatic Change, 17: 209-241.

OGALLO, L.J., *1989: The spatial and temporal patterns of the East African seasonal rainfall derived from principal component analysis.* International J. of Climatology, 9 (2): 145-167.

RICHMAN, M.B., *1991: Relationships between monthly precipitation over central and eastern North America and the Southern Oscillation. Proceedings 15th Climate Diagnostics Workshop.* Asheville, NC. October 29 to November 2, 1990. pp. 373-383.

U.S. CLIMATE ANALYSIS CENTER, *1989-90, Climatic Diagnostics Bulletin.* July 1989-May 1990. National Weather Service, Washington, DC.

U.S. CLIMATE ANALYSIS CENTER, *1988-91, Weekly Climate Bulletin.* December 3, 1988-June 1, 1991. National Weather Service, Washington, DC.

U.S. NATIONAL CLIMATIC DATA CENTER, *1989-91, Climate Variations Bulletin.* February 1989-May 1991, NOAA, Asheville, NC.

VINNIKOV, K. YA., P. YA. GROISMAN and K.M. LUGINA, *1990: Empirical data on contemporary global climate changes (temperature and precipitation).* J. of Climate, 3 (6): 662-677.

WANG, W-C. and K. LI, *1990: Precipitation fluctuation over semiarid region in northern China and the relationship with El Niño/ Southern Oscillation.* J. of Climate, 3: 769-783.

XU QUN, *1989: Significant influence of the interannual variation of direct solar radiation on the summer monsoon climates of China and Tropical Africa.* Papers presented at the Second WMO Workshop on the Diagnosis and Prediction of Monthly and Seasonal Atmospheric Variations over the Globe, WMO/TD, No. 261, pp. 114-118.

XU QUN, *1990: Significant change of winter solar radiation of China during recent 29 Years.* Scintia Sinica, Part B, No. 10, pp. 1112-1120.

XU QUN, *1965: The Plum Rains (Meiyu) of the Middle and Lower Yangtze Valley for most recent 80 years.* Acta Meteorological Sinica, 34 (4): 507-518.

5. DROUGHTS

ALLEY, W., *1984: The Palmer drought severity index: Limitations and assumptions.* J. of Climate and Applied Meteorology, 23: 1100-1109.

AUSTRALIAN BUREAU OF METEOROLOGY, *1989-90: Climate Monitoring Bulletin,* Nos. 42-52.

DRUYAN, L.M. and R.D. KOSTER, *1989: Sources of Sahel precipitation for simulated drought and rainy seasons.* J. of Climate, 2 (12): 1438-1446.

DYER, T.G.J., *1977: The assignment of rainfall stations into homogeneous groups. An application of principal component analysis.* Quarterly Journal of the Royal Meteorological Society, 103: 1005-1013.

GAFFNEY, D., *1990: Seasonal climate summary southern hemisphere (summer 1988-89),* Aust, Met. Mag. 38:1-6.

GLEICK, P.H. and L. NASH, *1991: The Societal and Environmental Costs of the Continuing California Drought.* Pacific Institute for Studies in Development, Environment, and Security, Berkeley, CA.

HASTENRATH, S., *1991: Diagnostics and prediction of northeast Brazil droughts.* Proceedings 15th Climate Diagnostics Workshop. Asheville, NC. October 29 to November 2, 1990. pp. 412-415.

HEIM, JR., R.R., *1991: Drought in the United States: 1990 end-of-year update and historical perspective.* Drought Network News 3 (1): 11-13.

HEIM, JR., R.R., *1990: Drought in the United States: 1989 end-of-year update and historical perspective.* Drought Network News, 2 (1): 8-9.

HEIM, JR., R.R., *1991: The 1989-90 drought and wet spell conditions in the contiguous United States.* Proceedings 15th Climate Diagnostics Workshop, Asheville, NC. October 29 to November 2, 1990. pp. 18-21.

HEDDINGHAUS, T.R., J.E. JANOWIAK, and R.P. MOTHA, *1987: Survey of various techniques used for drought assessment.* Preprints, Fifth Conference on Applied Climatology, 9-13 March 1987, Baltimore, MD, pp. 49-54.

HEDDINGHAUS, T.R. and P. SABOL, *1991: A review of the Palmer drought severity index and where do we go from here?.* Preprints, Seventh Conference on Applied Climatology, 10-13 September 1991, Salt Lake City, pp. 242-246.

JANOWIAK, J.E., *1988: An investigation of interannual rainfall variability in Africa.* J. of Climate, 1: 240-255.

JANOWIAK, J.E., C.F. ROPELEWSKI, and M.S. HALPERT, *1986: A method for monitoring*

regional precipitation deficiency and excess on a global scale. J. of Climate and Applied Meteorology, 25: 565-574.

KARL, T.R. and R.R. HEIM, JR., *1990: Are droughts becoming more frequent or severe in the United States?* Geophysical Res. Lett., 17 (11): 1921-1924.

KOGAN, F., *1991: Observations of the 1990 U.S. drought from the NOAA-11 polar orbiting satellite.* Drought Network News, 3: 7-11.

LANDSBERG, H.E., *1975: Drought, a recurrent element of climate.* Special Environmental Report No. 5, WMO, No. 403, Geneva, Switzerland, pp. 41-90.

LECOMTE, D., *1989: The rains return to the tropics.* Weatherwise, 42 (1): 8-12.

MASKELL, K., D.P. ROWELL and C.K. FOLLAND, *1991: The effect of global and regional sea surface temperature on seasonal Sahel rainfall.* Proceedings 15th Climate Diagnostics Workshop. Asheville, NC, October 29 to November 2, 1990. pp. 396-401.

MATARIRA, C.H., *1990: Drought over Zimbabwe in a regional and global context.* International J. of Climatology, 10: 609-625.

MESCHCHERSKAYA, A.V. and V.G. BLAZHEVICH, *1990: Catalogues of Temperature-Humidity Characteristics with Consideration for the Area of Distribution over Economic Regions of the Basic Grain-Producing Zone of the USSR*, p. 330 (in Russian).

NICHOLSON, S.E. and D. ETEKHABI, *1986: The quasi-periodic behavior or rainfall variability in Africa and its relationship with the southern oscillation.* Arch. Met. Geophy. BIO Ser. A34, 311-348.

OGALLO, L.J., *1987: Relationship between seasonal rainfall in East Africa and the southern oscillation.* J. of Climatology, 7: 1-13.

OGALLO, L.J., *1989: The spatial and temporal patterns of the East African seasonal rainfall derived from principal component analysis.* International J. Climatolology, 9: 145-167.

OGALLO, L.J., J.E. JANOWIAK, and M.S. HALPERT, *1988: Teleconnections between seasonal rainfall over East Africa and global sea surface temperature anomalies.* J. Met. Soc. Japan, 66 (6): 807-822.

OGLESBY, R.J. and D.J. ERICKSON III, *1989: Soil moisture and the persistence of North American drought.* J. of Climate, 2: 1362-1380.

REDMOND, K., *1991: Climate monitoring and indices* in D.A. Wilhite, D.A. Wood, and P.A. Kay, eds. Proceedings of the Drought Planning and Management Seminar and Workshop; pp. 29-33. IDIC Technical Report Series 91-1.

ROPELEWSKI, D.F. and M.S. HALPERT, *1987: Global and regional scale patterns associated with El Niño/Southern oscillation.* Mon. Wea. Rev., 115: 1606-1626.

ROPELEWSKI, D.F. and M.S. HALPERT, *1989: Precipitation patterns associated with the high index phase of the southern oscillation.* J. of Climate, 2: 268-284.

SMITH, D.K., *1989: Natural disaster reduction: how meteorological and hydrological services can help.* World Meteorological Organization, WMO-No. 722. 43pp.

WORLD METEOROLOGICAL ORGANIZATION, *1990: The role of the World Meteorological Organization in the International Decade for Natural Disaster Reduction.* WMO 745. 32pp.

6. FLOODS

AUSTRALIAN BUREAU OF METEOROLOGY, *1989-90: Climate Monitoring Bulletin,* Nos. 42-52.

LECOMTE, D., *1989: The rains return to the tropics.* Weatherwise, 42 (1): 8-12.

LU JIU-YUAN, *1992: Hydrological forecasting in China — the floods of 1991.* WMO Bulletin, 41 (1): 23-27.

SMITH, D.K., *1989: Natural disaster reduction: how meteorological and hydrological services can help.* World Meteorological Organization, WMO-No. 722. 43pp.

WORLD METEOROLOGICAL ORGANIZATION, *1990: The role of the World Meteorological Organization in the International Decade for Natural Disaster Reduction.* WMO 745. 32pp.

XU QUN, *1965: The Plum Rains (Meiyu) of the Middle and Lower Yangtze Valley for most recent 80 years.* Acta Meteorological Sinica, 34 (4): 507-518.

7. MONSOONS

BHATT, U.S., *1989: Circulation regimes of rainfall anomalies in the African-South Asian monsoon belt.* J. of Climate, 2 (10): 1133-1144.

DYER, T.G.J., *1977: The assignment of rainfall stations into homogeneous groups. An application of principal component analysis.* Q.J.R. Meteorol. Soc., 103: 1005-1013.

JANOWIAK, J.E., *1988: An investigation of interannual rainfall variability in Africa.* J. of Climate, 1: 240-255.

JOSEPH, P.V., B. LIEBMANN and H.H. HENDON, *1991: Interannual variability of the Australian summer monsoon onset: Possible influence of Indian summer monsoon and El Niño.* J. of Climate, 4 (5): 529-538.

MILLS, G.A. and SIXIONG ZHAO, *1991: A study of a monsoon depression bringing record rainfall over Australia.* Part I: Numerical predictability experiments. Monthly Weather Review, 119 (9): 2053-2073.

NICHOLSON, S.E. and D. ETEKHABI, *1986: The quasi-periodic behavior or rainfall variability in Africa and its relationship with the southern oscillation.* Arch. Met. Geophy. BIO Ser. A34, 322-348.

OGALLO, L.J., *1987: Relationship between seasonal rainfall in East Africa and the southern oscillation.* J. of Climatology, 7: 1-13.

OGALLO, L.J., *1989: The spatial and temporal patterns of the East African seasonal rainfall derived from principal component analysis.* International J. Climatolology, 9: 145-167.

OGALLO, L.J., J.E. JANOWIAK, and M.S. HALPERT, *1988: Teleconnections between seasonal rainfall over East Africa and global sea surface temperature anomalies.* J. Met. Soc. Japan, 66 (6): 807-822.

ROPELEWSKI, D.F. and M.S. HALPERT, *1987: Global and regional scale patterns associated with El Niño/Southern oscillation.* Mon. Wea. Rev., 115:1606-1626.

ROPELEWSKI, D.F. and M.S. HALPERT, *1989: Precipitation patterns associated with the high index phase of the southern oscillation.* J. of Climate, 2: 268-284.

WORLD METEOROLOGICAL ORGANIZATION, *1990: WCDP Global Climate System Review (June 1986-November 1988),* pp. 37-38, 47.

XU QUN, *1989: Significant influence of the interannual variation of direct solar radiation on the summer monsoon climates of China and Tropical Africa.* Papers presented at the Second WMO Workshop on the Diagnosis and Prediction of Monthly and Seasonal Atmospheric Variations over the Globe, WMO/TD, No. 261, pp. 114-118.

XU QUN, *1990: Significant change of winter solar radiation of China during recent 29 Years.* Scintia Sinica, Part B, No. 10, pp. 1112-1120.

XU QUN, *1965: The Plum Rains (Meiyu) of the Middle and Lower Yangtze Valley for most recent 80 years.* Acta Meteorological Sinica, 34 (4): 507-518.

8. SEVERE STORMS

AVILA, L.A., *1990: Atlantic tropical systems of 1989.* Monthly Weather Review, 118 (5): 1178-1185.

AVILA, L.A., *1991: Eastern North Pacific hurricane season of 1990.* Monthly Weather Review, 119 (8): 2034-2046.

AVILA, L.A., *1991: Atlantic tropical systems of 1990.* Monthly Weather Review, 119 (8): 2027-2033.

AVILA, L., *1991: Eastern Pacific hurricanes: A record year.* Weatherwise, 44 (1): 39-43, 54.

AVILA L., *1991: Eastern North Pacific hurricanes — 1990.* Mariners Weather Log, 35 (2): 24-30.

CASE, B., *1990: Hurricanes: Strong storms out of Africa.* Weatherwise, 43 (1): 30-31.

CASE, B. and M. MAYFIELD, *1990: Atlantic hurricane season of 1989.* Monthly Weather Review, 118 (5): 1165-1177.

CHUN, A.K.T., R.T. MARTIN, and H.E. ROSENDAL, *1990: Central North Pacific tropical cyclones, 1989.* Mariners Weather Log, 34 (2): 23-25.

DOBERITZ, R., *1990: Neun winterorkane in segie-fakten und hintergruende.* Der Wetterlotse, No. 519. pp. 84-94.

FERGUSON, E.W., F.P. OSTBY and P.W LEFTWICH, JR., *1989: Tornadoes: slow start, fast finish.* Weatherwise, 42 (1): 28-35.

FUJITA, T. and D. STIEGLER, *1989: Outstanding storms of the month: Hurricane Hugo, September 10-22, 1989.* Storm Data, 31 (9): 11-27.

JARVINEN, B.R., C.J. NEUMANN, and M.A.S. DAVIS, *1984: A tropical cyclone data tape for the North Atlantic Basin, 1886-1983: Contents, limitations, and uses.* NOAA Technical Memorandum NWS NHC 22, National Hurricane Center, Miami, FL, 21 pp.

LAWRENCE, M.B., *1990: Eastern North Pacific hurricane season of 1989.* Monthly Weather Review, 118 (5): 1186-1193.

LAWRENCE, M.B., *1989: Return of the hurricanes.* Weatherwise, 42 (1): 22-27.

LAWRENCE, M., *1990: Eastern Pacific tropical cyclones.* Weatherwise, 43 (1): 30-31.

LAWRENCE, M., *1990: Eastern North Pacific tropical cyclones, 1989.* Mariners Weather Log, 34 (2): 18-22.

MAYFIELD, M., *1991: Atlantic hurricanes: Storms stay at sea.* Weatherwise, 44 (1): 31-38.

MAYFIELD, M., *1991: North Atlantic hurricanes, 1990.* Mariners Weather Log, 35 (2): 16-22.

MAYFIELD, M. and B. CASE, *1990: North Atlantic tropical cyclones, 1989.* Mariners Weather Log, 34 (2): 12-17.

MAYFIELD, M. and M.B. LAWRENCE, *1990: Atlantic hurricane season of 1990.* Monthly Weather Review, 119 (8): 2014-2026.

OSTBY, F.P., E.W. FERGUSON and P.W. LEFTWICH, JR., *1990: Tornadoes: A strange year.* Weatherwise, 43 (1): 32-39.

READING, A.J., *1990: Caribbean tropical storm activity over the past four centuries.* International J. of Climatology, 10: 365-376.

SOLOW, A. and N. NICHOLLS, *1990: The relationship between the Southern Oscillation and tropical cyclone frequency in the Australian region.* J. of Climate, 3 (10): 1097-1101.

9. GLOBAL CLOUDINESS

ARISTOVA, L.N. and G.V. GRUZA, *1987: Climate Structure and Variability Data.* Satellite-Based Total Cloudiness Data. Northern and Southern Hemisphere. Obninsk, All-Union Research Institute of Hydrometeorological Information World Data Centre, 247 pp. (in Russian).

MATVEEV, L.T., *1986: Global field of cloudiness.* Hydrometeoizdat, Leningrad, 279 pp. (in Russian).

ROSSOW, W.B. and A.A. LACIS, *1990: Global, seasonal cloud variations from satellite radiance measurements.* Part II: Cloud properties and radiative effects. J. of Climate, 3: 1204-1253.

10.

STRATOSPHERIC OZONE

BISHOP, L. and R.D. BOJKOV, *1992: Total ozone trends 1958-91.* J. Geophysical Res. Submitted.

BOJKOV, R.D., *1991: Atmospheric ozone.* WMO Bulletin, 39 (4): 246-253.

DUTTON, E., J. DELUISI, and A. AUSTRING, *1985: Interpretation of Mauna Loa atmospheric transmission relative to aerosols, using photometric precipitable water amounts.* J. Atm. Chem., 3: 53-68.

EVANS, W.F.J., *1990: Ozone depletion in the Arctic vortex at Alert during February 1990.* Geophysical Res. Lett., 17 (2): 167-170.

GEOPHYSICAL RESEARCH LETTERS, *1990: Airborne Arctic Stratospheric Expedition.* Special March Supplement. 17 (4): 313-564.

NEWMAN, P., R. STOLARSKI, M. SCHOEBERL, L.R. LAIT and A. KRUEGER, *1990: Total ozone during the 88-89 Northern Hemisphere winter.* Geophysical Res. Lett., 17 (4): 317-320.

NEWMAN, P., R. STOLARSKI, M. SCHOEBERL, R. MCPETERS and A. KRUEGER, *1991: The 1990 Antarctic ozone hole as observed by TOMS.* Geophysical Res. Lett., 18 (4): 661-664.

STOLARSKI, R.S., M.R. SCHOEBERL, P. A. NEWMAN, R.D. MCPETERS and A.J. KRUEGER, *1990: The 1989 Antarctic ozone hole as observed by TOMS.* Geophysical Res. Lett., 17 (9): 1267-1270.

STOLARSKI, R.S., P. BLOOMFIELD, R. MCPETERS, and J. HERMAN, *1991: Total ozone trends deduced from Nimbus 7 TOMS data.* Geophys. Res. Letts., 18 (6): 1015-1018.

WESTPHAL, D.L. and O. B. TOON, *1991: The short-term temperature response to smoke from oil fires.* Geophysical Res. Lett. 18 (10): 1873-1876.

WMO, *1989: Scientific assessment of stratospheric ozone: 1989. Global Ozone Research and Monitoring Project — Report No. 20.* World Meteorological Organization.

WMO, *1991: Scientific assessment of ozone depletion: 1991. Global Ozone Research and Monitoring Project — Report No. 25.* World Meteorological Organization.

11.

TRACE GASES

ANDERSON, A., *1991: The environmental aftermath of the Kuwait-Iraq conflict.* Our Planet (United Nations Environment Programme), 3 (6): 4-7.

BLAKE, D. and F. ROWLAND, *1988: Continuing worldwide increase in tropospheric methane, 1978-1987.* Science, 239: 1129-1131.

BLUTH, G.J.S., S.D. DORION, C.C. SCHNETZLER, A.J. KRUEGER, and L.S. WALTER, *1992: Global tracking of the SO_2 clouds from the June, 1991 Mount Pinatubo eruptions.* Geophysical Research Letters, 19 (2): 151-154.

CLIMATE INSTITUTE, *1991: Kuwaiti oil fires threaten regional, not world climate.* Climate Alert, 4 (5): 2-3.

CONWAY, T., P. TANS, L. WATERMAN, K. THONING, K. MASARIE and R. GAMMON, *1988: Atmospheric carbon dioxide measurements in the remote global troposphere, 1981-1984, 1988.* Tellus, 40B: 81-115.

EHHALT, D., P. FRASER, D. ALBRITTON, R. CICERONE, M. KHALIL, M. LEGRAND, Y. MAKIDE, R. ROWLAND, L. STEELE, and R. ZANDER, *1988: Trends in Source Gases.* Chapter 8 in Report of the International Ozone Trends Panel 1988, WMO Global Ozone Research and Monitoring Project, Report No. 18, pp 543-569.

FRASER, P., P. HYSON, R. RASMUSSEN, A. CRAWFORD, and M. KHALIL, *1986. Methane, carbon monoxide, and methylchloroform in the Southern Hemisphere.* J. Atmos. Chem., 4:3-42.

FRASER, P., S. RENKETT, R. HARRISS, Y. MAKIDE and E. SANHUEZA, *1991: Source Gases: Concentrations, Emissions and Trends.* Chapter 1 in: Scientific Assessment of Ozone Depletion: 1991. WMO

Global Ozone Research and Monitoring Project, Report No. 25, World Meteorological Organization, pp. 1-1 to 1-47.

GEOPHYSICAL RESEARCH LETTERS, *1990: Airborne Arctic Stratospheric Expedition.* Special March Supplement. 17(4):313-564.

HAHN, J., *1991: Environmental effects of the Kuwaiti oil field fires.* Environ. Sci. Technol., 25 (9): 1530-1532.

HANSEN, J., A. LACIS, R. RUEDY, and M. SATO, *1992: Potential climate impact of Mount Pinatubo eruption.* Geophysical Research Letters, 19 (2): 215-218.

KEELING, C.D., R. BACASTOW, A. CARTER, S. PIPER, T. WHORF, M. HEIMANN, W. MOOK, and H. ROELOFFZEN, *1989: A three-dimensional model of atmospheric CO2 transport based on observed winds: 1.* Analysis of observational data in Aspects of Climate Variability in the Pacific and the Western Americas, D. H. Peterson (ed.), Geophysical Monograph No. 55, Amer. Geophys. Union. pp. 165-236.

KHALIL, M. and R. RASMUSSEN, *1990: Atmospheric methane: recent global trends.* Environ. Sci. Technol., 24: 549-553.

LASHOF, D., *1989: The dynamic greenhouse: Feedback processes that may influence future concentrations of atmospheric trace gases and climatic change.* Climatic Change, 14 (3): 213-242.

MAKIDE, Y., A. YOKOHATA, Y. KUBO, and T. TOMINAGA, *1987: Atmospheric concentrations of halocarbons in Japan in 1979-1986.* Bull. Chem. Soc. Japan, 60: 571-574.

MCCORMICK, M.P., *1992: Initial assessment of the stratospheric and climatic impact of the 1991 Mount Pinatubo eruption: prologue.* Geophysical Research Letters, 19 (2): 149.

MEGIE, G. (coordinator), *1989. Global Trends,* Chapter 2 in: Scientific Assessment of Stratospheric Ozone: 1989, WMO Global Ozone Research and Monitoring Project, Report No. 20, pp. 163-281.

STEELE, L., P. FRASER, R. RASMUSSEN, M. KHALIL, T. CONWAY, A. CRAWFORD, R. GAMMON, K. MASARIE, and K. THONING, *1987. The global distribution of methane in the troposphere.* J. Atmos. Chem., 5: 125-171.

STOWE, L.L., R.M. CAREY and P.P. PELLEGRINO, *1992: Monitoring the Mt. Pinatubo aerosol layer with NOAA/11 AVHRR data.* Geophysical Research Letters, 19 (2): 159-162.

THONING, K. W. and P. TANS, *1989. Atmospheric carbon dioxide at Mauna Loa Observatory 2.* Analysis of the NOAA GMCC data, 1974-1985. J. Geophys. Res., 94: 8549-8565.

WATSON, R., H. ROHDE, H. OESCHGER, and U. SIEGENTHALER, *1990. Greenhouse Gases and Aerosols,* Chapter 1 in Climate Change, The IPCC Scientific Assessment, J. Houghton, G. Jenkins and J. Ephraums, Eds. pp. 1-40, Cambridge Univ. Press, Cambridge UK.

12.

CRYOSPHERE

AGNEW, T. and A. SILIS, *1991: Winter sea ice extent on the eastern Canadian seaboard.* Canada Department of the Environment, Climatic Perspectives, 13 (2): 9-11.

ALENIUS, P. and L. MAKKONEN, *1981: Variability of the annual maximum ice extent of the Baltic Sea.* Arch. Met. Geoph. Biokl., Ser, B, 29:393-398.

ASSEL, R.A., *1989: Impact of global warming on Great Lakes ice cycles.* In: J.B. Smith and D.A. Tirpak (eds.), The potential effects of global climate change on the United States. Appendix A. Water Resources. U.S. Environmental Protection Agency, EPA-DW13932631-01-0, pp. 5.1-5.30.

BARRY, R.G., *1990: Changes in mountain climate and glacio-hydrological responses.* Mountain Res. Devel., 10: 161-170.

BARRY R.G., *1991: Observational evidence of changes in global snow and ice cover.* In: M.E. Schlesinger (ed.), Greenhouse-gas-induced climatic changes. A critical appraisal of simulations and observations. Elsevier, Amsterdam, pp. 320-345.

CHEN, J.Y. and A. OHMURA, *1991: Estimation of alpine glacier water resources and their changes since the 1870s.* In: H. Lang and A. Musy, eds., Hydrology in Mountainous Regions, I. Hydrological Measurements; the water cycle. Internat. Assoc. Hydrol. Sci., Publ. No. 193, pp. 127-35. Wallingford, U.K.

CHEN, J.Y. and M. FINK, *1990: Mass balance of Rhonegletscher during 1882/83 — 1986/87.* J. Glaciol., 36 (123): 199-209.

FOLLAND, C.K., T.R. KARL and K. YA. VINNIKOV, *1990: Observed climate variations and change.* In Climate Change: The IPCC Scientific Assessment, J.T. Houghton, G.J. Jenkins and J.J. Ephraums (editors), pp. 195-238. Cambridge Univ. Press, Cambridge.

FOSTER, J.L., *1989: The significance of the date of snow disappearance on the arctic.* Arctic and Alpine Res., 21 (1):60-70.

GINZBURG, B.M., *1975: Probabilistic characteristics of ice covering and breaking-up data for the USSR rivers and storage lakes.* Leningrad, Gydrometeoizdat (in Russian).

GINZBURG, B.M., K. N. POLYAKOVEA, *1991: On the secular trends in the beginning of ice covering data on the rivers European part of USSR.* Hydrometcenter of the USSR, Proceedings, Vol. 320.

GLOERSON, P. and W. J. CAMPBELL, *1991: Arctic Sea ice 1973-1987: seasonal, regional and inter-annual variability.* J. of Geophysical Res., 94 (C10): 14499-14523.

GLOERSEN, P. and W.J. CAMPBELL, *1991: Recent variations in Arctic and Antarctic sea-ice covers.* Nature, 352:33-36.

HAEBERLI, W., *1990: Glacier and permafrost signals of 20th-century warming.* Ann. Glaciol., 14:127-30.

JACKA, T.H., *1990: Antarctic and Southern Ocean sea-ice and climate trends.* Ann. Glaciol., 14: 99-101.

JONES, P.D., *1988: Hemispheric surface air temperature variations: recent trends and an update to 1987.* J. of Climate, 1: 654: 60.

LACHENBRUCK, A. H. and B. V. MARCHALL, *1986: Changing climate: geothermal evidence from permafrost in the Alaskan Arctic.* Science, 234: 689-696.

LAXON, S., *1990: Seasonal and inter-annual variations in Antarctic sea ice extent as mapped by radar altimetry.* Geophysical Res. Lett., 17 (10): 1553-1556.

LETREGUILLY, A., *1984: Bilans de masse des glacier alpins: methodes de mesure et repartition spatio-temporelle.* Laboratoire de Glaciologie, Publ. no. 439, CNRS, Grenoble, France.

MAYO, L.R. and R.S. MARCH, *1990: Air temperature and precipitation at Wolverine Glacier, Alaska; glacier growth in a warmer, wetter climate.* Ann. Glaciol., 14: 191-94.
MCLAREN, A.S., *1989: The under-ice thickness distribution of the Arctic Basin as recorded in 1958 and 1970.* J. Geophys. Res., 94: 4971-83.
MCLAREN, A.S., R.G. BARRY and R.H. BOURKE, *1990: Could Arctic ice be thinning?* Nature, 345: 762.
MEDRES, P. L., *1957: Ice regime of Lake Ladoga based on airborne ovservations data.* State Hydrological Institute. Proceedings, Vol. 66.
PALECKI, M.A. and BARRY, R.G., *1986: Freeze-up and break-up of lakes as an index of temperature changes during the transition seasons: A case study for Finland.* J. Clim. Appl. Met., 25: 893-902.
PATET, G. and M. AELLEN, *1990: Gletscher. In D. Vischer, ed., Schnee, Eis und Wasser der Alpen in einer wameren Atmospäre.* Versuchsansalt fur Wasserbau, Hydrologie und Glaziologie, Mitteilungen, 108. pp. 49-69. ETH, Zurich.
ROBINSON, D. A., *1987: Snow cover as indicator of climate change.* In: Large-Scale Effects of Seasonal Snow Cover, B. E. Goodison, R. G. Barry and J. Dozier, (eds.), IAHS Publ. No. 166, International Association of Hydrological Sciences Press, Wallingford, UK, pp. 15-25.
ROBINSON, D. A. and K. F. DEWEY, *1991: Recent secular variations in the extent of northern hemisphere snow cover.* Geophys. Res. Lett., 17 (10) 1557-1560.
ROBINSON, D.A., F.T. KEIMIG and K.F. DEWEY, *1991: Recent variations in northern hemisphere snow cover.* Proceedings, 15th Annual Climate Diagnostics Workshop, Asheville, NC. October 29 to November 2, 1990. pp. 219-24.
SCHINDLER, D. W. et AL., *1990: Effects of Climatic warming on the Lakes of the central boreal forest.* Science, 250: 967-970.
SEVASTYANOVA, N. V., *1991: Main regularities and probabilistic characteristics of Lake Ladoga ice covering.* Leningrad Hydrometcenter, coll. papers, Vol. 5 (18).
SKINNER, W. R., *1991: Lake ice conditions as a cryospheric indicator of climate variability in Canada.* Atmospheric Environment Service. Internal Report. July.
VERBOLOV, V.I., V. M. SOKOL'NIKOV, *1965: Hydrometeorological regime and heat balance of Lake Baikal.* Moscow, "Nauka" (in Russian).
WADHAMS, P., *1990: Evidence for thinning of the Arctic sea ice cover north of Greenland.* Nature, 345: 795-97.
WEATHERLY, J. W., J. E. WALSH and H. J. ZWALLY, *1991: Antarctic sea ice variations and seasonal air temperature relationships.* J. of Geophysical Res., 96 (C8) 15119-15130. August 15.

13.

OCEANS

BAKER, D.J., *1991: World ocean circulation and climate change: Research programmes and a global observing system.* In: Proceedings of the Second World Climate Conference. J. Jager and H.L. Ferguson (editors). Cambridge University Press and World Meteorological Organization. p. 195-201.
JOINT SCIENTIFIC COMMITTEE FOR THE WORLD CLIMATE RESEARCH PROGRAMME, *1991: The global climate observing system.* Report of the meeting at Winchester, United Kindgom, January 14-15, 1991. The Meteorological Office.
NICHOLLS, N., *1989: Sea surface temperatures and Australian winter rainfall.* J. of Climate, 2 (9): 965-973.
STANTON, B.R., *1991: Ocean circulation and ocean-atmosphere exchanges.* Climatic Change, 18 (2-3): 175-194.
U.S. DEPARTMENT OF COMMERCE *Climate Diagnostics Bulletin — Near real-time analyses ocean/atmosphere* (Periodical). NOAA, Climate Analysis Center.
U.S. DEPARTMENT OF COMMERCE: *Oceanographic Monthly Summary* (Periodical). NOAA, National Ocean Service.
WOODS, J.D., *1985: World Ocean Circulation Experiment,* Nature, Vol. 314, pp. 501-511.
WORLD METEOROLOGICAL ORGANIZATION, *1988: World Ocean Circulation Experiment, Implementation Plan,* Vols. I and II, WCRP 11 and 12 (WMO Technical Documents TD-242 and 243), Geneva.

14.

SEA AND LAKE LEVELS

GOVERNMENT OF CANADA, *1991: Monthly Water Level Bulletin — Great Lakes and Montreal Harbour.* Canadian Hydrographic Service and Inland Waters Directorate. 6p.
GOLITSYN, G.S. and G.N. PANIN, *1989: Contemporary changes of the Caspian Sea level.* Meteorologia and Gidrologia, 1: 57-64.
GOLITSYN, G.S., A.V.DZUBA, A.G. OSIPOV and G.N. PANIN, *1990: Regional climate changes and their impact on the Caspian Sea level rise.* Doklady, USSR Acad. Sci., 313 (5): 1224-1227.
RODIONOV, S.N., *1988: Recent climatic change in the Caspian Sea basin.* Gidrometeoizdat. 124p. (in Russian).

15.

DEFORESTATION AND DESERTIFICATION

BALLING, R.C., JR., *1988: The climatic impact of a Sonoran vegetation discontinuity.* Climatic Change, 13: 99-109.
BALLING, R.C., JR., *1989: The impact of summer rainfall on the temperature gradient along the United States — Mexico border.* J. of Applied Meteorology, 28: 304-308.
BALLING, R.C., JR., *1991: Impact of desertification on regional and global warming.* Bulletin of the American Meteorological Society, 72:232-234.
BRYANT, N.A., L.F. JOHNSON, A.J. BRAZEL, R.C. BALLING JR., C.F. HUTCHINSON, and L.R. BECK, *1990: Measuring the effect of overgrazing in the Sonoran Desert.* Climate Change, 17: 243-264.
CHARNEY, J.G., *1975: Dynamics of deserts and drought in the Sahel.* Quarterly Journal of the Royal Meteorological Society, 101: 193-202.
JONES, P.D., S.C.B. RAPER, R.S. BRADLEY, H.F. DIAZ, P.M. KELLY, and T.M.L. WIGLEY, *1986a: Northern hemispheric surface air temperature variations: 1851-1984.* J. of Climate and Applied Meteorology, 25: 161-179.
JONES, P.D., S.C.B. RAPER, and T.M.L. WIGLEY, *1986b: Southern hemispheric surface air temperature variations: 1851-1984.* J. of Climate and Applied Meteorology, 25: 1213-1230.
JONES, P.D., T.M.L. WIGLEY, and P.B. WRIGHT, *1986c: Global temperature variations between 1861 and 1984.* Nature, 322: 430-434.
MYERS, N.(editor), *1991: Tropical Forests and Climate.* Climatic Change, 19 (1-2): 1-264. Special Issue.
SALATI, E. and C.A. NOBRE, *1991: Possible climatic impacts of tropical deforestation.* Climatic Change, 19 (1-2): 177-196.

17.

THE 1980S — A MOST REMARKABLE DECADE FOR CLIMATOLOGY

HALPERT, M.S. and C.F. ROPELEWSKI, *1991: Climate assessment.* A decadal review 1981-1990. NOAA, National Weather Service — National Meteorological Center, Climate Analysis Center. Washington, DC 109 pp.
JONES, P.D. and T.M.L. WIGLEY, *1991: Recent global warmth during the 1980s and 1990.* Proceedings 15th Climate Deagnostics Workshop, Asheville, NC. October 29 to November 2, 1990. pp. 344-349.
U.S. DEPARTMENT OF COMMERCE, *1988 to 1991: Climate Diagnostics Bulletin.* NOAA, National Weather Service — National Meteorological Center, Climate Analysis Center, Washington, DC. Monthly isssue.
U.S. DEPARTMENT OF COMMERCE, *1988 to 1991: Weekly Climate Bulletin.* NOAA, National Weather Service — National Meteorological Center, Climate Analysis Center, Washington, DC. Weekly issue.
WORLD METEOROLOGICAL ORGANIZATION AND UNITED NATIONS ENVIRONMENT PROGRAMME, *1985: The Global Climate System. A critical review of the climate system during 1982- 1984.* World Climate Data Programme. 52 pp.
WORLD METEOROLOGICAL ORGANIZATION AND UNITED NATIONS ENVIRONMENT PROGRAMME, *1987: The Global Climate System. Autumn 1984 — Spring 1986.* World Climate Data Programme. CSM R84/86. 87 pp.
WORLD METEOROLOGICAL ORGANIZATION and UNITED NATIONS ENVIRONMENT PROGRAMME, *1990: The Global Climate System — Climate System Monitoring June 1986 — November 1988.* World Climate Data Programme. CSM R84/86. 70 pp.

LIST OF ABBREVIATIONS USED IN THIS REPORT

AOT	aerosol optical thickness
AVHRR	Advanced Very High Resolution Radiometer
CAC	Climate Analysis Center (Washington)
CFCs	chlorofluorocarbons
CSIRO	Commonwealth Scientific and Industrial Research Organization (Australia)
CSM	climate system monitoring
ENSO	El Niño/Southern Oscillation
FAO	Food and Agricultural Organization of the UN
GISS	Goddard Institute of Space Sciences, New York, USA
HCN	United States Historical Climate Network
IPCC	Intergovernmental Panel on Climate Change
ITCZ	intertropical convergence zone
MGO	Main Geophysical Observatory (St. Petersburg, Russia)
MLO	Mauna Loa Observatory
MSU	microwave sounding unit
NASA	National Aeronautics and Space Administration, USA
NCDC	National Climatic Data Center (Asheville, N.C.)
NESDIS	National Environmental Satellite Data and Information Service (Washington)
NOAA	National Oceanic and Atmospheric Administration, USA
OLR	outgoing long-wave radiation
ppbv	parts per billion (10^9) by volume
ppmv	parts per million (10^6) by volume
pptv	parts per trillion (10^{12}) by volume
PSC	polar stratospheric cloud
SCOR	Scientific Committee on Oceanic Research (ICSU)
SO (I)	Southern Oscillation (index)
SST	sea surface temperature
TOGA	Tropical Ocean and Global Atmosphere experiment
TOMS	total ozone mapping spectrometer
UNEP	United Nations Environment Programme
UTC	universal time coordinated
WCDMP	World Climate Data and Monitoring Programme
WCDP	World Climate Data Programme
WCP	World Climate Programme
WMO	World Meteorological Organization
WOCE	World Ocean Circulation Experiment

CONTRIBUTORS

B.M. Chhabra, India Meteorological Department, New Delhi, India
G.V. Gruza, Institute of Global Climate and Ecology, Moscow
Richard Heim, NOAA, National Climatic Data Center, Asheville, N.C., USA
Raino Heino, Finnish Meteorological Institute, Helsinki, Finland
Philip Jones, Climatic Research Unit, University of East Anglia, Norwich, UK
Bill Kininmonth, National Climate Centre, Bureau of Meteorology, Melbourne, Australia
Vernon Kousky, NOAA, Climate Analysis Center, Washington, D.C. USA
Luiz Molion, Space Research Institute, Manaus, Amazonas, Brazil
Laban Ogallo, University of Nairobi, Department of Meteorology, Nairobi, Kenya
Jim Peterson, NOAA, Environmental Research Laboratories, Boulder, Colo., USA
David Phillips, Canadian Climate Centre, Atmospheric Environment Service, Downsview, Ontario, Canada
Gudrun Rosenhagen, Deutscher Wetterdienst, Hamburg, Germany
Xu Qun, Jiangsu Meteorological Institute, Nanjing, China
Michael Crowe, World Climate Programme Department, Geneva, Switzerland
Heikki Tuomenvirta, WMO, World Climate Programme Department, Geneva, Switzerland
Robert C. Balling, Arizona State University, Tempe, Ariz., USA
M. Conte, Italy Meteorological Service, Rome, Italy
Henry Diaz, NOAA, Environmental Research Laboratories, Boulder, Colo., USA
J. Eischeid, NOAA, Environmental Research Laboratories, Boulder, Colo., USA
Pavel Ya. Groisman, State Hydrological Institute, Leningrad, Russian Federation
Frank Quinn, NOAA, Great Lakes Research Laboratory, Ann Arbor, Mich., USA
Richard Raddatz, Winnipeg Climate Centre, Environment Canada, Winnipeg, Man., Canada

Principal editor: David Philips
Graphics: Image One Productions, Ontario
Design: Bernard Chazine, Siena
Phototypesetting: *il* DOCG, Siena
Printed in Italy by: Centrooffset, Siena

1992

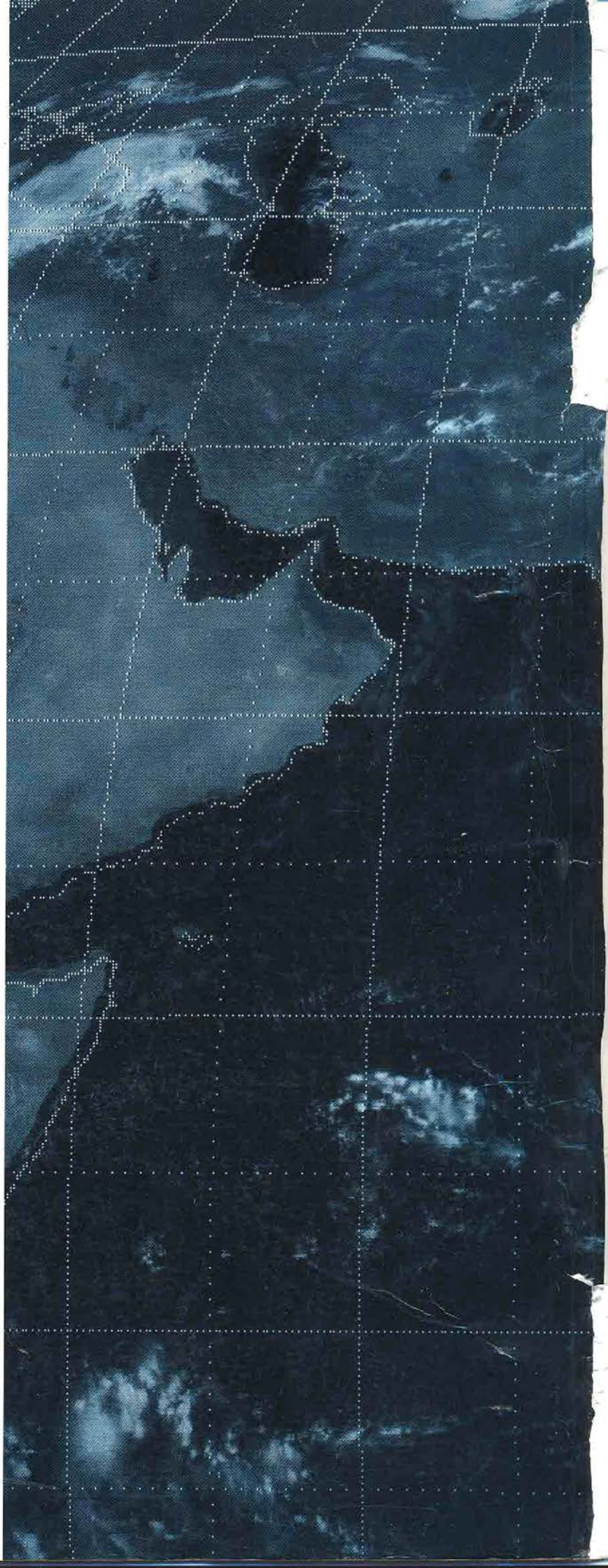

WORLD METEOROLOGICAL
ORGANIZATION
WORLD CLIMATE DATA
AND MONITORING PROGRAMME

UNITED NATIONS
ENVIRONMENT
PROGRAMME